HOKKAIDO UNIVERSITY

Title	Geospatial analysis on multiscale geomorphic processes and sediment connectivity in the Brahmaputra River basin
Author(s)	FAISAL, B.M Refat
Citation	北海道大学. 博士(環境科学) 甲第15714号
Issue Date	2024-03-25
DOI	10.14943/doctoral.k15714
Doc URL	http://hdl.handle.net/2115/91775
Type	theses (doctoral)
File Information	Faisal_BM_Refat.pdf

Instructions for use

Hokkaido University Collection of Scholarly and Academic Papers : HUSCAP

Geospatial analysis on multiscale geomorphic processes and sediment connectivity in the Brahmaputra River basin

ブラマプトラ川流域における地形プロセスと土砂接続性の地理空間情報解析

B. M. Refat Faisal

The dissertation submitted for the partial fulfillment of Doctor of Philosophy (Ph.D.), March 2024

Division of Environmental Science Development
Graduate School of Environmental Science
Hokkaido University, Japan

Geospatial analysis on multiscale geomorphic processes and sediment connectivity in the Brahmaputra River basin

ブラマプトラ川流域における地形プロセスと土砂接続性の地理空間情報解析

By
B. M. Refat Faisal
Graduate School of Environmental Science
Hokkaido University, Japan

Supervisor
Yuichi S. Hayakawa (Ph.D.)
Associate Professor
Faculty of Environmental Earth Science
Hokkaido University, Japan

March 2024

Abstract

Geomorphological knowledge is critical in understanding watershed-scale surface processes both in steep mountainous areas and flat lowlands, particularly if the mid- and downstream areas are densely populated and hazard assessments are highly required. The upper basin morphodynamics, hydrology, and sediment flux highly influence the repeated sediment disasters in the downstream areas, and our understanding of the large-scale fluvial geomorphic processes and basin-scale sustainable river management is crutial. However, our knowledge about such surface processes has relatively been limited in some areas in South Asia (particularly Bangladesh) due likely to the lack of comprehensive studies of geomorphology and related fields. In this study, the author first undertakes an overview of the geomorphological processes of the disaster-prone deltaic landscape of the Ganges–Brahmaputra–Meghna (GBM) focusing on fluvial processes at basin scale (Chapter 2). The review of previous studies found that most of the geomorphic researches in Bangladesh are exploring landslide inventory and susceptibility mapping in hilly areas; river channel or riverbank shifting, riverbank erosion and accretion in fluvial environments; watershed morphometric analysis and geomorphic unit identification in plain land; and coastline shifting or coastal erosion and accretion in coastal environments at a small scale. Then, the author discusses the fluvial dynamics and sediment transport of the GBM river system to address the knowledge gap in the context of deltaic plain land in Bangladesh, where upstream fluvial sedimentation processes impact the geomorphic connectivity from Himalayan to the Bay of Bengal. Although some studies on the fluvial dynamics and sediment dispersal in the upstream GBM river basin are present, the fluvial processes in the downstream domain of Bangladesh are not fully understood with a limited number of research with field-based approaches. Hence, some future perspectives of geomorphic research in Bangladesh are then mentioned to understand better the complex geomorphological settings in the entire GBM watershed and to strengthen the existing research capacity.

Following these reviews, in Chapter 3, the author attempts to characterize the morphometric and topographic features at the sub-basin scale along with the spatial sediment connectivity pattern of the middle Brahmaputra River basin (Teesta, Torsa, and Manas basins) covering ~75,000 km^2 that influences the hydro-geomorphic response of the deltaic landscape of lowland Bangladesh. This work considers a set of morphometric and topographic parameters including the stream network, longitudinal profiles, stream power

index (SPI), and topographic wetness index (TWI) for geomorphometric characterization. The linkage between the sediment sources to downstream areas also has been evaluated with the sediment connectivity index (IC) to understand better the sediment dynamics of the middle Brahmaputra River basin, draining towards lowland Bangladesh from the basin's upstream countries of India and Bhutan. The result of this study demonstrates a highly potential hydro-geomorphic response of the downstream areas attributed to steep topography, steep channel longitudinal profiles, high rainfall, and high sediment connectivity in upstream regions. However, the low topography, presence of anthropogenic stressors, almost flat longitudinal channel profiles with limited change in elevation, and lowered sediment connectivity potential in the mid-to-downstream areas depict sensitivity to the depositional processes therein, impacting the basin-scale geomorphic connectivity from the upstream to the downstream region. These results will be the basic information for exploring the large-scale hydro-geomorphic response and structural sediment dynamics to understand the complex geomorphological processes in the South Asia region.

Furthermore, for a widespread understanding of the upstream's hydro-geomorphic response as well as assessing geomorphological dynamics and protecting floodplain areas in downstream, the topographical changes in disaster-prone riverine floodplains at the local scale need to be measured, which has been limited in South Asia due to the lack of multitemporal, high-definition digital elevation models (DEMs) derived from modern techniques including airborne laser scanning, structure-from-motion (SfM) photogrammetry accompanied with Unmanned Aerial Vehicle (UAV), and field-based mapping approaches. Hence, as a local scale case, the author carried out a preliminary study at two locations of the Teesta River (Brahmaputra's tributary) in Bangladesh using the UAV-SfM techniques and generated high-resolution DEMs (Chapter 4). The selected locations represent dynamic changes of sediment and water on the floodplain over the years, and the UAV-SfM approach can be an effective method for monitoring those changes, but an archive of the past data has been unavailable. Here the author evaluated the topographic changes by comparing the UAV-SfM-derived DEMs of 2022 with global DEM products (NASADEM of 1999), which are often the only available choice of DEMs in this river floodplain. The elevation differences of these two sets of DEMs were in the range of −5.23 to −84.66 m, and volumetric changes of −4.11±0.15 to −86.25±0.20 million m^3, likely dominated by erosional processes towards the left side bank where the elevation errors are supposed to be several meters for UAV-DEM and ca. 5-12 m for NASADEM. Although it is not easy to accurately evaluate the absolute

values of the changes, these changes may be associated with the upper basin's hydrology, sediment flux, and anthropogenic stressors along the floodplain. The considerable changes in topography, including cross-sectional profiles, elevation, and sediment volume, indicate the importance of continuous river topographic monitoring that can be facilitated from the present workflow, which can optimize river management strategies in South Asia, particularly Bangladesh.

Hereafter, the author believes that this multiscale geospatial study will develop a holistic understanding of basin-wide fluvial geomorphic processes and sediment dynamics of the Brahmaputra River to the policymakers considering the key determinants (excessive sediment sequestering, riverbed aggradation, river hydrology, hydro-engineering structures, etc.) of geomorphic connectivity and may be helpful to improve the transboundary river basin management policies or strategies focusing on restoring the geomorphic connectivity, monitoring river floodplain, joint research initiatives, cross-boundary cooperation, and sustainable development among the basin-sharing countries.

Keywords: Ganges–Brahmaputra–Meghna (GBM), Fluvial-geomorphology, Brahmaputra, Multiscale, NASADEM, Sediment connectivity, Terrain analysis, Unmanned aerial vehicle (UAV), Structure-from-motion (SfM).

Table of contents

List of figures

List of tables

Chapter 1
General introduction

1.1 Background of the study

Information on terrain features or land surface processes is one of the most fundamental requirements for various studies in environmental science and applied geomorphology (Ehsani and Quiel, 2008). The most widely used data structure employed to store and accurately characterize information about topography in a Geographic Information System (GIS) environment is a land-surface model, i.e., the Digital Elevation Model (DEM) (Pike et al., 2009). Landform elements as physical constituents of terrain may be extracted from the DEM using various approaches including morphometric and topographic parameters (Dikau, 1989; Iwahashi and Pike, 2007), which have relationship with geomorphologic processes (Ehsani and Quiel, 2008). The landform properties control the geomorphic processes (Dehn et al., 2001), where consideration of the landforms might be different but a common perspective of many recent landform studies is to use a DEM (Ehsani and Quiel, 2008) (i.e., NASADEM), which can be compiled from various open sources like the United States Geological Survey (USGS) Earth Explorer (https://earthexplorer.usgs.gov/). The geomorphometric indices have been formulated to describe the landform characteristics and widely used around the globe (Crosby and Whipple, 2006; Olivetti et al., 2012). The understanding of processes that are causing changes on earth surface and related landform development represents one of the main challenges in geomorphology, where the remote sensing techniques allows the evaluation and quantification of landform change patterns at different spatial and temporal scale (Williams, 2012). Besides, the relation of sediment connectivity from a large drainage basin to the behavior of the river morphology is fundamental area of inquiry in fluvial studies.

In geomorphic science, the term connectivity has become widely used in the past two decades to describe the fluxes (water and sediment) in the geomorphic system that govern the configuration of the river channel, which influences land formation in geographically distant locations (Fryirs et al., 2007; Bracken et al., 2015; Wohl et al., 2019). The connectivity study investigates the interactions among the components of the geomorphic system (hillslope, valley bottom, channel segments), the response of the diverse geomorphic system to varying inputs (i.e., water and sediment fluxes), the landforms features that govern the connectivity

within a drainage basin, and the human alternations of geomorphic systems (i.e., flow regulations, channel diversion, etc.) at different spatio-temporal scales (Cenderelli and Wohl, 2003; Fryirs et al., 2007; Wohl et al., 2019). The sediment connectivity in geomorphology is the transfer of sediment between different stores or zones within the catchment system (e.g., between channel reaches or between hillslopes and channels), placing an emphasis on the distribution of sediment stores and sinks (Hooke, 2003; Harvey, 2012; Poeppl et al., 2017). The control of the morphological conditions on spatial sediment connectivity acts both through hillslope-channel coupling and decoupling, and through sediment transfer along the channel network. The connectivity research experienced a surge within various disciplines including geomorphology (Brierley et al., 2006; Bracken et al., 2015) to better understand linkages between sediment source areas and the corresponding sinks in catchment systems (e.g., Turnbull et al., 2008; Wainwright et al., 2011; Fryirs, 2013; Poeppl et al., 2017). The spatial characterization of connectivity patterns in the complex and heterogeneous mountainous catchment (e.g., Brahmaputra River basin) allows effective estimation of the contribution of a given part of the catchment as sediment source, and to define the sediment transfer paths (Cavalli et al., 2013). Furthermore, the implementation of connectivity in management concepts is especially important in a region where high erosion and sediment delivery rates cause severe problems (Najafi et al., 2021), as in the case of the largely ungauged Brahmaputra River. Besides, identifying the connectivity pattern is useful in basic and applied geomorphic research (Wohl et al., 2019), and this study explores the implications of sediment connectivity for river basin management in densely populated South Asian regions at the risk of repated sediment disasters.

The natural processes related to sediment erosion, transport, and deposition play a major role in shaping the morphology of mountainous catchments and may result in severe hazards when fluvial-sedimentation occurs in paroxysmal ways (Goldin, 2015). The Brahmaputra (Yarlung Tsangpo-Siang-Brahmaputra-Jamuna) (originated from the great glacier mass of Chema-Yung-Dung in the Kailas range of southern Tibet) is one of the most heavily sediment-laden large rivers of the world (after the Amazon and Yellow River), making the region prone to sediment disasters (i.e., flood causing the death on average around 6000 people per year in Bangladesh) and affecting enormous number of people's livelihood (400 million) (Yasuda et al., 2017; Pangare et al., 2021). This transboundary river (~580,000 sq. km; ~2880 km) is shared by four different countries (China-50.5%, India-33.6%, Bangladesh-8.1%, and Bhutan-7.8%) and there are international dimensions and

significant discord among the actors across the basin, which pose challenges to the management and distribution of its resources (e.g. hydropower potential, fertile agricultural lands, and substantial aquatic diversity) (Mahanta et al., 2014; Yasuda et al., 2017). For better management of this complex river basin, it is necessary to understand the fluvial-geomorphological context at basin-wide approach for potential future cooperation and strategies about the Brahmaputra River. As the ultimate carrier of freshwater and sediment in the South-Asian region, the Brahmaputra River drives the hydro-meteorological interactions, dynamics, and processes of the entire region (Pangare et al., 2021). Furthermore, as a complex river system, the Brahmaputra requires much more attention in analytical studies focusing on the morphological features and geomorphic connectivity to address the challenges of holistic transboundary river management among the riparian countries (China, India, Bhutan, and Bangladesh). Unfortunately, the understanding on land surface processes has relatively been limited in South Asia, particularly in transboundary Brahmaputra River basin (details are provided in Chapter 2).

Therefore, this study has been initiated to cover large areas of the Brahmaputra River flowing through different morphological zones (Himalaya belt, lower mountainous region, Brahmaputra valley, and deltaic floodplains) using remote sensing technologies (e.g., satellite sensing, unmanned aerial sensing) and GIS with field-based approaches towards achieving the better understanding of fluvial-geomorphic processes and sediment dynamics in South-Asia (Fig. 1.1). Particularly, this study focuses on the GBM's fluvial-geomorphic processes and their connectivity from the Himalayan to the Bay of Bengal (Chapter 2), and later on highlights the middle Brahmaputra's (includes snow and glacier-fed sub-basins on the southern Himalayan slopes) north bank tributaries (Teesta, Torsa, and Manas covering 75,000 sq. km) (Chapter 3) considering its potentiality of large additions to the flow of mainstream Brahmaputra and vigorous characteristics (i.e., steeper channel gradient, channel change, erosion rate, high flow, and sediment contribution, and precipitation intensity) (Coleman, 1969; Goswami, 1985; Mahanta et al., 2014; Pangare et al., 2021; Palash et al., 2023). Besides, this study emphasizes the lower Brahmaputra (includes non-snow sub-basins on the southern Himalayan slopes and floodplains) at Teesta (Brahmaputra's tributary) (Palash et al., 2023) to evaluate the topographical dynamics, introducing unmanned aerial vehicle-based structure-from-motion photogrammetry (UAV-SfM) and available global DEM products towards developing river basin management framework in South Asia's disaster-prone floodplain (Chapter 4), particularly densely populated Bangladesh. The author believes that

understanding the fluvial-geomorphic processes, geomorphic connectivity patterns, and topographic dynamics at multiscale (basin, sub-basin, and local scales) from this study will not only contribute to the existing academic body of knowledge but will also have the potential to contribute to effective management and regional collaboration among the basin-shared countries linking upstream to its downstream, often hindered by inadequate basin information. With this background in mind, this research aims to address the following questions.

1) How is the geomorphic processes and connectivity from the Himalayan to the Bay of Bengal impacted by upstream fluvial-geomorphic processes? And what kind of geomorphic research can be prioritized in this understudied region? (Chapter 2).
2) How are the geomorphic characteristics related to the sediment connectivity between upland and lowland systems on the Brahmaputra River basin? (Chapter 3).
3) How can the topographical dynamics be assessed from DEM products (UAV-SfM and global products) to optimize river management strategies in the disaster-prone floodplain of Teesta River (Brahmaputra's tributary)? (Chapter 4).

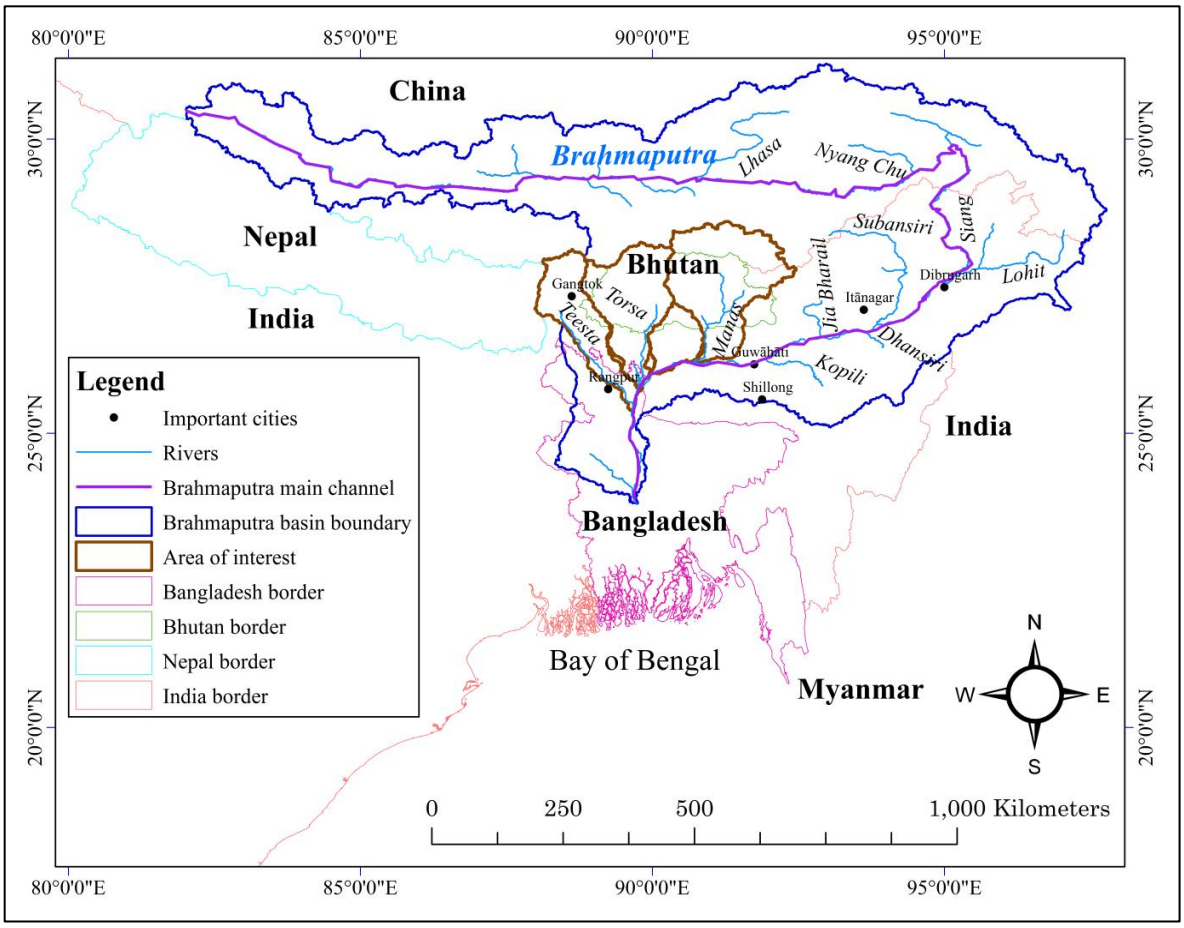

Fig. 1.1 Brahmaputra River system with transboundary flow path.

1.2 Objectives of the work

Within this context, the goal of the research reported here is to achieve a new and improved understanding of fluvial-geomorphic processes and sediment connectivity and to show the potential applicability of modern remote sensing approaches to uncover the topographical dynamics in densely populated developing areas (focus on Brahmaputra's downstream) that are prone to repeated sediment disasters (e.g., floods, river bank erosion). The specific objectives of this study are as follows-

a) To overview the geomorphological processes and their connectivity in hillslope, fluvial, and coastal areas in Brahmaputra's downstream to highlight some potential future geomorphic research considering the recent advancement and regional studies.
b) To assess the geomorphic characteristics to compare sediment connectivity parameters between upland and lowland systems on the Brahmaputra River basin.
c) Evaluate the topographical dynamics at Brahmaputra's tributary (Teesta River) using global and UAV-SfM derived DEM products.

1.3 Study approach and thesis structure

This thesis presents an integrated approach of remote sensing and field-based investigation for assessing the morphodynamics, sediment dynamics, and topography in the understudied Brahmaputra River basin at multiscale. The multiscale analysis is significant in the Himalayan River basin management that highlights the importance of different geographical scales across a river basin and the linkage between upstream-to-downstream and downstream-to-upstream. The multiscale approaches considered in this study focused on the entire river basin (transboundary regions over Bangladesh, India, Bhutan, China, and surroundings, approximately 10^5~10^6 km^2), tributaries (Teesta, Torsa, and Manas Rivers, 10^3~10^4 km^2), and more local levels (10^0~10^2 km^2), hereby referred to as basin, sub-basin, and local scales, respectively. Although the magnitude and nature of the land surface processes or events/problems differ at different points along the scale, it is crucial to consider the multiscale approach in the Himalayan River's geomorphic studies, which can link the local scale processes to basin-scale processes for integrated river basin management in the Brahmaputra River. The global availability of NASADEM with the introduction of UAV-SfM techniques and different hydrological data makes the effective assessment of multiscale fluvial-geomorphology and sediment connectivity in diverse environments ranging from the

Himalayan to the Bay of Bengal. The overall study approach is conceptualized briefly in Fig. 1.2.

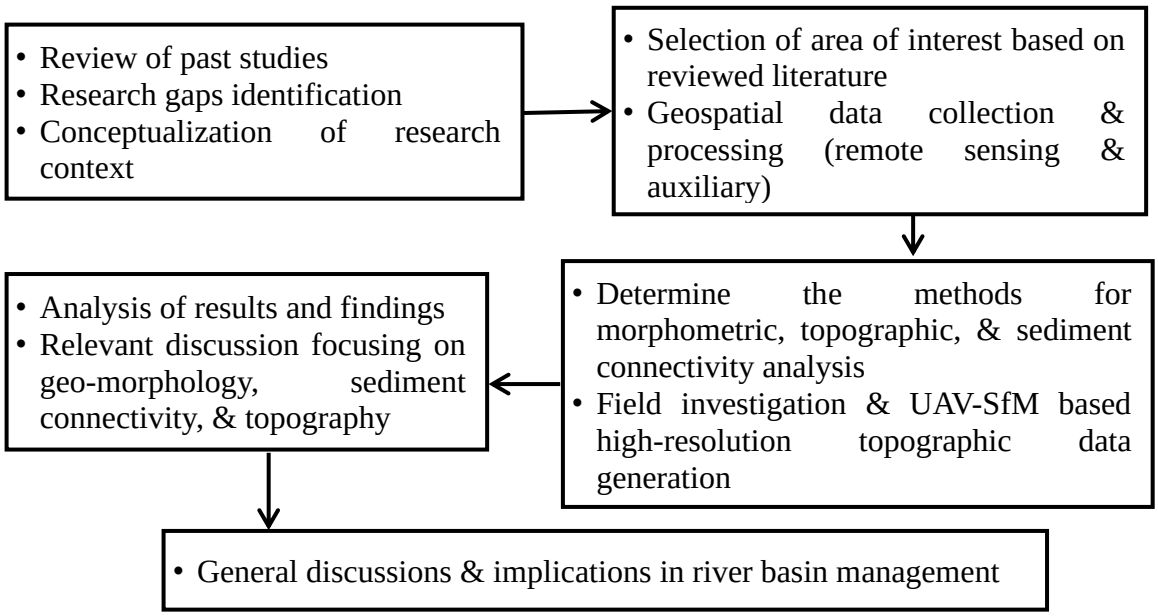

Fig. 1.2 Overall study approach.

Thesis structure: This thesis is structured as follows.

Chapter 2: Emphasize on geomorphological processes and their connectivity in hillslope, fluvial, and coastal areas in Bangladesh to find out the research gaps and way forwards for future studies (basin scale).

Chapter 3: Assessing the geomorphic characteristics to compare sediment connectivity parameters between upland and lowland systems in the Brahmaputra River basin (sub-basin scale).

Chapter 4: Describe the topographical dynamics based on global and UAV-SfM derived DEM products: A case study of transboundary Teesta River, Bangladesh (local scale).

Chapter 5: General discussion, describing the factors affecting multiscale geomorphic connectivity, importance of geomorphological studies, implications to river basin management, study limitations with way forwards for futher studies, and conclusions.

List of articles and conferences: This thesis is based on the following articles and conferences.

Articles:

- Faisal, B.M.R., Hayakawa, Y.S., 2023. Geomorphometric characterization and sediment connectivity of the middle Brahmaputra River basin. Geomorphology 429, 108665. https://doi.org/10.1016/j.geomorph.2023.108665
- Faisal, B.M.R., Hayakawa, Y.S., 2022. Geomorphological processes and their connectivity in hillslope, fluvial, and coastal areas in Bangladesh: A review. Progress in Earth and Planetary Science 9, 41. https://doi.org/10.1186/s40645-022-00500-8
- Faisal, B.M.R., Hayakawa, Y.S., Topographical dynamics based on global and UAV-SfM derived DEM products: A case study of transboundary Teesta River, Bangladesh. (Under review at international journal).

Conferences:

- B. M. Refat Faisal (Graduate student, Hokkaido University); Yuichi S. Hayakawa (Hokkaido University), Geomorphometric characterization and sediment connectivity in mountainous river basin: A study on Brahmaputra. International Sustainable Mountain Development and Tourism Conference. [2023/10/06-08, Phokhara, Nepal/Online].
- B. M. Refat Faisal (Graduate student, Hokkaido University); Yuichi S. Hayakawa (Hokkaido University), Topographical dynamics based on global and UAV-SfM derived DEM products: A case study of transboundary Teesta River, Bangladesh. Japan Geoscience Union Meeting 2023, HTT13-P02. [2023/05/21-26, Makuhari/Online]
- B. M. Refat Faisal (Graduate student, Hokkaido University); Yuichi S. Hayakawa (Hokkaido University); Tetsuya Takagi (JALUX Inc.), Topographic characterization of the middle Brahmaputra River basins. Abstracts, Japanese Geomorphological Union 2022 Fall Meeting, P05-SS. [2022/11/05-07, Sapporo/Online]
- B. M. Refat Faisal (Graduate student, Hokkaido University), Yuichi S. Hayakawa (Hokkaido University), Geomorphometric characterization of the middle Brahmaputra River basins. Abstracts, Japanese Geomorphological Union 2021 Autumn Meeting, P-02. [2021/12/04-05, Online].

Chapter 2

Geomorphological processes and their connectivity in hillslope, fluvial, and coastal areas in Bangladesh: A review

2.1 Introduction

The Ganges–Brahmaputra–Meghna (GBM) river system is the largest delta of the world, where the Brahmaputra is known as Jamuna River, and the confluence of Ganges and Jamuna River is known as Padma River (Sarker et al., 2014). The Meghna River (upper and lower Meghna) confluences with the Padma River at its upstream and downstream. The braided Jamuna, the meandering Ganges, the anastomosing upper Meghna, and the anabranching lower Meghna make the river planform more diverse and complicated (Sarker et al., 2014). Geographically, the major part of the GBM basin in Bangladesh is entirely lowland, which is surrounded by India on the west, the Myanmar on the east, Shillong Plateau on the north, and Bay of Bengal on the south (Steckler et al., 2010) (Fig. 2.1). However, most of the rivers of Bangladesh (405 rivers including 57 transboundary rivers) are originated from the Himalayan and East Indian mountains and flow through Bangladesh into the Bay of Bengal (BWDB, 2014; Dewan et al., 2017). In terms of mean annual discharge, the GBM river system is second only to the Amazon, and a major portion of this flow occurs in the summer season with immense monsoon rainfall, which causes widespread flooding in these drainage areas (Steckler et al., 2010). Therefore, the geomorphological features are changing very rapidly in downstream Bangladesh despite its remarkably flat topography due to the complex upstream fluvial process (Takagi et al., 2005). These fluvial dynamics are controlled by natural processes (discharge flow, sediment transport, debris flow, channel migration and floodplain erosion, and accretion) (Langat et al., 2019) and anthropogenic processes (dam constructions, river bank engineering, and land-use changes) (Surian and Rinaldi, 2003; Wellmeyer et al., 2005; Ortega et al., 2014). The geomorphic research describes both these natural and anthropogenic factors to explain the surface process, shape and dimension, spatiotemporal variability, and evolutionary characteristics of landscapes and landforms (Pareta and Pareta, 2015).

However, apart from Himalayan tributaries, numbers of tributaries from upland source areas are joining the Ganges–Brahmaputra (GB) river system and it also hosts a large

number of floodplain wetland and lakes (Singh et al., 2021). Furthermore, the geomorphic diversity of river formation and processes in the Himalayan foreland and hinterland are demonstrated by the climatic diversity along the strike of the Himalaya (Sinha, 2004). Because there is a close relationship among geomorphology, river engineering, hydrometeorology, and environment, the geomorphological study of the large Ganges–Brahmaputra River system is highly important to understand the process–form relationship of fluvial systems and landscape diversity. Also, an understanding of large GB river systems is critical as they support large human populations, where Ganges and Brahmaputra support a population of 400 million (Jain et al., 2012) and 83 million people (about 41% residents in Bangladesh), respectively (Mahanta et al., 2014). However, despite the enormity of the Ganges–Brahmaputra fluvial system and the general advancements in recent fluvial geomorphological studies (Oguchi et al., 2013, 2022), the hydro-geomorphic information in GBM is somewhat restricted (Ray et al., 2015; Fischer et al., 2017) and research availability has been fragmented at its downstream areas. On the other hand, significant research regarding the Ganges–Brahmaputra River hydrology, geomorphology, and sedimentology had been carried out by several researchers in India (Jain et al., 2012), covering the upper part of the Ganges–Brahmaputra basin. However, the integration of geomorphic and hydrological studies in the upstream and downstream reaches of the GBM basin has been limited.

Moreover, in the context of Bangladesh, which hosts two most diverse Ganges–Brahmaputra basins, not many studies on fluvial geomorphology and sediment dynamics have been conducted so for. Geomorphic research is still in the nascent phase in Bangladesh and previously studied by only a few researchers (Coleman, 1969; Umitsu, 1985, 1987, 1993; Best and Ashworth, 1997; Allison et al., 1998; Ashworth et al., 2000; Islam et al., 2001; Takagi et al., 2007; Goodbred et al., 2014; Brammer, 2014; Sarker et al., 2014; Dewan et al., 2017) focusing on channel diversion, erosion and accretion, sediment deposition, and few hydro-geomorphic systems. Earlier, Takagi et al. (2005) reviewed the geomorphological and geological researches of Bangladesh and tried to reflect some of the geomorphic research gap and realities and mentioned the limited scientific researchers. However, as discussed later, current geomorphic researches in downstream Bangladesh are mostly conducted at a small scale within the country. The insights obtained at small-scale studies are not sufficient to understand the large-scale landscape process (Baker, 1988; Lane and Richards, 1997; Jain et al., 2012). Moreover, the hydrological event that occurs in the upper part of a river basin may have a direct influence on downstream from a few to many hundreds of kilometers away

(Nepal, 2012; Nepal et al., 2014). Hence, the understanding of upstream–downstream linkages in hydrological processes of Ganges–Brahmaputra River basin is essential for water resources management of downstream Bangladesh.

Besides, there is an imperative need among the scientific community to understand better the geomorphic consequences of ongoing global environmental changes (Lane, 2013; Knight and Harrison, 2014; Harrison et al., 2019), where the mountainous landscapes including the diverse fluvial system deserve particular attention (Cienciala, 2021). These realizations highlighted the importance of geomorphic analysis at the cross-country scales because the fluvial system, including sediment connectivity and sediment dynamics, of downstream Bangladesh is mostly influenced by the upper and middle Ganges–Brahmaputra system (Subramanian and Ramanathan, 1996; Sinha, 2004; Singh, 2007). Therefore, there is a need to review the previous geomorphic studies with a holistic view of dealing with fluvial geomorphic research in downstream the deposition zone (Bangladesh) connecting the upstream Ganges–Brahmaputra basin. This sort of review study is required to find out the geomorphic research gap, to improve the understanding of geomorphic processes in complex downstream areas, and to unearth the flood-prone deltaic landscape connected with morphodynamics, hydrology, and sediment flux in the upper basins. In addition, an understanding of upstream dominated processes or events or sediment transport dynamics that shape the particular landform development of downstream areas is highly important in geomorphic science (Howard, 1994; Whipple and Tucker, 1999; Stark and Stark, 2001). Therefore, this study may help us answer the questions in geomorphology, how the magnitude and frequency of upstream event plays a more influential role in developing geomorphic characteristics of the downstream (Wolman and Miller, 1960; Rinaldo et al., 1991; Pelletier, 2003).

In such a context, a large part of this work focuses on reviewing the previous geomorphic research in downstream Bangladesh. Also, this article attempts to review some of the major aspects of the Ganges–Brahmaputra fluvial system that evaluates their relevance to understand the fluvial system of downstream Bangladesh taking into consideration the geomorphological diversity of the upper Ganges–Brahmaputra River system. Some of the potential implications for future geomorphic researches concerning downstream flat alluvial Bangladesh are also discussed here that can help minimize the multitude of river basin management problems. Therefore, we present an inclusive review of the Ganges–Brahmaputra fluvial system, starting from the mountainous catchments to the deltaic plain

concerning vast alluvial plain land in Bangladesh. In summary, the aim of this article is (a) to review the previous geomorphological research in Bangladesh with a focus on different geomorphic features, including landslides in hilly area, fluvial channel dynamics, plain land features, and coastal dynamics; (b) to critically analyze the fluvial dynamics and sediment pathways of active plain land Bangladesh that governs by the upper Ganges–Brahmaputra River system; and (c) to highlight some potential future geomorphic research for better understanding of the downstream geomorphic process in Bangladesh considering the recent advancement and regional studies.

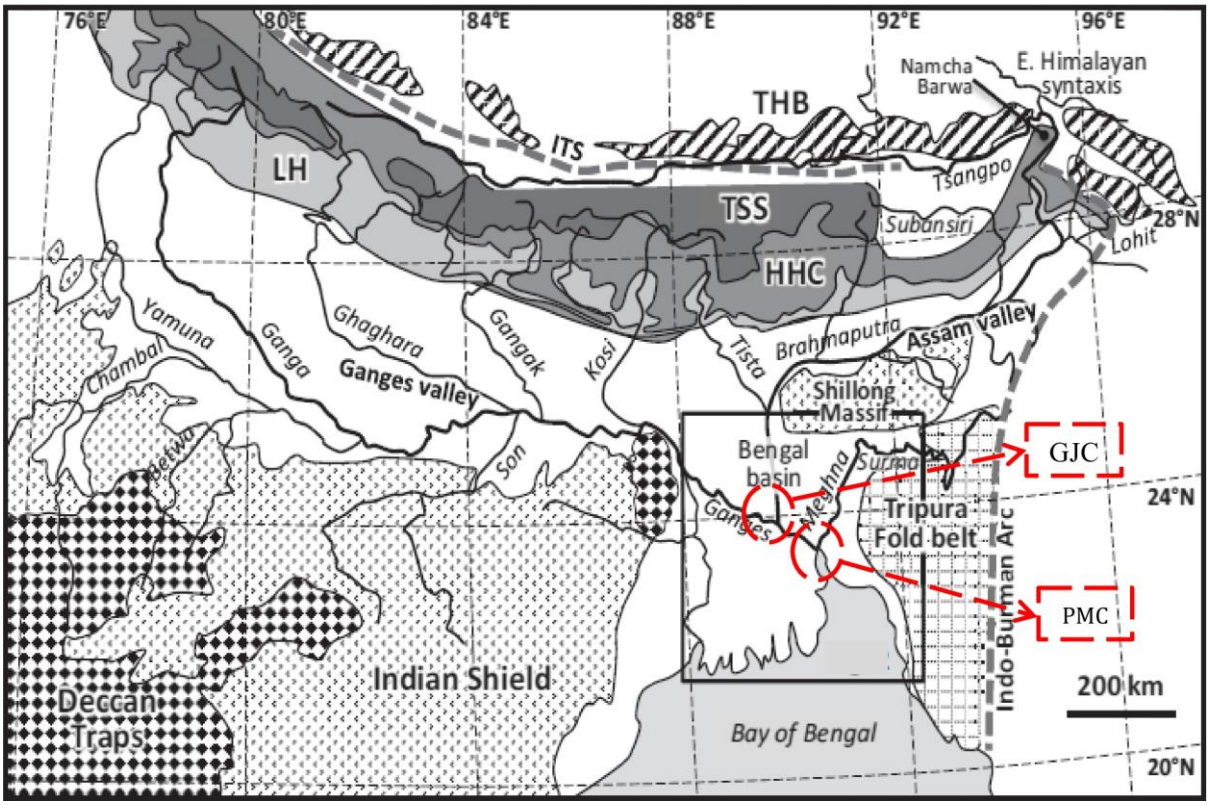

Fig. 2.1 Map of the Ganges–Brahmaputra–Meghna river basin representing major tributaries and sediment sources including Trans-Himalayan batholiths (THB), Tethyan Sedimentary Series (TSS), High Himalayan Crystalline Sequence (HHC), Lesser Himalayas (LH), Indus-Tsangpo suture (ITS) (after Goodbred et al., 2014). The rectangle focuses on the Bengal basin that influences the river migration and sediment dispersal across the Ganges–Brahmaputra–Meghna delta. GJC and PMC indicate the Ganges–Jamuna confluence and Padma–Meghna confluence, respectively (Gazi et al., 2020a).

2.2 Main text

2.2.1 Major geomorphic features in Bangladesh

Regarding the major geomorphic characteristics in Bangladesh, here the author reviews geomorphic research previously performed in the area at different scales, focusing on hillslopes, fluvial dynamics, plain land formation, and coastal dynamics.

2.2.1.1 Hilly area

A large variety of erosional and depositional features may be formed in mountainous and hillslope areas. The hilly or mountainous terrain is mainly found in the north and southeastern part of Bangladesh (18% of the total country area) and is mostly covered with dense vegetation (Rabby and Li, 2018). The hilly regions of southeast Bangladesh (Chittagong Hill Tracts) are underlain by Surma and Tipam rocks (Brammer, 1996), and the soil formation is complex and unstable (Islam et al., 2017). The young rock formation contains feldspars vulnerable to weathering (Ahmed et al., 2014), which make these regions more susceptible to landslide risks during heavy rainfall (> 40 mm/day) in the monsoon (June to October) season within a short period (2–7 days) (Khan et al., 2012; Sarker and Rashid, 2013a, b). In Chittagong Hill Tract (CHT) region, rainfall-induced landslides (Khan et al., 2012) are increasing and causing death and damage to property (Ahmed and Rubel, 2013; Rabby and Li, 2019; Rabby et al., 2020).

Furthermore, the southeastern hilly region of Bangladesh is regarded as a high-risk zone for flash floods and landslide events associated with intense rainfalls (Ahmed and Dewan, 2017; Rahman et al., 2017). Also, flash flood vulnerability studies have been carried out by Rahman and Salehin (2013) and Sarker and Rashid (2013a, b), but detailed watershed morphometric analysis has not been studied. Meanwhile, Adnan et al. (2019) assessed the flash flood susceptibility of the Karnaphuli and Sangu river basins in the southwest region with DEM-derived twenty-two morphometric parameters. The analysis revealed that more than 80% of the total area is susceptible to flash floods with moderate to a very high level of severity. On the other hand, morphometric analysis of major watersheds in the northwestern Bangladesh (Barind tract) has been carried out by Rahman et al. (2017). They found a dendritic drainage pattern with 1st to 6th stream order, moderate to a flat slope, moderate drainage density, semipermeable soil lithology, and homogenous soil texture. Similarly, small-scale morphometric analysis has been conducted by Jahan et al. (2018) in the Atrai–Sib River Basin (northern part of Bangladesh).

Moreover, the landslide scenario of this hilly region is aggravated by increased population, rapid urbanization, indiscriminate hill cutting and deforestation, and inappropriate land-use practices (Sarker and Rashid, 2013a, b; BUET-JIDPUS, 2015). Rabby and Li (2020) identified 730 landslides in Chittagong hilly area from January 2001 to March 2017 based on Google Earth images, field mapping, and literature search. The literature works on landslide

event were collected from local newspapers, Comprehensive Disaster Management Program (CDMP) phase II-2012, records of the disaster management department, and road and highway department of the people's republic of Bangladesh. However, comprehensive identification and response to the landslide occurrence in this remote hilly area are still difficult due to its inaccessibility covered by dense forest, faster vegetation regrowth after landslide, cloudy Landsat imageries, and unavailability of airborne light detection and ranging (LiDAR) images, aerial photographs, and unmanned aerial system (UAS)-based images (Rabby and Li, 2018).

Besides, Ahmed (2015) prepared landslide susceptibility mapping in one of the hilly areas of southeastern Bangladesh (Cox's Bazar) applying artificial hierarchy process (AHP), weighted linear combination (WLC), logistic regression, and multiple logistic regression techniques. Almost similar studies also have been carried out by Ahmed and Dewan (2017) and Rahman et al. (2017) in the Chittagong area of Bangladesh. Also, Rabby et al. (2020) evaluated the performance of several digital elevation models (DEMs) including global digital elevation models (GDEM) (30 m resolution), Shuttle Radar Topographic Mission (SRTM) (30–90 m), the Phased Array type L-band Synthetic Aperture Radar (PALSAR-DEM) (12.5 m) and Survey of Bangladesh (SoB) DEM (25 m) (generated from spot height) for landslide susceptibility mapping in one of the CHT region (Rangamati district) of Bangladesh. The comparative usability study of different DEMs concludes that except SoB-DEM (only source of local DEM in Bangladesh), all other global DEMs are suitable for the landslide suitability mapping in Bangladesh. The applicability of those landslide susceptibility maps to local areas in both scientific and social contexts is, however, still limited due partly to their coarse-resolution and the unavailability of field-based work on the landslides.

2.2.2 Fluvial features

2.2.2.1 Channel dynamics

In geomorphological studies, river channel formation and dynamics are the foremost topics (Petts, 1995). While the fluvial processes in Bangladesh connecting upstream areas are discussed in more detail in Sect. 2.3.1, here the author summarizes the overview of fluvial geomorphological studies in Bangladesh. The most comprehensive remote-sensing-based geomorphological study in Bangladesh about the Brahmaputra River channel has been

conducted by Takagi et al. (2007) over the time period of 1967–2002. They separated the Brahmaputra River into four phases, namely: (a) the late 1960s to early 1970s; (b) the mid-1970s to early 1980s; (c) the mid-1980s to early 1990s; and d) the mid-1990s to early 2000s. Phase (a) and phase (b) have been regarded as transitional phases with more complex conditions, which trigger frequent large floods and may significantly change the river system. Also, a state of dynamic equilibrium has been observed from the mid-1990s to the early 2000s due to small spatial variations both in the braided belt width and in the channel width. However, based on the study of the historical evolution of the Brahmaputra–Jamuna by Coleman (1969), Sarker et al. (2014) summarized that the rate of channel (Brahmaputra–Jamuna) widening (~ 152 my^{-1}) was high but the channel migration was effectively zero in last four decades (1970–2010). On the other hand, the Ganges catchment (Ganges and Padma) in Bangladesh annually receives 1200 mm of average rainfall (Sulser et al., 2010), which is one of the factors of the recurring large magnitude of seasonal floods during the monsoon period (July–October) (Gupta, 1995; Kale, 2003; Sharma, 2005). The study of Dewan et al. (2017) concludes that the Padma (Aricha–Chandpur) experienced a total of 183 km^2 of erosion (left bank 155 km^2 and right bank 28 km^2) which led to the occurrence of many extreme floods since 1973. Furthermore, Islam (2016) analyzed the Landsat MSS 1977 (9 Feb), Landsat TM 1989 (11 Nov), and Landsat ETM+ 2000 (17 Nov) data and assessed the fluvial channel dynamics of Padma River in Northwestern Bangladesh. This study showed a remarkable change in the position of the riverbank, river channel, as well as bars, along with the geometry and morphology over 23 years (1977 to 2000). Besides, the findings suggest that the bankline of Padma River is not stable and in recent decades it can be migrated continuously toward westward (Shamsuzzaman et al., 2005; Talukder and Islam, 2006).

The morphodynamics of two major confluences of Bangladesh Rivers, namely the Padma–Meghna confluence (PMC) and the Ganges–Jamuna confluence (GJC), have been studied recently by Gazi et al. (2020a) (Fig. 2.1). This study found that GJC moved to southwest direction and PMC moved to northwest direction over the period (1980–2019), but these directions of confluence migration were reversed before 1980s. At the same time, the width of PMC shows variation from 6.87 to 6.98 km, whereas the GJC confluence shows a decreasing trend of 8.10 to 2.80 km over the period (1972–2019). Further, Akhter et al. (2019) explore spatiotemporal changes of Teesta River channel morphology and forecast midline channel shifting in the reach over the period (1972–2017) through multi-date Landsat imageries (MSS/TM/ETM+/OLI) and SRTM-DEM (30 m) data and autoregressive integrated

moving average (ARIMA) model. This study found that, like other river systems of Bangladesh, the Teesta River width is becoming narrow in recent times than earlier decades (Takagi et al., 2007; Sarker et al., 2014; Bhuiyan et al., 2015; Dewan et al., 2017). Besides, over the period (1972 to 2010) and (2010 to 2017), the Teesta channel is shifting toward the right side (0.34 km/year) and left side (− 0.14 km/year), respectively. However, channel shifting rates of Teesta River are mostly affected by the temporally changing amount of sedimentation, but the spatial changes are more controlled by the differences in riverbank conditions. Further, the ARIMA model predicts the rightward direction of maximum midline channel shifting for 2017 to 2024 and leftward midline channel shifting between 2024 and 2031 because of reduced water flow at downstream of Teesta River, resulting from the construction of dams and embankments at upstream, which restricted the water flow and increased the number of bars (Ghosh, 2014; Khan and Islam, 2015).

2.2.2.2 Sediment dynamics

The GBM river system of Bangladesh is highly prone to channel shifting, erosion, accretion, and riverine island (locally Char) development due to high sediment transport or movement process in the monsoon season (Sarker et al., 2011). However, the sediment budget of the large braided river (Jamuna) largely depends on the river's flow path along the floodplain, suspended sediment transport regime, and average sedimentation rates (Allison et al., 1998; Takagi et al., 2007). In the Ganges and Brahmaputra River, 78% of the total suspended load is from the Brahmaputra River (Islam et al., 2001), where the siltation rate has been increased in recent years (Khalil et al., 1995). Like fluvial processes, the nature of sediment dispersal in the GBM catchment is also diverse but not fully understood or studied. The sediment dispersal in GBM catchments connecting the upstream catchments to the downstream reaches in Bangladesh is further discussed based on the existing literature in Sect. 2.3.2.

Examples of studies of fluvial sediment transport include the work of Islam et al. (2001), who used advanced very-high-resolution radiometer (AVHRR) images of 1996 and Landsat images of 1991. This work was designed to understand the seasonal and spatial variations of suspended sediment in the Ganges and Brahmaputra Rivers in Bangladesh for both high-discharge periods (June to October) and low-discharge periods (November to May). They found higher suspended sediment concentration (SSC) (1150 to 1375 mg/l) in the Ganges than the Brahmaputra (1000 to 1275 mg/l) in high-discharge period, whereas reverse scenario has been observed for low-discharge period. The significant fluctuations in SSC and

suspended sediment load along the Ganges and Brahmaputra River courses have been attributed to riverbank erosion and accretion, as well as the aggradation of riverbeds.

Similarly, Islam et al. (2002) examined the distribution of suspended sediment through Landsat images of 1989 and 1991 in the coastal sea around the Ganges–Brahmaputra River mouth, showing that transportation and deposition of suspended sediments experience seasonal variations (SSC varies from 200 to 700 mg/l during low-discharge period and 1300–1500 mg/l during high-discharge period). They also found that the suspended sediments are accumulated on the shallow shelf (between 5 to 10 m water depths) in the low-discharge period, and on the mid-shelf (between 10 to 75 m water depths) in the high-discharge period with an average rate of 2 cm/year. However, an empirical (exponential) relationship has been found between the gradual settle down of suspended sediments in the coastal area and its lateral distance from the turbidity maximum. Moreover, annual pluvial flooding during the monsoon period (Warner et al., 2018) due to short or prolonged precipitation (Falconer et al. 2009) in the southwestern coastal region of Bangladesh has become more intense and severe because of siltation in riverbeds and encroachment of drainage channels. This southwestern coastal region mainly comprises Ganges River floodplains, Ganges tidal floodplain, and old floodplain basins (Brammer, 2014). Consequently, Adnan et al. (2020) developed a sediment deposition model for southwestern coastal region of Bangladesh using flood data from Bangladesh Water Development Board (BWDB), precipitation data (1948–2012) from Bangladesh Meteorological Department, and DEM data from Advanced Land Observing Satellite (ALOS). This model predicts that the increase in land elevation could be up to 1.4 m in every 5 years, which would alleviate land subsidence and modify several geomorphological factors such as curvature, slope, aspect, and Stream Power Index (SPI). SPI is a measure of the erosive power of surface runoff, which is considered as one of the factors that determine the river channel erosion, basin-scale variability in channel processes, morphology, and sediment transport potentiality (Moore et al., 1991; Pei et al., 2010; Khosravi et al., 2016; Kaushal et al., 2020). This study reveals that the implementation of tidal river management (TRM) in southwestern Bangladesh could potentially improve the physical condition of the natural drainage basin by reducing the value of SPI, which reduces the erosion potential of the surface. Besides, the limitations of the sediment deposition model have been mentioned in this study with available experimental sedimentation data.

2.2.2.3 River bank management

Generally, floods often occur due to extreme condition of climatic triggers, and their effects are also conditioned by hydrological, geomorphological, and anthropogenic factors (Adnan et al., 2020). Bangladesh is prone to multiple flood hazards due to the frequent attacks of cyclones and the physiographic settings of large plain land (Rahman and Salehin, 2013). Consequently, riverbank erosion and accretion is a very common and dynamic process in the fluvial system of Bangladesh (Islam et al., 2014). A very recent study by Rashid et al. (2021) revealed that due to the route change, the Brahmaputra–Meghna in Bangladesh grabbed ~ 2817 km^2 of invaluable land resources and a newly developed ~ 4563 km^2 from 1971 to 2014. The National Plan for Disaster Management (NPDM) describes that the Padma River is quite sensitive to erosion and accretion processes, significantly affecting the society and economy to hinder the further development along the riverbank areas (Islam, 2000; NPDM, 2006). Billah (2018) studied the Padma River erosion and accretion scenario from 1975 to 2015, finding that the total amount of riverbank erosion in the 40-year period was 49,951 ha of land (rate of 1249 hay^{-1}) and accretion was 83,333 ha of land (rate of 2083 ha y^{-1}), also causing the riverbank shift. Furthermore, Gazi et al. (2020b) studied the erosion–accretion of Gorai–Madhumati River (a tributary of Ganges River), finding that the total river bank erosion of 80.84 km^2 and accretion of 82.9 km^2 over the years (1972–2018). The analysis also revealed that Gorai–Madhumati River experienced extreme sedimentation due to reduction in water discharge which consequently causes numerous problems in the river basin areas, and without attention and proper river management it will no longer exist with the present flowing condition. Also, the fluvial landform characterization studies of Biswas et al. (2021) depict that erosion and accretion of Madhumati River Basin (source of freshwater in southwestern hydrological region of Bangladesh) have increased during the flooding period of 1988 and 1998, and the basin boundary shifted toward east, which impacted negatively on floodplain resources, agricultural resources, and biodiversity.

A large number of people live in floodplains of Bangladesh with vulnerability to floods and river erosion, and the number of causalities due to floods has become higher than the other natural disasters (Tingsanchali and Karim, 2005). In this connection, Hoque et al. (2011) evaluated the RADARSAT images of 2004 (June 5, July 24, and Sep 9) and Landsat images of 2000 (Feb 28 and Oct 25) as well as ground data for flood monitoring and mapping in the northeastern part of Bangladesh, concluding that this region is more prone to floods

than the other parts of Bangladesh. They also concluded that RADARSAT data can clarify questions related to the mapping of inundation areas more clearly and quickly than the Landsat imageries, where Landsat is often unavailable due to the cloudiness in monsoon season over Bangladesh.

2.2.3 Plain land features

The northwestern part of Bangladesh has been divided geomorphologically into a) uplifted blocks of terraced land called as Barind Tract, b) Himalayan piedmont plains, c) alluvial lowland along the Brahmaputra–Jamuna River, and d) alluvial lowland along the Ganges River (Kubo, 1993). On the other hand, the southwestern portion of the basin is formed by the deposition of the mainstream Ganges River and its numerous tributaries and distributaries (Alam et al., 2003; Ravenscroft, 2003). Therefore, for understanding the landscape development, a comprehensive geomorphic mapping is required in plain land, which is still missing mostly for Bangladesh (Oya, 1979; Mahmud et al., 2017). Nevertheless, Mahmud et al. (2017) identified major geomorphic units of the western Ganges delta and divided the geomorphic features into fluvial deltaic plain (FDP) and fluvio-tidal deltaic plain (FTDP). Also, this study depicts that elevated concentration of arsenic (As) occurs mainly in deeper FDP due to the absence of permeable layer between shallow and deep aquifer, whereas chloride concentration shows an increasing trend in groundwater from FDP to FTDP (north to south). Furthermore, geomorphological maps of Dhaka city have been prepared by Kamal and Midorikawa (2004) and Karim et al. (2019). In the northern district (Pabna) of Bangladesh, Islam et al. (2015a, b) also identified the different geomorphic units, including active channels, abandoned channels, natural levees, flood plains, flood basins, and lateral channel bars.

However, morphometric analyses are a prerequisite for delineation of potential watershed (Aher et al., 2014) and water management aspects (Malik et al., 2019) where the hydrological information is unavailable. In this regard, Arefin and Alam (2020) focused on morphometric analysis for water resource management in the Dhaka city area. Their study suggests that surface water can be extracted from a fifth-order stream and can be supplied to the domestic area after water quality treatment. Furthermore, Arefin (2020a) identified the groundwater potential zones at the drought-prone Plio-Pleistocene highland in the northern part of Bangladesh using WLC and GIS-based multi-criteria evaluations for class normalization using Saaty's AHP (Saaty, 1977). This study determines clay soil regions with

high slopes and roughness as low groundwater potential zones in this area. Similarly, groundwater potentiality identification and prediction studies have been conducted in two metropolitan cities of Dhaka and Chittagong by Arefin (2020b) and Akter et al. (2020), respectively.

2.2.4 Coastal features

As a transitional zone between land and water, the coastal zone is one of the most dynamic and unstable geomorphic units in Bangladesh (Minar et al., 2013; Brammer, 2014). The coastal environment is governed by terrestrial and marine forces (Kabir et al., 2020), and the coastal vulnerability of Bangladesh is largely controlled by the geomorphic processes of the GBM river basins (Islam et al., 2015a, b). Also, the external forces, including water-logging, soil erosion, salinity intrusions, sea level rise, cyclone, storm surge, and tsunami, adversely affect the morphological settings of the coastal environment and negatively impact coastal area development activities (CZPo, 2005; Barua et al., 2010). Ahmed et al. (2018) focused on land dynamics of the entire coastal zone (western, central, and eastern) and determined a net gain of 237 km^2 (annual average of 7.9 km^2) of land from 1985 to 2015. This study also revealed that both erosion and accretion rates are higher in the central zone compared to the western and the eastern zones of the coastal area. Shibly and Takewaka (2012) studied the morphological changes along the western–central coast in 1989–2010, which obtains a large volume of discharge from the GBM river system through Sibsha, Pasur, and Baleswar River (Allison et al., 2003; Iftekhar and Islam, 2004). They found that the western–central shoreline in 2000–2010 was more stable than its previous decade (1989–2000). They also found that the mangrove-covered area is changing more significantly compared to the flat sandy beach, in contrast to the thought that mangrove stabilizes the land. Also, Alam and Uddin (2013) mentioned that, over the last 34 years (1977–2010), the coastal areas and the offshore Island of Bangladesh gained 139 km^2 of land from continuous erosion and accretion process. However, based on the Coastal Vulnerability Index (CVI) methods (Thieler and Hammar-Klose, 1999; Doukakis, 2005; Diez et al., 2007): Islam et al. (2015a, b) showed that the western coast of Char Fasson and the northern and southwestern coast of Bhola Island (Bhola Sadar) are the most vulnerable coastal regions of Bangladesh. Likewise, Miah et al. (2020) also applied CVI (Szlafsztein and Sterr, 2007, 2010; Mahapatra et al., 2014) by combining both the Physical Vulnerability Index and Social Vulnerability Index for the southeastern coast (Chittagong district) of Bangladesh. This study revealed 43% of the total southeastern

coastal area as highly vulnerable to flooding, storm surges, and cyclones, and the rural area is more prone to disaster impacts than the urban area.

2.3 Fluvial processes of GBM from upstream to downstream

As reviewed above, among various geomorphic features, fluvial processes are the major factor forming the landscape of Bangladesh. Here, the author reviews the studies on fluvial processes in further details. For the understanding of the downstream fluvial processes, fluvio-sediment dynamics of the upstream of GBM catchments are crucial and the author first summarizes river hydrology, river system, sediment transport, and discharge therein. Then, the author discusses geomorphic knowledge gap regarding the connectivity between the upstream and downstream domains and motivate larger-scale (beyond country scale) fluvial geomorphic studies.

2.3.1 Fluvial processes of Bangladesh in response to upstream GB

2.3.1.1 River hydrology

The annual flow pattern of large Himalayan (Ganges and Brahmaputra) and peninsular river (Mahanadi, Tapi, Kaveri, etc.) system suggests that these rivers are mostly characterized by non-monsoonal low or no flow (7–8 months), common monsoon flow (4–5 months), and occasional large magnitude flow during monsoon (Kale, 2005). Except for the catchment of the Brahmaputra in Tibet, all other drainage basins of the GBM River falls within the monsoonal regime of South and Southeast Asia, where rainfall pattern varies significantly, for example 743 mm/y in Tibetan Plateau, 1349 mm/y in Himalayan belt, and 2354 mm/y in floodplain (Immerzeel, 2008). Consequently, 80–95% of water discharge is observed in the Ganges and Brahmaputra during southwest monsoon (June to November) (Subramanian and Ramanathan, 1996), which led to a concurrent increase in sediment discharge (Mukherjee et al., 2009). For instance, the Ganges, Brahmaputra, and Meghna discharges 70,792,116 kg/s, over 70,792,116 kg/s and 14,158,423 kg/s, respectively, at lower reaches during monsoon flood season (Coleman, 1969). The monsoonal dominancy of annual discharge at the GB basin has also been mentioned in earlier studies of Kale (2005) and Mahanta et al. (2014). The monsoon-dominated rainfall and melting of the Himalayan snow from the upper GB river system cause a large magnitude of floods in downstream Bangladesh and therefore impact fluvial dynamics, but this process remains unclear or not studied (Fig. 2.2).

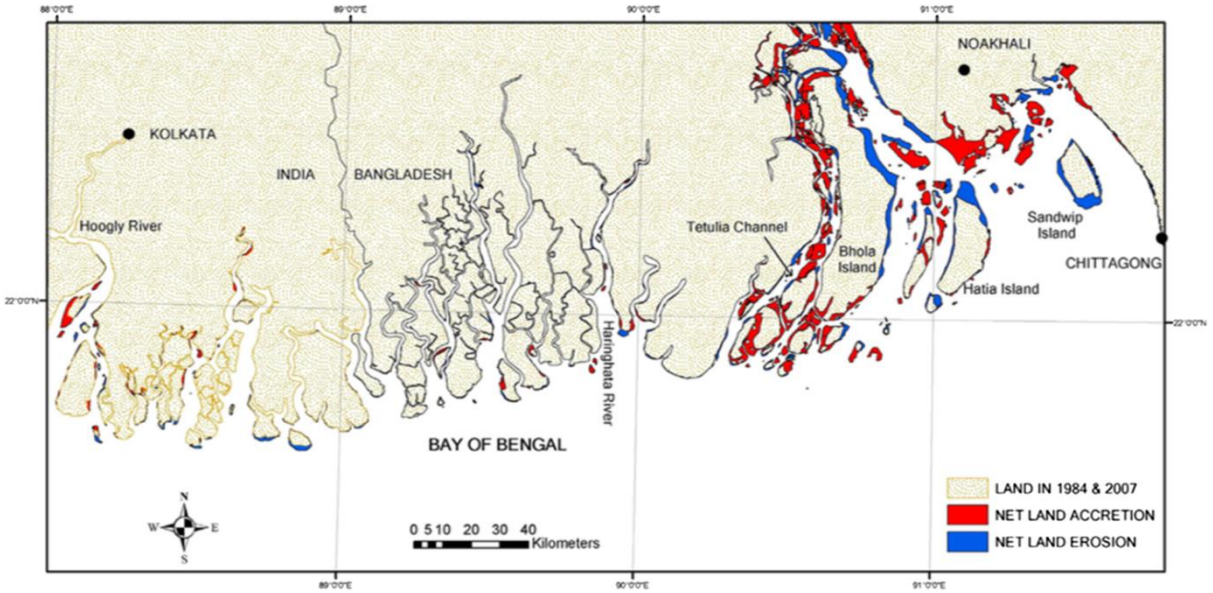

Fig. 2.2 Gains and losses of land on the Brahmaputra–Ganges–Meghna delta front in 1984–2007 (after Brammer 2014).

2.3.1.2 GBM River system dynamics

The drainage network map of Ganges–Brahmaputra–Meghna River (Fig. 2.3) shows that several tributaries of the Ganges (Yamuna, Ghagra, Gandak, Kosi, Chambal, Son, etc.) and the Brahmaputra are draining toward the Bay of Bengal (BoB) forming the major delta in the Bengal basin (Subramanian and Ramanathan, 1996; Sinha, 2004). The drainage development of the Ganges–Brahmaputra is generally derived from several factors such as tectonics and climatic patterns in the lowland area (Gupta, 1997; Friend et al., 1999). The longitudinal profile of the Ganges shows a sharp change in a gradient from steeper mountains to the gentler downstream plains (Fig. 2.4). The Brahmaputra River profile shows relatively low gradient in the upstream reach but drastically drops to the Assam plains (Gupta, 2007; Mahanta et al., 2014; Ray et al., 2015), resulting in abundant sediment deposition and formation of braided channels in the downstream reach (Pangare et al., 2021). Overall, the deviations of the Ganges–Brahmaputra River longitudinal profile are related to the Himalayan tectonics, water discharges, and sediment load characteristics of these basins (Seeber and Gornitz, 1983; Goswami, 1985; Gupta, 2007).

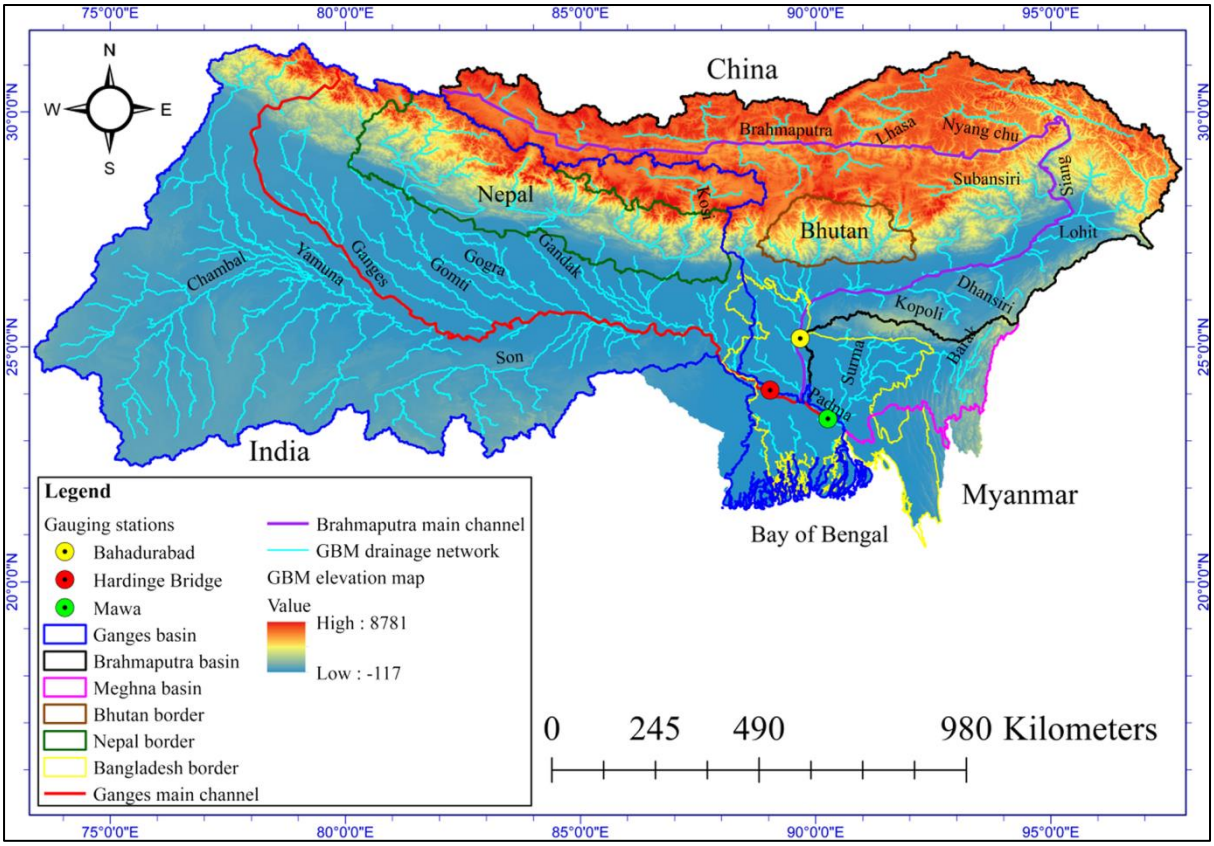

Fig. 2.3 GBM river basin elevation and drainage network. The elevation is prepared based on NASA-DEM (30 m resolution). The yellow, red, and green circles denote the in situ gauging stations for discharge estimations.

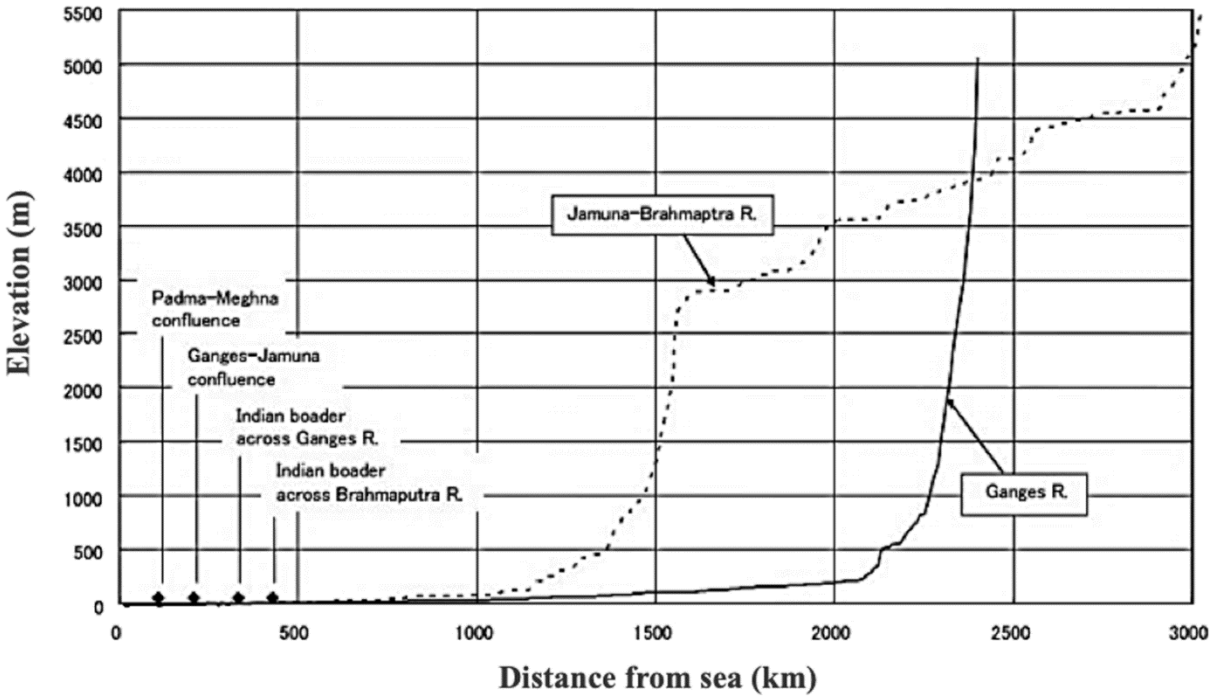

Fig. 2.4 Longitudinal profiles of Ganges–Brahmaputra–Meghna showing the entire flow path. Compiled from several sources (JICA report, 2005; Rahim et al., 2008).

In the southeastern center of the Tibetan Plateau, glaciers feed the Tsangpo-Brahmaputra River, and the increased rates of snow and glacial melt are likely to increase summer flows in the downstream Brahmaputra (Immerzeel, 2008; Bolch et al., 2010). Remarkably, the behavior of the Himalayan rivers (intense slope failure, landslide, and debris flow resulting from earthquake or intense rainfall) changes as they enter into the Indus–Ganga–Brahmaputra plain by shifting river course and changing morphology and bedforms due to heavy discharge and sediment load (Goswami, 1985; Sinha and Friend, 1994; Kale, 2005). For instance, the 1897 and 1950 earthquakes impacted Brahmaputra River sediment supply (bed load increases) and channel morphology in Assam, India (Coleman, 1969). An integrated drainage network has been formed at Brahmaputra River in India (Assam), where braided channels composed of mainly fine sand with various dimensions of rivers are developed, including straight, sinuous, meandering, tortuous, braided, anastomosing, anabranching, and reticulate features (Sarma, 2005). After crossing India (Assam), the Brahmaputra enters Bangladesh (about 47,000 km^2 of total 580,000 km^2 drainage basin) after traveling 220 km from the Indian border along the northern area (Kurigram) through Himalayan flows (Sarma, 2005; Sarker et al., 2014) and started to avulse linearly into the southward passage from the beginning of the eighteenth century (Bandyopadhyay et al., 2021). The bed scours depths of up to 40 m with a combined channel pattern of braided and anastomosing makes the Jamuna extremely dynamic and critical in devising engineering strategies, which implies the necessity of proper interpretation of ancient sediments and sea level changes (Bristow, 1987; Best and Ashworth, 1997; Thorne et al., 1993; Peters, 1993; Ashworth et al., 2000). In addition, the Jamuna is continually changing due to rapid rates of bar migration, bank erosion (up to 1 km per year), and shifting of braid belts (usually up to 5 km wide) (Klaassen and Masselink, 1992; Hossain, 1993; Ashworth and Lewin, 2012). Apart from natural processes, the Brahmaputra–Jamuna river is continuously facing various anthropogenic stressors like frequent land-use change, channelization, and regulations of normal river flow (Gupta et al., 2019) (i.e., Teesta barrage at its upstream, Jamuna multipurpose bridge, etc.), which emphasizes the implementation of sustainable solutions (Pradhan et al., 2021). For instance, the present site of the Jamuna multipurpose bridge was selected based on the geomorphological study conducted by Oya (1979).

On the other hand, draining from southern Tibetan uplift, the Ganges main channel had major movements in the historical period (after 1857), which caused highly irregular

shapes of valley (Hedge et al., 1989). The Ganges in India traverses through rugged mountains to flat alluvial plains, crossing various climatic zones with extensive erosional processes (Sinha, 2004; Jain et al., 2012). Nevertheless, regarding the source area (mountains catchments), alluvial plains, and deltaic plain, the Ganges river system shows unique fluvial processes where upstream flows control the landform development (Sinha, 2004). From two major branches of the Ganges (Bhagirathi and Padma in India), the Padma flows southeastward along the India–Bangladesh border and then takes eastward flow through Bangladesh (about 34,188 km^2 of total 980,000 km^2 drainage basin) to join with the Brahmaputra or Jamuna, forming the largest Ganges–Brahmaputra delta in the world (Islam et al., 1999). The bankline migration of the Ganges/Padma in Bangladesh shows that both the left and right banks do not follow the same direction (rightward) and are highly dependent on the localized factors and sedimentary features. Moreover, the Ganges is affected by human intervention, including the construction of Farakka Barrage by India in 1975 at 18 km upstream from the India–Bangladesh border, and is responsible for erosion both in India and in Bangladesh (Sarker, 2004; Rahman and Rahaman, 2018).

At the downstream GB basin, the Meghna has combined flow of Ganges–Brahmaputra/Jamuna into the Bay of Bengal, forming lower Bengal delta near Bangladesh coast. Hence, Bangladesh's coastal area has become more diverse and dynamic than it generally appears where rapid geomorphological changes are occurring in the Meghna estuary (Allison, 1998a, b; Brammer, 2014). The Meghna catchments experienced a net gain of 451 km^2 with a growth rate of 19.6 km^2/y over 1984–2007. Noticeably, despite gaining land in Meghna estuary, it showed considerable land losses along the east of Sandwip Island, north of Hatia, and northeast of Bhola Island, whereas erosion is gradually increasing eastward in the southwestern coast along the Hooghly estuary in India (Fig. 2.2) (Allison, 1998a, b; Brammer, 2014).

Fluvial studies of the upper Ganges in India had been thoroughly reviewed and updated by Sinha (2004) and Jain et al. (2012), respectively, whereas the fluvial research of the lower GBM (Bangladesh) regarding the causes of anomalous channel behavior, riverbank migration, erosion and accretion, sedimentation in tidal floodplains and coastal process is not fully investigated or conducted at small scale or has spare literature (as mentioned in Sect. 2.2).

2.3.2 Fluvial sediment dynamics of Bangladesh in response to upstream GB

2.3.2.1 GBM sediment production

The Trans-Himalayan batholiths, Tethyan Sedimentary Series, High Himalayan Crystalline Sequence, Lesser Himalayas, the Deccan Traps, the Shillong Massif, and Tripura fold belt are the source areas of GBM basin sediment, where the Indus-Tsangpo suture is connecting the sediment sources between Asia and India (Galy et al., 2010; Goodbred et al., 2014) (Fig. 2.1). Through the Indus-Tsangpo suture, the Brahmaputra traverse via Namcha Barwa syntaxis which encompasses only 4% of Brahmaputra's catchment but contributes about $45 \pm 15\%$ of sediment load (Singh and France-Lanord, 2002; Garzanti et al., 2004; Stewart et al., 2008; Goodbred et al., 2014). Beneath the syntaxis (drops for 2 km elevation), the Brahmaputra flows into low-lying Assam Valley and Himalayan foreland, where the rest of the load is supplied from the Himalayan tributaries (Goodbred et al., 2014).

On the other hand, after originating along the Tibetan border in north India, the Ganges headwater drained large areas of Himalayan front slope and its entry point to Bengal basin, the Ganges derived $90 \pm 5\%$ sediment load from the high Himalayan areas (Wasson, 2003; Singh et al., 2008; Lupker et al., 2012; Goodbred et al., 2014). Furthermore, the erosion intensity and sediment sources of upstream Himalayan Ganges catchments had been mapped in several studies (Narayan et al., 1983; Subramanian and Ramanathan, 1996; Sinha et al., 2002; Vaidyanathan et al., 2002). The different estimates of suspended sediment load from the GB river system have been documented in various studies and are summarized in Table 2.1. The sedimentation in the downstream reaches of the GB is related to the lowland fluvial processes and aggradation/degradational behavior of midstream alluvial reaches, which may create such variability of sediment load estimations among the researchers (Goswami, 1985; Islam et al., 1999; Jain et al., 2012). Nevertheless, the sediment load values comprise significant uncertainties, and exact values cannot be determined despite continuous decadal observations due to wide diurnal, seasonal, and annual variations in the sediment transport capacity of the GB Rivers (Subramanian and Ramanathan, 1996; Islam et al., 1999). The Brahmaputra has higher suspended load than the Ganges (Coleman, 1969; Milliman and Meade, 1983; Islam et al., 1999), because the eastern Himalayan range has higher precipitation and higher erosion rates than the western part (Galy and France-Lenord, 2001). Nevertheless, according to various estimates of sediment transport in several studies, it can be mentioned that the aggradation or degradation processes in the mid-

downstream alluvial reaches are quite complicated, causing significant variability of deposition rates in the downstream reaches (Jain et al., 2012).

Table 2.1 Estimates of suspended sediment load (million tons/year) of the Ganges–Brahmaputra River from different studies (updated after Islam et al., 1999)

Suspended sediment of Ganges river		Suspended sediment of Brahmaputra river	
(Mt/y)	(reference)	(Mt/y)	(reference)
375	NEDECO (1967)	750	NEDECO (1967)
1600	Holeman (1968)	800	Holeman (1968)
485	Coleman (1969)	617	Coleman (1969)
520	BWDB (1972)	541	BWDB (1972)
680	Milliman and Meade (1983)	1157	Milliman and Meade (1983)
328*	Abbas and Subramanian (1984)	402*	Goswami (1985)
729*	Abbas and Subramanian (1984)	710*	Subramanian (1987)
403	Singh (1988)	650	Hossain (1992)
316	Islam et al. (1999)	721	Islam et al. (1999)
550	CEGIS (2010)	590	CEGIS (2010)

* Estimated at Indian reach and rest of the estimate stands for Bangladesh.

NEDECO: The Netherlands Engineering Consultants Ltd.;

CEGIS: The Center for Environmental and Geographic Information Services.

2.3.2.2 Sediment discharge

The GBM river system in combination discharges 1×10^{12} m^3 of water and 1×10^{9} t of sediment per year to the Bay of Bengal (Goodbred and Kuehl, 1999; Wasson, 2003; Akter et al., 2016), of which 440×10^{6} t/y and 540×10^{6} t/y is contributed by Ganges and Brahmaputra, respectively (Milliman and Syvitski, 1992). According to Islam et al. (1999), the Ganges and the Brahmaputra in combination carried 1037 million tons/y of sediment into Bangladesh, of which about 525 million tons/y (51%) reaches the sea, 289 million tons/y (28%) deposited on land to balance the basin subsidence, and the remaining 223 million tons/y (21%) is deposited on the riverbeds. In turn, about 49% of the total sediment budget is trapped or deposited before the coastal region (Islam et al., 1999). This contributes to the intense monsoon flooding that facilitates the longer overbank flow (Ashworth and Lewin, 2012). The suspended sediment load estimation of the Ganges, Brahmaputra, and combined GB River was derived from the gauging data from the Hardinge Bridge, Bahadurabad, and Mawa stations (160 km downstream of Hardinge Bridge), respectively

(Fig. 2.3). The aggradation of the Brahmaputra River (> 14.7 mm/year) suggests that around 30–40% of GB sediment flux is estimated to be deposited in Bangladesh deltaic region before being transferred into the ocean (Goodbred and Kuehl, 1999; Jain et al., 2012). Moreover, the Ganges Riverbeds are aggrading about 3.9 cmy^{-1}, 2.5 times higher than the Brahmaputra in Bangladesh (Islam et al., 1999).

Recently, Dietrich et al. (2020) provides a first-order estimate of the yearly discharge of elements in the suspended sediment load to the BoB by the Ganges–Brahmaputra based on the dataset of Garzanti et al. (2011) that includes grain size, suspended sediment concentration, mineralogy, and element concentrations for suspended load samples collected at 0 to 24 m depths from locations in the Ganges (downstream of Hardinge Bridge), Brahmaputra (Sirajganj to Jamuna Bridge), and Padma (near Mawa) rivers during the monsoon season. This study shows that, on average, the GBM system transport 0.7×10^9 tons/y sediments to the BoB, contributing ~ 5% of the global riverine discharge of solid-phase elements. These elements are relatively enriched in Hf (hafnium), Zr (zirconium), Th (thorium), REEs (rare earth elements), Sn (tin), and Bi (bismuth), largely reflecting the nature of Himalayan source material. Moreover, it should be mentioned that future anthropogenic changes such as large-scale damming projects could significantly alter the delivery of sediment into the BoB, i.e., completion of the proposed National River Linking Project (NRLP) in India may reduce the annual suspended sediment load in the Ganges and Brahmaputra by 39–75% and 9–25%, respectively (Higgins et al., 2018). Also, future climate change scenarios projected the increase in sediment discharge by 34–37% in the Ganges and 52–60% in the Brahmaputra by the end of the twenty-first century (Darby et al., 2015).

Unfortunately, the quantitative sediment budget studies of Islam et al. (1999) and Dietrich et al. (2020) do not consider the sedimentation at lower Meghna (after Padma River between Mawa and the mouth of these rivers), which is naturally dynamic and also altered by various anthropogenic stressors. Also, the mechanism or process of sediment dispersal including sediment connectivity pattern from the erosion-dominated upper GB to the lower Meghna (tide and wave dominated) has not been fully mentioned or understood. At the lower GB, the main channel of the Meghna River, which is composed of braided and meandering channel sediments from the Brahmaputra/Jamuna and Ganges (Mukherjee et al., 2009), contributes significantly to the stratigraphy of main delta downstream (Goodbred et al., 2014). Furthermore, the downstream delta is also dominated by tidal wave rather than

runoff where Meghna–Surma (both fluvial and tidal) sediments contribute considerably (Islam et al., 2002). The sediment load of GBM delta is geochemically distinct, which makes this a potential location to unravel the dynamics of multiple fluvial systems interacting within a tectonically active basin (Goodbred et al., 2014; Li et al., 2020). Thus, the suspended load data, aggradation scenario, and projected sediment load estimation suggest disconnected or partially connected Himalayan foreland, where the eroded sediments from Himalayan could not reach the downstream sink area. Therefore, the geomorphic connectivity from the Himalayan to the BoB might be affected by sediment trapping before the mouth of these GBM rivers. Hence, the basin-wide integrated investigation from source to the mouth focusing on the lower Meghna reach may provide insights into quantifying annual sediment released by the GBM river system into the BoB. A conceptual diagram that shows the geomorphic connectivity impeded by sediment trapping within the GBM basin from the existing studies is presented in Fig. 2.5.

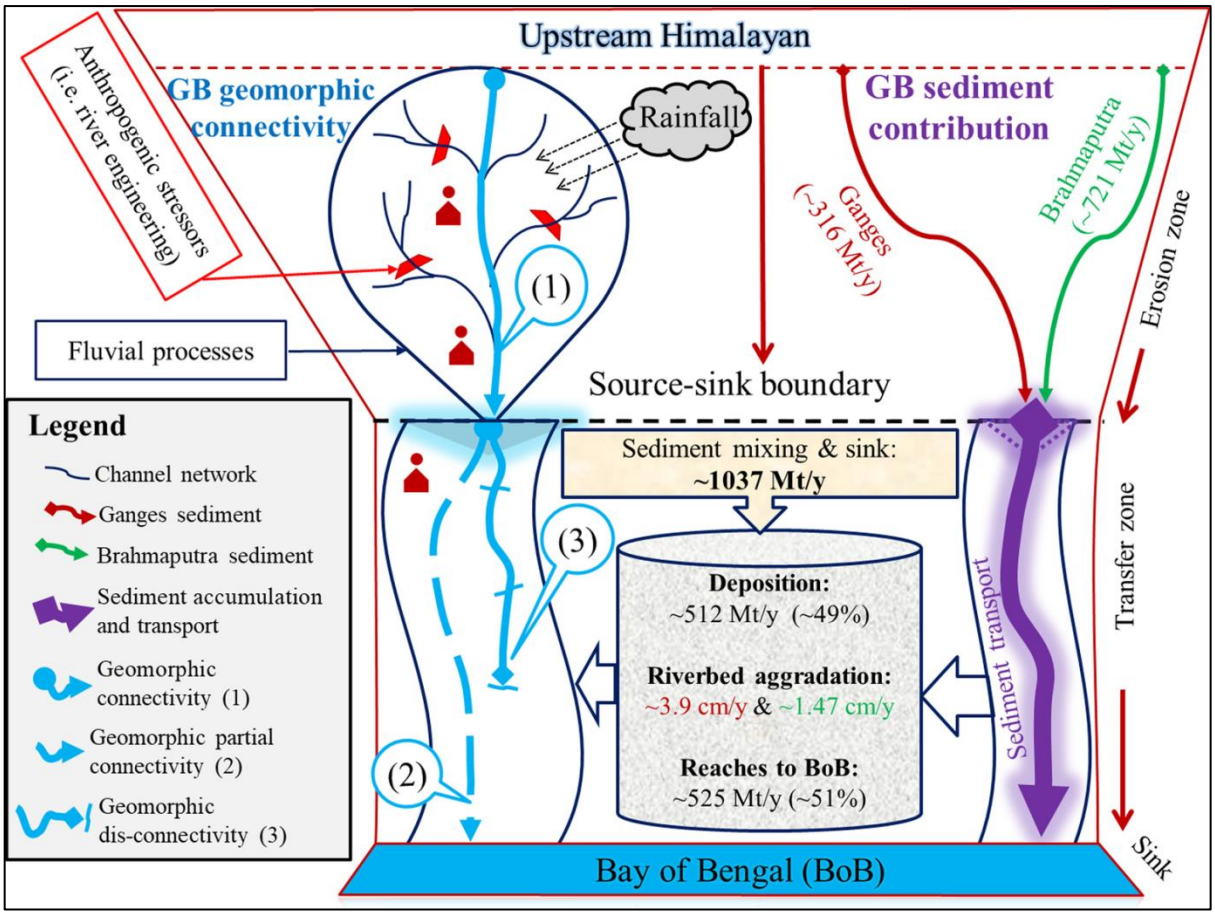

Fig. 2.5 A conceptual diagram showing the geomorphic connectivity from the Himalayan upstream to the BoB based on the existing literature (Goodbred and Kuehl, 1999; Islam et al., 1999, 2001; Wasson, 2003; Garzanti et al., 2011; Jain et al., 2012; Dietrich et al., 2020). On the right side, sediment contribution from upstream two major basins is shown. On the left side, the connected (1) and partially connected (2) or disconnected (3) geomorphic

systems are visualized from source to sink areas. The fluvial sedimentation processes (i.e., excessive sediment sequestering, riverbed aggradation) and anthropogenic stressors (i.e., river engineering, barrage, and dam construction) may change the geomorphic connectivity in the GBM river system. The altering geomorphic connectivity from connected to partially connected or disconnected, impeded by sediment trapping, may significantly impact the GBM river's hydro-geomorphic system. Mt/y denotes the million tons per year.

As noted, the GBM river supports over 150 million people at downstream reaches (Bangladesh), which are vulnerable to the impacts of relative sea level rise, climate changes, annual floods, shifts in land use, and water management (Brammer, 2014; Goodbred et al., 2014). Accordingly, based on the findings by Miah (1988) and Brammer (1990a, b), it was reported that more than 56.9% of total areas of Bangladesh are flooded annually due to monsoon rainfalls and increased water discharge from the upstream Himalayan area (BGS/DPHE, 2001). Also, Coleman (1969) estimated that during flood events, sand bars migrated at a rate of 300–450 m/day or even up to 600 m/day, and channel area increased about 300% in the Brahmaputra. Besides, Singh et al. (2007) reported that floods in the Ganges are also strongly influenced by high sediment discharge and water volume, and this has also been mentioned by the other studies (Wallick et al., 2007; Ahmed and Fawzi, 2011; Yao et al., 2011; Rozo et al., 2014). It is obvious that sustainable river management is demanded and challenged in the large GBM river, which tends to flow in international basins (Gupta, 2007; Rasul, 2014). However, the lack of publicly available long-term and spatially distributed hydrological data (discharge and river characteristics) at a basin-wide scale limits the understanding of hydrological and geomorphological processes of the GBM river basin (Kibler et al., 2014), which is a prerequisite for sustainable water resource management in this downstream region (Fischer et al., 2017). Being a downstream country, Bangladesh faces many challenges in coping with altering geomorphic characteristics of the large GBM river basin and is often dictated by decisions taken outside its border. Hence, the relevant case studies of geomorphic research in Bangladesh and subsequent discussion on large-scale fluvial sedimentation on the GBM river system will enhance our understanding, which may be helpful to improve the government policies or strategies regarding integrated river basin management more sustainably. Technical challenges related to river management may arise from a lack of scientific understanding of river basins or imperfect engineering skills to manage according to that understanding (Stanley and Boulton, 2000). The existing policies, plans, guidelines, and laws related to the integrated water resources management (IWRM) in Bangladesh also emphasize the understanding of the geomorphic process in GBM for

sustainable development (Alam and Quevauviller, 2014). Hence, the understandings of the fluvial geomorphic processes of upstream dominated large GBM river basins at a regional scale is essential to enhance the transboundary cooperation among the basin sharing countries like China, Nepal, Bhutan, and India.

However, the different case studies of fluvial geomorphic research at the downstream Ganges–Brahmaputra (Bangladesh) presented here do not involve a full potentiality of remote sensing techniques or tools in fluvial geomorphology. Therefore, applying the advanced remote sensing techniques and field-based approaches to fluvial research (e.g., Oguchi et al., 2022) in the future may provide a new dimension of fluvial geomorphic research in the hazard-prone deltaic landscape of Bangladesh. Also, our study is limited by collecting the estimates of suspended load at the different reaches of the Ganges–Brahmaputra River basin, which does not describe the sampling procedure and methods of suspended load calculation of each study mentioned in Table 2.1. Therefore, clarifying different methodologies of suspended load estimation may be necessary to understand better the large variations of suspended load estimations among the researchers and the sediment budget of the Ganges–Brahmaputra River basin from the Himalayan to the Bay of Bengal.

2.4 Future perspective of geomorphic research in Bangladesh

Modern quantitative geomorphological researches on hillslope, glacial, fluvial, and coastal processes have been significantly benefited from the availability of medium-to-high-resolution (10–90 m cell size) DEMs (e.g., SRTM, ASTER G-DEM, TanDEM-X) and satellite images (e.g., Landsat, MODIS, and Sentinel 1–3) at regional and global scales for free or at a low cost (Oguchi and Wasklewicz, 2011; Bishop, 2013; Hackney and Clayton, 2015; Otto et al., 2018; Oguchi et al., 2022). Although it is beyond the scope of this article to give a full overview of potential applications and improvements of geomorphic research considering the availability of remote sensing techniques and tools, here the author explores some research gaps between recent advancement of geomorphological researches and earlier geomorphic studies of Bangladesh and provide future perspectives on the better understandings of the geomorphic processes in the context of the upper Ganges–Brahmaputra dominated Bangladesh.

2.4.1 Mountain areas

Notably, there has been an exponential growth of scientific research on mountain and hillslope environments in recent decades (Stoffel and Marston, 2013; Slaymaker and Embleton-Hamann, 2018; Carrión-Mero et al., 2021). Landslide susceptibility mapping is one of the major topics frequently assessed in mountainous and hilly areas. Hence, the landslide susceptibility mapping based on quantum particle swamp optimization (QPSO)–alternating decision tree (ADTree) algorithm can be a promising tool for managing landslide disaster in complex mountainous terrain, successfully applied in Sikkim Himalayan (Islam et al., 2021). Although some studies on landslide susceptibility mapping or modeling have been carried out in hilly (CHT) areas of Bangladesh (Ahmed et al., 2014; Ahmed and Dewan, 2017; Rahman et al., 2017; Rabby and Li, 2020; Abedin et al., 2020), those approaches based on airborne LiDAR, Synthetic Aperture Radar (SAR), and UAS data are mostly missing. The use of such advanced remote sensing datasets with a high resolution or accuracy should benefit the improved assessments of mountain hazards at a local scale. Therefore, it is anticipated to perform remote sensing-based geomorphic research on hilly regions and steep slopes. The development of open access database of such remote-sensing datasets will contribute toestablishing a landslide early-warning system to protect the landslide vulnerable community of the CHT region.

2.4.2 Fluvial environments

After analyzing the fluvial processes of the Indian part of the Ganges–Brahmaputra delta, Subramanian and Ramanathan (1996) and Rudra (2014) mentioned the unavailability of time-series data in the upper GBM catchments and had some limitations. For instance, the work of Rudra (2014) was criticized and rectified by Bandyopadhyay et al. (2015) regarding the delineation of the Bengal basin, deltaic evolution, and discharge data for a better understanding of the fluvial geomorphic processes. However, the studies about the fluvial channel dynamics concerning Bangladesh have been started after 1990s and most of the geospatial studies have been dealing with river channel shifting (Sarker et al., 2014; Islam, 2016; Dewan et al., 2017; Akhter et al., 2019; Gazi et al., 2020a), riverbank line shifting, riverbank erosion, and accretion (Billah, 2018; Gazi et al., 2020b; Biswas et al., 2021). Accordingly, the research on the formation of an alluvial channel, causes of channel migration, anthropogenic impacts on fluvial system, and processes of anomalous channel variations at the downstream GBM River is still sparse or even missing. Further

extensive studies are therefore required to understand better the fluvial settings considering the upstream to downstream hydro-geomorphic connectivity. Besides, the encouragement for fluvial geomorphic research in this understudied region can be taken from fluvial research advancement mentioned by Stott (2013), Wohl (2014), Piégay et al. (2015), and Oguchi et al. (2022). Hence, it is necessary to extend the geospatial research on the fluvial channel dynamics and connectivity, especially with a detailed river basin morphometric analysis at various spatiotemporal scales for predicting the morphological changes along the GBM basin. For example, hotspot zonation of riverbank erosion could be assessed with advanced techniques in the downstream Bangladesh.

On the other hand, the advancement in the application of remote sensing and GIS for riverbank management, including flood monitoring and risk assessment, has significantly facilitated in the last two decades (Sanyal and Lu, 2004). Also, the use of satellite data for flood forecasting and monitoring is more frequent in developed countries than in the developing country like Bangladesh, where the geospatial data usability largely depends on the availability of cloud-free open access data. Nevertheless, in Bangladesh, most of the riverbank management studies are confined to post-flood monitoring (Hoque et al., 2011), flood susceptibility mapping (Rahman and Salehin, 2013; Sarker and Rashid, 2013a, b; Adnan et al., 2019; Sarkar et al., 2022), flood inundation mapping, and some small-scale watershed morphometric studies (Rahaman et al., 2017; Jahan et al., 2018). Consequently, a detailed hydro-geomorphological study of the major watershed floodplain at different spatial and temporal scales is required to make some meaningful flood hazard maps, prediction of extreme flood effects, flood forecasting, and warning based on watershed morphometric analysis and damage assessment in Bangladesh.

Furthermore, the large discharge and heavy sediment load affect the unstable conditions of the Ganges–Brahmaputra–Meghna Rivers, where channels are constantly migrating. However, despite the high possibilities of sediment disasters, only a few studies have been conducted considering the mechanisms of fluvial sediment transport and dynamics in the active downstream GBM basins. Some of the studies are linked to the distribution of suspended sediment concentration at a small scale in Bangladesh (Islam et al., 1999, 2001, 2002; Adnan et al., 2020). It should be noted that fluvial sediments are transported to Bangladesh from upstream source areas, and therefore studies on sediment dynamics need to describe the sediment connectivity and transportation pathways at a

watershed scale. Researches on sediment connectivity and hydrological connectivity are growing rapidly in different hydro-geomorphic setting across the world at various spatial and temporal scales, which includes 26 different countries including the Ganges basin in India (Cavalli et al., 2013; Najafi et al., 2021; Mishra et al., 2019; Swarnkar et al., 2020). However, such studies have not been carried out yet in the downstream basins in Bangladesh, which is a sink area connected to the large upstream basins of the Ganges–Brahmaputra River system and highly prone to repeated sediment disasters. Despite the significance of the entire Ganges–Brahmaputra River system, modeling of the basin-scale sediment dynamics based on climate change scenarios, connecting the upper (China, Nepal, Bhutan, and India) and lower (Bangladesh) Ganges–Brahmaputra basins, has been limited (Khan et al., 2018). Therefore, it is obligatory to extend the geomorphic studies, specifically on sediment yield estimation, sediment budgeting, rainfall–runoff relationship, sediment connectivity, and sediment transport mechanisms connecting upstream erosion zone to the downstream deposition zone in Bangladesh. Geospatial modeling of sediment dynamics for the downstream GBM river basin based on the rapidly changing river morphology is also necessary to facilitate the research findings for disaster countermeasures.

2.4.3 Plain land and coastal areas

Although comprehensive geomorphic mapping is essential for landscape development and urban development, this important section is mostly ignored for the national development program of Bangladesh. Most of the plain land geomorphic studies in Bangladesh have been related to geomorphic mapping or identification of geomorphic units (Kamal and Midorikawa, 2004; Islam et al., 2015a, b; Mahmud et al., 2017; Karim et al., 2019; Arefin and Alam, 2020) and identification of groundwater potential zones (Arefin, 2020a, 2020b; Akter et al., 2020), but their accuracy and precision have been somewhat limited. Therefore, comprehensive geomorphic studies of active plain land are required for proper landscape assessment and management in the densely populated areas in Bangladesh, where the framework of Thorne (2002) can be considered as a blueprint for geomorphic studies of large rivers like the Ganges and Brahmaputra.

The ununiformed sea level rise along the coast due to high sediment dispersal from the GBM river system makes the delta system more complex and vulnerable (Islam, 2011; Rashid et al., 2013; Sarwar, 2013; Karan, 2015). Nevertheless, the coastal geomorphology of Bangladesh is poorly understood, where most of the coastal geomorphic studies are restricted

to shoreline shifting (Shibly and Takewaka, 2012; Islam et al., 2013; Kabir et al., 2020), coastal erosion and accretion (Rahman, 2012; Alam and Uddin, 2013; Sarker et al., 2013; Sarwar and Woodroffe, 2013; Hussain et al., 2014), and morphological studies (Islam et al., 2015a, b; Miah et al., 2020) at small scale. Hereafter, further research is obligatory considering the long-term changes in the sediment supply from the GBM basin, associating the coastal morphological changes and relative sea level rise throughout the Bangladesh coast, which is critical to protect about 35 million people therein (Ahmad, 2019). For this purpose, some coastal geomorphological research trends and challenges mentioned in French and Burningham (2009) can be considered as well for further improvement in coastal geomorphic research in Bangladesh.

2.4.4 General plain land

The above-mentioned earlier geomorphic researches provide some understandings of the evolution pattern of landforms, channel diversion, discharge variability, and sediment estimation at a country scale, but geomorphic studies at larger spatiotemporal scales have been limited in Bangladesh. Also, the causes of discharge (water and sediment) variability patterns, aggradation, deposition, upstream to downstream sediment connectivity patterns, and human-induced perturbation on river geomorphology have not been mentioned or studied clearly. Furthermore, the projection of future behavior of river formation at different spatiotemporal scales based on fluvial geomorphology, hydrology, and meteorology does not exist in these areas, but these are important for understanding the watershed-scale landscape development and the sustainability of the river basin management.

2.5 Conclusions

Although the review of earlier geomorphic studies provided here generally focuses on some significant knowledge and research gaps in one country (Bangladesh), the author proposes the necessity of exploring the wider area studies on fluvio-geomorphic and sedimentation processes in the entire GBM basin, from the upstream erosion prone zone (China, Nepal, Bhutan, and India) to downstream deposition zone (Bangladesh). The bankline migration, human interventions, and tidal processes in the Ganges; avulsion, sedimentation, erosion and accretion, and river channel dimensions in the Brahmaputra; shoreline shifting, erosion, and migration of the Ganges–Brahmaputra confluence have often been investigated at a small scale (country scale). However, the aggradation in the Ganges floodplain and retention of

suspended sediment within the Brahmaputra channel are impacted by the upstream fluvio-sedimentation processes of the GBM river system, where the geomorphic connectivity from Himalayan to the Bay of Bengal is affected by sediment trapping before the mouth of the GBM rivers. Therefore, integrated regional research or basin-wide studies are required for comprehensive understanding of the fluvial processes and sediment dispersal mechanisms from upstream to downstream GBM concerning Bangladesh. In particular, the advanced remote sensing techniques (such as UAS imagery, LiDAR) for geomorphological research, which are encouragingly used in neighboring countries like China (Le Heron et al. 2019), India (Ramsankaran et al., 2020; Dhote et al., 2022), Bhutan (Dunning et al., 2009; Tempa et al., 2021), Nepal (Immerzeel et al., 2014; Kraaijenbrink et al., 2016; Van Woerkom et al., 2019), Pakistan (Khan et al., 2021), and in other parts of the worlds (Śledź et al., 2021), will improve the understandings of landscape evolution and fluvial dynamics not only in the upper Ganges–Brahmaputra but also the entire watershed scale including the downstream reaches in Bangladesh.

In summary, the literature review and discussion presented here provide very first step toward developing a detailed and documented understanding of the fluvio-geomorphic dynamics in the GBM River. We conclude that the fluvial geomorphic research at different spatial and temporal scales is a prerequisite for a large-scale basin management which is still missing here, for which the advancement from the present geomorphic research aptitude is necessary to solve a wide range of problems related to sustainable river basin management and disaster risk reduction. Also, the government policymaker can get a comprehensive idea from the subsequent discussion on the fluvial geomorphic research scale (borderless or basin-wide scale) and improve their policies or strategies accordingly to focus more on transboundary bilateral and multilateral collaboration (i.e., in situ gauging data sharing) with upstream countries like China, Nepal, Bhutan, and India.

Graphical abstract of Chapter 2:

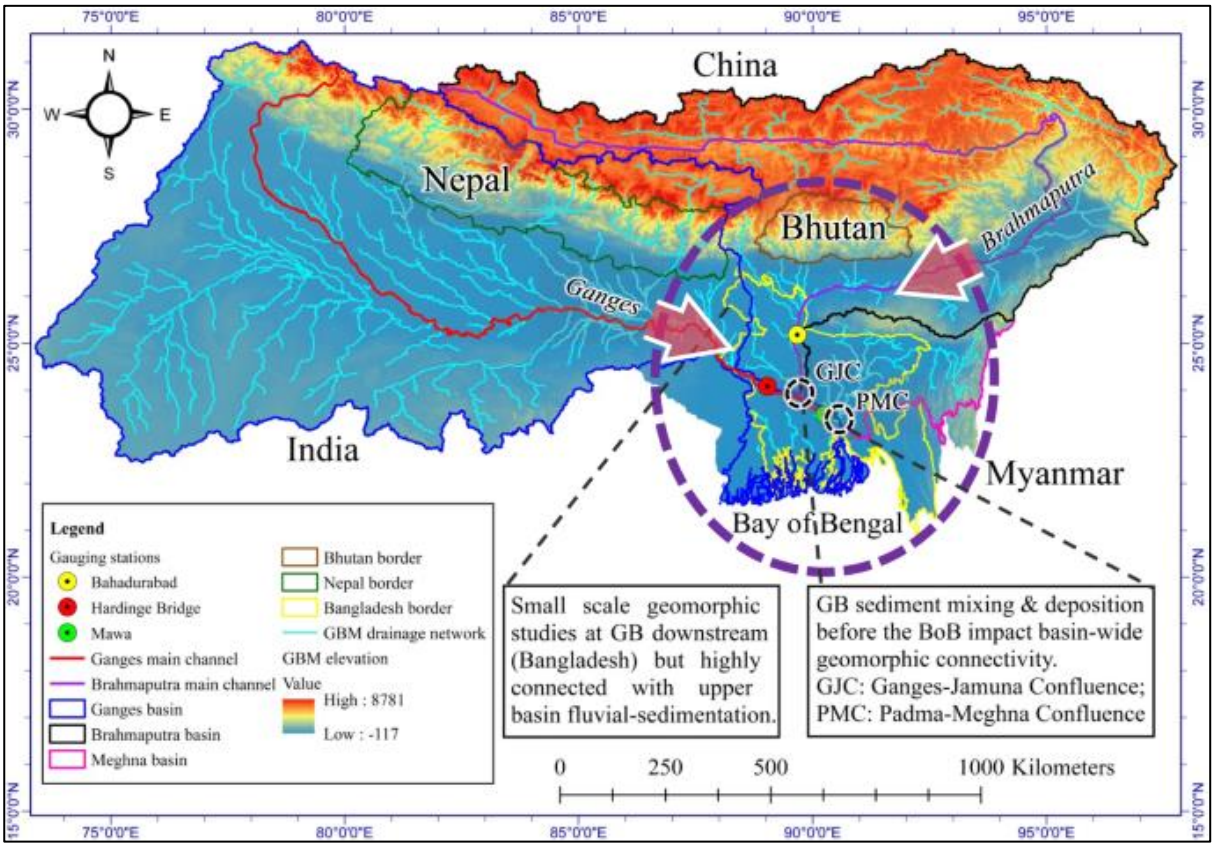

Highlights of Chapter 2:

- Small-scale geomorphic studies at GB downstream Bangladesh but highly connected with upper basin fluvial-sedimentation processes.
- Basin-wide geomorphic connectivity is highly impacted by GB's sediment mixing and deposition before the Bay of Bengal (BoB).

Chapter 3

Geomorphometric characterization and sediment connectivity of the middle Brahmaputra River basin

3.1 Introduction

Morphometry is the mathematical quantification of basin physiography (Clarke, 1966; Swarnkar et al., 2020; Oyedotun, 2020). It is crucial for characterizing geomorphological processes and understanding the evolutionary history of any basin (Sharma and Sarma, 2013). The morphological characteristics can be understood more clearly through linear, areal, and relief morphometric parameters (Mahala, 2020). Morphometric properties such as catchment area, stream network density, relief, terrain roughness, slope, and geology greatly influence the geomorphological changes and sediment connectivity in a basin (Fryirs et al., 2007; Cavalli and Marchi, 2008; Oguchi et al., 2013; Cavalli et al., 2013). Geomorphological studies also play an essential role in understanding the river system's longitudinal and lateral linkages (Sinha et al., 2005; Sinha et al., 2013). Moreover, morphometric analysis is crucial for sustainable watershed management, especially for upstream fluvial process-dominated downstream countries like Bangladesh, where integrated basin information is scarce (Sujatha et al., 2014; Rahmati et al., 2019).

Mountainous topography significantly impacts the spatial variation of hydrological conditions, including the spatial distribution of soil moisture and groundwater flow (Rahmati et al., 2019; Li et al., 2021). Notably, research of debris flow and sediment dynamics uses topographic factors like the topographic wetness index (TWI), the stream power index (SPI), the sediment transport index (STI), and the slope-length (LS) factor (De Reu et al., 2013; Rahmati et al., 2019). The use of digital elevation models (DEMs) to derive these topographic variables is faster, less subjective, and the obtained measurements are more reproducible than conventional techniques (Iqbal et al., 2005). In addition, using topographic indices for the large area that undergoes limited hydrological process monitoring, such as rainfall, runoff, and sediment yield, can provide helpful information for better watershed management. Moreover, the topographic factors correlate with drainage basin morphometry and impact the integrated watershed management (Sujatha et al., 2014).

Sediment connectivity is the degree to which a geomorphic system facilitates the transfer of sediment through its components such as hillslopes, channel networks, and valley bottoms (Fryirs and Brierley, 2013; Heckmann et al., 2018). The degree of connectivity between hillslopes and the channel and the transfer of water and sediment within the channel largely depends on the morphological diversity, where connectivity decreases with increasing landscape morphological complexity (Baartman et al., 2013). The connectivity processes also vary in space and time and can be modified by anthropogenic changes (drainage system changes, river engineering structures, land use, etc.) in the landscapes (Brierley et al., 2006; Jain and Tandon, 2010; Tarolli and Sofia, 2016; Llena et al., 2019). Measuring structural sediment connectivity is fundamental to representing the spatial configurations of the linkages among the components, which can be measured indirectly by using a geomorphic connectivity index instead of measuring connectivity in the field (Heckmann et al., 2018). Among several approaches to evaluating sediment connectivity, the use of geomorphometric indices (sediment connectivity index) make it possible to detect the areas that are prone to sediment transfer and the degree of sediment linkage through landscape units (Borselli et al., 2008; Cavalli et al., 2013; Persichillo et al., 2018; Zanandrea et al., 2019; Turley et al., 2021). This sediment connectivity index (IC), developed by Borselli et al. (2008) and then refined by Cavalli et al. (2013), is widely used and considered an effective means to quantitatively evaluate the transfer of sediments from hillslopes to downstream. This index helps identify the preferential sediment pathways and prioritize sediment source areas (Heckmann et al., 2018).

Although the downstream area of the Brahmaputra basin in South Asia is densely populated and highly prone to repeated sediment disasters, the research on hydro-geomorphic systems of the basin, considering the sediment linkage from upstream to downstream sink areas, has been limited (Faisal and Hayakawa, 2022). The sediment connectivity approach is essential in developing countries where the spatial data is often scarce and not easily accessible for field observation (Najafi et al., 2021). Moreover, there are few possibilities to model spatial patterns of sediment delivery and identify sediment source and sink areas because of the lack of effective and comprehensive strategies for basin-scale sediment management in the transboundary Brahmaputra River, which is shared by China, India, Bhutan, and Bangladesh in South Asia. Furthermore, understanding sediment connectivity informs us of sediment movement from source to sink in a catchment, which determines the long-term behavior of sediment flux and the aggradation or degradation patterns that are

manifest as a change in the landforms (Bracken et al., 2015; Poeppl et al., 2017; Najafi et al., 2021). Therefore, understanding geomorphic characteristics and sediment connectivity patterns in the upstream-dominated Brahmaputra River basin is essential in sustainable water resources management and land use planning of downstream countries affected by high erosion and sediment delivery rates from its upstream regions.

This work focuses on the transboundary Himalayan-fed middle Brahmaputra River, distinguished by highly variable seasonal flows, significant sediment discharge, and diverse morphological patterns (Subramanian and Ramanathan, 1996; Islam et al., 1999; Singh et al., 2004; Mahanta et al., 2014). Despite the enormity and geomorphic diversity of the Brahmaputra River, comparatively little attention has been paid by national and international researchers during the past few decades compared to the Ganges River system (Coleman, 1969; Goswami, 1985; Umitsu, 1987; Sinha and Friend, 1994; Subramanian and Ramanathan, 1996; Allison et al., 1998; Islam et al., 1999; Kale, 2005; Sinha et al., 2005; Takagi et al., 2007; Goodbred et al., 2014; Brammer, 2014; Sarker et al., 2014; Dewan et al., 2017; Bandyopadhyay et al., 2021). Furthermore, the review of geomorphological processes and their connectivity in hillslope, fluvial, and coastal areas of the downstream portions of the Ganges–Brahmaputra depicts that fluvial-geomorphic research in the deltaic landscape of Bangladesh is explored at a small-scale (country scale) (Faisal and Hayakawa, 2022). These small-scale studies are insufficient to understand large-scale landscape processes (Lane and Richards, 1997; Jain et al., 2012). Notably, the upper basin morphodynamics, hydrology, and sediment flux of the Brahmaputra River system influence the fluvial sediment dynamics of the downstream Bangladesh (Subramanian and Ramanathan, 1996; Singh, 2007; Faisal and Hayakawa, 2022). Furthermore, the hydrological processes in the upper part of a river basin may directly influence downstream areas from a few to many hundreds of kilometers away (Nepal et al., 2014). Moreover, understanding upstream-dominated processes or events or sediment transport dynamics that shape the particular landform development of downstream areas is critical in geomorphic science (Whipple and Tucker, 1999; Stark and Stark, 2001).

A research gap exists in the geomorphological investigation of the middle Brahmaputra River basin (Faisal and Hayakawa, 2022), but the geomorphic characterization and sediment connectivity at a basin-wide scale would increase our knowledge about this river system and its downstream consequences. To fill the gap, the present research intends to

analyze the morphometric characteristics, topographic features, and sediment connectivity along the right bank of the middle Brahmaputra River (Teesta, Torsa, and Manas) that are assumed to have a potential hydro-geomorphic response to the downstream area (Fig. 3.1). This article aimed to assess the geomorphic characteristics to compare sediment connectivity parameters (IC, SPI, etc.) between upland and lowland systems on the Brahmaputra River basins. The results from this study would be helpful in better understanding the basin-scale fluvial-geomorphic processes and may provide baseline information for further research.

3.2 Study area

3.2.1 Area of interest (AOI)

The Brahmaputra River (580,000 km^2 drainage area) is known as Yarlung/Tsang Po in China (Tibet), Siang/Dihang River in Arunachal Pradesh (India), Lohit/Dilao in Assam (India), and Jamuna in Bangladesh, characterized by marked variability in its substantial discharge and a considerable amount of sediment volume (~721 million t/yr) (Goswami, 1985; Sharma et al., 2012; Faisal and Hayakawa, 2022). The geology of the Brahmaputra basin is comprised of the Higher Himalaya (schists, gneisses, marbles with amphiboles, Migmatites, and Miocene leucogranites), the Lesser Himalaya (schists, quartzites, graphitic schists, and limestone) and the Siwaliks formation (Singh and France-Lanord, 2002; Singh, 2007; Goodbred et al., 2014). The northern tributaries joining the Brahmaputra in Assam largely drain metamorphic rocks of the Higher Himalayas in Bhutan and Sikkim (Garzanti et al., 2004). The low-grade sedimentary rocks of the Lesser Himalaya outcrop locally along the Assam Valley tributaries in the Brahmaputra catchment (Richards et al., 2006; Goodbred et al., 2014). The Assam and Bangladesh plains carry the Brahmaputra's fluvial sediments consisting of alluvial features such as natural levees, point bars, oxbow lakes, and channel bars (Goswami, 1998; Singh, 2007).

Most of the Brahmaputra's sediment load is derived from its high Himalayan portion and many landslides in this region, transferring sediment downstream and causing large floods with substantial flood deposits (Wasson, 2003; Rajbanshi et al., 2022). Rainfall during the southwest monsoon (June–September) is a significant source of water and contributes to the annual discharge of the Brahmaputra. However, Himalayan meltwater and groundwater contributions are crucial during summer (Singh, 2007). In this study, the author wants to emphasize the mountainous northern (right bank) tributaries of the middle Brahmaputra River (Fig. 3.1) considering its dynamic characteristics (i.e., high flow and sediment contribution,

extensive channel modification, steeper channel gradient, and flashy nature) compared to the south bank tributaries (Sharma et al., 2012; Pangare et al., 2021). For example, the Teesta, Torsa, and Manas contribute significantly to the discharge of the main Brahmaputra (Sarma, 2004; Saha and Bhattacharya, 2021; Pangare et al., 2021) and may influence the sediment flux as well as sediment transfer at its entire catchment.

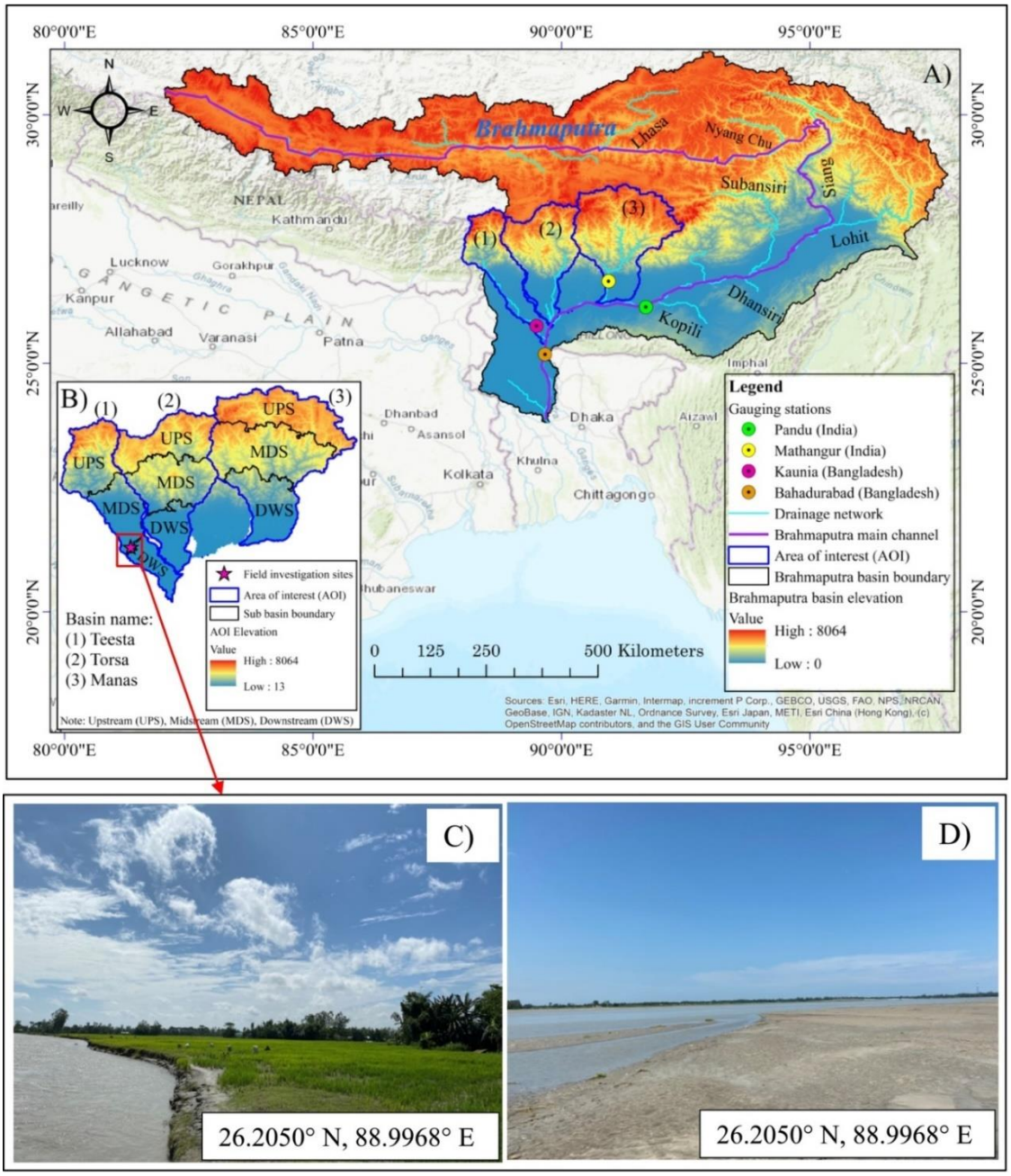

Fig. 3.1 A) Overview of Brahmaputra River basin with background topography showing the flow path connecting the upstream region to downstream and surrounding areas, B) the area of interest; upstream (UPS), midstream (MDS), and downstream (DWS), C–D) field photos were taken by the authors on 20 Aug 2022 from the field investigation site (indicated in B), Teesta River (Brahmaputra's tributary) in northern Bangladesh; where C) and D) respectively show the erosion along the bank and sedimentation within the channel.

Therefore, north bank tributaries joining the mainstream Brahmaputra River channel adjacent and upstream to the Bangladesh border, namely Teesta, Torsa, and Manas basins, have been selected for the present study. The selected basins fall within the Pandu to Goalundo reach (Sarma, 2004). After rising from the northern Himalayan, the Teesta traverses 309 km to join the Jamuna below Rangpur town in Bangladesh (Sarma, 2004). The Torsa travels about 145 km through the Chumbi valley of Bhutan before entering India near Ramgati, called Amo Chu. The Torsa travels a distance of 100 km through North Bengal, and after flowing past Balampur, it joins the Jamuna 15 km downstream from the last Indian tributary, the Gangadhar (Saha and Bhattacharya, 2019, Saha and Bhattacharya, 2021). The Manas originates from the northern slope of Mount Kula Kangri in Tibet and flows 140 km through Bhutan; then, it bifurcates near the Indian border and travels through the Assam valley before meeting the Brahmaputra. The area of interest for this study is about 75,000 km^2, which connects different parts of India and Bhutan and flows through the main Brahmaputra channel to downstream Bangladesh farther south (Rasul, 2015; Ray et al., 2015). Table 3.1 identifies the significant characteristics of the selected basins.

Table 3.1 Major characteristics of basins under this study

Characteristics	Basin		
	(1) Teesta	(2) Torsa	(3) Manas
Basin area (km^2)	17,639	23,680	33,102
Mean elevation (m)	3173	2479	3298
Annual average rainfall (mm) (2010-2019)	2408	1763	1200
Average annual yield in Million Cubic Meter (MCM)	21,413	14,980	2925
Major land-cover	Trees (40.68%), Crops (17.46%), Shrubs (13.27%), Built up (11.09%), Bare ground (8.25%), Water (2.38%)	Trees (54.77%), Shrubs (19.44%), Crops (8.44%), Built up (5.08%), Bare ground (5.81%), water (1.31%)	Trees (45.04%), Shrubs (25.76%), Bare ground (14.34%), Crops (5.50%), Built up (3.09%), water (1.37%)

Note: Based on Brahmaputra Board, 1995; TRMM, 2011; Mahanta et al., 2014; NASA JPL, 2020; Karra et al., 2021; Pangare et al., 2021

3.2.2. Meteorological conditions

The entire Brahmaputra basin, excluding the Tibetan portion, falls within the Southeast Asian monsoon regime, highly influenced by extreme monsoon rainfall with a mean annual rainfall of 2300 mm (Mahanta et al., 2014). The monsoon rain (June to September) accounts for 60–70 % of the yearly rainfall in the entire Brahmaputra basin, while the pre-monsoon season (March to May) produces only 20–25 % of the annual rainfall (Mahanta et al., 2014). The large concentrated rainfall pattern in the monsoon season may increase the basin discharge, generating a high sediment yield and dynamics (Mahanta et al., 2014; Pangare et al., 2021). Hence, the tropical rainfall measuring missions (TRMM) data from (2010–2019) have been analyzed to observe the rainfall pattern over the studied basins. The time series analysis of rainfall data also suggests strong monsoonal influence (June to September) with an average annual rainfall of 1200 mm to 2408 mm along these basins (Fig. 3.2).

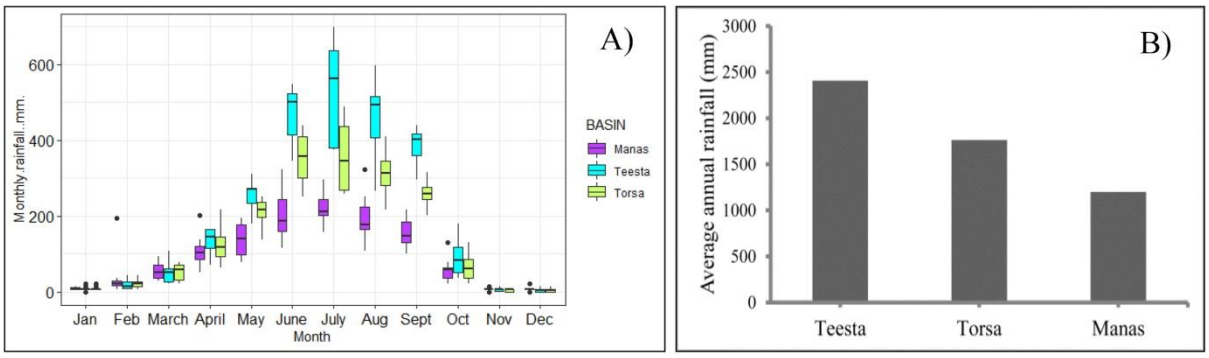

Fig. 3.2 Inter-basin A) monthly rainfall cycle and B) average annual rainfall variations throughout 2010–2019.

In addition, the enormous and variable flows distinguish the hydrological regimes, where about 70–80 % of the total Brahmaputra discharge is from the southwest monsoon (Singh, 2007). The hydrographs of available average annual discharge along the studied basins indicates monsoonal (June to September/October) flow dominancy (Fig. 3.3). For example, at Bahadurabad (Bangladesh) gauging station (where the Teesta at downstream Bangladesh joins the Brahmaputra), the average monsoon flow is 35,712 m^3/s. In contrast, during the non-monsoonal season (January–April), the average flow is 5186 m^3/s (Rahaman and Varis, 2009). Therefore, the mainstream and the tributaries of the Brahmaputra spill over their banks, causing devastating floods in the Assam plains and Bangladesh annually during the southwest monsoon (Kale, 2003). The similar scenario of rainfall patterns and annual discharge at different parts of the Brahmaputra basin were mentioned in previous studies (Mahanta et al., 2014; Rao et al., 2020; Pangare et al., 2021). The rainfall and discharge

patterns have been considered here to discuss the effects of hydro-meteorological conditions on these basins' characteristics and sediment dynamics.

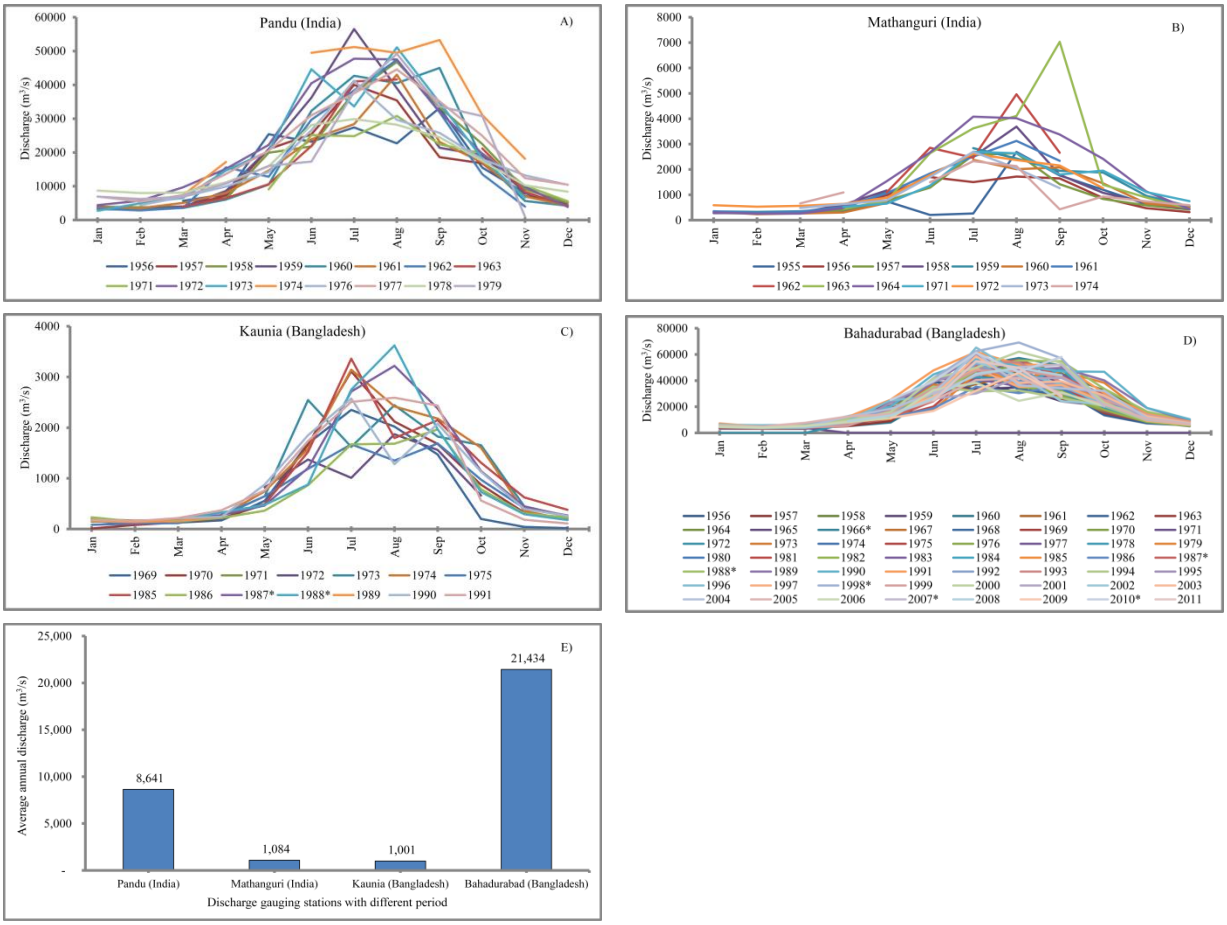

Fig. 3.3 Monthly discharge hydrographs from different gauging stations along the study area; A. Pandu (India) (1956-1963, 1971-1979); B) Mathanguri (India) (1955-1964, 1971-1974); C) Kaunia (Bangladesh) (1969-1975, 1985-1991); D) Bahadurabad (Bangladesh) (1956-2011); E) Average annual discharge at different gauging stations. * denotes the major flood occurrence.

3.3 Data and methods

3.3.1 Geospatial data

Table 3.2 provides a summary of the dataset used in this study. Freely accessible NASADEM_HGT (30 m and void-filled), created by the NASA-MEaSUREs program (publicly released in February 2020), have been downloaded from NASA-LPDAAC (Land Processes Distributed Active Archive Center) (NASA JPL, 2020; Buckley et al., 2020). This NASADEM is reprocessed from the radar-based SRTM (Shuttle Radar Topographic Mission) with many improvements to its quality, notably void reduction and artifacts removal using auxiliary data from various datasets such as ASTER GDEM, PRISM (Panchromatic Remote-

sensing Instrument for Stereo Mapping), GLAS (Geoscience Laser Altimeter System), and ICESat (Ice, Cloud, and Land Elevation Satellite) in processing techniques (Crippen et al., 2016; Buckley et al., 2020; Oguchi et al., 2022; Tran et al., 2023). The vertical accuracy of NASADEM has been revealed as 5.3 m (USA) (Buckley et al., 2020), 6.39 m (Estonian) (Uuemaa et al., 2020), 6.59 m (China) (Li et al., 2022), and 12.08 m (New Zealand) (Uuemaa et al., 2020). Moreover, the NASA Jet propulsion laboratory (creators of the dataset) claims that the radar does an excellent job in penetrating the vegetation canopy, so the digital terrain model (DTM) bias is not significant (Franks et al., 2020). Since NASADEM is relatively new, few articles have been published in the relevant fields of study and performed well compared to other freely available global DEM datasets, e.g., ASTER, AW3D30, MERIT, SRTM, and TanDEM-X (Franks et al., 2020; Uuemaa et al., 2020; Li et al., 2020; Tran et al., 2023).

Table 3.2 Data used in the present study

Input data	Data source	Specifications	Reference
NASA-DEM	NASA-MEaSUREs (https://earthexplorer.usgs.gov/)	30 m spatial resolution and released in 2020.	NASA JPL, 2020; Buckley et al., 2020
Annual average rainfall	TRMM (https://disc2.gesdisc.eosdis.nasa.gov/opendap/)	TRMM_3B43 version 7; 0.25° by 0.25° spatial resolution over the period of 2010-2019.	TRMM, 2011
Land-use and land-cover	ESRI 2021 (https://livingatlas.arcgis.com/landcover/)	ESA Sentinel-2 (10 m) released in July 2021.	Karra et al., 2021
Average annual yield (MCM)	IUCN 2014 (https://www.iucn.org/content/physical-assessment-brahmaputra-river)	IUCN report on physical assessment of the Brahmaputra river: A Bangladesh-India Initiative.	Mahanta et al., 2014
River discharge data	Global Runoff Data center (GRDC) (https://www.bafg.de/GRDC/EN/01_GRDC/grdc_node.html).	Gauging stations and time periods: (1) Pandu (1956-1963, 1971-1979); (2) Mathanguri (1955-1964, 1971-1974); (3) Kaunia (1969-1975, 1985-1991); (4) *Bahadurabad (1956-2011)	GRDC, 2021; *Rao et al., 2020
Global polygon for terrain classification	Geospatial Information Authority of Japan (GSI) 2022 (https://gisstar.gsi.go.jp/terrain2021/)	MERIT DEM-90 m (v1.0.3) merging mainly the SRTM3-90 m (v.2.1) and the ALOS (AW3D-30 m) (v.1) and released in June 2022.	Iwahashi and Yamazaki, 2022

Here, space borne rainfall data from TRMM-3B43, which was a joint mission between NASA and the Japan Aerospace Exploration Agency (JAXA), have been used to extract the meteorological information (rainfall) from 2010 to 2019 over the area of interest (TRMM, 2011). The TRMM system uses precipitation RADAR, microwave imager, and visible infrared scanner merged with station data to estimate rainfall (Huffman et al., 2007; NASA, 2017). Furthermore, freely accessible Brahmaputra River discharge data from three gauging stations (shown in Fig. 3.1) along the present study area have been accessed from the global runoff datacenter (GRDC) website (GRDC, 2021). Unfortunately, these discharge datasets are widely spaced with a large data gap (7 to 10 yr) and historic (time series data collection ends around 1990) (Goswami, 1985; Islam et al., 1999; Sarma, 2005). The available time series insitu discharge datasets (Table 3.2) are used to discuss the large-scale flow dynamics and sediment connectivity patterns along these basins. In addition, the most comprehensive and updated instrumental discharge data of Bahadurabad (Bangladesh) gauging station over the last six decades (1956–2011) have been collected from Rao et al. (2020) for this study. However, the combination of NASADEM, TRMM rainfall, and river discharge data at gauging stations provides a new dimension in the investigation of hydro-geomorphological characteristics of the study area.

The global land-use/land-cover (LULC) 2020 maps derived from European space agency (ESA) Sentinel-2 imageries at 10 m resolution released by Environmental System Research Institute Inc. (ESRI) under creative commons BY-4.0 license in July 2021 have been used in this study (Karra et al., 2021). Furthermore, in association with IUCN (International Union for Conservation of Nature and Natural Resources) and collaborative research between India and Bangladesh, the physical assessment report of Brahmaputra basin-2014 provides previously unavailable annual sediment yield data for future research in the under-investigated Brahmaputra basin (Brahmaputra Board, 1995; Mahanta et al., 2014; Pangare et al., 2021). Our study intends to use this yield estimation data collected from Brahmaputra Board (India) and an extensive joint field investigation between India and Bangladesh. The ground-based sediment yield data collection and availability are highly appreciated because the field data collection in the transboundary Brahmaputra River is somewhat risky with limited accessibility, hindering a systematic field-based investigation.

The author also used a global polygon for terrain classification data released in June 2022 by the Geospatial Information Authority of Japan (GSI) as a proxy for the topographic applications (Iwahashi and Yamazaki, 2022). The geometric signatures of terrain polygons such as lnSLOPE, lnHAND (Height Above the Nearest Drainage), and Texture (density of pits and peaks) that quantitatively classify the topography help obtain an overview of the ground efficiently in a wide area (Iwahashi et al., 2021).

3.3.2 Methodology

The datasets mentioned above have been used to analyze the selected basins' hydro-geomorphic characteristics and sediment connectivity. For this study, each selected basin is divided into three sub-basins (Fig. 3.1B), upstream (UPS), midstream (MDS), and downstream (DWS), based on the flow length algorithm (Smith, 1997; Cho, 2020). The methodologies of deriving the meteorological factor, morphometric parameters, topographic parameters, and sediment connectivity index are mentioned below with their applicability and limitations. The statistical analyses were mainly performed using software R (version 4.1.0) (R Development Core Team, 2020). Multicollinearity was checked for the morphological and topographic data. Then generalized linear mixed models (GLMMs) were used to analyze the interactive and univariate effects on sediment connectivity, where the "glmmADMB" package was used (Alam et al., 2021).

3.3.2.1 Meteorological factors

The meteorological studies focus on the TRMM rainfall data analysis because of unevenly distributed and poorly maintained real-time rain gauge data, complicated transboundary issues, and limited accessibility along the Brahmaputra River basin (Shrestha et al., 2008; Bajracharya et al., 2015). Comparative studies of satellite-based and gauge-based rainfall estimation documented that monthly TRMM products are more reliable than other estimations (Huffman et al., 2007; Immerzeel, 2008; Medhioub et al., 2019), where the systematic bias is significantly reduced in the low altitude river basins (Yong et al., 2014). In addition, the gridded rainfall dataset of the India meteorological department (IMD) and gauge rainfall (47 stations) observations of Bangladesh water development board (BWDB) tested the suitability of using the TRMM dataset over the Ganges–Brahmaputra–Meghna river basin (Prasanna et al., 2014). Furthermore, the rain gauge-based validation of the TRMM dataset in the Brahmaputra basin encourages us to use it for meteorological analysis (Shukla et al.,

2014; Bajracharya et al., 2015; Tarek et al., 2017). Therefore, TRMM-3B43 version 7 products of 0.25° by 0.25° fine spatial resolution and monthly temporal resolution have been downloaded and processed (Huffman et al., 2007; Huffman et al., 2010; NASA, 2017). These gridded rainfall datasets are available in NetCDF format and converted to raster layer using multidimensional tools of ArcGIS model builder language. TRMM-3B43 products of (mm/h) unit converted to (mm/month) by multiplying the hourly rain rate with the total hours in that particular month and then the annual scale (Shukla et al., 2014). Brahmaputra River discharge datasets accessed in ASCII format at a monthly scale have been converted to annual-scale (m^3/s) for the specific available years.

3.3.2.2. Geomorphometric factors

The morphometric parameters of linear (stream order, stream length, bifurcation ratio), areal (circularity ratio, stream frequency, drainage density, and compactness coefficient), and relief aspects (basin relief, relief ratio, and ruggedness number) have been computed along with longitudinal profiles. The formula for calculating each morphometric parameter with its respective reference has been provided in Table 3.3. ArcGIS software analysis has measured the watersheds' areas, perimeter, and length. The channel network was determined by the stream threshold approach with several trials and errors (Jenson and Domingue, 1988; Heine et al., 2004). The reality and consistency of extracted channel network were visualized from Google Earth satellite images and field investigation at Brahmaputra's tributary (Teesta, Bangladesh). The longitudinal channel profiles were generated to understand the topographic features and channel anomalies (O'Callaghan and Mark, 1984; Ozulu and Gökgöz, 2018).

Table 3.3 Methodology adopted for computing morphologic and topographic parameters

Parameters name	Equation	References
Stream order (u)	Hierarchical rank	Strahler, 1964
Stream number (N_u)	$N_{u=}N_1+N_2+N_3+.....+N_n$	Horton, 1945
Stream length (L_t) (km)	$L_{t=}L_1+L_2+L_3+.....+L_n$	Strahler, 1964
Stream frequency (Fs)	$F_s = N_u/A$; Where A is basin area.	Horton, 1932
Bifurcation ratio (R_b)	$R_b = N_u/N_u+1$; where N_u+1 is number of segments of the next higher order.	Strahler, 1964
Drainage density (D_d) (km/km^2)	$D_d = L_u/A$; where L_u is total stream length of order 'u'.	Horton, 1932

Circularity ratio (R_c)	$R_c = 4\pi \times A/P^2$; Where, A is the area enclosed within the boundary of watershed divide (Basin area)	Strahler, 1964
Compactness coefficient (Cc)	$C_c = 0.2824 \times (P/\sqrt{A})$; where P is the length of the watershed divide which surrounds the basin	Gravelius, 1914
Basin relief (R) (m)	R= Max H – Min H	Strahler, 1952
Relief ratio (R_r)	$R_r = R/L_b$; Where L_b is the distance between the outlet and farthest point on the basin boundary (Basin length).	Schumm, 1956
Ruggedness number (R_n)	$R_n = D_d \times (H/1000)$; Where D_d is drainage density, and H is basin height.	Patton and Baker, 1976
Topographic Wetness Index (TWI)	$TWI = \ln(A_s/\tan\beta)$ ... ... (1) Where, A_s is the specific catchment area and β is the slope gradient in radians.	Moore et al.,1993
Stream Power Index (SPI)	$SPI = A_s \times \tan\beta$ ... ... (2) Where, A_s is the specific catchment area and β is the slope gradient in radians	Moore et al., 1993
Sediment Transport Index (STI)	$STI = (m+1)(A_s/22.13)^m \times (\sin\beta/0.0896)^n$ ... ... (3) Where, A_s is the specific catchment area (m^2 m^{-1}), β is the slope gradient in degrees, m is 0.4, and n is 1.3.	Moore et al., 1991
LS (slope-length) factor	$LS = (n+1)(A_s/22.13)^n \times (\sin\beta/0.0896)^m$ ... ... (4) Where, n = 0.4, and m = 1.3	Moore and Burch, 1986
Topographic Position Index (TPI)	$TPI = Z_0 - (1 - nZ_n)/n$ ... ... (5); Where, Z_0 is the elevation of the point under evaluation, Z_n is the elevation of the points within the local window, and n is the total number of surrounding points employed in the evaluation.	Gallant and Wilson, 2000

3.3.2.3. Topographic factors

Topographic factors such as the topographic wetness index (TWI), the stream power index (SPI), the sediment transport index (STI), the LS (slope-length) factor, and the topographic position index (TPI) have been considered in this study as they provide helpful information about geomorphological characteristics of river basins (Table 3.3). Furthermore, a range of previous geomorphic studies also applied these factors, notably Pei et al. (2010), De Reu et al. (2013), Papaioannou et al. (2014), Rahmati et al. (2019), and Swarnkar et al. (2020). The topographic indices are often evaluated using geographic information system (GIS) (De Roo, 1998; Chen and Yu, 2011). Our study also uses an ArcGIS model builder language environment to compute rapid topographical analysis of large basins. Different topographic

indices for geomorphic characterization largely depend on the quality, availability, and resolution of the DEM (Sørensen and Seibert, 2007; Grabs et al., 2009). Also, it is not certain that increasing DEM resolution will improve topographic indices' performance (Oguchi et al., 2022) as topography has less control over the groundwater flow (Grabs et al., 2009). Here, the author used newly released and freely accessible 30-m NASADEM as a significant input of topographic factor analysis.

Here, TWI is calculated based on Moore et al. (1993) (Table 3.3, Eq. (1)), which provides an alternative for understanding the spatial pattern of wetness (Sørensen et al., 2006; Grabs et al., 2009). The SPI reflects the stream power, which is considered here as one of the factors that determine river channel erosion, basin-scale variability in channel processes, morphology, and sediment transport potential (Moore et al., 1991; Pei et al., 2010; Kaushal et al., 2020) (Table 3.3, Eq. (2)). However, the values of TWI and SPI are influenced by the calculating algorithm of specific catchment area (A_s) and gradient (Tanβ) as the computation of A_s depends on the flow direction algorithm (Chen and Yu, 2011). The STI is calculated by Moore et al. (1991) (Table 3.3, Eq. (3)) to characterize the erosion and deposition processes (Kalantari et al., 2014; Mojaddadi et al., 2017). Furthermore, the LS factor (dimensionless) reveals the fact that erosion increases with slope angle and slope length (Winchell et al., 2008; García Rodriguez and Giménez Suarez, 2010), and here, it has been calculated by applying a numerical model described by Moore et al. (1991) (Table 3.3, Eq. (4)). Moreover, TPI measures topographic slope positions and subdivides the landscapes into morphological classes based on topography (De Reu et al., 2013). In the present study, TPI is calculated based on the equation derived by Gallant and Wilson (2000) (Table 3.3, Eq. (5)) at 2 × 2 windows as it was successfully applied with field verification at highly sloping hilly terrain in India (Chauniyal and Dutta, 2018). The TPI value ranges from positive to negative values, representing ridges and valleys, respectively, where zero values correspond to flat areas (Gallant and Wilson, 2000; Amatulli et al., 2020).

Here, the functions and computation of morphometric and topographic factors in Table 3.3 use ArcGIS model builder visual programming language, and are then converted to semi-automated morphometric assessment tools (SMAT) (Fig. 3.4). It has three components (a) a morphometric and topographic assessment tool (MTAT), (b) a longitudinal profile extraction tool (LPET), and (c) a TRMM data extraction tool (TRET). The SMAT tools, developed from the current workflow, shortened the computation time of meteorology

(rainfall), morphometric, and topographic parameters and are provided in the supplementary material.

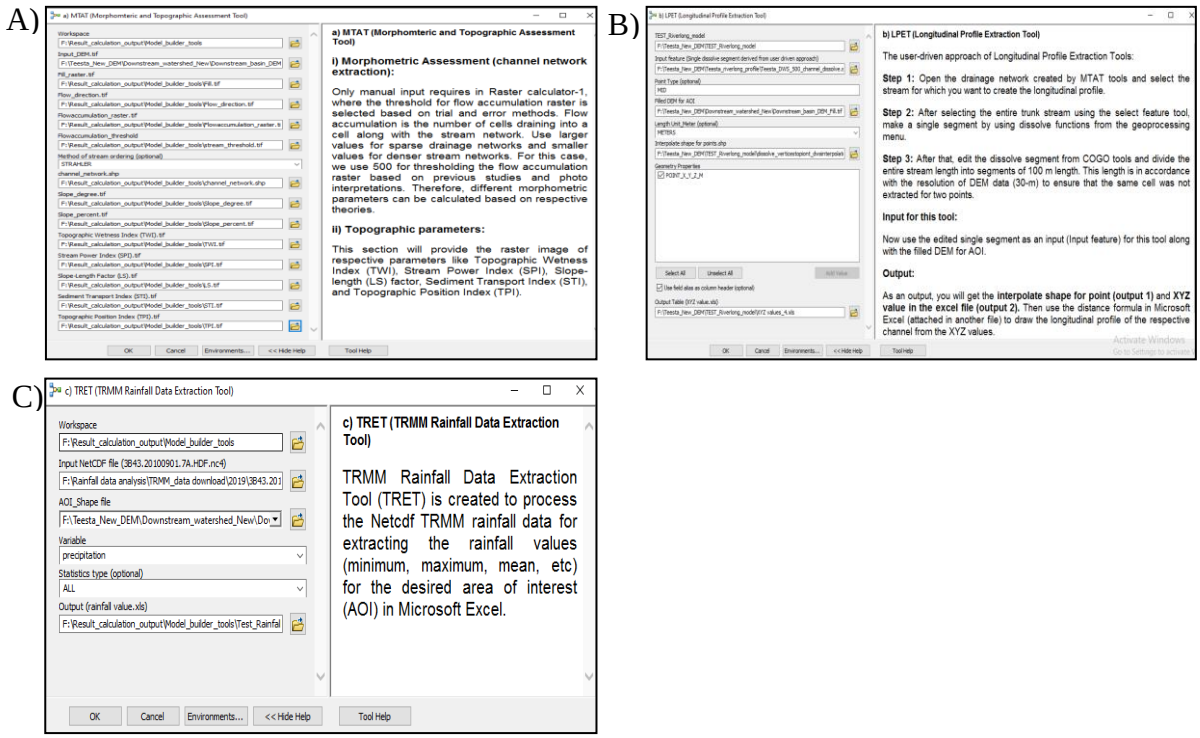

Fig. 3.4 Workflow of deriving morphometric parameters converted to Semi-automated Morphometric Assessment Tools (SMAT); A) Morphometric and Topographic Assessment Tool (MTAT), B) Longitudinal Profile Extraction Tool (LPET), and C) TRMM Rainfall Data Extraction Tool (TRET). Can be accessed from https://drive.google.com/file/d/1-85dzHShrtMFtiyndGAd_3sp1cWVWlqz/view?usp=sharing

3.3.2.4. Index of sediment connectivity

The sediment connectivity index estimates the potential connection or sediment mobilization between the sediments eroded from hillslopes and the stream system, considering the land surface and topographic characteristics (Borselli et al., 2008). The IC was primarily applied in relatively smaller basins covering ~10 to ~150 km^2 with a very high-resolution (~2.5 m) DEM (Cavalli et al., 2013). Mishra et al. (2019) and Swarnkar et al. (2020) applied this IC in the larger basin area (~50,000 to 70,000 km^2) of the Ganges with coarser SRTM-DEM (~90 m and ~30 m resolution) to understand the sediment connectivity between hillslopes and channels. Hence, taking encouragement from SedInConnect tool designer Crema and Cavalli (2018) and previous work (Mishra et al., 2019; Zanandrea et al., 2019; Swarnkar et al., 2020), this connectivity index is applied to the middle Brahmaputra basin as a novel approach, where sediment dynamics are not fully understood. Here, sediment connectivity analysis is carried out using the stand-alone freely available SedInConnect 2.3 tools

(https://github.com/HydrogeomorphologyTools), introduced by Crema and Cavalli (2018). The functionalities and algorithm of the TauDEM 5.3.7 tool (Terrain Analysis Using Digital Elevation Models) (https://hydrology.usu.edu/taudem/taudem5/downloads5.0.html) is used to reflect a more usual pattern of sediment connectivity through the basins (Tarboton, 1997; Cavalli et al., 2013). This connectivity index (IC) is defined as follows:

$$IC_k = log_{10}(D_{up}/D_{dn}) = log_{10}\left(WS_k\sqrt{A_k}/\sum i = k, n_k\, d_i/W_i S_i\right) \ldots\ldots (6)$$

where IC_k is the sediment connectivity index (dimensionless) at the particular cell; k is the cell number; D_{up} is the upslope component; D_{dn} is the downslope component; W is an average weight factor (usually considered as C-factor of RUSLE equation, dimensionless) of the upslope contributing area; S_k is the average slope (m/m) of the upslope contributing area at a particular cell (k); A_k is the upslope contributing area (m^2) at cell (k); n_k is the total number of the cell in the basin; d_i is the length of the ith cell along the flow path (m); W_i is the weight (C factor) at the ith cell (dimensionless); S_i is the slope (m/m) at the ith cell. The IC is defined in the range of $[-\infty,+\infty]$, with connectivity increasing for larger IC values.

The calculation of the IC is mainly based on topography. However, land-use cover information can be integrated into the analysis by utilizing weighting factors, e.g., C-factor, as shown by Borselli et al. (2008). The author used NASADEM (30 m resolution) for topography and channel network as the target. The C-factor is considered as the weight factor generated from the Sentinel-2 derived land-use/land-cover map of 2021, which may provide better insight into the connectivity pattern as heterogeneous landscape favors using the C-factor as weighting factor (Cavalli et al., 2014; Cantreul et al., 2018). The C-factor values of individual cells are acquired from the published literature for a range of land-use/land-cover classes mentioned in Table 3.1 (FAO, 1978; Wischmeier and Smith, 1978; Morgan, 2009; Ganasri and Ramesh, 2016; Swarnkar et al., 2020). Using the C-factor as weight in the IC computation would help us model the impedance to runoff and sediment fluxes from local land use and soil surface (Borselli et al., 2008). Here, both the input layers (i.e., NASADEM and C-factor map) are resampled to the same pixel size (30 m) for the calculation of IC (Eq. (6)). According to several researchers (notably Zanandrea et al. (2019); Mishra et al. (2019); Swarnkar et al., 2020; Martini et al. (2020); Liu et al. (2021)), this DEM resolution is sufficient to evaluate sediment connectivity. In addition, particle size of sediments is another influential factor for the calculation of sediment connectivity, particularly for relatively small,

steep watersheds with diverse particle size including boulder, gravel, sand, and mud. However, our study focuses on wider areas with less variable sediment particle size (mainly sand and mud), so this study assume the effects of differing particle size on the calculated IC in a broader scale is minimal (Garzanti et al., 2004; Fryirs and Brierley, 2013). Therefore, the IC values derived from topography and land-use/land-cover characteristics would help us to better understand the sediment connectivity pattern in these large basins.

3.4 Results

3.4.1 Geomorphometric analysis

The result of geo-morphometric parameters are presented in Table 3.4. The Strahler's stream order suggests that 7^{th} (Teesta), and 8^{th} (Torsa and Manas) order stream networks are present along these basins (Fig. 3.5A). Compared to the midstream and upstream sub-basins, higher stream frequencies have been observed downstream (Fig. 3.5B). Considering the whole basin (WB), the stream frequency ranges from (1.12 to 1.14 km^{-2}) where the highest stream frequency is found at Teesta (1.14 km^{-2}) compared to others. High stream frequency, larger catchment area, and high discharge in downstream areas may suggest the dominancy of channel processes and, therefore, more erosion (Fryirs and Brierley, 2013; Oyedotun, 2020). Drainage density is related to climate, the type of rocks, relief, vegetation cover, surface roughness, and several hydrological processes such as infiltration capacity, soil saturation, and overland flow, which impact the production of runoff and sediment load in the basin (Rudraiah et al., 2008; Swarnkar et al., 2020). For the whole basin, the drainage density (D_d) results suggest comparatively higher values in the Teesta basin (1.07 km/km^2) compared to the Torsa basin(0.98 km/km^2), and the Manas basin (0.96 km/km^2) (Fig. 3.5C). The variability of infiltration numbers shows the dominancy of MDS and DWS over the UPS except for the Manas basin. The infiltration number is relatively higher in the whole basin of Teesta (1.21) compared to Torsa (1.10), and Manas (1.08). This result infers that the Teesta basin has a lower infiltration capacity with high runoff, followed by the Torsa and Manas basin because the infiltration number implies that the higher the value of the infiltration number, the lower will be the infiltration with higher runoff (Bhatt and Ahmed, 2014). The result of the compactness coefficient (C_c) for the whole basin shows the highest values in Manas (3.43), whereas the lowest is found for Torsa (2.95). In the whole basin, the circulator ratio (R_c) ranges from 0.16 to 0.24, where higher values are found for Manas (0.24), followed by Torsa (0.23), and Teesta (0.16). The circulatory ratio varies from 0 to 1 (where a higher

value shows a more circular basin shape) (Miller, 1953). The low values for the circulatory ratio in these basins indicate that basin shapes are not circular and suggests that they reflect an early stage of topographical maturity, which may significantly affect their hydrological response (Rai et al., 2017). High variations of bifurcation ratio have been observed from upstream to downstream sub-basins, where the highest bifurcation ratio has been observed in the MDS of Teesta (2.27) (Fig. 3.5D). As a whole basin, Teesta shows a relatively higher bifurcation ratio (R_b) (1.87) compared to the Manas (1.75) and Torsa (1.77) basins. Bifurcation ratios between 3 and 5 means the drainage system is less influenced by tectonics (Strahler, 1964), therefore, values in this study (<3–5) infers the dominance of modern geomorphic processes rather than tectonics.

Table 3.4 Comparison of morphometric parameters at selected basins and sub-basins

Basin	Sub-basin	F_s	R_b	R_c	D_d	D_t	C_c	If	R	R_r	R_n
Teesta	UPS	1.17	1.79	0.20	0.94	1.10	1.49	1.10	7901	13.80	7.44
	MDS	1.12	2.27	0.20	1.19	1.34	1.62	1.34	4336	6.98	5.15
	DWS	1.22	1.85	0.13	1.11	1.36	1.44	1.36	99	0.18	0.11
	WB	1.14	1.87	0.16	1.07	1.21	3.12	1.21	7901	6.61	8.42
Torsa	UPS	1.07	1.87	0.18	0.92	0.99	2.08	0.99	5981	7.49	5.50
	MDS	1.14	1.81	0.18	0.93	1.07	2.11	1.07	4726	5.83	4.41
	DWS	1.18	1.80	0.18	0.58	1.35	1.58	1.35	2656	4.37	3.05
	WB	1.12	1.77	0.23	0.98	1.10	2.95	1.10	7208	6.36	7.07
Manas	UPS	1.10	1.96	0.13	0.95	1.04	2.64	1.04	4736	4.67	4.50
	MDS	1.13	1.87	0.22	0.88	1.00	2.79	1.00	6944	6.49	6.13
	DWS	1.13	1.92	0.22	1.06	1.19	1.83	1.19	4444	6.32	4.71
	WB	1.12	1.82	0.24	0.96	1.08	3.43	1.08	7490	5.69	7.20

Note: abbreviations of parameters are according to Table 3.3

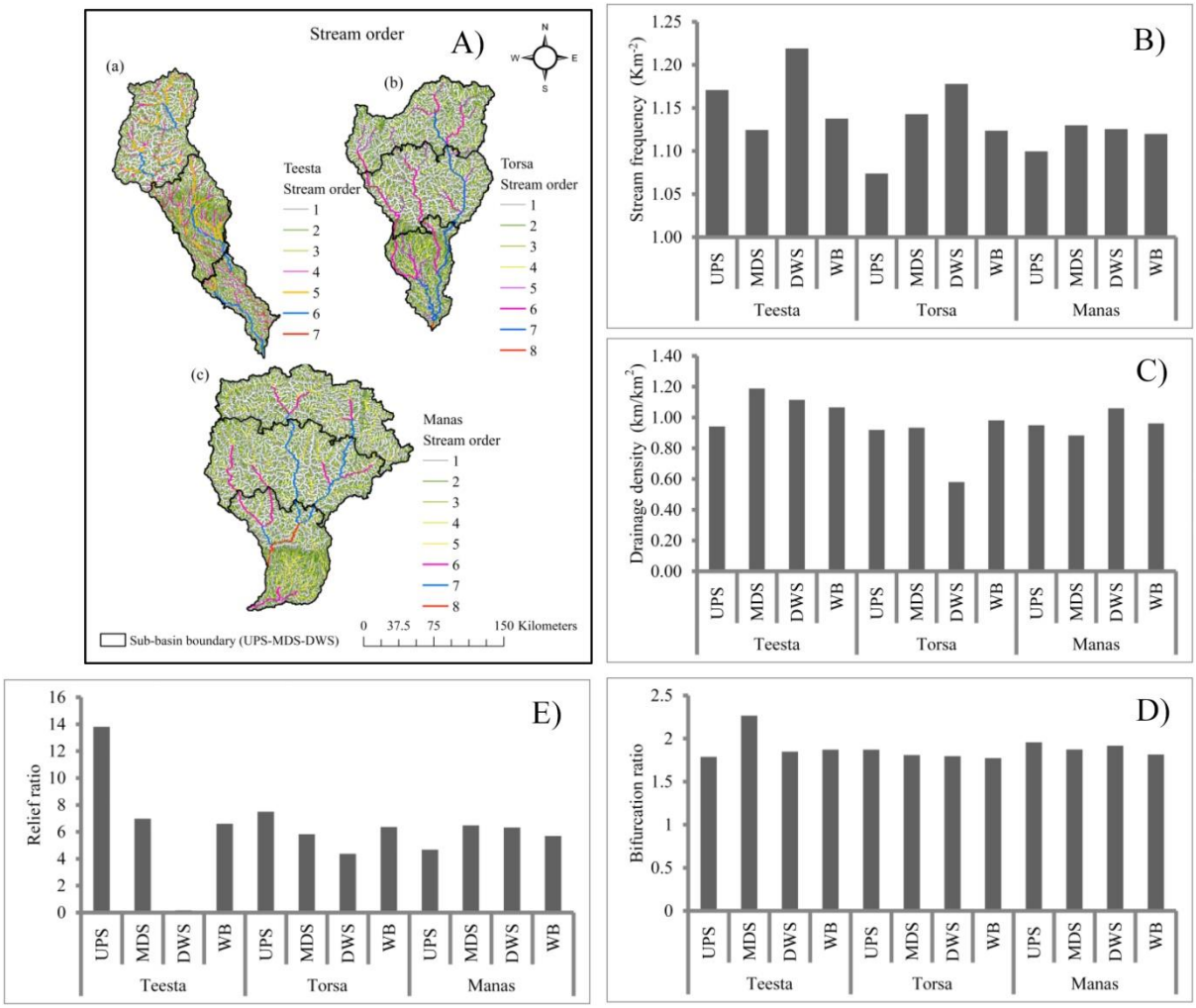

Fig. 3.5 A) Stream order (Strahler, 1964) maps for (a) Teesta, (b) Torsa, and (c) Manas basin. Bar plots of B) stream frequency, C) drainage density, D) bifurcation ratio, and E) relief ratio are shown for all the basins and sub-basins.

The basins in this study are characterized by a large basin relief, which is highest in Teesta (7901 m) followed by Manas (7490 m) and Torsa (7208 m), and indicates the steepness of these basins (Parveen et al., 2012; Rai et al., 2017). The relief ratio (R_r) of the Teesta, Torsa, and Manas basins is 6.61, 6.36, and 5.69, respectively (Fig. 3.5E). The relief ratio has a direct relationship with slope gradient, so the relief ratio of the Torsa and Teesta basins is also high (Rudraiah et al., 2008). For the whole basin, the ruggedness number (R_n) varies from 7.07 to 8.42. Teesta shows higher values (8.42), which implies more rugged terrain compared to other basins (Patton and Baker, 1976; Debelo et al., 2017). The variation in R_n values reflects slope and relief differences among these sub-basins and basins.

3.4.2 Longitudinal profiles analysis

The longitudinal profile depicts the change in the channel bed elevation over the river's entire length from its origin to its mouth (Rhoads, 2020). Fig. 3.6 shows that longitudinal profiles are concave-upward to relatively flat. The upstream region in these basins mostly shows a steep profile with sharp transitions. The Teesta, Torsa, and Manas's midstream region mainly shows gradually decreasing profiles. In contrast, almost flat segments with irregularities are observed in downstream areas, where the elevation change is limited but might be very sensitive to depositional characteristics. The deviations of the most observed concave nature of long profiles with irregularities in these basins may depict the response of long profiles to tectonics, change in base level, water discharges, and sediment load characteristics of these basins (Goswami, 1985; Whipple and Tucker, 1999; Jiang et al., 2016). The errors or irregularities along the valley bottom profiles may arise from converting discrete altitude measurements into gridded elevation information of coarse-grained (10 to 30 m resolution) DEM data (Hayakawa and Oguchi, 2006; Schwanghart and Scherler, 2017; Rhoads, 2020).

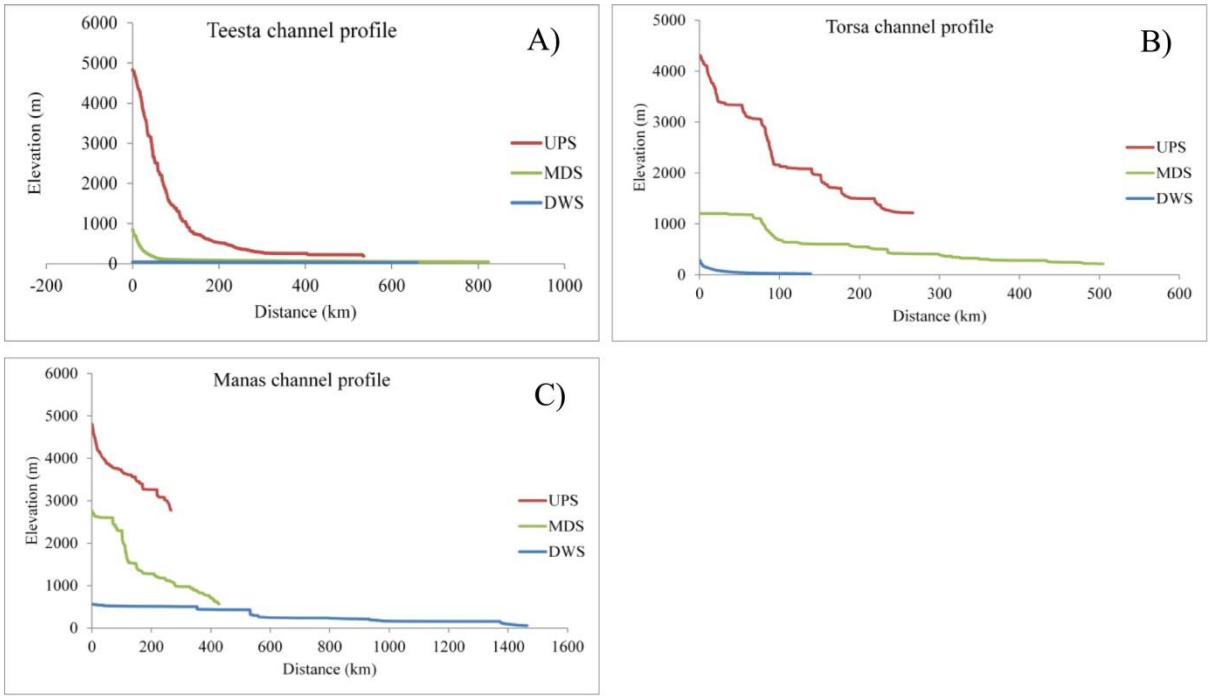

Fig. 3.6 Longitudinal channel profiles of A) Teesta, B) Torsa, and C) Manas. UPS, MDS, and DWS reaches have been considered to show the variations in channel profiles. The distance is from the upstream end of each section.

3.4.3 Topographic analysis

The topographic factors are described from upland to downslope areas in Table 3.5. Generally, a channel slope >25° is preferred for debris or sediment flow initiation, which

decreases with increasing catchment area (Takahashi, 1981; Hungr et al., 1984; Rickenmann and Zimmermann, 1993; Van Dine, 1996). Here, in the upstream region, the average slope is >25° except at Manas (23.41°) basin. The slope in the midstream region drops drastically at Teesta (7.97°). Downstream, the lowest slope is found for Teesta (1.72°), followed by Torsa (4.31°) and Manas (17.24°). The average slope varies significantly across the whole basin, where a higher gradient is found for Manas (23.76°), followed by Torsa (21.78°) and Teesta (16.13°). The slope difference at the whole basin scale shows that with a steeper slope, Manas has a relatively higher potential for flow or sediment initiation than the Torsa and Teesta basins. Overall, the gradient varies highly, reflecting the heterogeneous terrains' behavior. Slope significantly controls complex terrain's erosion and deposition potential (Rafaelli et al., 2001), and the head area slope generally determines the sediment delivery (Fontana and Marchi, 1998). The runoff, sediment yield, or sediment transport capacity increased as the slope gradient increased (Xiao et al., 2017; Jourgholami et al., 2021). Here, the steeper slope has been observed in the upstream areas, showing the potentiality for flow or sediment initiation. In contrast, the slope decreased dramatically along the midstream and downstream reaches, reducing the sediment connectivity or transport potential and favors deposition.

Table 3.5 Basin topographic features analyzed (abbreviations are according to Table 3.3)

Basin	Sub-basin	Slope (degree)	TWI	SPI	STI	LS	TPI
Teesta	UPS	27.70	5.80	-1.02	0.39	0.16	-1.67
	MDS	7.97	7.63	-4.09	0.46	0.23	-0.67
	DWS	1.72	8.55	-4.98	0.42	0.21	-0.19
	WB	16.13	7.00	-2.75	0.68	0.31	0.22
Torsa	UPS	27.12	5.80	-1.13	0.39	0.16	-1.34
	MDS	26.43	5.81	-1.19	0.42	0.17	-0.77
	DWS	4.31	8.05	-4.63	0.39	0.20	-0.92
	WB	21.78	6.37	-1.87	0.68	0.29	0.12
Manas	UPS	23.41	6.10	-1.19	0.65	0.26	0.33
	MDS	28.14	5.79	-0.91	0.65	0.25	0.37
	DWS	17.24	6.93	-2.63	0.63	0.29	0.30
	WB	23.76	2.15	-1.43	0.68	0.28	0.10

Further, the TWI has been used to assess the presence of saturation, which is essential for ephemeral gully formation (Foster, 1990) and influences the runoff processes and suspended sediment flows (Sharma, 2010). Generally, large TWI values are seen at the lower slope or on the valley floor of large catchment areas. Here, TWI at UPS varies from 5.80 to 6.10, with the highest values in Manas (6.10). In the midstream and downstream reaches, the TWI ranges from 5.79 to 7.63 and 6.93 to 8.55, respectively, where comparatively higher

values are found in downstream reaches. As for the whole basin, the highest TWI has been found for Teesta (7.00), followed by Torsa (6.37) and Manas (2.15). The steeper slope upstream and high TWI at the downstream zone of the Manas basin can initiate high flows compared to Torsa and Teesta basins. Moreover, a significant positive relationship between TWI and slope suggests high sediment flow potential at UPS because of a higher gradient and lower TWI. In contrast, DWS suggests lower sediment flow caused by a steeper slope and higher TWI (Fig. 3.7A). The analysis of TWI illustrates that high values are mostly found along the downstream region (mostly flat terrain) while low values are typical in the upstream region (mostly steeper terrain). Therefore, the areas with high TWI (i.e., downstream) will have a greater risk of gully erosion than areas with low TWI value (i.e., upstream) (Sharma, 2010).

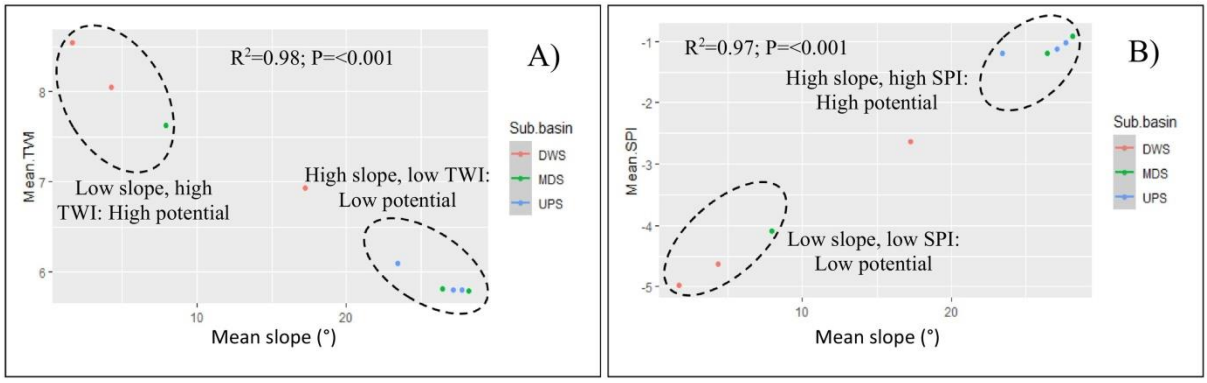

Fig. 3.7 Relationship of topographic features A) mean slope and mean TWI; B) mean slope and mean SPI in each UPS, MDS, and DWS sub-basins. The slope is in degrees.

Furthermore, the SPI has been used to evaluate the erosion and potential energy of overland flow that is available to cause sediment transport where a high SPI indicates a more significant potential for soil erosion (Moore et al., 1993). Upstream, the SPI ranges from −1.19 to −1.02, where the highest values are found for Teesta (−1.02), followed by Torsa (−1.13), and Manas (−1.19). At midstream and downstream areas, the SPI ranges (−4.09 to −0.91) and (−4.98 to −2.63), respectively, where higher values are found in Manas, followed by Torsa and Teesta. Similarly, in the whole basin, the highest SPI values are found in Manas (−1.43), followed by Torsa (−1.87) and Teesta (−1.87). Intra-basin comparison shows that upstream sub-basins show comparatively higher SPI values, possibly caused by higher elevation. The significant positive relationship between slope and SPI depicts its high potential at UPS (high slope, high SPI) and lower potential at DWS (low slope, low SPI) for sediment transport (Fig. 3.7B). Furthermore, the steeper slopes with high SPI and low TWI are expected to have high flow and sediment potential. High SPI with steeper slopes at

upstream reaches of the Teesta, Torsa, and Manas basins can initiate high flows, but low SPI and high TWI with flatter slope downstream may imply the sediment deposition within the channel.

The STI of upstream areas varies from 0.65 to 0.39, and higher values have been observed in the Manas basin. In midstream and downstream regions, the STI ranges from 0.42 to 0.65 and 0.39 to 0.63, respectively. For the whole basin, Teesta, Torsa, and Manas show similar values (0.68). The low STI value at downstream reflects the slow mobility and, consequently, the accumulation of sediments. Furthermore, a high LS factor value suggests a higher rate of soil loss (Vijith and Dodge-Wan, 2019). The LS factor values at UPS range from 0.16 to 0.26, where higher values are found in Manas, followed by Torsa (0.16) and Teesta (0.16). At MDS and DWS, the LS values range from 0.17 to 0.25 and 0.20 to 0.29, respectively. Inter-basin comparison of LS values shows that Teesta has a higher LS value (0.31) compared to Torsa (0.29) and Manas (0.28). High LS and STI values are expected to initiate the high erosion and flows at the UPS zone, whereas the MDS and DWS may experience deposition scenarios. The LS factor directly impacts erosion and transport potential from the source region to downstream, where a high LS factor value shows greater potential (i.e., UPS of Teesta) (Arabameri et al., 2018; Vijith and Dodge-Wan, 2019). Previous studies by Das et al. (2022) found a similar trend of LS values in the Indian Himalayan region.

The application of TPI is limited in the Himalayan region (Chauniyal and Dutta, 2018). Here, TPI is estimated to infer the slope pattern and landforms of the study area. According to Weiss (2001), the landform can be classified as ridges: TPI > 1.0, upper slope: 1.0 > TPI > 0.5, middle slope: 0.5 > TPI > −0.5 (angles >15°), flat: 0.5 > TPI > −0.5 (angles <15°), lower slope: -0.5 > TPI > −1.0, and valley: TPI < −1.0. In our study, the TPI varies from −1.67 to 0.33, −0.77 to 0.37, and −0.92 to 0.30 in upstream, midstream, and downstream, respectively. Here, the negative TPI values are found in Teesta and Torsa from upstream to downstream. The positive values of TPI from upstream to downstream in Manas depict its ridge formation, while the negative values in Torsa and Teesta reveal its valley formation. However, as a whole basin, none of the basins has negative values of TPI, where the highest values are found for Teesta (0.22) followed by Torsa (0.12) and Manas (0.10). The TPI values of the whole basin fall within the range 0.5 > TPI < -0.5, which identified these basins as middle slope regions, where UPS and DWS are dominated by a steeper slope

and a lower slope, respectively. Roy and Das (2021) classified a similar pattern of landforms conducted in the eastern Himalayan catchment near the Brahmaputra's northernmost tributary (Teesta). The TPI result shows large variations in topography though the results may vary because of the basin's radius, scale, or surface roughness (Grohmann and Riccomini, 2009). Here, the spatial distribution of TPI illustrates the formation of upper slope to valley-type landforms where the sediment may accumulate at DWS because of the flat landscape (Gallant and Dowling, 2003).

Furthermore, this study's topographic features (i.e., TWI and SPI) show significant correlations with the standardized terrain geometric signatures (ZlnSLOPE, ZlnHAND, and ZTexture) that represent the ground feature efficiently (Iwahashi et al., 2021; Iwahashi and Yamazaki, 2022). This correlation represents the validity of topographic patterns obtained from the present study (Fig. 3.8). Moreover, the terrain classification map in Fig. 3.9 represents the hilly mountainous to the lowland features, resembling the spatial distribution of topographic features derived from this study.

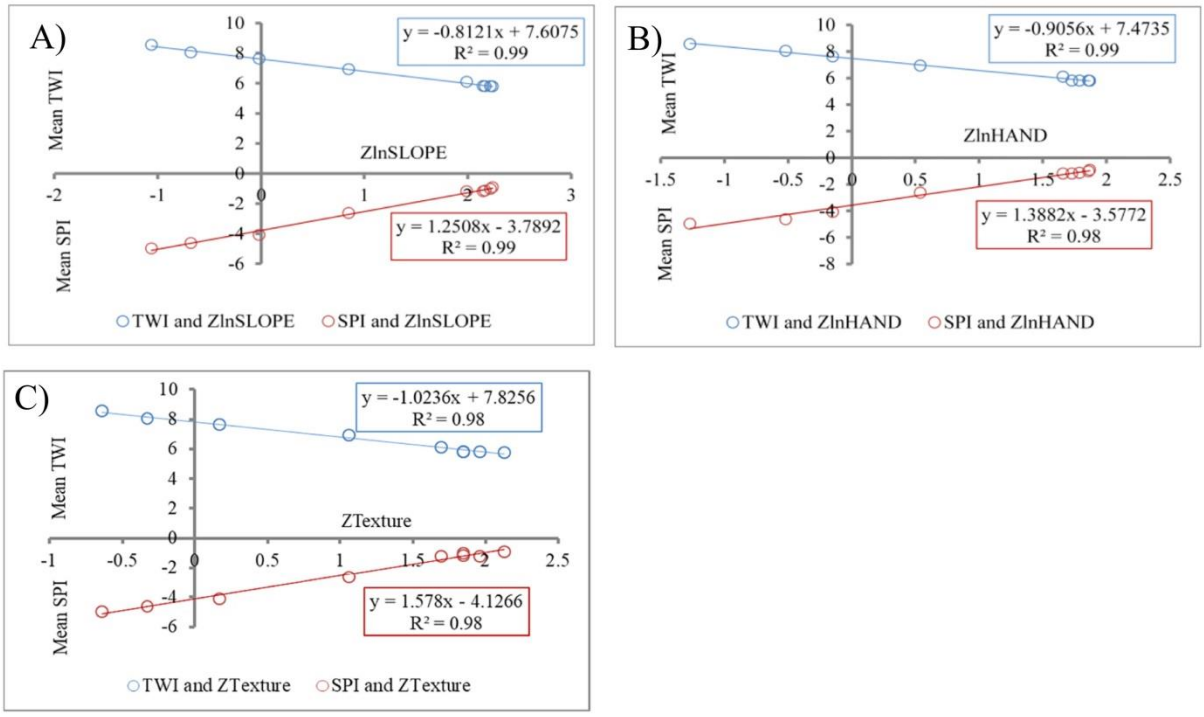

Fig. 3.8 Correlation of terrain geometric signatures and topographic features A) ZlnSLOPE with TWI and SPI, B) ZlnHAND with TWI and SPI, and C) ZTexture with TWI and SPI. $P < 0.001$ shows a significant level.

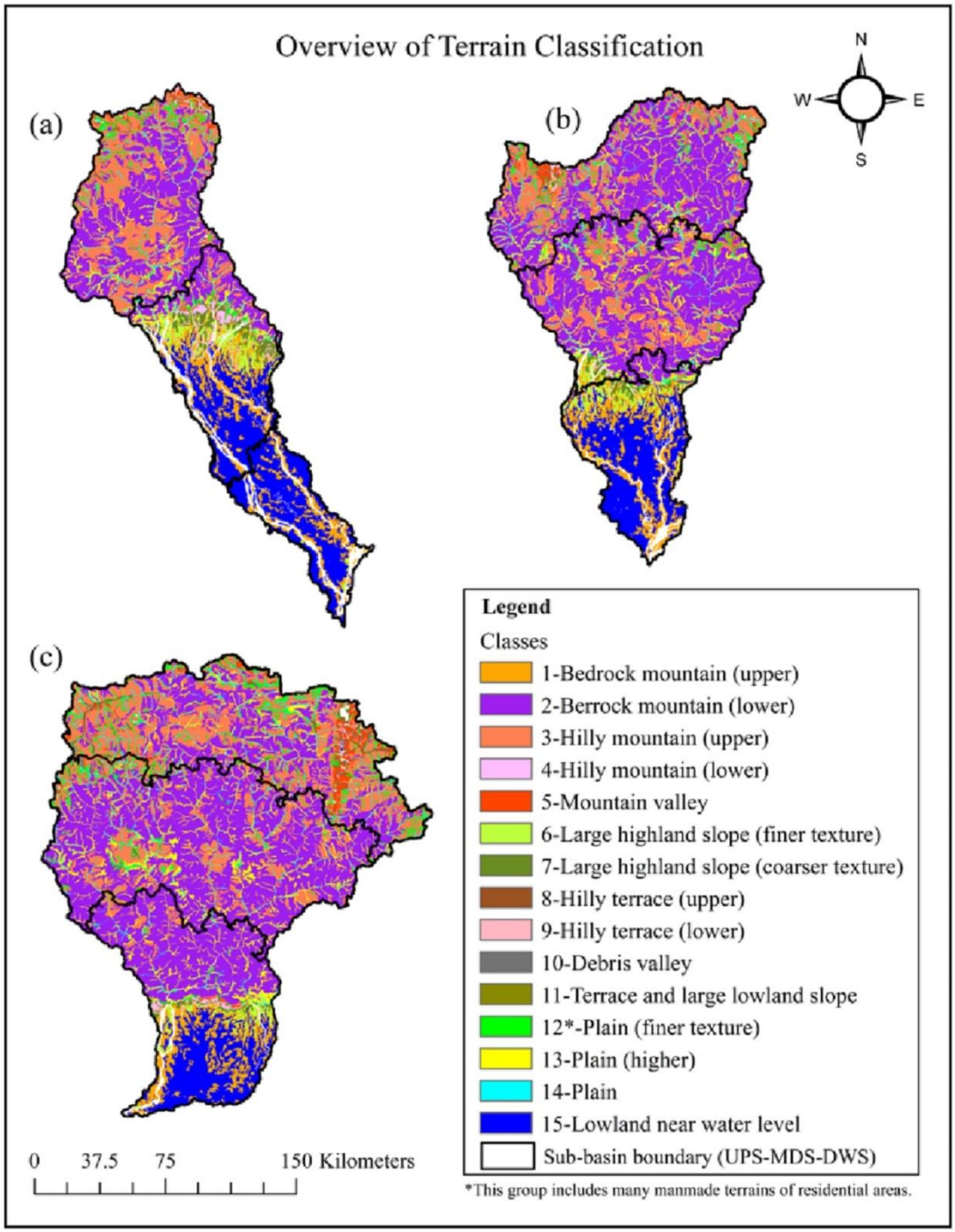

Fig. 3.9 Terrain classification with geomorphological features of a) Teesta, b) Torsa, and c) Manas basin based on the data of Iwahashi and Yamazaki (2022).

3.4.4 Index of connectivity (IC) analysis

3.4.4.1 Spatial analysis of IC

The spatial IC patterns of studied basins show non-homogenous connectivity potentials (Fig. 3.10). The region close to the channel network represents the higher potential connectivity and the area far from the channel network generally shows lower connectivity potential. The pattern of sediment connectivity is essential in large-scale river basins because the degree of connectivity is fundamental to understanding the response to natural and anthropogenic disturbances (Wohl et al., 2019). The distribution and descriptive statistics of IC values for different basins are presented in Fig. 3.11 and Table 3.6, respectively.

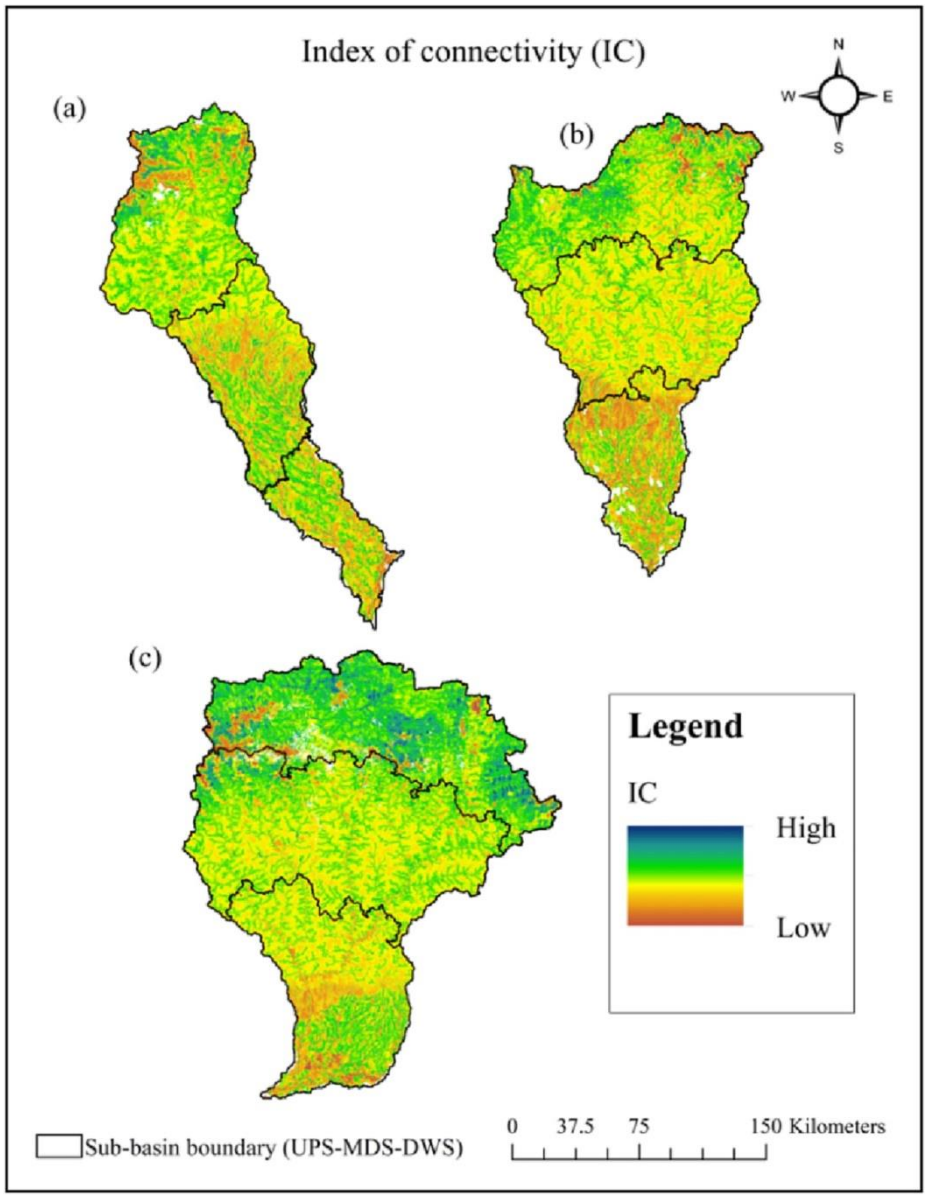

Fig. 3.10 Spatial distribution of index of connectivity for (a) Teesta, (b) Torsa, and (c) Manas basin.

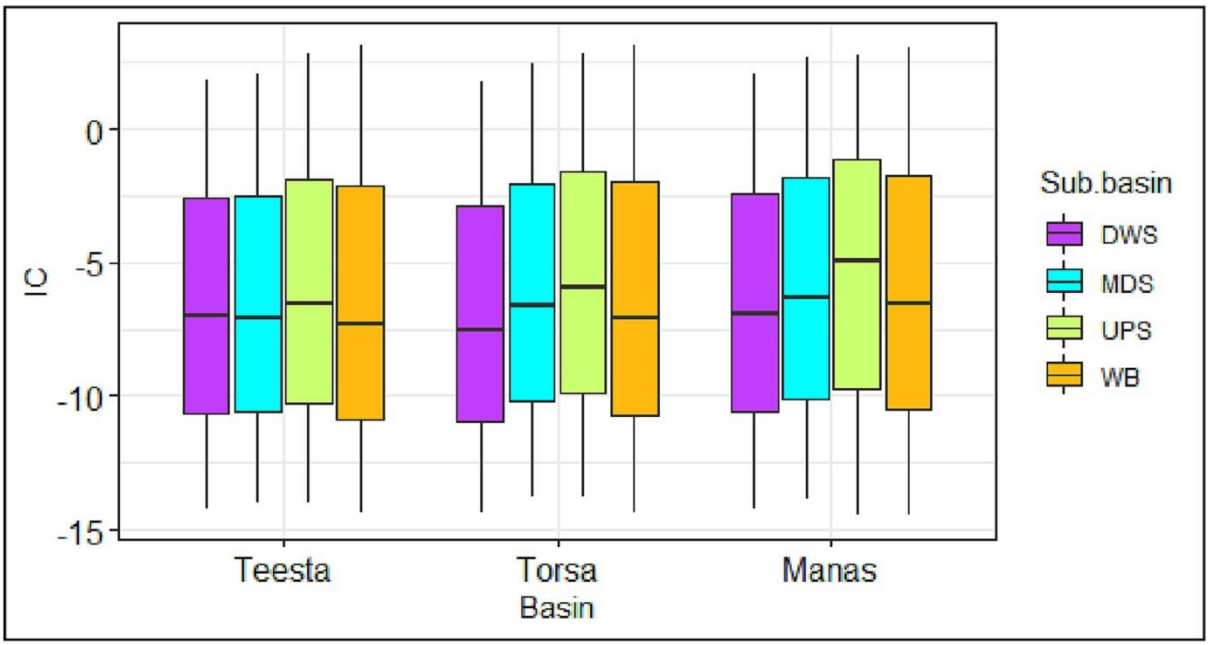

Fig. 3.11 Distribution of IC for each basin and sub-basins are shown in box plots.

Table 3.6 Descriptive IC statistics of studied basins

Basin	Sub-basin	Min	Max	Mean	Std.
Teesta	UPS	-14.02	2.80	-6.55	1.89
	MDS	-14.01	2.08	-7.08	2.02
	DWS	-14.21	1.81	-7.02	2.22
	WB	-14.42	3.10	-7.30	1.94
Torsa	UPS	-13.77	2.79	-5.96	1.91
	MDS	-13.78	2.47	-6.63	1.27
	DWS	-14.39	1.75	-7.50	2.15
	WB	-14.39	3.09	-7.09	1.73
Manas	UPS	-14.48	2.76	-4.98	2.27
	MDS	-13.83	2.70	-6.34	1.54
	DWS	-14.21	2.08	-6.92	1.88
	WB	-14.49	3.06	-6.52	1.96

The inter-sub-basin comparison of IC values shows that higher IC values have been observed mainly along the UPS zone rather than along the MDS and DWS zones. The higher mean IC values (>−6.55) along the UPS zone represent higher potential connectivity within the channel because of high hillslope slopes from upstream areas. In the MDS and UPS reaches, higher values are observed compared to the DWS, which shows moderate to low (<−6.92) IC values. Compared with UPS, the mean IC values at MDS are decreased by 0.53, 0.67, and 1.36 in Teesta, Torsa, and Manas, respectively. Also, at DWS, the mean IC value is reduced by 0.45, 1.90, and 1.94 in Teesta, Torsa, and Manas, respectively, compared to UPS. The decreased mean IC values from UPS to MDS and DWS reflect the decrease in sediment

connectivity in these basins. The IC variations from upstream to downstream are distinct, with high and slightly connected areas visible to higher and lower slope areas. Higher slopes in the UPS zone and agriculture patches or built-up areas along the DWS zone may contribute to high IC variations from its upstream to downstream (Mishra et al., 2019; Swarnkar et al., 2020).

Furthermore, the inter-basin comparison shows higher IC values for Manas (−6.52), followed by Torsa (−7.09) and Teesta (−7.30). The difference in mean IC values among these basins is not so high but still distinctive. The connectivity pattern may be attributed to the upstream-downstream linkage of the basin, where topography and land use play a dominant role. However, lower IC values along the DWS of Torsa (−7.50) and Teesta (−7.02) show disconnected terrain, affecting the overall sediment connectivity or routing in these basins. The lower average annual discharge (1001 m^3/s) at Kaunia (Bangladesh) station from (1985 to 1991) and the decrease of water flow at Dalia point from (1985 to 2006) (Mondal and Islam, 2017) of Teesta can confirm the lower IC values and lower connectivity potential at the DWS of Teesta (Fig. 3.3 E). In addition, the anthropogenic disturbances along the Teesta basin were reported in several cases (Khan and Islam, 2015; Goyal and Goswami, 2018), which may significantly affect these basins' sediment connectivity and transport.

The differential IC values suggest varied connectivity where the UPS are slightly better connected and, hence better or more efficient sediment transport than MDS and DWS. The lower IC values along the DWS suggest a poorly developed channel and lower sediment transport efficiency because of valley-shaped landforms and a more downward slope favoring deposition. The significant standard deviation of IC values also illustrates the variability of connectivity patterns among these basins (Table 3.6).

3.4.4.2 Connectivity index and ground-based evidence

Positive correlations between the magnitude of the hydrological process and the sediment connectivity or transport were reported in several earlier studies (Hu et al., 2019; Arabkhedri et al., 2021; Zanandrea et al., 2021). Correlations between mean IC values and the ground-based average annual yield of respective basins, collected from the IUCN physical assessment report on the Brahmaputra River basin prepared from the India-Bangladesh joint field investigation (Mahanta et al., 2014; Pangare et al., 2021), however, shows a slightly negative correlation (Fig. 3.12A). On the other hand, the mean IC values plotted against the geometric signatures (ZlnSLOPE, ZlnHAND, and ZTexture) of terrain classes, which is a

proxy for the topographic application and the sediment supply potential (Iwahashi et al., 2021), show positive correlations (Fig. 3.12B). Although the sample size of this study is too small to statistically validate the results, these may suggest that the relationships between sediment connectivity and yield may not follow the general trend in large-scale basins. For this, more data collection of IC and site-specific ground-based sediment yield observation would be required.

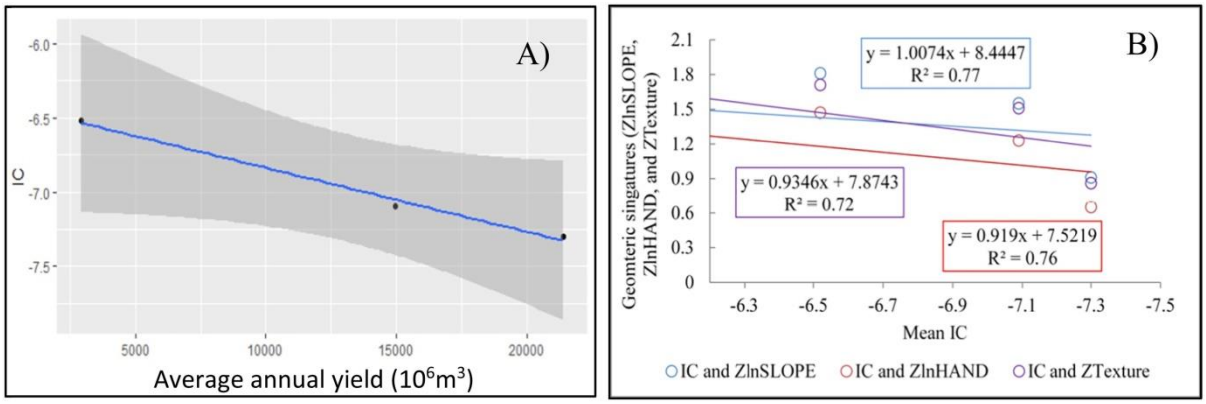

Fig. 3.12 Correlations between A) mean IC and ground-based average annual yield (blue line and gray shading denote the regression line and 95 % confidence interval, respectively), and B) Mean IC and geometric signatures of terrain classes (P value<0.05).

3.4.5 Inter-relationship among morphometric and topographic variables

Like the morphometric studies of Faghih et al. (2015), Pant et al. (2020), and Różycka and Migoń (2021), correlation analysis has been performed here to examine interrelationships among fifteen (15) different morphometric and topographic variables. Pearson's correlation is frequently used for this purpose and the results of the correlation matrix are given in Fig. 3.13. The correlation matrix of morphometric and topographic variables depicts a significant positive correlation between D_t-F_s, F_s-If, If-D_t, Cc-R_n, slope-SPI, and STI-TPI. Also, significant negative correlations between slope-D_t, slope-TWI, If-SPI, and TWI-SPI have been observed. Various positive and negative correlations depict the interrelationship and importance of these parameters for characterizing the basin.

In addition, the GLMMs test signifies the effect of morphometric and topographic factors (independent variable) on sediment connectivity (IC) (response variable), where SPI shows the best fit model (lower AIC) compared to other factors (Table 3.7). The Akaike information criterion (AIC) is considered an estimator of a model's relative goodness fit for a given dataset, where the lower AIC value represents the best model (Akaike, 1974).

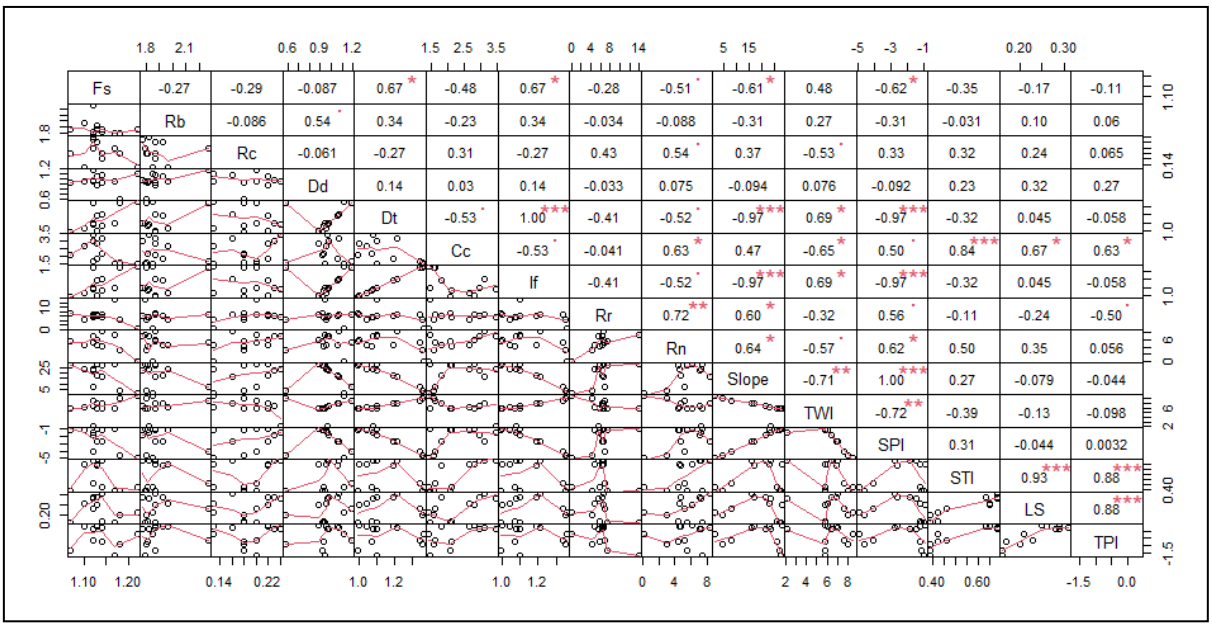

Fig. 3.13 The correlation matrix represents the relationships and relative importance of morphometric and topographic indices (abbreviations are according to Table 3.3). The right half shows the Pearson correlation matrix with the significance level (***P<0.001; **P<0.01, *P<0.05). The left half is the data distribution and bivariate scatter plot with fitted lines.

Table 3.7 Results of Generalized linear mixed models (GLMMs) testing the effects of morphometric and topographic factors on connectivity (IC). The models were summarized as A) multivariate, B) univariate, and C) Null model in the table

Explanatory variables	Log-likelihood	Akaike information criterion (AIC)	P value
A) Multivariate model			
SPI× R_n×F_s× D_d×R_b	1.89	18.20	<0.001***
B) Univariate models			
SPI	-8.60	27.20	<0.001***
R_n	-9.02	28.00	<0.001***
F_s	-7.90	29.50	0.022 *
D_d	-11.91	33.80	<0.001***
R_b	-11.88	33.80	0.0087 **
C) Null model	-11.91	31.80	

Note: When there are multiple explanatory variables that often have correlations with each other, this can lead to a distortion of the effects of the explanatory variables on the response variables due to collinearities with redundant effects. For this reason, explanatory variables without strong correlations (correlation coefficient > 0.7; $p < 0.05$) to others were selected to be included in GLMMs to avoid multicollinearity (Dormann et al., 2013). The GLMMs were constructed by considering stream power index (SPI), ruggedness number (R_n), stream frequency (F_s), drainage density (D_d), and bifurcation ratio (R_b) as main factors, IC as a response variable, and sub-basin nested within the basin as a random variable. Multivariate and univariate models denote the interaction and univariate effects on response variable, respectively. All models were compared separately with null models.

3.5 Discussion

3.5.1 Morphometric characteristics of the basin

Noticeable differences in the morphometry of stream network, drainage density, stream frequency, bifurcation ratio, relief ratio, and longitudinal profiles determine the hydro-geomorphic response of individual basins. These basins generally show a higher stream order of 7^{th} to 8^{th} with the dominance of first order streams indicating the existence of a highly permeable lithology leading to a lower infiltration rate, suggesting greater discharge potential (Bindu et al., 2012; Oyedotun, 2020). The average annual discharge of 21,434 m^3/s at Bahadurabad (Bangladesh) station from 1956 to 2011 can validate the discharge potentialities of these basins. The lower mean bifurcation ratio of <3 shows that these basins are not much influenced by tectonics and geological structure (Sreedevi et al., 2009; Arulbalaji and Gurugnanam, 2017). The drainage density values from our study (range: 1.19 to 0.96) may result from the weak or impermeable subsurface material, sparse vegetation, and mountainous relief (Ozdemir and Bird, 2009; Kanhaiya et al., 2018). The low or moderate slope in downstream areas leads to a higher drainage density, whereas the lower drainage density characterizes a steeper slope at upstream reaches in these basins. As a result, lower surface runoff may be experienced downstream, but an opposite hydrological situation may occur in upstream regions. The drainage density is positively correlated with the relief and erosion process (Sangireddy et al., 2016; Oyedotun, 2020), rapid storm event runoff (Montgomery and Dietrich, 1989; Tucker and Bras, 1998), and hence the sediment supply to the fluvial network (Clubb et al., 2016). However, higher drainage density in these basins may result in potential hydrological responses such as high catchment runoff and potential sediment supply to the downstream fluvial system. The high basin relief of Teesta (7901 m), Manas (7490 m), and Torsa (7208 m) that suggest steepness, accompanied by higher rainfall patterns (Table 3.1), may determine the hydro-geomorphic characteristics, including flood pattern, erosional processes, and sediment transport in these basins (Hadley and Schumm, 1961; Burrough et al., 2015). Thus, the high relief ratio of these basins may intensify the erosion processes and increase the sediment transport capacities that are produced by upstream portions. Various morphometric features discussed here may significantly control geomorphological processes and the hydrological behavior of downstream areas.

The upstream region shows a mostly steepened longitudinal channel, indicating the potential erosion and sediment transport from the upstream headwater region. Our sediment

connectivity analysis also suggests higher IC and connectivity potential at most upstream reaches than midstream and downstream. The channel steepness patterns and irregularities show that the studied basins are erosional landscapes controlled by regional tectonic uplift, water, and sediment discharge (Goswami, 1985; Shi et al., 2020). Downstream, mostly dissecting profiles with errors or irregularities have been observed where the elevation change is limited but may be sensitive to the deposition of sediment. It can also be assumed that, after traveling a long distance, the sediments may be deposited in downstream areas, which are the characteristics of riffle-pool sequences at lowland rivers (Wohl and Merritt, 2008; Rhoads, 2020). The typical concave profiles associated with downstream decreases of elevation characterize the wider valleys, which may impede sediment connectivity and transport potentials of these basins. With the decline of gradient in the downstream direction, the main channel of the Brahmaputra basin receives sediment inflow from many tributaries, creating a possible clogging of the sediment, giving it an intensely braided character (Rajbanshi et al., 2022). The excessive channel deposits, locally called chars (river islands) visualized from the field investigation, are typical characteristics of a braided river that may significantly alter the geomorphology of Brahmaputra's channel planform (Takagi et al., 2007; Rajbanshi et al., 2022).

It is known that the topographic factors affect the sediment discharge and connectivity in a river basin (Cheng et al., 2017). The responses of different topographic factors suggests that steep slopes with high SPI, STI, and lower TWI are expected to have high sediment connectivity and transport potential in the UPS region. On the other hand, a more gently sloping basin with lower SPI, STI, and higher TWI shows lower sediment connectivity and transport potentials at midstream and downstream favoring deposition. The recent field investigation at Teesta downstream in Bangladesh also reveals the presence of depositional features, where bankline erosion is widespread and sediments accumulated (Fig. 3.1C–D). Furthermore, the terrain classification data of Iwahashi and Yamazaki (2022), proxy to the topographic applications, correlates significantly with our study's topographic pattern and effectively reflects our observations. However, topographic factors derived from a 30–m DEM resolution may affect the values of the indices, which can be investigated in future research (Chen and Yu, 2011; Panagos et al., 2015).

3.5.2 Sediment connectivity of the basins

In geomorphology, sediment connectivity studies are valuable to understand the sediment dynamics (Heckmann et al., 2018; Wohl et al., 2019), characterizing the geomorphic system (Buter et al., 2022), and addressing geomorphic vulnerabilities (Alca'ntara-Ayala, 2002), which is considered here for understudied Brahmaputra River. The meteorology, drainage basin and topographic characteristics, and connectivity index affect the sediment dynamics of these basins (Table 3.8). The spatial mapping of hillslope to channel connectivity shows considerable variations and inhomogeneity in these basins (Fig. 3.10). The slopes, debris fans, and alluvial plains are considered key drivers influencing the sediment conveyance from hillslope to channel within the sediment cascade (Fryirs et al., 2007; Messenzehl et al., 2014). Here, the presence of bedrock mountains, mountainous valleys with large highland slopes, and lowlands near the water table from upstream to downstream might be one reason for such an inhomogeneous connectivity pattern in these basins (Sharma et al., 2012). However, limited ground-based average annual yield data, field investigations, and quantitative geometric signatures based terrain classification greatly support our sediment connectivity analysis.

Table 3.8 Comparison of the overall response to sediment connectivity

Basin	Remarks based on meteorology, geo-morphometry, topographic, and connectivity features
Teesta	Steep terrain, high relief ratio, higher SPI, STI, and IC at UPS, and higher annual rainfall infer a highly connected system, but dissected stream profiles and lower topographic control at MDS and DWS limit connectivity potentials.
Torsa	Steep terrain, high relief, higher SPI, STI, and IC values at UPS with moderate annual rainfall infer a highly connected system for potential sediment transportation. However, connectivity decreases at DWS caused by lower SPI and topographic control.
Manas	Moderate relief ratio, gentle stream profiles, and lower annual rainfall infers a moderately connected system instead of relatively higher IC values at UPS compare to MDS and DWS.

High IC values with higher slope, SPI, and STI depict a highly connected zone (coupled with stream network) along the UPS, resulting in increased sediment transport efficiency as mentioned by previous studies (López-Vicente et al., 2013; Jing et al., 2022). The high IC pattern in the upstream region corresponds with the presence of highland slopes, hilly mountains, and steep valleys (Sarma, 2004; Singh, 2007; Iwahashi et al., 2021). On the other hand, low IC values with lower slope, SPI, and STI along the MDS and DWS depict a

minimally connected zone where the transported sediments maybe deposited. These lower IC values indicate the propensity of these areas to be decoupled from the stream network because of gentler slopes and longer flow paths (Fryirs et al., 2007). The considerable number of large and mid-channel bar developed along with bank migration within the studied basin (Singh, 2007; Sharma et al., 2012; Ashworth and Lewin, 2012), especially in middle and downstream areas, may configure lower connectivity aspects, which may alter the Brahmaputra's planform characteristics (Rajbanshi et al., 2022). In turn, the frequent changes of channel planform may influence the basin-scale geomorphology (Rajbanshi et al., 2022) and increase flood risks (Rao et al., 2020), which is predicted based on Brahmaputra's basin hydrology (Alam et al., 2016) and sediment flux (Rahman et al., 2018).

The upstream-downstream linkages of geomorphological processes in Himalayan River basins were severely impacted by anthropogenic structures, i.e., channel diversions, hydroelectric projects, dams, embankments, etc. (Nepal et al., 2014). The dams in Ganga–Brahmaputra control the discharge, which caused a 31 % reduction in its downstream sediment contribution compared to the past and is expected to be aggravated in the future (Gupta et al., 2012; Higgins et al., 2018; Bandyopadhyay et al., 2023). The anthropogenic disturbances on the large river systems may result in the reduction or loss of connectivity and the nature of sediment supply (Jain and Tandon, 2010; Fryirs and Brierley, 2013; Sinha and Ravindra, 2013; Oyedotun, 2016). Hence, the anthropogenic modifications (hydroelectric projects, dams, barrages, channel diversions, hydro-engineering structures) noticed along the studied basins (Fig. 3.14) may decrease sediment connectivity or (dis)connectivity in the mid-to-downstream region and potentially reduce the flow-sediment flux to the main channel. For instance, the diversion of upstream water of the Teesta basin by Gozoldoba (India) and Teesta barrage (Bangladesh) led to a severe water shortage and the channel drying up in downstream Bangladesh (Mondal and Islam, 2017; Goyal and Goswami, 2018; Singh et al., 2021; Pangare et al., 2021) (Fig. 3.15). Hence it might be one of the reasons for the substantial decrease of sediment connectivity of Teesta at MDS and DWS compared to the upstream areas. Also, the alternation of the natural flow of the Torsa and Manas rivers caused by hydro-engineering structures was reported earlier, which might influence the decreased sediment connectivity along the midstream and downstream regions of these basins (Sharma et al., 2012; Yasuda et al., 2017; Higgins et al., 2018; Saha and Bhattacharya, 2019). The study of Poeppl et al. (2017) underlines the impacts of human-induced alternation of fluvial

processes, connectivity, and geomorphic changes in the catchment systems, but are beyond the scope of this article.

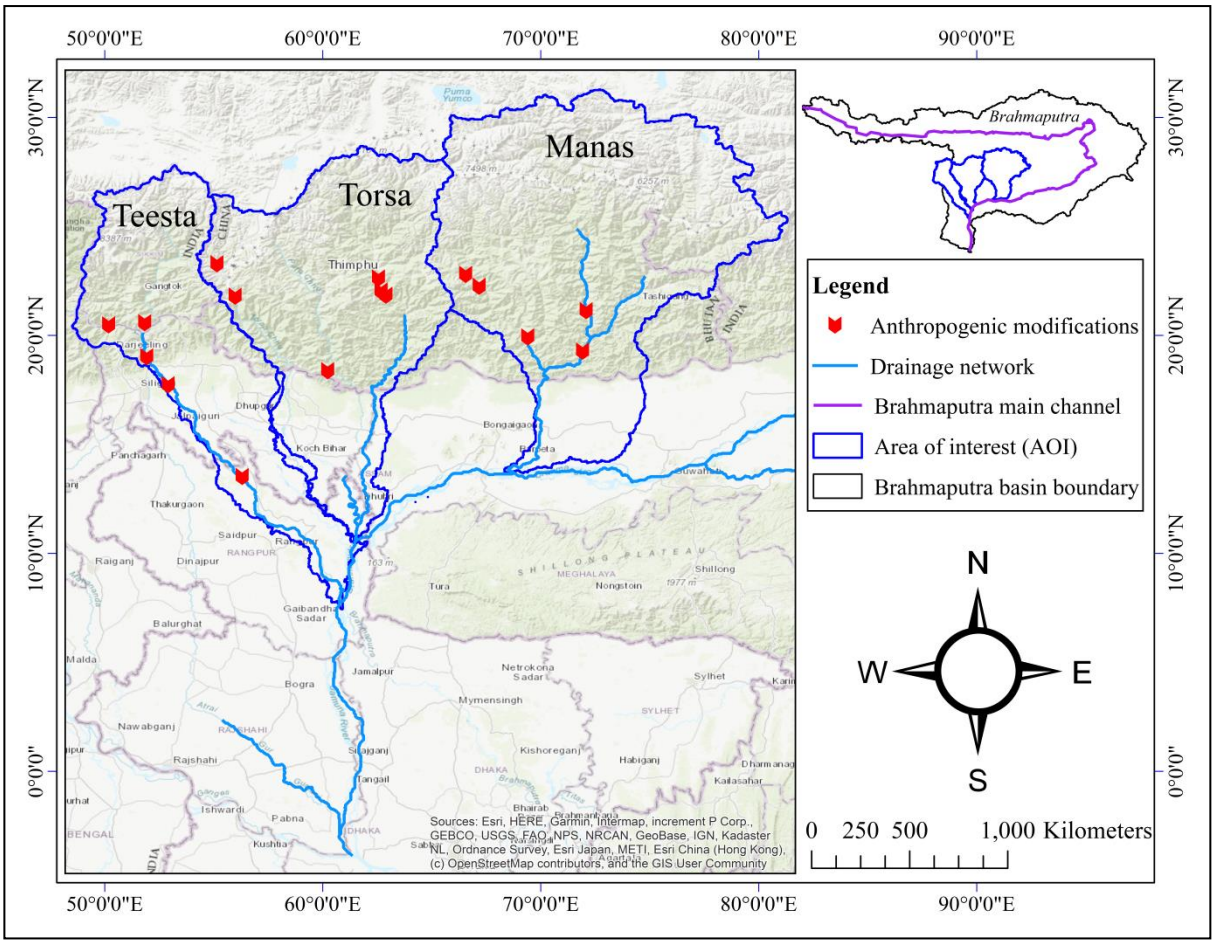

Fig. 3.14 The spatial distribution of anthropogenic inferences (dams, barrages, hydroelectric plants, channel diversion, and hydro-engineering structures) along Brahmaputra basins (Teesta, Torsa, and Manas) is shown with background topography as an example. The enlisted (16) anthropogenic modifications are the i) Teesta low DAM-III, ii) Rammam hydroelectric project-III, iii) Teesta low DAM- IV project, iv) Gazoldoba barrage & diversion at Teesta (India), v) Teesta barrage & diversion (Bangladesh), vi) Punatsangchhu-I hydroelectric project, vii) Punatsangchhu-II hydroelectric project, viii) Basochhu hydropower project, ix) Kurichu hydroelectric project, x) Mandechchhu hydroelectric project, xi) Tangsibji micro hydropower plant, and xii-xvi) Hydro-engineering structures. The location and name of the anthropogenic modifications are based on google earth satellite imagery.

Furthermore, land cover directly affects sediment connectivity (López-Vicente et al., 2013; Llena et al., 2019), and here the decreased connectivity from the up-to-downstream region may be attributed to the presence of high vegetation coverage and lower agricultural patches or barren land (Table 3.1), which may potentially impede the sediment transfer. The heterogeneities of the spatial pattern of sediment connectivity presented in this study can have drastic impacts on the overall behavior at basin-scale river system because the changes

in connectivity may lead to changes in morphodynamics and sediment budgets (Fryirs et al., 2007; Turnbull et al., 2008). Connectivity studies in different parts of the world, for example, India (Mishra et al., 2019; Swarnkar et al., 2020), China (Xie et al., 2020), Japan (López-Vicente et al., 2017), Spain (Llena et al., 2019), the Italian Alps (Cavalli et al., 2013; Martini et al., 2020), the Swiss Alps (Messenzehl et al., 2014), and Brazil (Zanandrea et al., 2019) shows how the connectivity at different scales (e.g., hillslope, river reach, sub-catchment) affect the sediment dynamics and geomorphic processes. Similarly, our connectivity analysis identified the upstream watershed as a sensitive part of the landscape where the channel network or the morphodynamics (e.g., hillslope-channel network, upslope erosion, activation of sediment source by landsliding) severely impacts the connectivity in downstream areas and hence the basin-wide fluvial-geomorphic processes.

Fig. 3.15 A) Teesta barrage in Bangladesh, B) diversion of channel from the barrage for irrigation, C) deposition within the channel, and D) erosion along the bank.

The highly connected upstream region may increase the Brahmaputra's sediment flux, but the reduced connectivity downstream may cause sediment storage within the floodplain and contribute to the riverbed aggradation (Fryirs et al., 2007; Poeppl et al., 2020). The

partial connectivity or (dis)connectivity scenario observed here may form a barrier to sediment movement (transport-limited system), restraining the large volume of sediment transfer supplied from upstream along the lowland plain (Brierley and Fryirs, 2005; Fryirs and Brierley, 2013). The (dis)connectivity affects the internal dynamics of the sediment cascade both spatially and temporally, which provides a basis to examine cumulative responses to disturbance, whether natural or human-induced (Fryirs and Brierley, 2013). In partially connected or disconnected systems, materials eroded and transported from upstream parts of catchments may be deposited in accumulation zones (lowland plains or broad alluvial plains) over different periods, marked by alluviation, aggradation, and long-term sediment storage (Brierley and Fryirs, 2005; Jain and Tandon, 2010; Fryirs and Brierley, 2013). The sediment storage scenario (~49 % of eroded sediments) and riverbed aggradation rate (~1.47 cm/yr in the Brahmaputra) before the mouth of the Ganges–Brahmaputra (GB) rivers (Islam et al., 1999; Garzanti et al., 2011; Ashworth and Lewin, 2012; Dietrich et al., 2020; Faisal and Hayakawa, 2022), convincingly supports our study's observation, with the decreased connectivity or (dis)connectivity the depositional features may become prominent and hence may affect basin-wide geomorphic linkages.

3.5.3 Sediment transport potentials and implications

The sediment dynamics of these basins may be controlled by climatic, hydrological, geomorphometric, and sediment connectivity patterns. The SPI works as a proxy of discharge, which is related to the upslope contributing area and represents topographic steepness (Fontana and Marchi, 2003). Furthermore, Swarnkar et al. (2020) showed that sediment connectivity and stream power have equal importance in efficient sediment transport to the downstream region. Furthermore, the lower AIC value from the GLMMs test defines SPI as one of the influential factors on sediment connectivity potentials (Table 3.7). Therefore, SPI and IC have been integrated to demonstrate the combined effects on these basins' sediment transport potentials or accessibility. Then, the sediment transport potential maps (STPM) are prepared for respective basins (Fig. 3.16), which provides a general portrait of sediment transfer potentials and conveys critical information to identify the reaches that may receive higher sediment supply and transport along the main channel. The STPM raster images have been classified into five classes using natural breaks classification with successive classes of ‘very low,’ ‘low,’ ‘average,’ ‘high,’ and ‘very high,’ indicating increasing potential sediment transport (Xie et al., 2020). Our analysis suggests higher

sediment transport potential along the UPS region. In contrast, the MDS and DWS regions have low to very low sediment transport potential and may favor sediment deposition. These depositional phenomena may increase the severity of hydrological floods and erosion in the downstream region. For instance, approximately 2000 km of river reaches of Bangladesh annually experience bank erosion because of the floods, which resulted in the increase of homeless or landless people or even loss of human life (28,700 and 600 deaths caused by the flood of 1974 and 2007, respectively) (Siddiqui et al., 2018; Mondal et al., 2020; Pradhan et al., 2021).

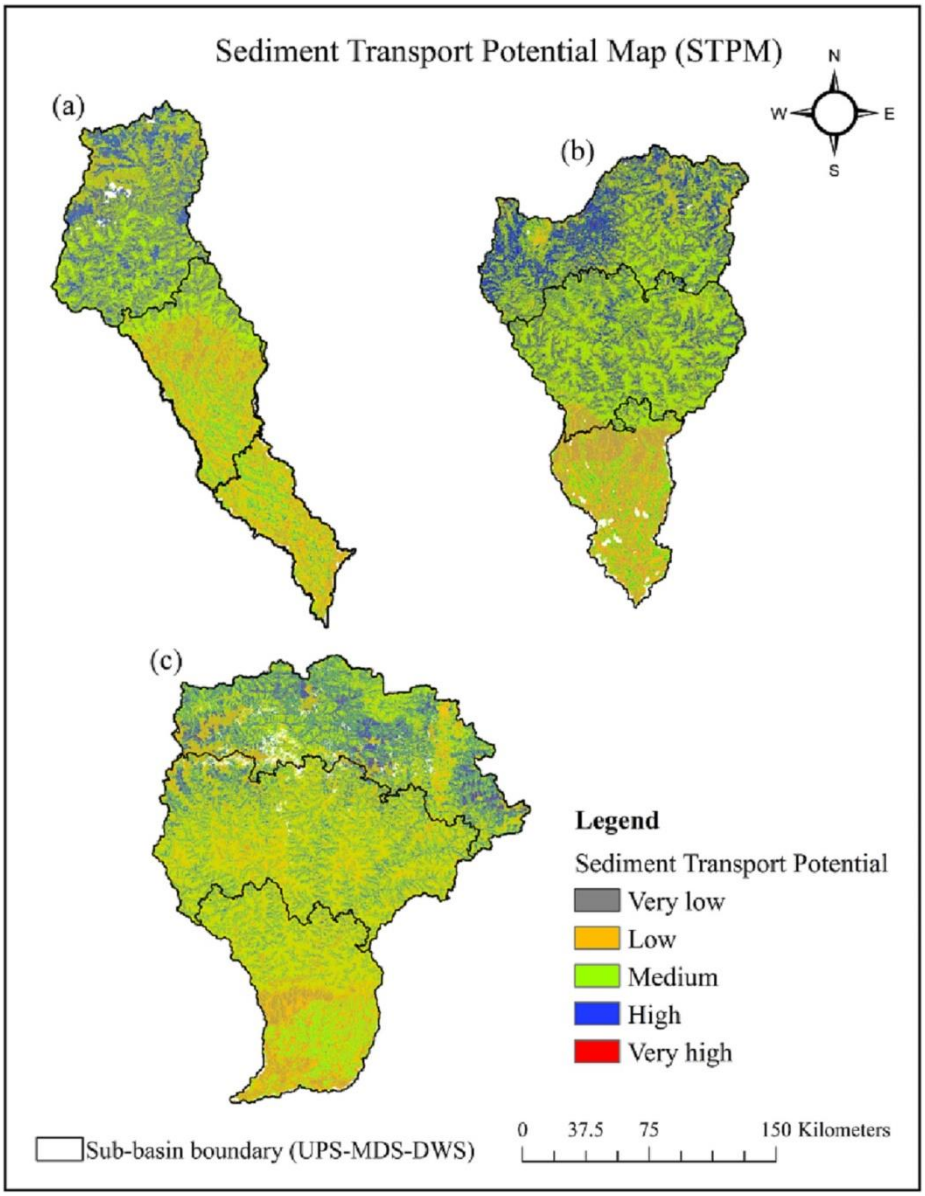

Fig. 3.16 Sediment transport potential maps for (a) Teesta, (b) Torsa, and (c) Manas basin.

Hence, in the simplified representation of sediment transport potential maps, areas characterized by high to very high or low to very low value classes could become observation

hotspots for future hydrological or sediment disaster management focusing downstream. For instance, identifying hot spot connectivity areas, strategic dredging or de-siltation of sediments, river interlinking, and improvements in channel navigation that consider the potential sediment transfer pathways and geomorphic processes can be effective for disaster management in the deltaic landscape of a downstream country in South Asia that is densely populated (about 41 % of the basin's population of 83 million resides in Bangladesh) (Mahanta et al., 2014; Foerster et al., 2014; Wohl et al., 2019; Martini et al., 2019). Our study provides the sediment transport pathways, a prerequisite for an efficient sediment management framework (White and Apitz, 2008) and sustainable river basin management (World Bank, 2015), encouragingly practiced in neighboring countries like India (Mishra et al., 2019; Swarnkar et al., 2020), China (Xie et al., 2020; Jing et al., 2022), and other parts of the world (Poeppl et al., 2020). Moreover, the conceptual considerations gained with morphometric GIS approaches and field investigation provides a valuable representation of sediment dynamics and fluvial geomorphic processes, particularly at the basin scale. However, it should be mentioned that the current approach to representing potential sediment transfer does not consider the whole spectrum of the sediment transfer process, e.g., high runoff, precipitation events, monsoonal floods, landslides events, etc. Furthermore, sediment size exerts significant influence on the sediment transport and depositional processes in the river system, which is highly variable and requires extensive grain size analysis for a better representation of sediment runoff in these large basins (Fryirs and Brierley, 2013; Oyedotun, 2016). Addressing these issues requires a more sophisticated approach with increased input data (higher resolution multitemporal DEM, more ground-based observations, river discharge data, etc.). In addition, it should be noted that the sediment transport potential may be changed, reduced, or disconnected by various anthropogenic structures on the upstream channel for multiple purposes like hydroelectric power generation, irrigation, navigation, water supply, flood moderation, etc. (Pradhan et al., 2021). Therefore, river engineering structures like embankments, dams, barrages, etc., should be planned in such a sustainable way that does not disturb the hydro-geomorphic regime and, simultaneously, lower the risk of recurrent sediment disasters in downstream regions. In addition, the proposed workflow, which is developed from open-source data, can be replicated in other areas where the high-resolution data are not available or inaccessible, but large-scale sediment transport processes need to be investigated effectively.

3.6 Conclusions

The middle Brahmaputra River basin's geomorphic diversity and sediment connectivity have been studied using meteorological factors (rainfall and discharge variability), geomorphometric and topographic variables, and a sediment connectivity index. These basins are characterized by contrasting morphometry, steep and dissected channel profiles, different topographic responses, and inhomogeneous sediment connectivity patterns that affect the river system's overall connectivity and sediment transport potentials from upstream to downstream. The highly connected system at the upstream zone with steep topography and higher rainfall intensity demonstrates its higher sediment transport potential. Nevertheless, the connectivity reduces in the mid-to-downstream area with mild or low topographic features, lowering the sediment transport potential and resulting in deposition, which may affect the basin-wide geomorphic processes. Despite limitations in DEM resolution and functionalities of IC and topographic indices, the computation of IC and other topographic parameters from the present study in an understudied basin gives a general portrait of sediment transport behavior, providing the first step towards integrated river basin management. This study contributes to the current literature and would be helpful to local administrators or policymakers in future river adjustments and planning, where understanding sediment connectivity or sediment transport pathways is crucial for large-scale sediment management and integrated river basin management. Additionally, understanding large-scale sediment connectivity and its impacts on sediment transport because of monsoon dynamics, climate change scenarios, and human interventions in the upper Brahmaputra is the most challenging problem in such large basins, which needs to be investigated in the future. Therefore, the current approach of integrating the geomorphic characteristics, topographic features, and connectivity index from freely available remote sensing data and easily implementable geospatial tools may encourage different groups of researchers to carry out multi-temporal geomorphic analysis (event-based, monthly, seasonal and annual scale) taking this study result as baseline information for future investigations. Furthermore, the availability of high-resolution multi-temporal DEM and ground-based sediment yield observations can provide further insights into the factors controlling fluvial dynamics and sediment connectivity in such diverse transboundary river basins.

Graphical abstract of Chapter 3:

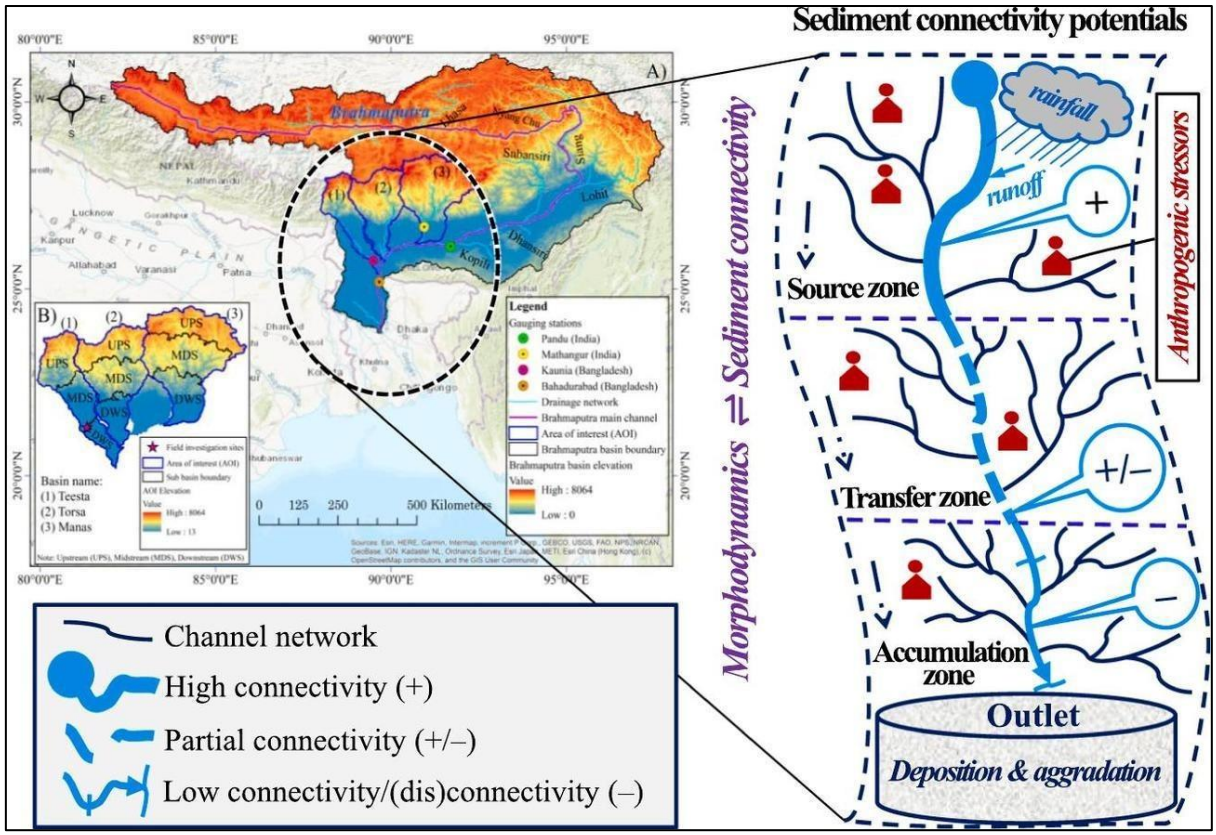

Highlights of Chapter 3:

- Morphodynamics and sediment connectivity patterns are key determinants of fluvial-sediment dynamics in Brahmaputra River basin.
- The sediment connectivity varies across the basins and is highly influenced by the upstream's hydro-geomorphic responses.
- Partial connectivity or (dis)connectivity in mid-to-downstream is sensitive to deposition, impacting geomorphic linkage.
- Understanding large-scale geomorphic processes is required for sustainable river management in disaster-prone South-Asia.

Chapter 4

Topographical dynamics based on global and UAV-SfM derived DEM products: A case study of transboundary Teesta River, Bangladesh

4.1 Introduction

In fluvial geomorphology, river topography measurement is a significant concern and a basic descriptor for understanding the geomorphic processes (Woodget et al., 2014; Özcan and Özcan, 2021). The analysis of spatiotemporal modifications of the river, which are suddenly changing the flow pattern and hydro-geomorphology due to natural and anthropogenic factors, requires better hazard assessment since these processes can result in flood phenomena and suffering to human society (Rinaldi et al., 2017; Fanta-Jende et al., 2020). In this regard, river topographic model plays a critical role in investigating a range of the earth's surface processes and detailed monitoring of the fluvial environment (Watson et al., 2019; Salandra et al., 2022). For topographic studies, freely accessible global digital elevation model (DEM) products such as National Aeronautics and Space Administration DEM (NASADEM, released in 2020), ALOS Global Digital Surface Model (AW3D30, released in 2020), TerraSAR-X add-on for Digital Elevation Measurement (TanDEM-X, released in 2018), Multi-Error-Removed Improved-Terrain (MERIT, released in 2017), Advanced Spaceborne Thermal Emission and Reflection satellite (ASTER, released in 2006), and Shuttle Radar Topography Mission (SRTM, released in 2003) are often used in the absence of finer resolution data which is limited for multitemporal assessment (Watson et al., 2019; Uuemaa et al., 2020). Among the existing freely available global DEM data sets, the NASADEM, reprocessed from the STRM-1999 measurement offer near-global land surface coverage at 30 m spatial resolution has been considered here as baseline topography because of its recent improvements and accuracy (NASA JPL, 2020; Uuemaa et al., 2020; Tran et al., 2023; Faisal and Hayakawa, 2023). The orbital nature of satellites hampered the revisit frequency (i.e., low temporal resolution) to the same location, so it is not easy to track dynamically changing rivers (Rhee et al., 2018).

The recent advents in Unmanned Aerial Vehicles (UAVs) are advantageous over satellite and piloted aircraft in data acquisition which is widely used in monitoring dynamic changes in river morphology (Van Iersel et al., 2016; Rusnák et al., 2018; Cai et al., 2022), natural hazards management (Giordan et al., 2018), and water resource management

(Acharya et al., 2021). The high-resolution DEMs generated from UAVs following the structure-from-motion (SfM) multi-view stereo photogrammetry (SfM-MVS) workflow are becoming increasingly common for assessing earth surface processes (Smith et al., 2015). Several studies, for example, Annis et al. (2020), Avand et al. (2022), Oguchi et al. (2022), and Salandra et al. (2022), demonstrated the importance of high-resolution DEMs for more accurate geomorphological and topographical analysis. The advances in survey equipment (i.e., UAVs, LiDAR) and data processing software (i.e., Agisoft Metashape) enables the production of rapid and accurate high-resolution topographic data (i.e., DEMs), over the decades in river environments (Picco et al., 2023). The characterization of hydro-geomorphological features, channel planform changes, and sediment dynamics (erosion and deposition processes) can be performed using high-resolution topographic analysis, which can significantly improve our understanding of fluvial regimes (Salandra et al., 2022). The advanced remote sensing techniques (i.e., LiDAR-light detection and ranging, UAV-SfM) are encouragingly used in South Asian countries like China, India, Bhutan, Nepal, and Pakistan for fluvial-geomorphic research (Faisal and Hayakawa, 2022). In contrast, the UAV-based approaches in fluvial geomorphological and topographical studies are still scarce or have not started in the context of the Ganges-Brahmaputra-Meghna (GBM) river system in downstream Bangladesh that is highly influenced by upper basin's morphodynamics, hydrology, sediment flux, and anthropogenic stressors (Faisal and Hayakawa 2022, 2023).

The recent advancement of fluvial research mentioned by Oguchi et al. (2022) and the geomorphic research gaps in large South Asian GBM Rivers by Faisal and Hayakawa (2022, 2023) necessitates the UAV-based topographic survey to assess the geomorphic features at Brahmaputra's river system that changes dramatically. In Bangladesh, several scholars have employed multi-temporal satellite imageries to investigate the Teesta River (Brahmaputra's tributary), focusing on channel dynamics (Khan and Hossain, 2001; Khan et al., 2015; Ashrafi et al., 2016; Akhter et al., 2019), channel bar evolution (Ghosh, 2014; Khan and Islam, 2015), and water flow patterns (Mullick et al., 2010; Mondal and Islam, 2017). Besides, several studies about morphological dynamics also exist in the upper part of transboundary Teesta River in India, such as Mandal and Chakrabarty (2016), Goyal and Goswami (2018), and Lukram and Tandon (2022). Unfortunately, little or no attention has been paid to the past literature on topographic change studies due to unavailability of multitemporal topographic data in the Teesta River that may have significant implications for understanding the sedimentation pattern and river floodplain management in disaster-prone

South Asian region. The present area of interest mostly relies on freely accessible terrain data sources. Hence, the topographic survey for introducing high-resolution terrain data has become necessary for investigating this region's topography and associated geomorphic dynamics. Therefore, the present work focuses on utilizing UAV imageries and newly available NASADEMs to assess the river's topographical dynamics as well as to show the potential applicability of advanced modern remote sensing techniques in developing areas of South Asia, Bangladesh along the Brahmaputra's right bank tributary (Teesta River).

The combination of advanced UAV-SfM techniques and satellite remote sensing embedded with field-based approaches may be helpful for topographic change studies, as the multitemporal DEMs were unavailable for the present area of interest. Recently, several studies have been conducted in different parts of the world deriving the topographical and morphological dynamics comparing the UAV-DEMs to the global DEM products, such as Hsieh et al. (2016) (Taiwan), Watson et al. (2019) (Nepal), Tang et al. (2019) (China), and Parizi et al. (2022) (Iran). Although the UAV survey will cover small area compared to the enormity of the Teesta River, this study definitely fills the knowledge gaps of the previous studies. The present study is attempted as a novel case study in deriving UAV-SfM-based high-resolution topography (UAV-DEM) and later compared with the available global DEMs (NASADEM) to evaluate the topographical dynamics and fluvial-geomorphic processes in South-Asian context focusing at Teesta River, Bangladesh (Fig. 4.1). Hence, the author assumes that the dynamics of topographic and volumetric changes (erosion and deposition) of a flood-vulnerable transboundary Teesta River in the Bangladesh floodplain can be quantified from the calculation of the difference between subsequent DEMs (DEM of Difference-DoD) during a specific time interval via two DEM data sets (UAV-DEM 2022 and NASADEM 1999) (Wheaton et al., 2010; Picco et al., 2023). Therefore, this article aimed to a) assess the topography and geomorphological features focusing on changes in elevation, volumetric estimates, and river cross-sectional profiles at disaster-prone Teesta River, and b) introducing UAV-SfM techniques for high-resolution data acquisition in the lowland river environment as a baseline topographic survey. The study's outcomes will help to understand the topographical dynamics and fluvial-sedimentation processes which can play crucial role in taking adaptive strategies for river floodplain management and reduce the people's suffering from repeated sediment disasters.

4.2 Materials and methods

4.2.1 Study area and UAV mission planning

This study has been conducted in the transboundary Teesta River that flows through the highlands in Sikkim, the hills of West Bengal, and the floodplains of West Bengal (India) and Bangladesh (Fig. 4.1). This river has a length of 414 km, drains an area of around 12,159 km^2, and traverses two different countries "India" (83%) and "Bangladesh" (17%) (Alford, 1992). In Bangladesh, the Teesta River traverses (170 km) through the extreme northern part of Bangladesh (Nilphamari, Lalmonirhat, Kurigram, Rangpur, and Gaibandha district) and are crucial for almost 10 million people in this region (BBS, 2016; Islam, 2016). The Teesta floodplain covers around 14% of the country's total cultivated land and is one the largest geomorphic units of Bangladesh (Akhter et al., 2019). It plays a crucial role in flushing silt and sediment deposited during the dry season, the region's lifeline for irrigation, agriculture, farming, fishing, and navigation (Prasai and Surie, 2013). The sediments are mainly recent floodplain deposits comprising of clay, silt, fine, and medium grain sand (Islam et al., 2014). The study area falls in a sub-tropical monsoon (June to September), mostly dry climatic region (pre-monsoon and post-monsoon), where mean annual rainfall is more than 1900 mm (decadal 2010-2019 average of 2408 mm) with mean temperature of 35°c and 15°c in the summer and winter seasons, respectively (Rahman et al., 2011; Akhter et al., 2019; Faisal and Hayakawa, 2023). The annual average discharge of Teesta River ranges from (280−470 m^3/s) over the 2011−2022 period, where extreme low-flow conditions (<50 m^3/s) (Fig. 4.2) during the dry season are likely to occur more frequently after India implements the Gozoldoba barrage in 1993 (Higano and Islam, 2002; Islam, 2016; Pangare et al., 2021).

Unfortunately, the exclusive control of Teesta's upstream water in the dry season at Gozoldoba (India) makes the Teesta barrage (operation started in 1990) in useless and fails the irrigation project in northern Bangladesh (Khan, 2001; Mondal and Islam, 2017; Goyal and Goswami, 2018). Furthermore, the sudden release of excessive water in the rainy season causes flood and bank erosion, leading to severe suffering for the people in Bangladesh (Higano and Islam, 2002). Given the large area of the Teesta River in Bangladesh (>2071 km^2), this study selects two cross-sections considering the minimal UAV survey coverage, assumed to be representative of the river's topographical and morphological features investigation focusing on dynamics changes of sediment and water on the floodplain over the years (Mondal and Islam, 2017; Akhter et al., 2019). The selected two cross-sections (CS-1

and CS-2) were relatively upstream and downstream from the location of the Teesta barrage (Fig. 4.1C), which is one of the anthropogenic interventions along the main river channel.

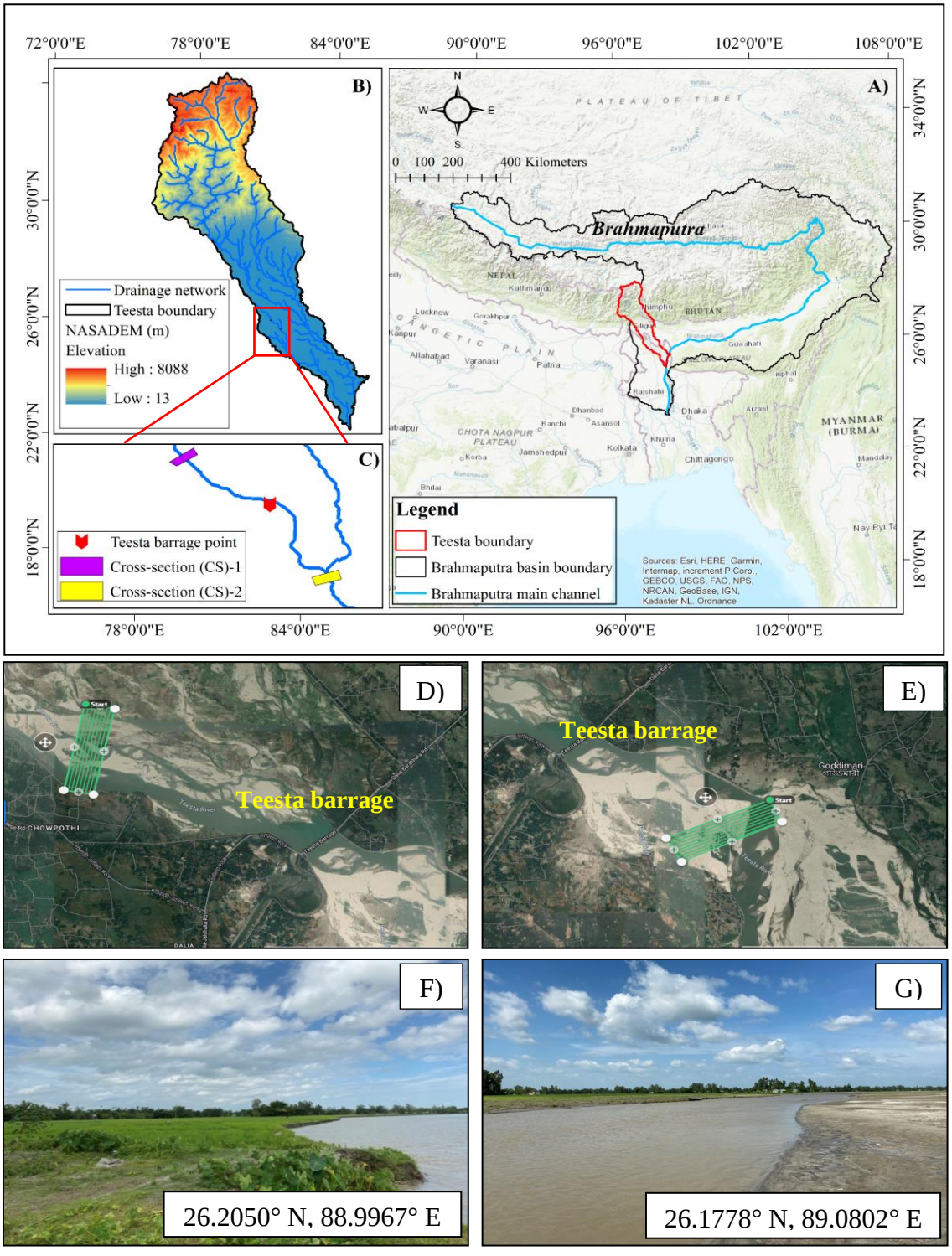

Fig. 4.1 A) Overview of study sites in Teesta River (Brahmaputra's tributary) showing the transboundary flow regime, B) elevation map with drainage channel, C) enlarged view of selected cross-sections, D-E) example of mission plan in DroneDeploy for CS-1 and CS-2, and F-G) field pictures showing the erosion along the bank at CS-1 and CS-2 taken in Aug 2022.

The UAV survey was planned in DroneDeploy, where Google Earth Pro was used to select the mission coordinates. The UAV used for the image recording is the DJI Mavic 2 Pro (equipped with a 20-megapixel, 1-inch RGB CMOS sensor and 35 mm f 2.8 lens with a 77° field of view), adjusted the altitude in Height Above Ellipsoid (HAE) to elevation using EGM96 (Earth Gravitational Model 1996) geoid model. The UAV automatically captured imagery, and each image was georeferenced with 3D coordinates from the UAV's global navigation satellite system (GNSS) receiver. Multiple flights with more than 75% front overlaps and 60% side overlaps were ensured to reduce the dome effect and uncertainty in elevation measurement (James and Robson, 2012; Hayakawa and Obanawa, 2020). With this flight plan (Table 4.1), 775 and 1,050 photos were collected from CS-1 and CS-2, respectively (Fig. 4.1 D-E).

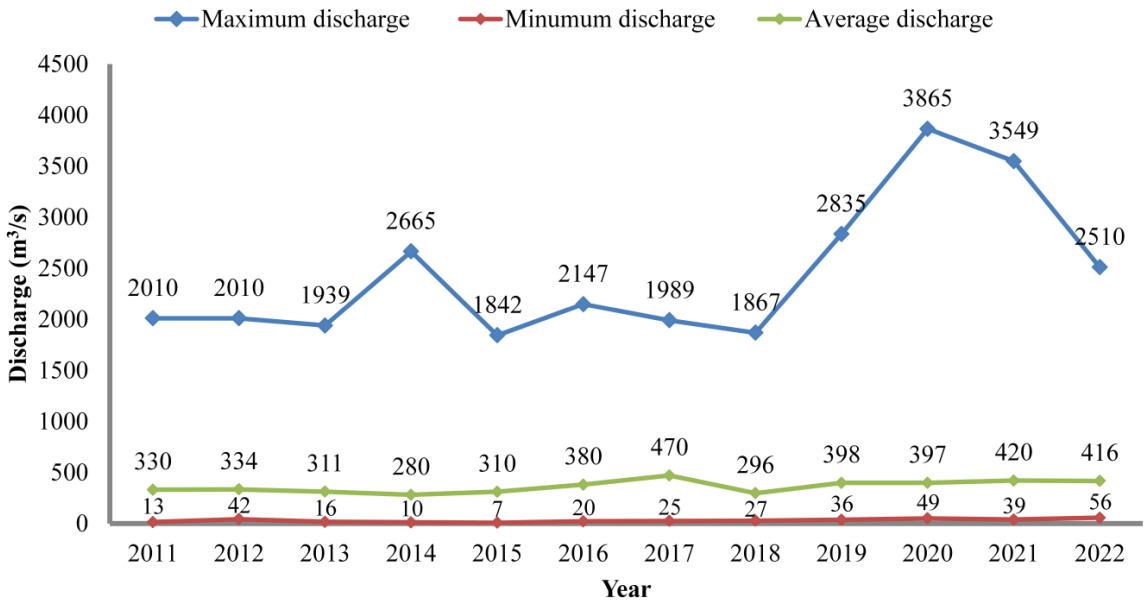

Fig. 4.2 Yearly discharge experienced by study reach measured at Dalia (Teesta barrage) gauging station from (2011-2022) (Data source: Hydrology directorate, BWDB).

4.2.2 Data processing

4.2.2.1 UAV data processing

The collected UAV imageries were processed using SfM-MVS photogrammetry software, Agisoft Metashape Professional (version 1.8.1 Build 13915, 64-bit), which can produce accurate DEMs from suitable photographs and are used for geomorphic observations, i.e., debris flow, landslide area, sediment deposits, etc. (Tsunetaka et al., 2020; De Haas et al., 2021). The standard workflow has been followed to generate the DEMs and orthophotos from the collected photographs (Smith et al., 2015; Saito et al., 2018; Hayakawa and Obanawa, 2020; Giulietti et al., 2022; Agisoft, 2022). The photograph datasets were imported into Metashape, and the 'estimate image quality' program was run for all the photographs before the image alignment. An image quality value of 0 to 1 indicates the sharpness of the photograph (Wang and Watanabe, 2022), and here the photographs with a value >0.7 were used for subsequent processing. Here, some unnecessary photographs (e.g., repeated photographs) were deleted to reduce the processing work.

Distorted pictures resulting from the windy conditions on the flight day and water surface reflectance limit the image alignment in data processing (Hinge et al., 2019). Here, original UAV image coordinates obtained by uncorrected single positioning of the aircraft GNSS receiver were used for image alignment. After that, image alignment of medium quality was applied to generate the point clouds. Then these point clouds were further processed to generate high-resolution DEMs (as new DEM) and orthorectified images at WGS 1984 (UTM Zone 46N) coordinate system. We adopted this approach because of the unavailability of external GNSS receiver station, ground control point (GCP), referenced map, and difficulty in accessing possible check points locations in the land-side area. We needed extensive locations along the survey site to place if the check points or GCPs were to be placed for reducing model error (James and Robson, 2012; Hayakawa and Obanawa, 2020), but the accessibility was quite limited (Fig. 4.1F-G). The error of generated DEM in the absence of GCPs mostly comes from rational function model error and may impact on the accuracy of generated DEM (Wang et al., 2019). The characteristics of UAV surveys and the generated DEMs and Orthorectified images are given in Table 4.1.

4.2.2.2 NASADEM processing

The NASADEM_HGT (30m, void-filled), created by the NASA-MEaSUREs program and publicly released in February 2020, have been downloaded for the area of interest from NASA-LPDAAC (Land Processes Distributed Active Archive Center) website (available at https://earthexplorer.usgs.gov/) (NASA JPL, 2020; Buckley et al., 2020). The necessary processing including mosaicking, raster projection, and clipping of acquired data have been performed in ArcGIS (ESRI). This study selected NASADEM (as reference surface or old DEM of 1999) from global DEMs products because it is relatively new and considered as the most accurate compared to other freely available DEM datasets, e.g., ASTER, AW3D30, MERIT, SRTM, and TanDEM-X (Franks et al., 2020; Uuemaa et al., 2020; Li et al., 2020; Tran et al., 2023; Faisal and Hayakawa, 2023).

It is reprocessed from the radar-based SRTM 1999 (Farr et al., 2007) with many improvements to its quality, notably void reduction and artifacts removal through improved phase unwrapping using auxiliary data from various datasets such as ASTER GDEM, PRISM (Panchromatic Remote-sensing Instrument for Stereo Mapping), GLAS (Geoscience Laser Altimeter System), and ICESat (Ice, Cloud, and Land Elevation Satellite) in processing techniques (Crippen et al., 2016, Buckley et al., 2020; Oguchi et al., 2022; Tran et al., 2023). The vertical accuracy of NASADEM has been revealed as 5.3 m (USA) (Buckley et al., 2020), 6.39 m (Estonian) (Uuemaa et al., 2020), 6.59 m (China) (Li et al., 2022), 12.08 m (New Zealand) (Uuemaa et al., 2020), and 12.6 m (Tibetan Plateau) (Chen et al., 2022). Furthermore, the NASA Jet Propulsion Laboratory (creators of the dataset) claims that the radar does an excellent job of penetrating the vegetation canopy, so the digital terrain model (DTM) bias is not significant (Franks et al., 2020).

4.2.3 Methods

4.2.3.1 DEM of difference (DoD) and volumetric estimates

The differencing of sequential DEMs to create a DEM of difference (DoD) is particularly relevant to geomorphic studies because a DoD may provide spatially distributed surface model of topographic and volumetric change over time (James et al., 2012). Recently, the DoD maps have been widely used in various studies regarding sediment transport, erosion volume estimation, landslides, and earthflow (Rumsby et al., 2008; Tseng et al., 2013; Hsieh et al., 2016; Hayakawa and Obanawa, 2020; Wang and Watanabe, 2022). In this study, DoD

maps have been produced for two cross-sections over the study area. For this, the fine-resolution UAV-DEMs (0.10 m & 0.11 m) have been resampled to medium-resolution (30 m) products for the homogeneity of the resolution by using bilinear interpolation method (Tang et al., 2019). Then, two sets of DEMs (UAV-DEM & NASADEM) are transformed into WGS 1984 (UTM Zone 46 N) coordinate system for subsequent analysis. Here, the DoD maps are prepared by subtracting the earlier terrain elevation (NASADEM of 1999) from the later one (UAV-DEM of 2022) using the raster calculator in ArcGIS (Hsieh et al., 2016; Watson et al., 2019; Wang and Watanabe, 2022). A level of significant change detection (LoD) was determined to filter out uncertain topographical change and considered for subsequent volumetric change analysis (Wheaton et al., 2010; Milan et al., 2011).

The standalone Geomorphic change detection (GCD) 7.5.0 tool (available at https://gcd.riverscapes.net/) is used to estimate volumetric changes (Wheaton et al., 2010), which is widely applied for quantifying the spatial pattern of geomorphic changes (James et al., 2012; Kaliraj et al., 2017; Rajakumari et al., 2022). In volume change estimations, the negative values indicate erosion, and positive values indicate deposition (Corsini et al., 2009; Hsieh et al., 2016; Yang et al., 2021), where the volume estimation error can also be gained, as shown in Table 4.2.

4.2.3.2 Cross-sectional profile

The terrain profile is a standard analytical method to discuss terrain evolution and provides valuable information about a landscape responding to a changing base level (Kirby and Whipple, 2001; Wobus et al., 2006). Here, profile extraction analysis has been conducted with the DEMs (NASADEM of 1999 and UAV-DEM of 2022) to identify the changes in topographic features across the two river cross-sections through ArcGIS environment (Hsieh et al., 2016; Cirillo, 2020). For the straight-line profiling method, the starting and ending points were first selected, and elevation values between the points were calculated to generate the terrain profile based on the distribution of elevations. The results were then used to better understand the dynamic changes of river elevation and sedimentation pattern (erosion/deposition) on the floodplain over the years.

4.3 Results

4.3.1 UAV DEMs resolution and error

The main characteristics of the UAV-generated DEMs of two cross-sections is provided in Table 4.1. The resolution of the created DEMs in this study was 0.10 m and 0.11 m at CS-1 and CS-2, respectively with orthorectified images of 0.04 m. The generated DEMs assessed a relative camera position error of 5.24 m and 6.35 m in CS-1 and CS-2, respectively which were processed using original UAV image georeferencing. The generation of high-quality DEM in inaccessible areas without GCPs has been applied in many studies (Wang et al., 2019) but the optimized sparse point cloud with identifiable GCPs across the study sites would improve the quality of generated model (James et al., 2017).

Table 4.1 Characteristics of the UAV survey and generated DEMs in study sites

Survey sites	Platform	Sensors	Flight altitude (m)	Total flight duration (min)	Images taken	DEM resolution (m)	Orthorectified image resolution (m)
CS-1	UAV (DJI MAVIC 2 PRO)	1 inch CMOS (effective pixels: 20MP, 35 mm f 2.8 lens with a 77° FOV)	120	37	775	0.10	0.04
CS-2			120	53	1050	0.11	0.04

4.3.2 DEM of difference (DoD)

The terrain elevation change from two periods of DEM data is presented in Table 4.2. The mean elevation difference for CS-1 and CS-2 is −5.23 m and −84.66 m, respectively. The DoD maps (Fig. 4.3) at river cross-sections over time representing the spatial pattern of geomorphic change. Here, the negative values stand for the decrease in terrain elevation in these images, which may be caused by surface erosion. On the other hand, positive values represent an increase in terrain elevation, which may be due to surface deposition. Through the DoD images presented here, the terrain evolution of the river channel can be observed. Also, the DoDs have been used here to quantitatively estimate the volumetric changes which are related to the sediment budgets. However, the elevation changes signal (larger than ±50 m) derived from the DoD maps may be affected by the artifacts, i.e., scratches on the photographs, but not sensitive to the measurements of volumetric change when varied above this threshold (Schwat et al., 2023).

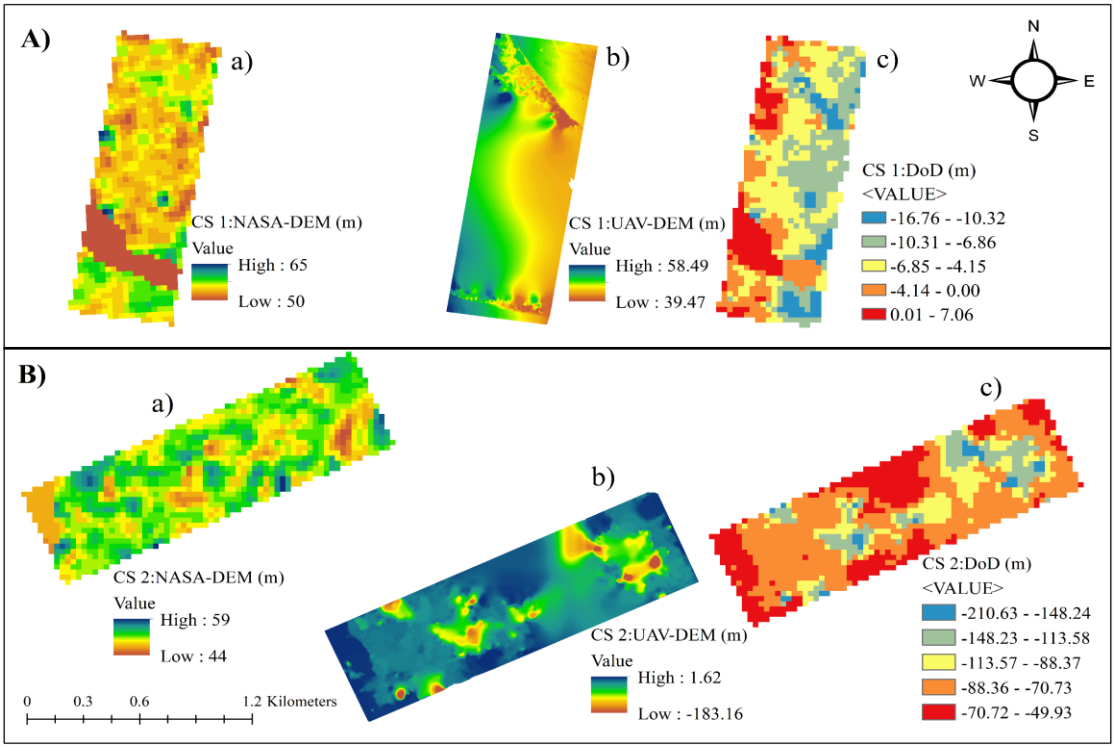

Fig. 4.3 DEMs and DoD maps are generated from NASADEM 1999 and UAV-DEM 2022 for CS-1 (A) and CS-2 (B).

4.3.3 Volume estimation

The total volumes of erosion and deposition, together with the net volume change, including errors, are given in Table 4.2. During the period (1999-2022), the estimated erosion and deposition volumes were 4.30 million m^3 and 0.18 million m^3, respectively, in CS-1. Instead of neglecting the estimation error and supplementary debris, at least 4.30 million m^3 of sediment may be eroded from the upstream sources to this CS-1. On the other hand, at CS-2, about 86.25 million m^3 of erosion are estimated. The result indicates that erosion was the dominant process in the Teesta River floodplain, with lower deposition over the study period. The estimate of net volumetric change is CS-2 is higher than the CS-1. The estimated erosion in these two cross-sections suggests this river's dominancy of erosional features aggravated by monsoonal flow, as the UAV survey was conducted in monsoon season. The negative net volumetric change for these two sites indicates that the earthflow from the upstream should be the main source of the sediments and result in high erosion. This high erosion may be impacted by the construction of the Teesta barrage and the diversion of the channel for the irrigation project (Fig. 4.5D), which is within the proximity of our present study sites. Also, previous studies mentioned the dominance of erosion in the last several decades because of high rate of sedimentation and the rise of 1 m bed level every ten years in Teesta River

channel (Khan, 2001; Akhter et al., 2019; Sultana, 2022). Furthermore, volumetric changes estimation based on the Teesta River's bathymetric survey conducted by Bangladesh Water Development Board-2011 supports our study's observation of erosional dominancy along the present study sites (BWDB, 2011; Tarannum et al., 2018).

From this study, it is not possible to find real-time data on the discharge events that caused these huge erosional episodes. Therefore, it is unpredictable when and where the next discharge will occur. However, it can be mentioned that the monsoonal flow patterns control the erosional and sedimentation processes in such a large transboundary river basin. The net volume of change is often used as a sediment budget term in sediment dynamics study. Therefore, estimating the volumetric change from the change detection can be helpful to develop morphological sediment budget to infer the rates of sediment transport for the studied river (James et al., 2012).

Table 4.2 DEM difference and volumetric changes in the study sites

Study sites	DEM difference *	Mean elevation difference (m)	Standard deviation	Erosion		Deposition		Volume change (m^3) ($\times 10^6$)
				Area (m^2)	Volume (m^3) ($\times 10^6$)	Area (m^2)	Volume (m^3) ($\times 10^6$)	
CS 1	UAV DEM– NASA DEM	–5.23	3.98	688,957	4.30 ± 0.13	106,530	0.18 ± 0.02	−4.11±0.15
CS 2		–84.66	13.98	1,010,101	86.25 ± 0.18	0	0	–86.25±0.20

* The NASADEM and UAV-DEM represents the topography of 1999 and 2022, respectively.

4.3.4 Topographic features in the river sites

Fig. 4.4 shows the high-resolution topographic products (slope gradient) of two cross-sections. The river flow path and the bankline in the study sites, presenting a flatland appearance, can be easily identified from the DEM maps. Most of these two cross-sections sloped eastwardly, where the slope gradient was below 5°, determining the presence of flat areas. On the other hand, the slope gradient around the bankline or near the char lands (locally known as Char) exceeds 20°. The orthomosaic images generated from the study (Fig. 4.4) visualize the agricultural lands along the bank lines, with some human settlements that were not permanent. Due to the main river course changes, bankline erosion is widespread in the study sites, and therefore the sediments accumulated at the lower flat area.

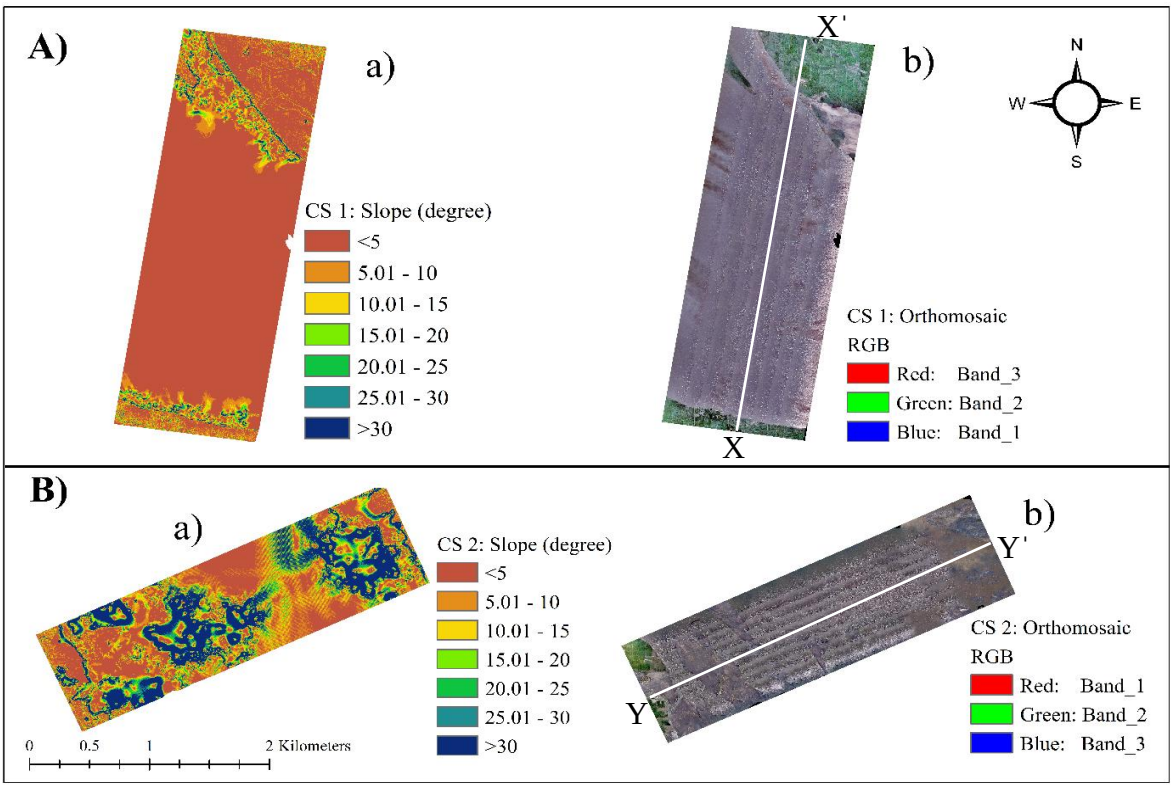

Fig. 4.4 Slope gradient and orthomosaic images of CS-1 (A) and CS-2 (B) created from UAV photographs. See Fig. 4.5 for the cross-sectional profiles denoted here.

4.3.5 Cross-sectional profile analysis

Next to elevation and volumetric change estimates, the DEMs are helpful for evaluating the profiles of river cross-sections. In our study NASADEM 1999 has been used as the reference for the profile analysis. The selected transects from two river cross-sections illustrate the profile analysis, indicating an ongoing erosion process. Fig. 4.4A (X-X') and 4.4B (Y-Y') indicate the transect locations on the orthomosaic of 2022 for profile analysis. Fig. 4.5 (A-B) shows the elevation profiles for these transects derived from the DEMs, indicating the deepening of the river channel within this period (1999-2022) with approximate errors.

Here, active sedimentation and erosion processes are significantly visible near the left bank side from the cross-sectional profiles, though several meters of uncertainty may exist. The elevation change demonstrated the erosion variations within the profile position. The erosion process is relatively small for profile (A), with approximately 7 m elevation change at the lower middle section in CS-1. On the other hand, the higher erosion is visible at the profile (B), in CS-2 towards the left side bank. The Teesta barrage and diversion of the river channel for irrigation and periodic sand extraction for financial benefits at the upper part of CS-2 may aggravate this high erosion process. Also, the bed scours depth of more than 13

m was reported at Teesta River in Nilphamari (present study site) by the Institute of Water and Flood Management (IWFM-BUET 2018-2022) (Mondal, 2022), which was estimated up to 40 m in the Brahmaputra River channel (locally known as Jamuna River) (Ashworth et al., 2000), supports the erosion processes observed here. Furthermore, the multi-temporal satellite remote sensing (MSS/TM/ETM+/OLI)-based and bathymetric survey-based study explored that erosion, sand bar development, and channel shifting rate towards the left side bank has increased over the 46-year periods (1972-2017) along the study sites because of the high rate of sedimentation (BWDB, 2011; Akhter et al., 2019; Mondal, 2022). Besides, high erosive condition (15.32 to 31.72 sq.km) that caused the bank failure were evident over the last few decades in several cross-sections of the Teesta River floodplain in the Nilphamari district, including our present study site (Tarannum et al., 2018; Sultana, 2022).

Nevertheless, it should be mentioned that considerable uncertainty remains in channel depth due to the glitter, over-estimation of water level, data processing software, resolution difference and mirroring effects of water, which may affect the interpretations of these profiles (Schwanghart and Scherler, 2017; Hemmelder et al., 2018). In general, the elevation error ranges from 5-12 m for NASADEM (Buckley et al., 2020; Uuemaa et al., 2020; Li et al., 2022; Uuemaa et al., 2020; Chen et al., 2022; Tran et al., 2023), whereas the UAV's single positioning of GNSS may provide error of ~8-13 m or more (DoD, 2020; Elkhrachy, 2021; De Haas et al., 2021; Grunwald et al., 2023). Hence, this error and recent studies necessitates improving the accuracy of elevation data with modern UAVs connected to RTK global navigation satellite systems in the most remote and challenging geographic locations, like this study area (Elkhrachy, 2021; De Haas et al., 2021).

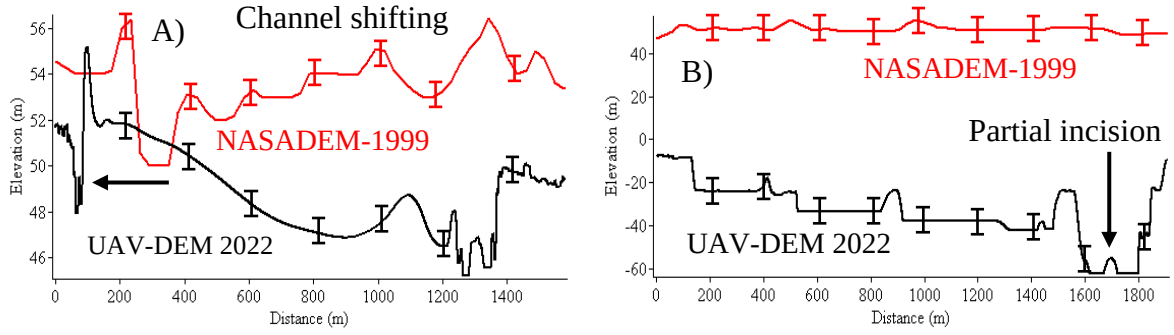

Fig. 4.5 Changes in cross-sectional profiles. Here, A) and B) corresponds to the CS-1 (X-X' transect) and CS-2 (Y-Y' transect) shown in Fig. 4.4. The red and black lines indicate the elevation profile of NASADEM 1999 and UAV-DEM 2022, respectively, with approximate errors (>10 m).

4.4 Discussion

4.4.1 Topographical and morphological dynamics

This paper presents a study using DEMs to map topographic changes and associated morphological dynamics, including elevation differencing, volumetric change estimates, and river cross-sectional profiles, in an understudied region where repetitive topographic measurement is absent. The availability of high-resolution river topographic data, possible through UAVs and global DEM products, allows performing topographical change detection analysis over the years (1999-2022). Nevertheless, this information is critical to understanding the river's topographical and morphological dynamics that are prone to repeated sediment disasters from its upper basin sediment flux. Furthermore, topographic factors affect the sediment discharge in a river basin (Cheng et al., 2017). Therefore, the DoD difference between the UAV-DEM and NASADEM for the area of interest (Table 4.2) shows the benefit of conducting UAV surveys even if ground control point is unavailable due to inaccessibility to field sites.

This study noticed the decrease of elevation from –5.23 to –84.66 m and net volumetric difference of –4.11 to –86.25 million m^3 in CS-1 and CS-2 on Teesta River's left side bank. The sedimentation between these periods varied largely per cross-section towards the left side bank of this river and seemed to dominate with the erosional process. The volume changes over the 1999–2022 periods are mainly expedited by the anthropogenic modifications of the main river channel, such as the construction of the Teesta barrage, channel diversion for irrigation, and sand mining observed from the field investigations (Fig. 4.6). Furthermore, earlier studies documented the increase of erosion at Teesta barrage's proximity (Khan, 2001; Sultana, 2022; Mondal, 2022). The visual observations on the land-side of these cross-sections (Fig. 4.6A) also support the feasibility of such a large amount of erosion processes. Hence, using DoD derived from the DEMs has proven helpful in identifying the sedimentation pattern resulting from erosion and deposition scenarios in the floodplain. The volumetric dynamics studies prefer the DEMs from the same data source for more accurate estimations, which may affect the assessment here (Tang et al., 2019).

However, the availability of high-resolution data (same source and similar accuracy level) derived from Unmanned Aerial System (UAS) is often not available in this region. The topographical changes recorded over the period (years 1999–2022) revealed

significant variations of the topographic profile dominated by erosional process. The interaction of upstream fluvial incision, high and low discharge patterns, base-level change, and anthropogenic stressors (e.g., channelization, sand mining, hydroelectric projects-3405 MW installed of over 8000 MW potentiality in Teesta, and hydro-engineering structures) may result in the changes along these profiles (Montgomery and Brandon, 2002; Goyal and Goswami, 2018; Van Denderen et al., 2022). Since river cross-sectional profiles preserve valuable information on landscape evolution and are fundamental to understanding the river morphological changes, this profile analysis can be helpful in monitoring the sedimentation patterns and management of the disaster-prone landscape.

Over the years, the flashy and unpredictable nature of sedimentation in this river basin left the inhabitants in a more risky situation. Also, the sudden release of huge volumes of water from the upstream reservoir makes the sediment pattern more unpredictable and more uncertain floods in this region in recent decades (Mondal and Islam, 2017). The erosion dominated sedimentation pattern and enormous volumetric changes may affect the bankline stability, development of mid-channel sand bars (locally known as char) (Fig. 4.6B), and multithreaded channel system in Teesta River (Akhter et al., 2019; Sultana, 2022). The increased number of mid-channel bars led to the sudden shifting of the channel (Ghosh, 2014), where Teesta's channel shifted towards the right (0.34 km/year) and left side (-0.14 km/year) over the period (1972-2017) (Akhter et al., 2019). The sedimentation patterns may control the channel dynamics because the river discharge flow through the narrower channel increases the flow velocity, resulting in abrupt bank erosion (Graf, 2000; Croke et al., 2008).

Moreover, the excessive and unplanned extraction of sand (Fig. 4.6C) from the sand-dominated bed profile (approximately 10 m) in the study sites has been common practice (Biswas et al., 2018). That may also alter the river morphological characteristics such as channel incision (Rai et al., 2019), changes in riverbed (Best, 2018), erosion of river banks (Bravard et al., 1997), and decrease of sediment flux at downstream of the river delta (Anthony et al., 2015). The channel incision process is a gradual geomorphological phenomenon. But, the point of concern is that the pace of incision may significantly be expedited from the excessive sand mining, which may result in drastic morphological changes within 10-100 years in its natural course where such changes would have occurred over millennia (Simon and Rinaldi, 2006; Rai et al., 2019).

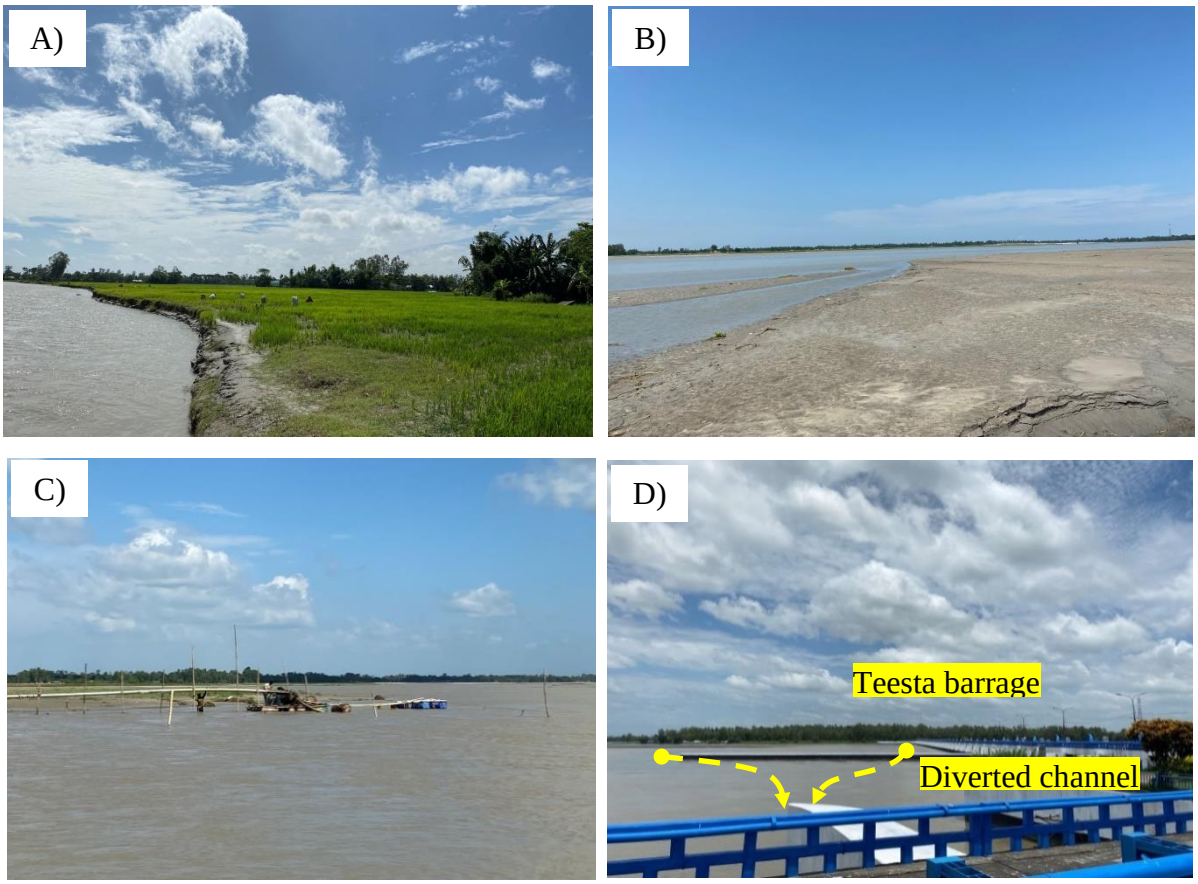

Fig. 4.6 A) Erosion along the bank, B) sedimentation within the channel and bar development C) dredging for sand extraction, and D) channel diversion for irrigation at Teesta.

4.4.2 High-resolution topographic baseline, limitations, and challenges

This study showed that UAV images are suitable for monitoring the changes in river topography and geomorphology in a region where high-resolution imagery is often unavailable. To the best of our knowledge, this study successfully estimates the topography using UAV-SfM in the Teesta River sites for the first time. It is evident that high-resolution DEMs derived from the present UAV survey represents an important new baseline topographic dataset for river studies considering the existing freely available global DEM dataset, e.g., NASADEMs (Watson et al., 2019; Tang et al., 2019).

The availability of real-time kinematic (RTK) enabled UAVs in developing countries like Bangladesh will further improve the survey data and, at the same time, reduce the requirements for extensive ground control point surveys in inaccessible riverine areas (Fazeli et al., 2016; Forlani et al., 2018). With the limited scope, this study only conducted UAV topographic survey single time to generate high-resolution DEMs and then used the existing medium-resolution global DEMs to analyze the topographic change due to the

unavailability of high-resolution multitemporal DEMs. Hence, data obtained from different DEM generation techniques and the resampling processes to homogenous resolution (high-resolution to medium resolution) may lead to estimation errors or uncertainty, which would eventually impact the topographic change analysis (Joerg and Zemp 2014). Besides, due to the unavailability of good control points like cross marks on the road, permanent features, or the referenced maps, this study relies on the aircraft's GNSS errors to estimate the uncertainty of the UAV-generated DEMs, which were several meters. Besides, this topographic study did not consider the monsoonal effect, which is one of the limiting factors raised by the study's limited scope. Some approximations, such as the presence of water bodies in the riverbed, water surface reflectance, and differences in DEM sources and resolution, may also constrain our analysis. Nevertheless, the author believes that such approximations would not dramatically influence the analysis and the interpretations.

The availability of RTK-enabled aircraft, external GNSS receiver, and evenly distributed ground control points with geographical coordinates were challenging, but addressing these issues may improve the elevation data quality. Furthermore, some key challenges remain in UAV-based riverine floodplain monitoring, such as wind, rain, surface reflectance, image focus, image resolution, and processing equipment (Hashemi-Beni et al., 2018; Acharya et al., 2021). Besides, a quantitative assessment of the accuracy and precision of the UAV-derived products compared to RTK-GPS enabled UAS and terrestrial laser scanning (TLS) are beyond the scope of this paper. Though, it is expected that the topographic data acquired via TLS would be more accurate compared to SfM-derived products in geomorphic investigations (Tsunetaka et al., 2020). Furthermore, UAV survey and high-resolution DEM generation techniques may also attract attention to the research community in that region. Where the applicability of advanced remote sensing techniques (such as UAV-SfM and LiDAR) for geomorphological investigation is very limited compared to neighboring countries like China (Le Heron et al., 2019), India (Ramsankaran et al., 2020; Dhote et al., 2022), Bhutan (Dunning et al., 2009; Tempa et al., 2021), Nepal (Immerzeel et al., 2014; Kraaijenbrink et al., 2016; Van Woerkom et al., 2019), Pakistan (Khan et al., 2021), and in other parts of the worlds (Śledź et al., 2021).

4.4.3 Advances in river floodplain management

Evaluating recent topographic change in a riverine environment relevant to the sustainability of human populations in the disaster-prone area requires up-to-date fine-resolution DEMs,

such as those derived using UAV imagery in this study. In our case, single-time UAV image acquisitions and use of global DEM products for volumetric change estimate along the river cross-sections are low to link sedimentation patterns. In this context, the high temporal UAV data acquisition campaigns after each important discharge event or season scale can provide important information regarding the river sedimentation pattern and hence the management of sediment disasters in these disaster-prone deltaic landscapes. The processing of hundreds or thousands of images using the SfM algorithm is computationally intensive but fast, straightforward, and produces detailed results (Clapuyt et al., 2016; Hemmelder et al., 2018). With the advancement of UAV developments and innovations, UAV operations are becoming easy to monitor the river floodplain. Despite some challenges in river topographic measurement, UAV-based DEM should be considered as the optimal choice for investigations over river floodplains due to its advantages of portability, high data processing speed, low flying height, convenient flying preparation, and the ease of generating orthoimage and DEM data (Hayakawa and Obanawa, 2020).

Despite some limitations and challenges, the current approach of terrain evaluation utilizing free and on-demand DEMs can be helpful for other areas where repetitive terrain information is scarce but requires effective topographic investigation. Furthermore, land managers and mapping agencies responsible for monitoring river dynamics and management could use the methods presented in this paper, especially the UAV-SfM data generation techniques for the advancement of river floodplain management. The effective monitoring requires sufficient knowledge of fluvial-sedimentation processes in the riverine floodplain, and in this regard, encouragement can be taken from fluvial research advancement mentioned by Stott (2013), Wohl (2014), Piégay et al. (2015), and Oguchi et al. (2022). In the advancement of riverine floodplain management, the UAV-SfM photogrammetry can be an effective and powerful tool to map morphological dynamics and processes focusing on the river basin maintenance plan, delineation of flood-prone areas (Şerban et al., 2016), estimation of flood volume and extent (Escobar Villanueva et al., 2019), flood risk modeling (Coveney and Roberts, 2017), assessing the impact of flooding (Langhammer and Vackova, 2018), sediment discharge analysis, and responding to flood emergencies (Salmoral et al., 2020).

Furthermore, understanding river topographic and related morphological dynamics will promote the development of a river floodplain management framework, where

the studies of Morris-Oswald and Sinclair (2005), APFM (2012); Kiedrzyńska et al. (2015), Sharma et al. (2019), Serra-Llobet et al. (2022), and Chan et al. (2022) can be exemplary. The existing river floodplain management approaches in transboundary river (total 57 rivers) dominated Bangladesh should not focus on the traditional hard engineering approach (Haque et al., 2019), which may not be enough to mitigate substantial risks from the natural (e.g., climate change, sea-level rise, and land subsidence) and anthropogenic factors (e.g., channelization, hydro-engineering structures, excessive sand mining, large population, and rapid socio-economic growth) (Chan et al., 2022). Therefore, the advancement of river management needs to focus on utilizing the UAV-based framework (Fig. 4.7) to support decision-making in hazard assessments and disaster responses in South Asia's disaster-prone countries, particularly Bangladesh.

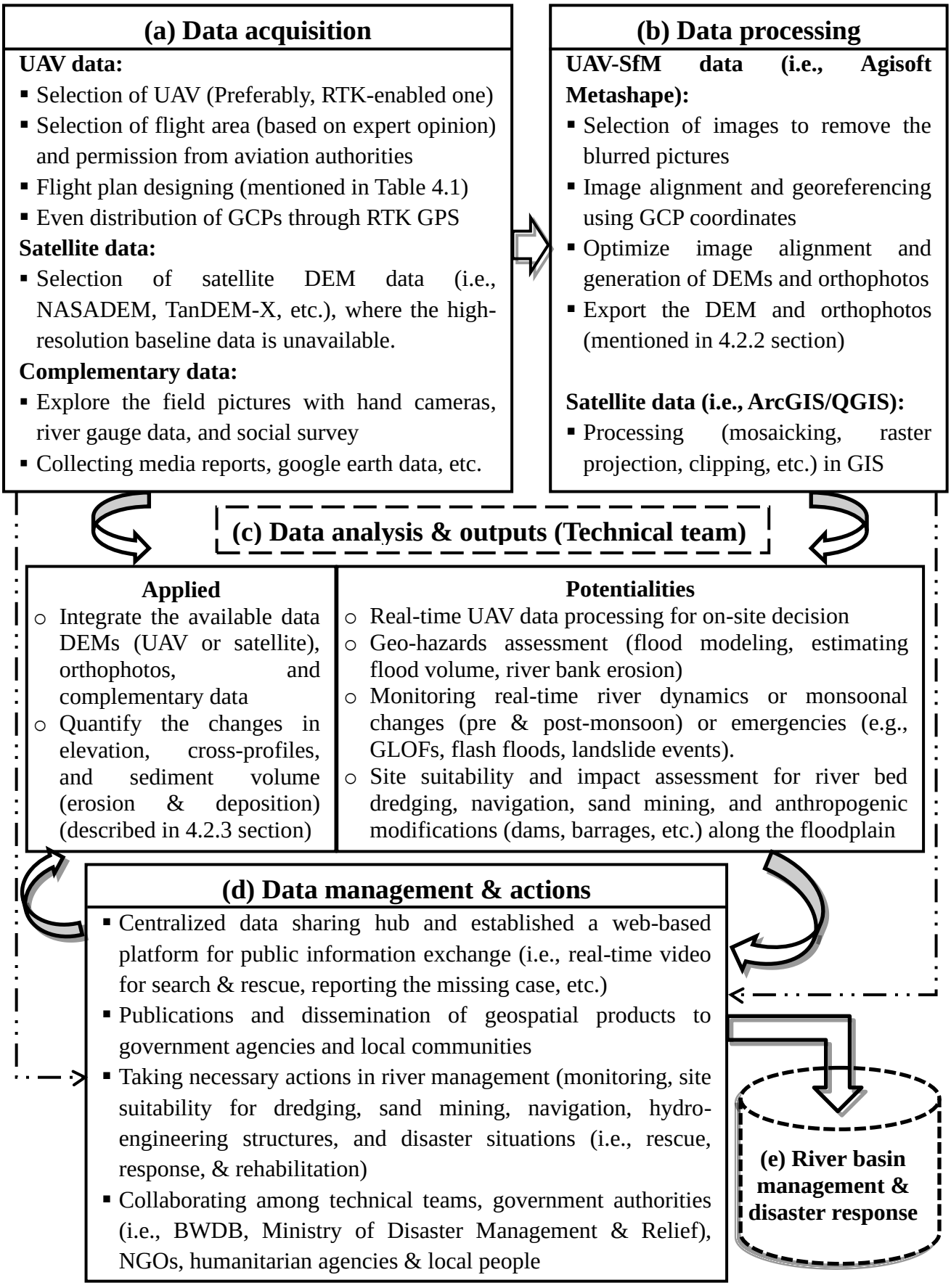

Fig. 4.7 Framework for river basin management and natural disaster with UAVs.

4.5 Conclusions

This study demonstrates the utility of an integrated geographic information system combined with UAV-SfM-derived DEMs and globally available DEMs (NASADEM), considering topographical and geomorphological dynamics in a disaster-prone riverine floodplain. The workflow presented here has been successfully applied to identify the topographic and geomorphic changes, as well as assess the sedimentation pattern in the river channel based on multiple topographic outputs (DEMs, DoDs, cross profiles). The author noticed the changes in elevation (−5.23 to −84.66 m), sediment volume (−4.11±0.15 to −86.25±0.20 million m^3), and erosion-dominated cross-sectional profiles towards the left side bank in the transboundary Teesta River over a period of 23 years (1999-2022). The current approach of data acquisition, especially the UAV-SfM-derived DEMs and orthomosaic images, can encourage interested researchers to take this study as baseline information for future investigation, where the UAV data can be available on request to the authors. In addition, time series investigations with advanced remote sensing techniques (such as UAV-SfM and LiDAR etc.) for detailed monitoring of topographic variables considering the monsoonal dynamics are essential to assess future instability scenarios in this dynamic, unpredictable, and disaster-prone river floodplains. The findings from this study will provide a better understanding of the river's topographical dynamics, geomorphological processes, and sedimentation scenario to national-river managers. Also, the proposed river basin management framework will elevate river floodplains management and disaster response in South Asia’s densely populated deltaic landscape, particularly Bangladesh and/or similar situations elsewhere.

Chapter 5
General discussion

5.1 Factors affecting the multiscale geomorphic connectivity

Morphodynamics and sediment connectivity patterns are key determinants of the fluvial-sediment dynamics and geomorphic connectivity in the Brahmaputra River basin. The author conducted multiscale (basin, sub-basin, and local) studies, which is a critical issue in river basin management because the understanding of complex natural fluvial systems, erosion and weathering processes, human interferences, selection of hydro-morphological monitoring sites, management of fluvial risk, resource utilization, and sustainability of the basin is intimately linked from its large-scale processes to small-scale measurements (Nepal et al., 2014; Ortega et al., 2014; Rinaldi et al., 2017; Lombana and Martínez-Graña, 2021). Besides, this multiscale approach in Himalayan Rivers that flow across different geographical regions is essential to promote the integrated river basin management framework, which can address the needs of different users of basin water considering the heterogenicity of the basin and linkage between upstream and downstream (Nepal et al., 2019).

Here, the geomorphic connectivity varies across the basins and is highly influenced by the upstream's hydro-geomorphic responses. The geomorphic connectivity at multiscales show connected, partially connected, or disconnected systems from its upstream, mid-and downstream, respectively, affected mainly by the sediment trapping before the mouth of the basin’s outlet, intensified by the higher fraction of anthropogenic stressors, and hence impacting the fluvial-geomorphic processes. The fluvial sedimentation processes (i.e., excessive sediment sequestering, riverbed aggradation) and anthropogenic stressors (i.e., river engineering, barrage, hydroelectric projects, and dam construction) (Fig. 3.14) are one of the factors that may affect the basin-wide geomorphic connectivity in the Brahmaputra River system. The evidence of anthropogenic stressors on morphological characteristics and sediment dynamics along this basin is also mentioned in earlier studies (Kale, 2002; Goyal and Goswami, 2018; Higgins et al., 2018; Best, 2019; Palash et al., 2023; Raff et al., 2023). Also, in the future, a boom in hydropower dam construction activity in Asia, mainly in China, India, and Nepal is reported (Zarfl et al., 2015). Recent studies demonstrate that sediment delivery could decline by 15-80% (Raff et al., 2023) with the full implementation of planned dams and river diversions along the Ganges-Brahmaputra delta (Zarfl et al., 2015; Higgins et

al., 2018). The future changes in the Ganges-Brahmaputra sediment supply and their potential consequences for the downstream delta suggest unprecedented levels of change in sediment supply (±50–90%) over the next 50-100 years, either through the reductions of discharge from existing and proposed artificial damming and channel diversion, increase of monsoonal precipitation and higher river discharge, or a combination of these factors, where the artificial damming significantly affecting the (dis)connectivity of sediment supply to the delta (Darby et al., 2015; Dunn et al., 2018; Higgins et al., 2018; Raff et al., 2023). Besides, river hydrology (discharge and sedimentation) is dominated by monsoonal flow, which may significantly affect the hydro-geomorphic response and, therefore, the geomorphic connectivity at the basin scale (Chapter 2). Moreover, the GBM basin's precipitation analysis over 1985-2015 suggests monsoonal dominancy (June-September) with high spatial and interannual variability, especially towards the southern border and Himalayan ridge (Curtis et al., 2018). The high monsoonal variability along with the strengthened precipitation (77% of the total rainfall) readily mobilizes the abundant sediments from the upper catchment, which are critical for managing water resources and hydrological hazards in this South-Asian hydrological unit (Curtis et al., 2018; Raff et al., 2023). This monsoonal precipitation feeds this immense GBM's river system and is considered a potential predictor for discharge dynamics in the downstream delta region, where downscaled hydroclimate predictions are encouraged for further study (Curtis et al., 2017; Curtis et al., 2018). Also, the future projections of hydro-climatology in the Brahmaputra basin suggest that the strengthening of monsoon precipitation (8-28%) (Caesar et al., 2015) could increase the runoff (16%) (Masmood et al., 2015) and sediment delivery (34-60%) (Raff et al., 2023) by the end of 21st century, which will worsen sediment disasters (flooding, erosion) in the downstream delta (Lutz et al., 2014; Higgins et al., 2018). Therefore, the geomorphic connectivity pattern would be crucial for considering the future instability scenario in this transboundary river basin, where more geo-scientific diplomacy is required for the sustainability of the delta environment.

However, as insights of basin-scale processes (Chapter 2) are interconnected with the medium (sub-basin) scale processes (Rinaldi et al., 2017; Nepal et al., 2019), the baseline information on geomorphic variables, terrain configuration, and sediment connectivity patterns at the (sub-basin) scale (Chapter 3) is essential for understanding the basin-wide geomorphic linkage. Here, the connected and partially connected, or disconnected geomorphic systems exist from source to sink areas of the Brahmaputra's hydro-geomorphic

system. The altering geomorphic connectivity from connected to partially connected or disconnected may be attributed to topography, longitudinal channel profiles**,** rainfall variation, land cover, sediment connectivity potentials**,** and intense sediment trapping (Chapter 3). The deposition resulting from sediment trapping along the mid-to-downstream region is attributed to the partially connected or (dis)connected system in the Brahmaputra River system, impacting the basin-scale geomorphic linkage from the upstream to the downstream region. Also, high runoff, precipitation, and landslides in the upstream region disrupt the natural flow of discharge (water and sediment) and play crucial role in changing geomorphic connectivity.

Furthermore, as the (basin) large-to-medium (sub-basin)-scale processes (Chapter 3) are often inferred from small-scale forms (Ortega et al., 2014; Rinaldi et al., 2017), the interpretation of current topographic conditions and sedimentation behavior at a local scale (Chapter 4) for managing the upstream-dominated fluvial risk is crucial for the sustainability of local people and the surrounding landscape. Here, the changes in topography recorded over the period (1999–2022) revealed significant variations in elevation, volumetric estimates, and cross-sectional profiles along the Brahmaputra's tributary (Teesta River), dominated by the erosional process. This erosion-dominated sedimentation pattern may affect the geomorphic connectivity by developing the mid-channel sand bars, raising, or lowering of the riverbed, multithreaded channel, and incision channel, decreased sediment flux downstream (Chapter 4).

Therefore, the above-mentioned factors play a critical role in basin-scale geomorphic connectivity, where the integration of a multiscale approach of fluvial-geomorphic study in a basin makes it possible to establish a scenario of fluvial processes, geomorphic linkage, sediment connectivity, and topographic dynamics in a more detailed manner, which would be significant for sustainable river basin management issues. However, in the context of integrated river basin management, the Driver-Pressure-State-Impact-Response (DPSIR) framework offers a useful approach for managing the transboundary river basin, recently adapted to the Hindu Kush Himalayan region (Nepal et al., 2019). Hence, the DPSIR framework has been applied here (Fig. 5.1) to assess the driving forces of geomorphic connectivity, the resulting pressure, the connectivity's state, the drivers' impact, and the future response to be considered in Brahmaputra River basin management (Kristensen, 2004; Rahman et al., 2016; Nepal et al., 2019).

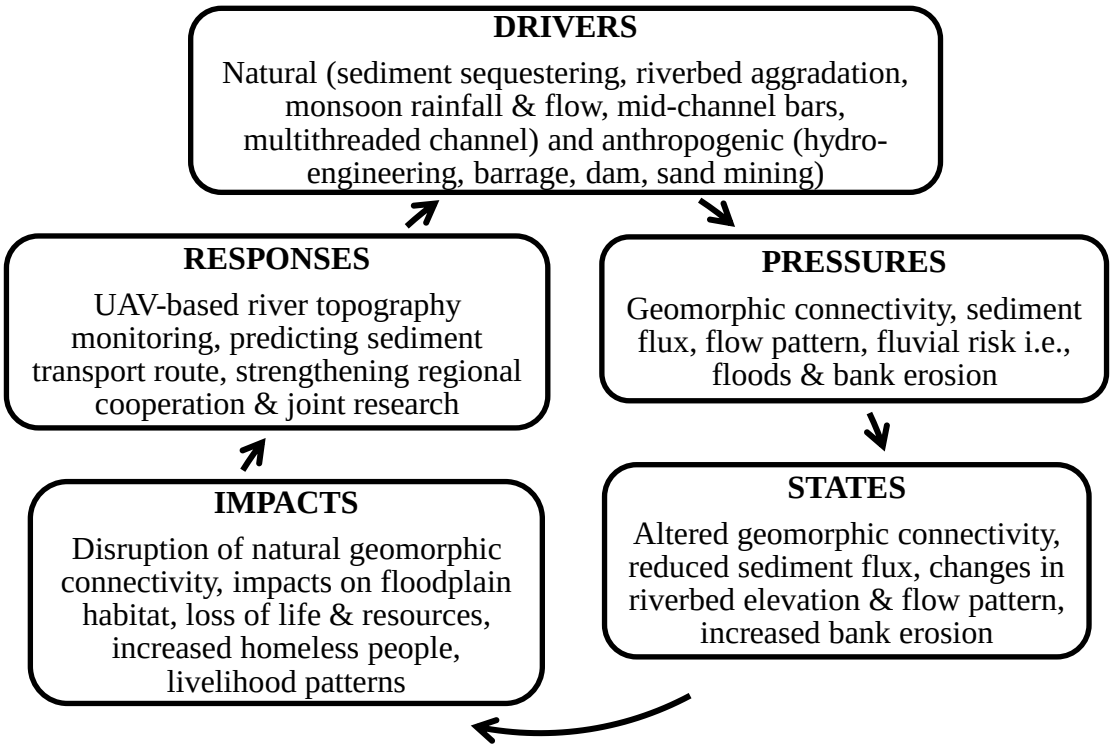

Fig. 5.1 Driver-Pressure-State-Impact-Response (DPSIR) framework in geomorphic connectivity for integrated river basin management in the Brahmaputra.

5.2 Importance of fluvial-geomorphic studies to river management

This study deals with the role of fluvial geomorphologic processes, sediment connectivity, and topographic dynamics in fluvial system of the largest river basins in South Asia, Brahmaputra, which requires integrated river management. The following section stipulates the key importance of this study in the context of Brahmaputra River basin management.

It is established that the fluvial-geomorphic system is a prominent morphological feature that greatly influences landscape modifications. The changes in fluvial-geomorphic features, sedimentation patterns, topography, and anthropogenic activities have increased the level of modifications of the natural fluvial system and led to river management relevance. In addition, the interplay of tectonic activity, climate change, sea level rise, hydrologic change, global temperature growth, and rainfall intensity has induced the relevant modifications of fluvial discharges, urging the integration of geomorphological investigations in river basin management (Yamagata et al., 2015; Giano, 2021). Therefore, the knowledge of land surface processes through analyzing geomorphic features, sediment connectivity patterns, and topographical dynamics at a basin-wide scale gained from this study would be noteworthy in river management approaches of South Asia's densely populated country, particularly lowland Bangladesh. Moreover, the number of geomorphic analysis frameworks developed

over the last decades in Europe, Australia, and Asia focused on the understanding of current fluvial processes and sediment dynamics in river management, foreseeing future river geomorphological investigations (Kondolf and Bizzi, 2022). Hence, this study would be noteworthy to develop an integrated river basin management framework in this transboundary river, which has significant discord among the basin's actors and requires effective cooperation.

In mountainous terrain, strong geomorphic connectivity between the slopes and high-order streams induces permanent fluvial risk (flooding, bank erosion and sedimentation in the channel, channel avulsion, and severe low flows) for local people living near the river (e.g., Chand et al., 2019; Thapa et al., 2022). Furthermore, it also affects the lower river terraces or alluvial fans as demonstrated in the Brahmaputra River basin. Managing fluvial risk resulting from the interaction of erosion and sedimentation processes on the slopes and valley bottom is of fundamental importance in river management (Arnaud-Fassetta et al., 2009). Also, engineering hydraulics, including the designing of stable channels, navigation routes, channel alternation, construction of dams and barrages, and hydroelectric projects, has been a source of land surface processes understanding, requiring detailed analysis of fluvial channels, sediment entrainment, transport, and deposition (Lewin et al., 2018). The sustainable solution to the problems that arise from these streams engineering often requires the knowledge of fluvial geomorphology and sedimentation processes, discussed in this study.

Besides, sediment transport dynamics is often the key problem in river channel design, causing sediment-related river maintenance. In this regard, the knowledge of fluvial-geomorphology and sediment connectivity patterns gained from this study will contribute to the understanding of sediment sourcing and predicting sediment transport rates, which would be crucial for the transboundary river basin management, like the Brahmaputra (Sear et al., 1995; Vazquez-Tarrío et al., 2024). Furthermore, the assessment of fluvial geomorphological processes and sedimentation scenario from the modern remote sensing approaches (i.e., UAV-SfM) are the key to landscape-based urban development design, particularly in developing areas like Bangladesh. Also, this study will allow the various stakeholders (academicians, international community, government organizations, NGOs, and others) to promote the dialogue for the functioning of the natural fluvial system considering geomorphic connectivity and river restoration (Espinosa et al., 2018). Based on the relevant importance of river basin management discussed above, this study's findings can contribute to

the Brahmaputra River basin's integrated river basin management aspects, which require particular attention at a basin-wide scale to maintain its natural fluvial system.

5.3 Implications of this study towards river basin management

As a first step towards integrated river basin management, this study provides a comprehensive understanding of fluvial-geomorphic processes and sediment dynamics connecting the upstream region to the downstream of the Brahmaputra River basin. It highlights the following key points regarding its implications.

5.3.1 Restoring the geomorphic connectivity

The conventional structural measures in river management, such as levees (dikes), dams, and engineered channels, are perceived as effective means of eliminating flood risk and controlling the river flows (Auerswald et al., 2019). However, preventing high flows or floodwaters through hard-engineering approaches from spreading over floodplains can concentrate the flow and result in higher flow peaks downstream and upstream, exacerbating flooding problems (Heine and Pinter, 2012). As the fluvial geomorphic processes, sediment connectivity patterns, and topography become understood, there would be more opportunities to restore the geomorphic connectivity and functionalities of the river floodplains compared to the conventional hard engineering approach, thereby may reduce the flow peaks downstream (Van Rees et al., 2021). Besides, the flood management plan disregards the influence of sediment transport on flooding (Vázquez-Tarrío et al., 2024). Understanding the land surface processes, including the connectivity patterns mentioned here, may improve the river management policies in restoring the geomorphic connectivity considering the multiple benefits such as combining flood risk reduction, ecosystem restoration, and adaptability to climate change (Serra-Llobet et al., 2021; Vázquez-Tarrío et al., 2024). Adaptability to the increase of sediment discharge by 52-60% or 34-60% by the end of the twenty-first century (Derby et. al., 2015; Raff et al., 2023), projected by future climate change scenario in the Brahmaputra River basin requires the restoration of the geomorphic connectivity, where this study's observed connectivity pattern can play a significant role. Also, this study contributes to the sustainable development principles by understanding the limitations of hard-engineering approaches in the transboundary Brahmaputra River basin. Therefore, this understanding will help to initiate the coping strategies to restore the geomorphic connectivity at a basin-wide scale, considering the experience of developed countries like the United Kingdom, the Netherlands, the United States, and Japan (Chan et al., 2022).

5.3.2 Monitoring the river floodplain dynamics and baseline topography

The responsible agencies related to water management in Bangladesh (such as Bangladesh Water Development Board-BWDB, Bangladesh Inland Water Transport Authority-BIWTA, and Ministry of Water Resources) can focus more on continuous floodplain monitoring with the introduced modern UAV-SfM techniques, particularly delineation of flood-prone areas, estimation of flood volume, flood risk modeling, sediment discharge, and responding to flood emergencies (Tarolli, 2014; World Bank, 2015; Acharya et al., 2021; Mishra et al., 2022). For instance, severe flooding of the upper Teesta River valley in the eastern Himalayan state of Sikkim originated from the South Lhonak Lake's GLOFs (Glacial Lake Outburst Flood) outburst, killed at least 14 people, and left over a hundred missing with severe damage to the buildings, highways, and Chungthang dam downstream since 4th October 2023 (Sattar, 2023; Chauhan, 2023). This case shows the consequences of upstream events and their extent over tens of kilometers downstream, resulting in the loss of human life and significant damage to property and infrastructure. Hence, this study can play a crucial role in risk management strategies and emergency response to this kind of anticipated flooding disaster for the downstream communities with the proposed river basin management framework (mentioned in Fig. 4.7), considering the topographic survey (satellite/UAV-based) following the occurred event and the sediment connectivity patterns along the river channel.

Furthermore, the UAV-based high-resolution data obtained here can be used as a baseline topographic dataset for future investigations and can encourage other relevant researchers to investigate the geomorphic processes and sedimentation patterns considering the monsoonal dynamics. Also, the repetitive monitoring of river floodplains may be facilitated by the introduced river topographic data collection techniques for the river managers and authorities to make decisions in disastrous situation, i.e., the Sikkim glacial lake outburst on 4th October 2023. Furthermore, this approach can be applied to other floodplains that are assumed to be more dynamic and critical for river management in this disaster-prone region. The repetitive topographic data collection through the RTK-enabled UAVs at seasonal and temporal scales or event-based in future studies would be significant for this disaster-prone deltaic region, particularly estimation of flood volume and extent, river bank erosion, seasonal dredging, and site-specific sand mining, following the frameworks mentioned in Fig. 4.7.

5.3.3 Documented understanding on strengthening cross-boundary cooperation

Integrated river basin management is often hindered by the lack of basin-wide collaboration, disconnected or contradictory policies, conflict of interest (water sharing, disaster management), and failure to understand the importance of maintaining transboundary river flow due to the absence of documented understanding. This study finding necessitates the strengthening of active transboundary cooperation among river-sharing countries like China, India, Bhutan, and Bangladesh. Although some mutual agreements exist among these countries, the effectiveness must focus more on the holistic approach respecting mutual interest and understanding the basin-wide fluvial-geomorphic processes. Hence, this study provides a documented understanding of the fluvial geomorphic processes from the hillslope to the coast, sediment connectivity patterns, and topographical dynamics at the GBM river basin, leading to an adequate understanding for assuming future scenarios (e.g., Derby et. al., 2015; Raff et al., 2023). This will help policymakers such as the Joint River Commission (JRC), Ministry of Water Resource, Bangladesh, to negotiate with better concepts and build regional cooperation among the Brahmaputra-Ganges River co-riparian countries based on geo-scientific significance in collaboration with the World Bank's South Asia Water Initiative (SAWI) (Leb et al., 2018). Furthermore, this study will also be valuable not only for the government institutions but also to other stakeholders of this river basin, such as non-government organizations (NGOs), conservationists, and different indigenous groups.

5.3.4 Joint research initiatives and data sharing

The findings from this study can contribute to initiating the joint research to ensure the relevance and appropriate actions in river policy meetings participated by Bangladesh and other basin sharing countries (China, India, Nepal, and Bhutan). It was recognized that China and India consider the research results in their policies and act likely (Yasuda et al., 2017). Hence, as an active stakeholder of transboundary Brahmaputra River, Bangladesh requires more collaborative research or joint research among basin-sharing countries to improve the understanding of fluvial-sedimentation processes and future scenarios at a basin-wide scale. A clear scope of future joint research and collaboration among the actors of this Brahmaputra basin exists that can significantly support the resourceful landscape and its dependent livelihood in the developing country of the South-Asian region, particularly Bangladesh. Also, the relevant researchers or experts from developed countries, i.e., Japan, can collaborate to enhance the river basin management options considering the UAV-based framework (Fig.

4.7) with bilateral or multilateral projects focusing on advanced topographic survey through UAV and Lidar along the floodplains that are assumed to be crucial for the management of river basin (Hayakawa et al., 2017; Saito et al., 2018; Ogura et al., 2023). Furthermore, this study improves the data collection hub along the GBM river basin, focusing on suspended sediment load (Table 2.1), river discharge (Fig. 3.3 and Fig. 4.2), high-resolution elevation data (Fig. 4.3), and different geospatial data generation techniques (i.e., Fig. 3.4).

5.3.5 Sustainable river basin development

The information on the basin-scale fluvial-geomorphic processes, sediment connectivity patterns, and topographic dynamics (elevation change, river cross-sectional profile, and volumetric estimate) from mainstream rivers is required to underpin the sustainable river basin development focusing on sand and gravel mining, hydropower potentials, navigation, and distribution of groundwater resources. Also, understanding current scenarios of the Brahmaputra basin encompassing the geomorphic features and fluvial-sedimentation scenarios will help portray plausible future development plans considering the equity and sustainability of available resources (hydro-power, agriculture, fisheries, and sand mining) at the entire basin (World Bank, 2015; Pradhan et al., 2021). Also, the maintenance of natural fluvial geomorphic connectivity, considering the general pattern observed in this study, can minimize the threat of isolation of aquatic populations and local extinction (Bunn and Arthington, 2002), will play a crucial role in the Brahmaputra River's ecological sustainability. Besides, this study can support the planning and designing of sand mining, dams, and hydroelectric projects, considering the potential geomorphic features and connectivity patterns at a basin-wide scale. Furthermore, sustainable management requires an interdisciplinary approach linking geomorphological knowledge to hydro-engineers, earth scientists, social scientists, and political parties to maximize the benefits of the large resourceful transboundary river like Brahmaputra.

Hence, based on the discussion mentioned above, the implications of this study in transboundary river basin management have been summarized in Fig. 5.2, considering the importance and relevant organizations linked with integrated river basin management (IRBM).

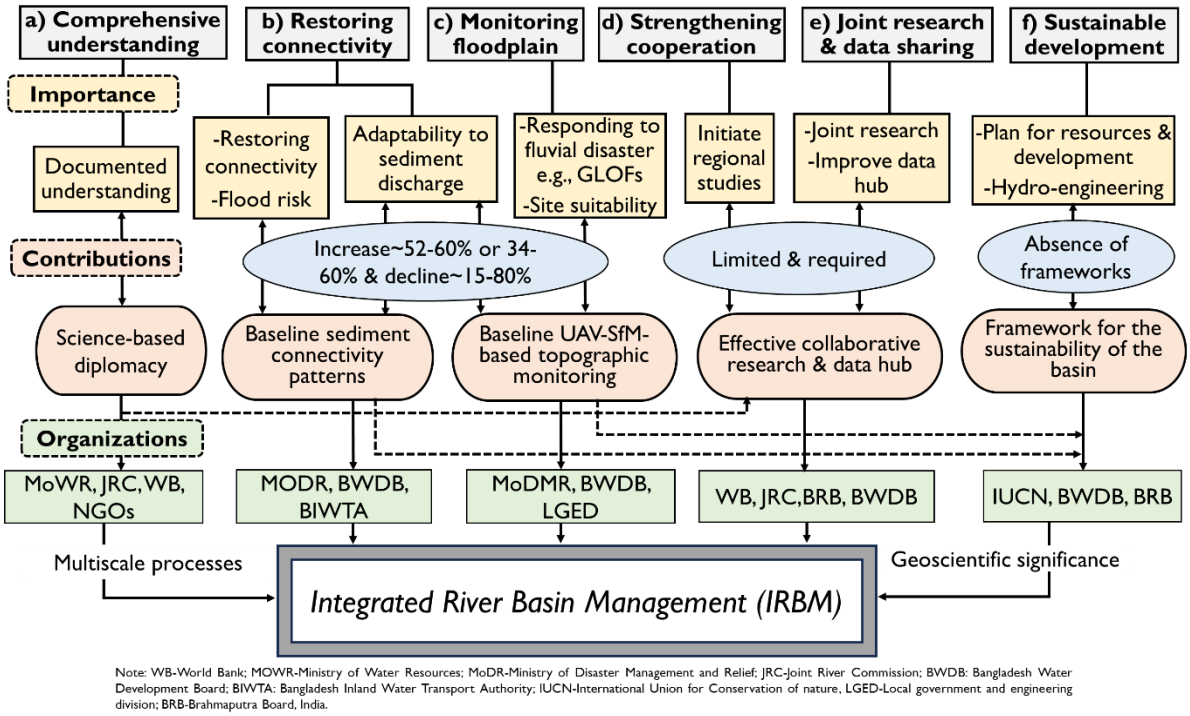

Fig. 5.2 Implications of this study in integrated river basin management.

5.4 Limitations of this study and way forwards

Despite the study region's novelty and significance, there are some limitations that can be addressed in future studies.

Chapter 2 describes the overview of the geomorphological processes and their connectivity in hillslope, fluvial, and coastal areas in GBM downstream Bangladesh. However, it was beyond our scope to give a complete overview of potential applications and improvements of geomorphic research, considering the availability of remote sensing techniques and tools. Also, our study is limited by collecting the estimates of suspended load at the different reaches of the Ganges–Brahmaputra River basin, which does not describe the sampling procedure and methods of suspended load calculation. Therefore, clarifying different methodologies of suspended load estimation in future studies can contribute to understanding better the large variations of the Ganges–Brahmaputra river's suspended load estimations and the sediment budget from the Himalayan to the Bay of Bengal.

Chapter 3 describes the geomorphometric characterization and sediment connectivity of the middle Brahmaputra River basin, where the computation of connectivity and topographic parameters are limited by DEM resolution (30 m). Also, one of the limitations of the present study lies in the limited availability of observed river discharge data for model

validation. Besides, monsoon dynamics, climate change scenarios, and human alternations along the mainstream river need to be considered in future studies to understand sediment transport dynamics better. Furthermore, more gauging station data focusing on sediment size are required for more accurate geomorphological investigations, which is challenging and somewhat restricted in this transboundary Brahmaputra River basin. Therefore, it is expected that collaborative geomorphic research among basin-shared countries like China, India, and Bhutan addressing these issues will elevate our understanding of land surface processes in densely populated South Asian regions.

Chapter 4 describes the potential applicability of modern remote sensing techniques for investigating the topographical and geomorphological dynamics using DEMs (UAV-SfM and NASADEM), considering the elevation change, volumetric estimate, and cross-sectional profiles of Brahmaputra's tributary. The estimation of these changes might be affected by the DEM's resolution difference, estimation accuracy, and the limited scope of the UAV survey. Besides, the time series topographic investigation with UAVs considering the monsoonal dynamics (pre- and post-monsoon survey in a year) in several cross-sections of river floodplains at local scale (10^0~10^2 km^2) are required to assess future instability scenarios in Brahmaputra's tributary (Teesta River). Besides, the applicablities of microsatellites considering the Himalayan-lowland interactive system need to be assessed for continuous multitemporal topography assessment in this South Asian region in collaboration with Japanese universities (e.g., Diwata-1) (Ives and Messerli, 1989; Takahashi, 2013). However, it is worth mentioning the potentialities of Interferometric Synthetic Aperture Radar (InSAR) based DEM (i.e., TanDEM-X) as the baseline topography (Avtar et al., 2015) in future research considering the proposed river floodplain management framework (Fig.4.7).

Hence, addressing the above-mentioned limitations and further multipurpose studies in the future would help better assess the fluvial-geomorphic processes more effectively for the improved, sustainable, and integrated river basin management strategies in South Asia's densely populated disaster-prone region.

5.5 Conclusions

This research focuses on the geospatial investigation of multiscale (basin, sub-basin, and local scales) fluvial-geomorphic processes and geomorphic connectivity in the Brahmaputra River basin of South Asia (China, India, Nepal, Bhutan, and Bangladesh), where the

information or knowledge on land surface processes is very crucial for the sustainability of the entire GBM basin's management and its surrounding landscape. The basin scale study (Chapter 2) considering the transboundary regions over Bangladesh, India, Bhutan, and China (approximately 10^5~10^6 km^2) found that the fluvial-geomorphic processes and their connectivity from the Himalayan to the Bay of Bengal (BoB) are not clearly understood or mentioned due to small-scale and limited field-based approaches at downstream domain but are impacted by the Ganges-Brahmaputra's upstream fluvial-sedimentation processes. The alternation of geomorphic processes and their connectivity (connected-to-partially connected or dis-connected) in the entire fluvial system is mainly due to the excessive upstream sediment contribution from the Ganges-Brahmaputra and inside sediment trapping before the mouth of the BoB, downstream Bangladesh. Hence, with the documented understanding of the fluvial-geomorphic processes, this study recommends wider area geomorphic studies rather than small-scale studies in the Ganges-Brahmaputra-Meghna basin to better understand the fluvial-sedimentation processes towards integrated river basin management among the basin-shared countries.

Therefore, the sub-basin scale (Chapter 3) study has been conducted along the tributaries of the Brahmaputra River basin (Teesta, Torsa, and Manas Rivers, approximately 10^3~10^4 km^2) considering the upstream-downstream linkage and found that the morphodynamics and sediment connectivity patterns are the key determinants of fluvial-sediment dynamics in this river basin. Here, the sediment connectivity varies from connected to partially connected or (dis)connected across the basins and is highly influenced by the upstream's hydro-geomorphic responses and anthropogenic modifications (i.e., hydroelectric projects, dams, barrage, channel diversion, etc.) along the floodplain channel. The partial connectivity or (dis)connectivity in mid-to-downstream is sensitive to deposition and, therefore, impacts the geomorphic linkage. Understanding these sediment connectivity patterns from the basin's upstream to its downstream domain can play a crucial role in fluvial sediment-related disaster management (i.e., GlOFs outburst flood in Teesta River valley of Sikkim Himalayan on 4th October 2023) and is required for the sustainability of disaster-prone landscape of South Asia, particularly for the lowland.

Furthermore, the last part of this study (Chapter 4) assesses the topographical dynamics of Brahmaputra's tributary (Teesta River, Bangladesh) as a nobel case study of utilizing the UAV-SfM techniques at the local scale (10^0~10^2 km^2) considering the cross-sectional profiles and volumetric estimate along the floodplain that are dynamics and crucial

for the sustainability of the surrounding landscape. This study demonstrates the erosion-dominated cross-sectional profiles and sedimentation patterns impacted by the upstream fluvial processes and anthropogenic modifications along the floodplain (i.e., Teesta barrage and channel diversion). Also, the UAV-SfM-based river basin management framework developed from this study can be applied to other cross-sections of the river floodplain considering its dynamic characteristics, proneness to repeated sediment disasters (i.e., floods, river bank erosion), and significance towards the human and environment.

However, the joint venture multipurpose research considering the findings, limitations, and way forwards of this study among the basin-shared countries like China, India, Bhutan, and Bangladesh, focusing on the cross-boundary data sharing, restoring geomorphic connectivity of the natural fluvial system, predicting sediment transport route, continuous river topography monitoring, geoscientific installation of hydro-engineering structures (i.e., hydroelectric dams, barrage, navigation route, etc.) and sustainable utilization of transboundary natural resources (sand mining, fisheries, agriculture, etc.) would improve the integrated river basin management issues in this densely populated landscape of South-Asia. Besides, this approach of gathering information on the fluvial-geomorphic processes and the sediment connectivity patterns in mountainous river basins based on the geospatial techniques can be applied to other mountainous regions (e.g., Japan, Nepal, etc.) at risk of sediment disasters from its upstream. Notably, this study significantly contributes to the current literature on geomorphic science and river basin management issues as the geomorphological knowledge is interlinked to the hydro-engineers, earth scientists, social scientists, river managers or administrators, and political parties, particularly in a disputable transboundary river like the Brahmaputra.

Acknowledgments

The decision to pursue the doctoral program was really tough from my family's point of view and would not be possible without the kindness of the Almighty Allah and great support from the family members, especially my parents, beloved wife (Mst. Liza Pervin), sister (Israt Zarin), siblings, in-laws' members, and absolute love from my two daughters (Taherima Adiyat Nazifa (2.6y) & Rizwana Zafreen Manha (0.8y)). This theiss is dedicated to my beloved daughters and family members for their sacrifice.

First, I would like to express my heartiest gratitude to my supervisor Dr. Yuichi S. Hayakawa, Associate Professor, Hokkaido University, Japan for accepting me in his laboratory and for his kind support, guidance, assistance, and continuous encouragement. I am also thankful and indebted to him for providing me with the opportunities to enrich my knowledge and capabilities to conceptualize the research theme, without his uninterrupted support, this Ph.D. would not be achievable. Also, I am grateful to my supervisor for providing me the opportunity to participate in several UAV-based field investigations related to earth surface processes in several parts of Japan (Hokkaido, Shizuka) and relevant local or international conferences.

I really appreciate the guidance and contribution of the faculty members of Hokkaido University and the Ph.D. evaluation committee members for their constructive comments and suggestions on my research, which truly improved the quality of the dissertation. I am grateful to the Bangladesh Space Research and Remote Sensing Organization (SPARRSO), the Ministry of Defense, Bangladesh, and the Japanese Government (MEXT) scholarship 2020, for kind support during this study period.

I am indebted to my friend Dr. Md. Khorshed Alam (Post-doc, Hokkaido University) and his wife, Dr. Mehjabin Jeny (Post-doc, Hokkaido University), for their kind support during my entire stay in Japan. I thank all my lab members, coursemates, and colleagues in Bangladesh, especially Md. Nur Hossain Sharifee (CSO) and S M Ahsan Habib (SSO). Also, I am grateful to Mohammed Jamal Uddin (Professor, Jahangirnagar University), Md. Abul Kashem Majumder (Hydro-geologist), and Md. Anando (Undergraduate student, Jahangirnagar University), for their thoughtful assistance in the field investigation.

Lastly, I would like to thank myself for completing this academic journey, which can be helpful for my professional carrier and next endeavor.

References

Abbas, N., Subramanian, V., 1984. Erosion and sediment transport in the Ganges River basin (India). J. Hydrol. 69, 173–182.

Abedin, J., Rabby, Y.W., Hasan, I., Akter, H., 2020. An investigation of the characteristics, causes, and consequences of June 13, 2017, landslides in Rangamati District Bangladesh. Geoenviron. Disast. 7, 23.

Acharya, B.S., Bhandari, M., Bandini, F., Pizarro, A., Perks, M., Joshi, D.R., Wang, S., Dogwiler, T., Ray, R.L., Kharel, G., 2021. Unmanned aerial vehicles in hydrology and water management: applications, challenges, and perspectives. Water Resour. Res. 57 (11), e2021WR029925.

Adnan, M.S.G., Dewan, A., Zannat, K.E., Abdullah, A.Y.M., 2019. The use of watershed geomorphic data in flash flood susceptibility zoning: a case study of the Karnaphuli and Sangu river basins of Bangladesh. Nat. Hazards 99, 425–448.

Adnan, M.S.G., Talchabhadel, R., Nakagawa, H., Hall, J.W., 2020. The potential of tidal river management for flood alleviation in South Western Bangladesh. Sci. Total Environ. 731, 138747.

AgiSoft PhotoScan Professional (Version 1.8.1 Build 13915, 64 bit) [Software]. 2022. Available online: https://www.agisoft.com/pdf/metashape-pro_1_8_en.pdf (accessed on 29 Sep 2022).

Aher, P.D., Adinarayana, J., Gorantiwar, S., 2014. Quantification of morphometric characterization and prioritization for management planning in semi-arid tropics of India: a remote sensing and GIS approach. J. Hydrol. 511, 850–860.

Ahmad, H., 2019. Bangladesh coastal zone management status and future. J. Coast Zone Manag. 22, 1–7.

Ahmed, A., Drake, F., Nawaz, R., Woulds, C., 2018. Where is the coast? Monitoring coastal land dynamics in Bangladesh: an integrated management approach using GIS and remote sensing techniques. Ocean Coast Manag. 151, 10–24.

Ahmed, A.A., Fawzi, A., 2011. Meandering and bank erosion of the river Nile and its environmental impact on the area between Sohag and El-Minia, Egypt. Arab J. Geosci, 4(1), 1–11.

Ahmed, B., 2015. Landslide susceptibility modelling applying user-defined weighting and data-driven statistical techniques in Cox's Bazar municipality. Bangladesh. Nat. Hazards 79 (3), 1707–1737.

Ahmed, B., Rahman, M.S., Rahman, S., Huq, F.F., Ara, S., 2014. Landslide inventory report of Chittagong Metropolitan Area, Bangladesh. BUET-Japan Institute of Disaster

Prevention and Urban Safety (BUET-JIDPUS). Bangladesh University of Engineering and Technology (BUET), Dhaka-1000, Bangladesh.

Ahmed, B., Rubel, Y.A., 2013. Understanding the issues involved in urban landslide vulnerability in Chittagong metropolitan area. Association of American Geographers (AAG), Washington, DC.

Ahmed. B., Dewan, A., 2017. Application of bivariate and multivariate statistical techniques in landslide susceptibility modeling in Chittagong City Corporation, Bangladesh. Remote Sens. 9 (4), 304.

Akaike, H., 1974. A new look at the statistical model identification. IEEE Trans. Automat. Contr. 19 (6), 716–723.

Akhter, S., Eibek, K.U., Islam, S., Islam, A.R.M.T., Chub, R., Shuanghe, S., 2019. Predicting spatiotemporal changes of channel morphology in the reach of Teesta River, Bangladesh using GIS and ARIMA modeling. Quatern. Int. 513, 80–94.

Akter, A., Uddin, A.M.H., Wahid, K.B., Ahmed, S., 2020. Predicting groundwater recharge potential zones using geospatial technique. Sustain. Water Resources Manag. 6, 24.

Akter, J., Sarker, M.H., Popescu, I., Roelvink, D., 2016. Evolution of the Bengal Delta and its prevailing processes. J. Coast. Res. 32 (5), 1212–1226.

Alam, M., Alam, M.M., Curray, J.R., Chowdhury, M.L.R., Gani, M.R., 2003. An overview of the sedimentary geology of the Bengal Basin in relation to the regional tectonic framework and basin-fill history. Sed. Geol. 155 (3), 179–208.

Alam, M., Quevauviller, P., 2014. An evaluation of Integrated Water Resources Management (IWRM) activities in Bangladesh. Asia Pac. J. Energy Environ. 1 (1), 22.

Alam, M.K., Negishi, J.N., Pongsivapai, P., Yamashita, S., Nakagawa, T., 2021. Additive effects of sediment and nutrient on leaf litter decomposition and macroinvertebrates in hyporheic zone. Water 13 (10), 1340.

Alam, M.S., Uddin, K., 2013. A study of morphological changes in the coastal areas and offshore islands of Bangladesh using remote sensing. Am. J. Geograph. Inf. Syst. 2 (1), 15–18.

Alam, S., Ali, M.M., Islam, Z., 2016. Future streamflow of Brahmaputra River basin under synthetic climate change scenarios. J. Hydrol. Eng. 21 (11), 05016027.

Alca´ntara-Ayala, I., 2002. Geomorphology, natural hazards, vulnerability and prevention of natural disasters in developing countries. Geomorphology 47 (2–4), 107–124.

Alford, D., 1992. Hydrological aspects of the Himalayan region. ICIMOD occasional paper 18, International Centre for Integrated Mountain Development, Kathmandu, Nepal. https://doi.org/10.53055/ICIMOD.115 (accessed on 20 Jan 2024).

Allison, M.A., 1998a. Historical changes in the Ganges–Brahmaputra delta front. J. Coast. Res. 14, 1269–1275.

Allison, M.A., 1998b. Geologic framework and environmental status of the Ganges–Brahmaputra Delta. J. Coast. Res. 14 (3), 826–836.

Allison, M.A., Khan, S.R., Goodbred, J.S.L., Kuehl, S.A., 2003. Stratigraphic evolution of the late Holocene Ganges–Brahmaputra lower delta plain. Sed. Geol. 155, 317–342.

Allison, M.A., Kuehl, S.A., Martin, T.C., Hassan, A., 1998. Importance of flood-plain sedimentation for river sediment budgets and terrigenous input to the oceans: insights from the Brahmaputra-Jamuna River. Geology 26, 175–178.

Amatulli, G., McInerney, D., Sethi, T., Strobl, P., Domisch, S., 2020. Geomorpho90m-global high-resolution geomorphometry layers. Sci. Data 7, 162.

Annis, A., Nardi, F., Petroselli, A., Apollonio, C., Arcangeletti, E., Tauro, F., Grimaldi, S., 2020. UAV-DEMs for small-scale flood hazard mapping. Water 12 (6), 1717.

Anthony, E.J., Brunier, G., Besset, M., Goichot, M., Dussouillez, P., Nguyen, V.L., 2015. Linking rapid erosion of the Mekong River delta to human activities. Sci. Rep. 5, 14745.

APFM (Associated Programme on Flood Management), 2012. Integrated Flood Management Tools Series (Issue 13): conservation and restoration of rivers and floodplains. Compiled in association with World Meteorological Organization (WMO) and the Global Water Partnership (GWP). https://library.wmo.int/doc_num.php?explnum_id=7332

Arabameri, A., Pradhan, B., Pourghasemi, H.R., Rezaei, K., Kerle, N., 2018. Spatial modelling of gully erosion using GIS and R programing: a comparison among three data mining algorithms. Appl. Sci. 8 (8), 1369.

Arabkhedri, M., Heidary, K., Parsamehr, M.R., 2021. Relationship of sediment yield to connectivity index in small watersheds with similar erosion potentials. J. Soils Sediments 21, 2699–2708.

Arefin, R., 2020a. Groundwater potential zone identification at Plio-Pleistocene elevated tract, Bangladesh: AHP-GIS and remote sensing approach. Groundw. Sustain. Dev. 10, 100340.

Arefin, R., 2020b. Groundwater potential zone identification using an analytic hierarchy process in Dhaka City, Bangladesh. Environ. Earth Sci. 79, 268.

Arefin, R., Alam, J., 2020. Morphometric study for water resource management using principal component analysis in Dhaka City, Bangladesh: a RS and GIS approach. Sustain Water Resour. Manag. 6, 38.

Arnaud-Fassetta, G., Astrade, L., Bardou, E., Corbonnois, J., Delahaye, D., Fort, M., Gautier, M., Jacob, N., Peiry, J., Piégay, H., Penven, M., 2009. Fluvial geomorphology and flood-risk management. Geomorphol. Relief, Process. Environ. 15-n° 2, 109–128.

Arulbalaji, P., Gurugnanam, B., 2017. Geospatial tool-based morphometric analysis using SRTM data in Sarabanga watershed, Cauvery River, Salem district, Tamil NaduIndia. Appl. Water Sci. 7 (7), 3875–3883.

Ashrafi, Z.M., Shuvo, S.D., Mahmud, M.S., 2016. Changes in course pattern of the Teesta River after the effect of an engineering project. AGU Fall Meeting Abstracts, EP51A–0859.

Ashworth, P.J., Best, J.L., Roden, J.E., Bristowà, C.S., Klaassen, G.J., 2000. Morphological evolution and dynamics of a large, sand braid-bar, Jamuna River, Bangladesh. Sedimentology 47, 533–555.

Ashworth, P.J., Lewin, J., 2012. How do big rivers come to be different? Earth Sci. Rev. 114(1–2a), 84–107.

Auerswald, K., Moyle, P., Seibert, S. P., Geist, J., 2019. HESS Opinions: socio- economic and ecological trade-offs of flood management-benefits of a transdisciplinary approach. Hydrol. Earth Syst. Sci. 23, 1035–1044.

Avtar, R., Yunus, A. P., Kraines, S., Yamamuro, M., 2014. Evaluation of DEM generation based on Interferometric SAR using TanDEM-X data in Tokyo. Phys. Chem. Earth parts A/B/C 83–84, 166–177.

Avand, M., Kuriqi, A., Khazaei, M., Ghorbanzadeh, O., 2022. DEM resolution effects on machine learning performance for flood probability mapping. J. Hydro Environ. Res. 40, 1–16.

Baartman, J.E.M., Masselink, R., Temme, A.J.A.M., Keesstra, S.D., 2013. Linking landscape morphological complexity and sediment connectivity. Earth Surf. Proc. Land. 38 (12), 1457–1471.

Bajracharya, S.R., Palash, W., Shrestha, S., Khadgi, V.R., Duo, C., Das, P.J., Dorji, C., 2015. Systematic evaluation of satellite-based rainfall products over the Brahmaputra basin for hydrological applications. Adv. Meteorol. 398687.

Baker, V.R., 1988. Geological fluvial geomorphology. Geol. Soc. Am. Bull. 100, 1157–1167.

Bandyopadhyay, S., Das, S., Kar, N.S., 2015. Discussion: changing river courses in the western part of the Ganga-Brahmaputra delta by Kalyan Rudra (2014), Geomorphology, 227, 87–100. Geomorphology 250, 442–453.

Bandyopadhyay, S., Das, S., Sekhar Kar, N., 2021. Avulsion of the Brahmaputra in Bangladesh during the 18th–19th century: a review based on cartographic and literary evidence. Geomorphology 384, 107696.

References

Bandyopadhyay, S., Kar, N.S., Dasgupta, S., Mukherjee, D., Das, A., 2023. Island area changes in the Sundarban region of the abandoned western Ganga–Brahmaputra–Meghna Delta, India and Bangladesh. Geomorphology 422, 108482.

Barua, P., Chowdhury, M.S.N., Sarker, S., 2010. Climate change and its risk reduction by mangrove ecosystem of Bangladesh. Bangladesh Res. Publ. J. 4, 208–225.

BBS (Bangladesh Bureau of Statistics), 2016. Statistical yearbook of Bangladesh, Dhaka. http://www.bbs.gov.bd/site/page/29855dc1-f2b4-4dc0-9073-f692361112da/Statistical-Yearbook (accessed on Jan 2023).

Best, J., 2019. Anthropogenic stresses on the world's big rivers. Nature Geosci. 12, 7–21.

Best, J., Ashworth, P., 1997. Scour in large braided rivers and the recognition of sequence stratigraphic boundaries. Nature 387, 275–277.

BGS/DPHE, 2001. Arsenic contamination of groundwater in Bangladesh, vol. 2: final report. In: Kinniburgh, D.G., Smedley, P.L., (Eds.), British Geological Survey (BGS) Technical Report WC/00/19, Keyworth, pp. 255.

Bhatt, S., Ahmed, S.A., 2014. Morphometric analysis to determine floods in the Upper Krishna basin using Cartosat DEM. Geocarto Int. 29 (8), 878–894.

Bhuiyan, M.A.H., Kumamoto, T., Suzuki, S., 2015. Application of remote sensing and GIS for evaluation of the recent morphological characteristics of the lower Brahmaputra-Jamuna River, Bangladesh. Earth Sci. India 8, 551–568.

Billah, M.M., 2018. Mapping and monitoring erosion-accretion in an alluvial river using satellite imagery–the river bank changes of the Padma River in Bangladesh. Quaestiones Geographicae 37 (3), 87–95.

Bindu, G., Neelkantan, R., Ragunath, R., 2012. Assessment of morphometric characteristics of Chittar river basin, Triruvantpuram district, Kerala: a remote sensing and GIS based study. J. Indian Geomorphol. 1, 127–132.

Bishop, M.P., 2013. 3.1 Remote sensing and GIScience in geomorphology: introduction and overview. In: Shroder, J.F., (Eds.), Treatise on geomorphology. Academic Press, San Diego, pp. 1–24.

Biswas, P. K., Ahmed, S.S., Pownceby, M. I., Haque, N., Alam, S., Zaman, M. N., Rahman, M.A., 2018. Heavy mineral resource potential of Tista River sands, Northern Bangladesh. Appl. Earth Sci. 127, 3, 94–105.

Biswas, R.N., Islam, M.N., Islam, M.N., Shawon, S.S., 2021. Modeling on approximation of fluvial landform change impact on morphodynamics at Madhumati River Basin in Bangladesh. Model Earth Syst. Environ 7, 71–93.

Bolch, T., Yao, T., Kang, S., Buchroithner, M.F., Scherer, D., Maussion, F., Huintjes, E., Schneider, C., 2010. A glacier inventory for the western Nyainqentanglha Range and the Nam Co Basin, Tibet, and glacier changes 1976–2009. Cryosphere 4, 419–433.

Borselli, L., Cassi, P., Torri, D., 2008. Prolegomena to sediment and flow connectivity in the landscape: a GIS and field numerical assessment. Catena 75 (3), 268–277.

Bracken, L.J., Turnbull, L., Wainwright, J., Bogaart, P., 2015. Sediment connectivity: a framework for understanding sediment transfer at multiple scales. Earth Surf. Process Landf. 40, 177–188.

Brahmaputra Board, 1995. Additional volume for master plan of Brahmaputra Basin, Part-1: Main Stem. Published by Brahmaputra Board, India.

Brammer, H., 1990a. Floods in Bangladesh. 1.Geographical background to the 1987 and 1988 floods. Geogr. J. 156, 12–22.

Brammer, H., 1990b. Floods in Bangladesh. II. Flood mitigation and environmental aspects. Geogr. J. 156, 158–165.

Brammer, H., 1996. The geography of the soils of Bangladesh. University Press Ltd., Dhaka.

Brammer, H., 2014. Bangladesh's dynamic coastal regions and sea-level rise. Clim. Risk Manag. 1, 51–62.

Bravard, J.P., Amoros, C., Pautou, G., Bornette, G., Bournaud, M., Creuzé des Châtelliers, M., Tachet, H., 1997. River incision in south-east France: morphological phenomena and ecological effects. Regulated rivers: research & management 13 (1), 75–90.

Brierley, G., Fryirs, K., Jain, V., 2006. Landscape connectivity: the geographic basis of geomorphic applications. Area 38, 165–174.

Brierley, G.J., Fryirs, K.A., 2005. Geomorphology and river management: applications of the river styles framework. Blackwell Publications, Oxford, UK.

Bristow, C.S., 1987. Brahmaputra River: channel migration and deposition. In: Ethridge, F.G., Flores, R.M., Harvey, M.D., (Eds.), Recent developments in fluvial sedimentology: SEPM Special Publication 39, pp. 63–74.

Buckley, S.M., Agram, P.S., Belz, J.E., Crippen, R.E., Gurrola, E.M., Hensley, S., Kobrick, M., Lavalle, M., Martin, J.M., Neumann, M., Nguyen, Q.D., Rosen, P.A., Shimada, J.G., Simard, M., Tung, W.W., 2020. NASA-DEM user guide. NASA Jet Propulsion Laboratory, January, California, USA. https://lpdaac.usgs.gov/documents/1318/NASADEM_User_Guide_V12.pdf (accessed on 15 March 2021).

BUET-Japan Institute of Disaster Prevention and Urban Safety (JIDPUS), 2015, Developing a dynamic Web-GIS based early warning system for the communities living with

landslide risks in Chittagong Metropolitan Area, Bangladesh; Bangladesh University of Engineering and Technology (BUET), Dhaka.

Bunn, S.E., Arthington, A.H., 2002. Basic principles and ecological consequences of altered flow regimes for aquatic biodiversity. Environ. Manage. 30 (4), 492–507.

Burrough, P.A., McDonnell, R., McDonnell, R.A., Lloyd, C.D., 2015. Principles of geographical information systems. Oxford University Press, UK.

Buter, A., Heckmann, T., Filisetti, L., Savi, S., Mao, L., Gems, B., Comiti, F., 2022. Effects of catchment characteristics and hydro-meteorological scenarios on sediment connectivity in glacierised catchments. Geomorphology 402, 108128.

BWDB (Bangladesh Water Development Board), 1972. Sediment investigations in main rivers of Bangladesh, 1968 & 1969. BWDB water supply paper no. 359. BWDB, Bangladesh.

BWDB (Bangladesh Water Development Board), 2011. Rivers of Bangladesh. BDWB reports in August 2011. Dhaka, Bangladesh.

BWDB (Bangladesh Water Development Board), 2014. Flood forecasting and warning centre, annual flood report 2014. Dhaka-1000, Bangladesh. www.ffwc.gov.bd. (accessed on June 2021).

Caesar, J., Janes, T., Lindsay, A., Bhaskaran, B., 2015. Temperature and precipitation projections over Bangladesh and the upstream Ganges, Brahmaputra and Meghna systems. Environ. Sci.: Processes Impacts, 17 (6), 1047–1056.

Cai, M., Gao, J., Fan, X., Liu, S., Shen, W., He, C., 2022. Estimation of river discharge using Unmanned Aerial Vehicle (UAV) based on manning formula for an ungauged alpine river in the eastern Qilian mountains. Water 14 (13), 2100.

Cantreul, V., Bielders, C., Calsamiglia, A., Degré, A., 2018. How pixel size affects a sediment connectivity index in Central Belgium. Earth Surf. Proc. Land. 43 (4), 884–893.

Carrión-Mero, P., Montalván-Burbano, N., Morante-Carballo, F., Quesada-Román, A., Apolo-Masache, B., 2021. Worldwide research trends in landslide science. Int. J. Environ. Res. Public Health 18 (18), 9445.

Cavalli, M., Crema, S., Marchi, L., 2014. Guidelines on the sediment connectivity ArcGIS toolbox and stand-alone application (No Release 1.0, Issue June). pp. 1–33.

Cavalli, M., Marchi, L., 2008. Characterization of the surface morphology of an alpine alluvial fan using airborne LiDAR. Nat. Hazards Earth Syst. Sci. 8, 323–333.

Cavalli, M., Trevisani, S., Comiti, F., Marchi, L., 2013. Geomorphometric assessment of spatial sediment connectivity in small Alpine catchments. Geomorphology, 188, 31–41.

CDMP-II, 2012. Comprehensive disaster management programme-II. A report on the landslide inventory and land-use mapping, DEM preparation, precipitation threshold value and establishment of early warning devices. Ministry of Food and Disaster Management, Disaster Management and Relief Division, Government of the People's Republic of Bangladesh.

CEGIS (Center for Environmental and Geographic Information Services), 2010. Impacts of climate change on the morphological processes of the main rivers and Meghna Estuary of Bangladesh. Dhaka, Bangladesh: CEGIS, pp. 133.

Cenderelli, D.A., Wohl, E.E., 2003. Flow hydraulics and geomorphic effects of glacial-lake outburst floods in the Mount Everest region, Nepal. Earth Surf. Process Landf. 28, 385–407.

Chand, M.B., Watanabe, T., 2019. Development of supraglacial ponds in the Everest region, Nepal, between 1989 and 2018. Remote Sens. 11, 1058.

Chan, F.K.S., Yang, L.E., Mitchell, G., Wright, N., Guan, M., Lu, X., Wang, Z., Montz, B., Adekola, O., 2022. Comparison of sustainable flood risk management by four countries – the United Kingdom, the Netherlands, the United States, and Japan–and the implications for Asian coastal megacities, Nat. Hazards Earth Syst. Sci. 22, 2567–2588.

Chauniyal, D.D., Dutta, S., 2018. Application of topographic position index for classification of landforms in Dudhatoli region of Garhwal Himalaya Uttarakhand. J. Indian Geomorphol. 6, 28–41.

Chauhan, A., 2023. Glacial lake outburst flood kills 14 in Sikkim, 102 people missing: What is GLOF, and why does it happen? The Indian Express (published on 06 October 2023, online). https://indianexpress.com/article/explained/explained-climate/glacial-lake-outburst-flood-glof-sikkim-8968562/ (accessed on 18 October 2023).

Chen, C.Y., Yu, F.C., 2011. Morphometric analysis of debris flows and their source areas using GIS. Geomorphology 129, 387–397.

Chen, W., Yao, T., Zhang, G., Li, F., Zheng, G., Zhou, Y., Xu, F., 2022. Towards ice-thickness inversion: an evaluation of global digital elevation models (DEMs) in the glacierized Tibetan Plateau. The Cryosphere 16, 197–218.

Cheng, N.N., He, H.M., Yang, S.Y., Lu, Y.J., Jing, Z.W., 2017. Impacts of topography on sediment discharge in Loess Plateau China. Quat. Int. 440, 119–129.

Cho, H., 2020. A recursive algorithm for calculating the longest flow path and its iterative implementation. Environ. Model. Soft. 131, 104774.

Cienciala, P., 2021. Vegetation and geomorphic connectivity in mountain fluvial systems. Water 13, 593.

Cirillo, D., 2020. Digital field mapping and drone-aided survey for structural geological data collection and seismic hazard assessment: case of the 2016 central Italy earthquakes. Appl. Sci. 10 (15), 5233.

Clapuyt, F., Vanacker, V., Van Oost, K., 2016. Reproducibility of UAV-based earth topography reconstructions based on structure-from-motion algorithms. Geomorphology 260, 4–15.

Clarke, J.I., 1966. Morphometry from maps. In: Dury, G.H., (Eds.), Essays in geomorphology. Heinemann, London, pp. 235–274.

Clubb, F.J., Mudd, S.M., Attal, M., Milodowski, D.T., Grieve, S.W.D., 2016. The relationship between drainage density, erosion rate, and hilltop curvature: implications for sediment transport processes. J. Geophys. Res. Earth Surf. 121 (10), 1724–1745.

Coleman, J.M., 1969. Brahmaputra River: channel processes and sedimentation. Sed. Geol. 3, 129–239.

Corsini, A., Borgatti, L., Cervi, F., Dahne, A., Ronchetti, F., Sterzai, P., 2009. Estimating mass-wasting processes in active earth slides—Earth flows with time-series of High-Resolution DEMs from photogrammetry and airborne LiDAR. Nat. Hazards Earth Syst. Sci. 9, 433–439.

Coveney, S., Roberts, K., 2017. Lightweight UAV digital elevation models and orthoimagery for environmental applications: data accuracy evaluation and potential for river flood risk modelling. Int. J. Remote Sens. 38 (8–10), 3159–3180.

Crema, S., Cavalli, M., 2018. SedInConnect: a stand-alone, free and open source tool for the assessment of sediment connectivity. Comput. Geosci. 111, 39–45.

Crippen, R., Buckley, S., Belz, E., Gurrola, E., Hensley, S., Kobrick, M., Lavalle, M., Martin, J., Neumann, M., Nguyen, Q., 2016. NASADEM global elevation model: methods and progress. Int. Arch. Photogramm.Remote Sens. Spatial Inf. Sci. 125–128, XLI-B4.

Croke, J.C., Purvis-Smith, D., Thompson, C.J., Lymburner, L. 2008. The effect of local-scale valley constrictions on flood inundation and catchment-scale sediment delivery in the Fitzroy River Basin, Australia. IAHS-AISH Publication, 325, 200–207. https://iahs.info/uploads/dms/14514.31-200-207-25-325-Croke.pdf

Crosby, B.T., Whipple, K.X., 2006. Knickpoint initiation and distribution within fluvial networks: 236 waterfalls in the Waipaoa River, North Island, New Zealand. Geomorphology 82 (1), 16–38.

Curtis, S., Crawford, T., Rahman, M., Paul, B., 2017. Monsoon dynamics in the Ganges-Brahmaputra-Meghna Basin. In: Proceedings of the first international electronic conference on the hydrological cycle, 12–16 November 2017, MDPI, Basel, Switzerland.

Curtis, S., Crawford, T., Rahman, M., Paul, B., Miah, M.G., Islam, M.R., Patel, M. A., 2018. Hydroclimatological analysis of precipitation in the Ganges–Brahmaputra–Meghna River Basin. Water 10 (10), 1359.

CZPo (Coastal Zone Policy), 2005. Ministry of water resources, Government of the People's Republic of Bangladesh, Dhaka.

Darby, S.E., Dunn, F.E., Nicholls, R.J., Rahman, M., Riddy, L., 2015. A first look at the influence of anthropogenic climate change on the future delivery of fluvial sediment to the Ganges–Brahmaputra–Meghna delta. Environ. Sci. Process Impacts 17 (9), 1587–1600.

Das, S., Bora, P.K., Das, R., 2022. Estimation of slope length gradient (LS) factor for the sub-watershed areas of Juri River in Tripura. Model. Earth Syst. Environ. 8, 1171–1177.

De Haas, T., Nijland, W., McArdell, B.W., Kalthof, M.W.M.L., 2021. Case report: optimization of topographic change detection with UAV structure-from-motion photogrammetry through survey co-alignment. Front. Remote Sens. 2, 626810.

De Reu, J., Bourgeois, J., Bats, M., Zwertvaegher, A., Gelorini, V., De Smedt, P., Chu, W., Antrop, M., De Maeyer, P., Finke, P., Van Meirvenne, M., Verniers, J., Crombé, P., 2013. Application of the topographic position index to heterogeneous landscapes. Geomorphology 186, 39–49.

De Roo, A.P.J., 1998. Modelling runoff and sediment transport in catchments using GIS. Hydrol. Process. 12, 905–922.

Debelo, G., Tadele, K., Korich, S.A., 2017. Morphometric analysis to identify erosion prone areas on the upper Blue Nile using GIS: case study of Didessa and Jema sub-basin Ethiopia. Int. Res. J. Eng. Technol. 04 (08), 1773–1784.

Dehn, M., Gärtner, H., Dikau, R., 2001. Principles of semantic modeling of landform structures. Comput. Geosci. 27, 1005–1010.

DoD (Department of Defense), 2020. Global positioning system standard positioning service performance standard, (5th eds.). US Department of Defense: Arlington, TX, USA. https://www.gps.gov/technical/ps/2020-SPS-performance-standard.pdf

Dewan, A., Corner, R., Saleem, A., Rahman, M.M., Haider, M.R., Rahman, M.M., Sarker, M.H., 2017. Assessing channel changes of the Ganges-Padma River system in Bangladesh using Landsat and hydrological data. Geomorphology 276, 257–279.

Dhote, P.R., Thakur, P.K., Chouksey, A., Srivastav, S.K., Raghvendra, S., Rautela, P., Ranjan, R., Allen, S., Stoffel, M., Bisht, S., Negi, S.B., Aggarwal, S.P., Chauhan, P., 2022. Synergistic analysis of satellite, unmanned aerial vehicle, terrestrial laser scanner data and process-based modelling for understanding the dynamics and morphological changes around the snout of Gangotri Glacier, India. Geomorphology 396, 1080052.

Dietrich, M., Best, K.B., Raf, J.L., Ronay, E.R., 2020. A first-order geochemical budget for suspended sediment discharge to the Bay of Bengal from the Ganges-Brahmaputra river system. Sci. Total Environ. 726, 66.

Diez, P.G., Perillo, G.M.E., Piccolo, M.C., 2007. Vulnerability to sea level rise on the coast of Buenos Aires province. J. Coast. Res. 23, 119–126.

Dikau, R., 1989. The application of a digital relief model to landform analysis in geomorphology. In: Raper, J., (Eds.), Three dimensional applications in geographical information systems. Taylor & Francis, London, pp. 51–77.

Dormann, C.F., Elith, J., Bacher, S., Buchmann, C., Carl, G., Carré, G., Marquéz, J.R.G., Gruber, B., Lafourcade, B., Leitão, P.J., Münkemüller, T., Mcclean, C., Osborne, P.E., Reineking, B., Schröder, B., Skidmore, A.K., Zurell, D., Lautenbach, S., 2013. Collinearity: a review of methods to deal with it and a simulation study evaluating their performance. Ecography 36 (1), 27–46.

Doukakis, E., 2005. Coastal vulnerability and risk parameters. Eur. Water 11 (12), 3–7.

Dunning, S.A., Massey, C.I., Rosser, N.J., 2009. Structural and geomorphological features of landslides in the Bhutan Himalaya derived from terrestrial laser scanning. Geomorphology 103, 17–29.

Dunn, F. E., Nicholls, R. J., Darby, S. E., Cohen, S., Zarfl, C., Fekete, B. M., 2018. Projections of historical and 21st century fluvial sediment delivery to the Ganges-Brahmaputra-Meghna, Mahanadi, and Volta deltas. Sci. Total Environ. 642, 105–116.

Ehsani, A.H., Quiel, F., 2008. Geomorphometric feature analysis using morphometric parameterization and artificial neural networks. Geomorphology 99 (1–4), 1–12.

Elkhrachy, I., 2021. Accuracy assessment of low-cost Unmanned Aerial Vehicle (UAV) photogrammetry. Alex. Eng. J. 60 (6), 5579-5590.

Escobar Villanueva, J.R., Iglesias Martinez, L., Perez Montiel, J.I., 2019. DEM generation from fixed-wing UAV imaging and LiDAR-derived ground control points for flood estimations. Sensors 19 (14), 3205.

Espinosa, P., Horacio, J., Ollero, A., De Meulder, B., Jaque, E., Muñoz, M. D., 2018. Chapter-9: When urban design meets fluvial geomorphology: a case study in Chile. In: Thornbush, M.J., Allen, C.D., (Eds.), Urban geomorphology: landforms and processes in cities, Elsevier, pp. 149–17.

ESRI ArcGIS Desktop: Release 10.3; Environmental Systems Research Institute: Redlands, CA, USA, 2015.

Faghih, A., Nourbakhsh, A., Kusky, T.M., 2015. GIS-Based analysis of relative tectonic activity along the Kazerun Fault Zone, Zagros Mountains, Iran, insights from data mining of geomorphic data. J. Earth Sci. 26, 712–723.

Faisal, B.M.R., Hayakawa, Y.S., 2022. Geomorphological processes and their connectivity in hillslope, fluvial, and coastal areas in Bangladesh: a review. Prog. Earth Planet. Sci. 9, 41.

Faisal, B.M.R., Hayakawa, Y.S., 2023. Geomorphometric characterization and sediment connectivity of the middle Brahmaputra River basin. Geomorphology 429, 108665.

Falconer, R., Cobby, D., Smyth, P., Astle, G., Dent, J., Golding, B., 2009. Pluvial flooding: new approaches in flood warning, mapping and risk management. J. Flood Risk Manag. 2, 198–208.

Fanta-Jende, P., Steininger, D., Bruckmüller, F., Sulzbachner, C., 2020. A versatile UAV near real-time mapping solution for disaster response–concept, ideas and implementation. Int. Arch. Photogramm. Remote. Sens. Spat. Inf. Sci. 43, 429–435.

FAO (Food and Agriculture Organization), 1978. Methodology for assessing soil degradation. In: Report on the FAO/UNEP Expert Consultation, Rome.

Farr, T.G., Rosen, P.A., Caro, E., Crippen, R., Duren, R., Hensley, S., Kobrick, M., Paller, M., Rodriguez, E., Roth, L., Seal, D., Shaffer, S., Shimada, J., Umland, J., Werner, M., Oskin, M., Burbank, D., Alsdorf, D., 2007. The Shuttle Radar Topography Mission. Rev. Geophys 45 (2), RG2004.

Fazeli, H., Samadzadegan, F., Dadrasjavan, F., 2016. Evaluating the potential of RTK-UAV for automatic point cloud generation in 3D rapid mapping. Int. Arch. Photogramm. Remote Sens. Spat. Inf. Sci. XLI-B6, 41, 221–226.

Fischer, S., Pietron, J., Bring, A., Thorslund, J., Jarsjo, J., 2017. Present to future sediment transport of the Brahmaputra River: reducing uncertainty in predictions and management. Reg. Environ. Change 17, 515–526.

Foerster, S., Wilczok, C., Brosinsky, A., Segl, K., 2014. Assessment of sediment connectivity from vegetation cover and topography using remotely sensed data in a dryland catchment in the Spanish Pyrenees. J. Soils Sediments 14 (12), 1982–2000.

Fontana, G.D., Marchi, L., 1998. GIS indicators for sediment sources study in alpine basins. In: Kovar, K., Tappeiner, U., Peters, N.E., Craig, R.G., (Eds.), Hydrology, water resources and ecology in headwaters. IAHS Publication 248, International Association of Hydrological Sciences, Wallingford, pp. 553–560.

Fontana, G.D., Marchi, L., 2003. Slope-area relationships and sediment dynamics in two alpine streams. Hydrol. Process. 17 (1), 73–87.

Forlani, G., Dall'Asta, E., Diotri, F., Cella, U.M.d., Roncella, R., Santise, M., 2018. Quality assessment of DSMs produced from UAV flights georeferenced with on-board RTK positioning. Remote Sens. 10 (2), 311.

Foster, G.R., 1990. Process based modelling of soil erosion by water on agricultural land [M]. In: Boardman, J., Foster, I.D.L., Dearing, J.A., (Eds.), British Geomorphological Research Group Symposium Series: Soil erosion on agricultural land. Wiley, Chichester, pp. 429–445.

Franks, S., Storey, J., Rengarajan, R., 2020. The new Landsat collection-2 digital elevation model. Remote Sens. 12 (23), 3909.

Franks, S., Storey, J., Rengarajan, R., 2020. The new Landsat collection-2 digital elevation model. Remote Sens. 12 (23), 3909.

French, J.R., Burningham, H., 2009. Coastal geomorphology: trends and challenges. Prog. Phys. Geogr. 33 (1), 117–129.

Friend, P.F., Jones, N.F., Vincent, S.J., 1999. Drainage evolution in active mountain belts: extrapolation backwards from present day Himalayan river patterns. Spec. Publ. Int. Assoc. Sedimentol. 28, 305–311.

Fryirs, K.A., 2013. (Dis)connectivity in catchment sediment cascades: a fresh look at the sediment delivery problem. Earth Surf. Process. Landf. 38 (1), 30–46.

Fryirs, K.A., Brierley, G.J., 2013. Geomorphic analysis of river systems: An approach to reading the landscape. John Wiley and Sons, Chichester.

Fryirs, K.A., Brierley, G.J., Preston, N.J., Kasai, M., 2007. Buffers, barriers and blankets: the (dis)connectivity of catchment-scale sediment cascades. Catena 70, 49–67.

Gallant, J.C., Dowling, T.I., 2003. A multiresolution index of valley bottom flatness for mapping depositional areas. Water Resour. Res. 39, 1347.

Gallant, J.C., Wilson, J.P., 2000. Primary topographic attributes. In: Wilson, J.P., Gallant, J.C., (Eds.), Terrain analysis: principles and applications. Wiley, New York, pp. 51–85.

Galy, A., France-Lanord, C., 2001. Higher erosion rates in the Himalaya: geochemical constraints on riverine fluxes. Geology 29 (1), 23–26.

Galy, V., France-Lanord, C., Peucker-Ehrenbrink, B., Huyghe, P., 2010. Sr–Nd–Os evidence for a stable erosion regime in the Himalaya during the past 12 Myr. Earth Planet Sci. Lett. 290, 474–480.

Ganasri, B.P., Ramesh, H., 2016. Assessment of soil erosion by RUSLE model using remote sensing and GIS-A case study of Nethravathi Basin. Geosci. Front. 7 (6), 953–961.

García Rodriguez, J.L., Giménez Suarez, M.C., 2010. Historical review of topographic factor of LS, of water erosion models. Aqua-LAC 2, 56–61.

Garzanti, E., Andó, S., France-Lanord, C., Censi, P., Vignola, P., Galy, V., Lupker, M., 2011. Mineralogical and chemical variability of fluvial sediments 2. Suspended-load silt (Ganga–Brahmaputra, Bangladesh). Earth Planet Sci. Lett. 302 (1–2), 107–120.

Garzanti, E., Vezzoli, G., Ando, S., France-lanord, C., Singh, S.K., Foster, G., 2004. Sand petrology and focused erosion in collision orogens: the Brahmaputra case. Earth Planet Sci. Lett. 220, 157–174.

Gazi, M.Y., Hossain, F., Sadeak, S., Uddin, M.M., 2020b. Spatiotemporal variability of channel and bar morphodynamics in the Gorai–Madhumati River, Bangladesh using remote sensing and GIS techniques. Front. Earth Sci. 14, 828–841.

Gazi, M.Y., Roy, H., Mia, M.B., Akhter, S.M., 2020a. Assessment of morpho-dynamics through geospatial techniques within the Padma–Meghna and Ganges–Jamuna River confluences, Bangladesh. KN J. Cartogr. Geogr. Inf. 70, 127–139.

Ghosh, K., 2014. Planform pattern of the lower Teesta River after the Gazaldoba barrage. Indian J. Geogr. Environ. 13, 127–137.

Giano, S.I., 2021. Fluvial geomorphology and river management. Water 13, 1608.

Giordan, D., Hayakawa, Y.S, Nex, F., Tarolli, P., 2018. Preface: The use of remotely piloted aircraft systems (RPAS) in monitoring applications and management of natural hazards. Nat. Hazards Earth Syst. Sci. 18, 3085–3087.

Giulietti, N., Allevi, G., Castellini, P., Garinei, A., Martarelli, M., 2022. Rivers water level assessment using UAV photogrammetry and RANSAC method and the analysis of sensitivity to uncertainty sources. Sensors 22 (14), 5319.

Goldin, B., 2015. Geomorphometric analysis and sediment dynamics in mountainous basins: spatial and temporal scales. UNIPD Doctoral thesis, University of Padua, Italy.

Goodbred, S.L. Jr., Kuehl, S.A., 1999. Holocene and modern sediment budgets for the Ganges–Brahmaputra river system: evidence for highstand dispersal to flood-plain, shelf, and deep-sea depocenters. Geology 27, 559–562.

Goodbred, S.L., Paolo, P.M., Ullah, M.S., Pate, R.D., Khan, S.R., Kuehl, S.A., Rahaman, W., 2014. Piecing together the Ganges–Brahmaputra–Meghna River delta: use of sediment provenance to reconstruct the history and interaction of multiple fluvial systems during Holocene delta evolution. Geol. Soc. Am. Bull. 126 (11–12), 1495–1510.

Goswami, D.C., 1985. Brahmaputra River, Assam, India: physiography, basin denudation, and channel aggradation. Water Resour. Res. 21 (7), 959–978.

Goswami, D.C., 1998. Fluvial regime and flood hydrology of the Brahmaputra River, Assam. In: Kale, V.S., (Eds.), Flood studies in India. Geological Society of India, Memoir, Bangalore, vol. 41, pp. 53–76.

Goyal, M.K., Goswami, U.P., 2018. Teesta river and its ecosystem. In: Singh, D.S., (Eds.), The Indian rivers. Springer Hydrogeology, Springer Nature Singapore Pte Ltd., pp. 537–551.

Grabs, T., Seibert, J., Bishop, K., Laudon, H., 2009. Modeling spatial patterns of saturated areas: a comparison of the topographic wetness index and a dynamic distributed model. J. Hydrol. 373, 15–23.

Graf, W.L., 2000. Locational probability for a dammed, urbanizing stream: Salt River, Arizona, USA. Environ. Manag. 25, 321–335.

Gravelius, H., 1914. Grundrifi der gesamten Gewcisserkunde. Band I: Flufikunde (Compendium of Hydrology, Vol. I. Rivers, in German). Goschen, Berlin.

GRDC, 2021. Discharge data obtained from the Global Runoff Data Centre. Koblenz, Germany-Federal Institute of Hydrology (BfG). https://www.bafg.de/GRDC/EN/01_GRDC/grdc_node.html (accessed on Jan 2021).

Grohmann, C.H., Riccomini, C., 2009. Comparison of roving-window and search-window techniques for characterising landscape morphometry. Comput. Geosci. 35, 2164–2169.

Grunwald, G., Ciećko, A., Kozakiewicz, T., Krasuski, K., 2023. Analysis of GPS/EGNOS positioning quality using different ionospheric models in UAV navigation. Sensors 23 (3), 1112.

Gupta, A., 1995. Magnitude, frequency and special factors affecting channel form and processes in the seasonal topics. In: Costa, J.E., Miller, A.J., Potter, K.W., Wilcock, P.R., (Eds.), Nature and anthropogenic influences in fluvial geomorphology. American Geophysical Union, Washington, DC, pp. 125–136.

Gupta, A., 2007. Large rivers: geomorphology and management, Chapter 17–19. Wiley, England.

Gupta, H., Kao, S., Dai, M., 2012. The role of mega dams in reducing sediment fluxes: a case study of large Asian rivers. J. Hydrol. 464–465.

Gupta, N., Mishra, A., Agrawal, N.K., Shrestha, A.B., 2019. Potential impacts of climate change on water resources and adaptation policies in the Brahmaputra River Basin. Working paper 2019/8; ICIMOD: Kathmandu, Nepal.

Gupta, S., 1997. Himalayan drainage patterns and the origin of fluvial megafans in the Ganges foreland basin. Geology 25, 11–14.

Hackney, C., Clayton, A.I., 2015. Unmanned aerial vehicles (UAVs) and their application in geomorphic mapping. British Society for Geomorphology, Geomorphological techniques, Chapter 2, section l.7, pp. 1–12.

Hadley, R.F., Schumm, S.A., 1961. Sediment sources and drainage basin characteristics in upper Cheyenne River basin. In: US Geological Survey water-supply paper 1531-B, 198.

Haque, C.E., Azad, M.A.K., Choudhury, M.U.I., 2019. Discourse of flood management approaches and policies in Bangladesh: mapping the changes, drivers, and actors. Water 11 (12), 2654.

Harrison, S., Mighall, T., Stainforth, D.A., Allen, P., Macklin, M., Anderson, E., Knight, J., Mauquoy, D., Passmore, D., Rea, B., Spagnolo, M., Shannon, S., 2019. Uncertainty in geomorphological responses to climate change. Clim. Change 156, 69–86.

Harvey, A.M., 2012. The coupling status of alluvial fans and debris cones: a review and synthesis. Earth Surf. Process Landf. 37 (1), 64–76.

Hashemi-Beni, L., Jones, J., Thompson, G., Johnson, C., Gebrehiwot, A., 2018. Challenges and opportunities for UAV-based digital elevation model generation for flood-risk management: A case of Princeville, North Carolina. Sensors 18 (11), 3843.

Hayakawa, Y.S., Obanawa, H., 2020. Volumetric change detection in bedrock coastal cliffs using terrestrial laser scanning and UAS-based SfM. Sensors 20 (12), 3403.

Hayakawa, Y.S., Oguchi, T., 2006. DEM-based identification of fluvial knickzones and its application to Japanese mountain rivers. Geomorphology 78 (1), 90–106.

Hayakawa, Y.S., Fujita, H., Lee, S., Sagara, T., 2017. Developing a data-sharing system for geospatial research: A case study on the Joint Research Assist System (JoRAS). Int. J. Spat. Data Infr. 12, 141–160.

Heckmann, T., Cavalli, M., Cerdan, O., Foerster, S., Javaux, M., Lode, E., Smetanova, A., Vericat, D., Brardinoni, F., 2018. Indices of sediment connectivity: opportunities, challenges and limitations. Earth Sci. Rev. 187, 77–108.

Hedge, M., Mathur, V.K., Mandal, P.S., 1989. Erratic meander of the river Ganga at Kanpur. In: 3rd International workshop on alluvial river problems (TIWARP), University of Roorkee, Roorkee; Oxford and IBH publishing Co. Pvt. Ltd., New Delhi, pp. 239–246.

Heine, R. A., Pinter, N., 2012. Levee effects upon flood levels: an empirical assessment. Hydrol. Process. 26 (21), 3225–3240.

Heine, R.A., Lant, C.L., Sengupta, R.R., 2004. Development and comparison of approaches for automated mapping of stream channel networks. Ann. Am. Assoc. Geogr. 94, 477–490.

Hemmelder, S., Marra, W., Markies, H., De Jong, S.M., 2018. Monitoring river morphology & bank erosion using UAV imagery–A case study of the river Buëch, Hautes-Alpes, France. Int. J. Appl. Earth Obs. Geoinf. 73, 428–437.

Higano, Y., Islam, M.F., 2002. Rural poverty alleviation through large-scale irrigation planning: problem and prospects of the Dalia barrage project, Bangladesh. Bulletin of Research Institute of Economic Science 32, 371–384.

Higgins, S., Overeem, I., Rogers, K., Kalina, E., 2018. River linking in India: downstream impacts on water discharge and suspended sediment transport to deltas. Elementa Sci. Anthr. 6, 20.

Hinge, L., Gundorph, J., Ujang, U., Azri, S., Anton, F., Rahman, A.A., 2019. Comparative analysis of 3D photogrammetry modeling software packages for drones survey. Int. Arch. Photogramm. Remote Sens. Spatial Inf. Sci. XLII-4/W12, 95–100.

Holeman, J.N., 1968. Sediment yield of major rivers of the world. Water Resour. Res. 4(4), 737–747.

Hooke, J.M., 2003. Coarse sediment connectivity in river channel systems: a conceptual framework and methodology. Geomorphology 56, 79–94.

Hoque, R., Nakayama, D., Matsuyama, H., Matsumoto, J., 2011. Flood monitoring, mapping and assessing capabilities using RADARSAT remote sensing, GIS and ground data for Bangladesh. Nat. Hazards 57, 525–548.

Horton, R.E., 1932. Drainage basin characteristics. Trans. Am. Geophys. Union 13, 350–361.

Horton, R.E., 1945. Erosional development of streams and their drainage basins; hydro-physical approach to quantitative morphology. Geol. Soc. Am. Bull. 56, 275–370.

Hossain, M.M., 1992. Total sediment load in the lower Ganges and Jamuna. J. Inst. Eng. Bangladesh 20, 1–8.

Hossain, M.M., 1993. Economic effects of riverbank erosion: some evidence from Bangladesh. Disasters 17, 25–32.

Howard, A.D., 1994. A detachment-limited model of drainage basin evolution. Water Resour. Res. 30, 2261–2285.

Hsieh, Y-C., Chan, Y-C., Hu, J-C., 2016. Digital elevation model differencing and error estimation from multiple sources: a case study from the Meiyuan Shan landslide in Taiwan. Remote Sens. 8 (3), 199.

Hu, P., Gao, X., Mu, G., Zhao, W., Sun, P., Li, L., 2019. Runoff-sediment dynamics under different flood patterns in a Loess Plateau catchment, China. Catena 173, 234–245.

Huffman, G.J., Adler, R.F., Bolvin, D.T., Nelkin, E.J., 2010. The TRMM multisatellite precipitation analysis (TMPA) chapter 1. In: Hossain, F., Gebremichael, M., (Eds.), Satellite rainfall applications for surface hydrology. Springer Verlag, Berlin, pp. 3–22.

Huffman, G.J., Bolvin, D.T., Nelkin, E.J., Wolff, D.B., Adler, R.F., Gu, G., Stocker, E.F., 2007. The TRMM multisatellite precipitation analysis (TMPA): quasi-global, multiyear, combined-sensor precipitation estimates at fine scales. J. Hydrometeorol. 8 (1), 38–55.

Hungr, O., Morgan, G.C., Kellerhals, P., 1984. Quantitative analysis of debris hazards for design of remedial measures. Can. Geotech. J. 21, 663–677.

Hussain, M.A., Tajima, Y., Gunasekara, K., Rana, S., Hasan, R., 2014. Recent coastline changes at the eastern part of the Meghna Estuary using PALSAR and Landsat images. IOP Conf. Ser. Earth Environ. Sci. 20 (1), 012047.

Iftekhar, M.S., Islam, M.R., 2004. Managing mangroves in Bangladesh: a strategy analysis. J. Coast. Conserv. 10, 139–146.

Immerzeel, W., 2008. Historical trends and future predictions of climate variability in the Brahmaputra Basin. Int. J. Climatol. 28 (2), 243–254.

Immerzeel, W.W., Kraaijenbrink, P.D.A., Shea, J.M., Shrestha, A.B., Pellicciotti, F., Bierkens, M.F.P., De Jong, S.M., 2014. High-resolution monitoring of Himalayan glacier dynamics using unmanned aerial vehicles. Remote Sens. Environ. 150, 93–103.

Iqbal, J., Read, J.J., Thomasson, A.J., Jenkins, J.N., 2005. Relationships between soil landscape and dryland cotton lint yield. Soil Sci. Soc. Am. J. 69, 872–882.

Islam, A.R.M.T., 2016. Assessment of fluvial channel dynamics of Padma River in Northwestern Bangladesh. Univ. J. Geosci. 4 (2), 41–49.

Islam, A.R.M.T., Saha, A., Ghose, B., Pal, S.C., Chowdhuri, I., Mallick, J., 2021. Landslide susceptibility modeling in a complex mountainous region of Sikkim Himalaya using new hybrid data mining approach. Geocarto Int. https://doi.org/10.1080/10106049.2021.2009920

Islam, A.R.M.T., Sein, Z.M.M., Ongoma, V., Islam, M.S., Alam, M.F., Ahmed, F., 2015a. Geomorphological and land use mapping: a case study of Ishwardi under Pabna district, Bangladesh. Adv. Res. 4 (6), 378–387.

Islam, A.Z.M.Z., Kabir, S.M.H., Sharifee, M.N.H., 2013. High-tide coastline method to study the stability of Kuakata coast of Bangladesh using remote sensing techniques. Asian J. Geoinform. 13 (1), 23–29.

Islam, M. F., 2016. The Teesta River and its basin area. In: Islam, M. F., (Eds.), Water use and poverty reduction. Springer Tokyo, Japan. pp. 13–42.

Islam, M., Hossain, M., Murshed, S., 2015b. Assessment of coastal vulnerability due to sea level change at Bhola Island, Bangladesh: using geospatial techniques. J. Indian Soc. Remote Sens. 43, 625–637.

Islam, M.A., Islam, M.S., Islam, T., 2017. Landslides in Chittagong hill tracts and possible measures. In: Proceedings of the international conference on disaster risk mitigation, Dhaka, Bangladesh, 23–24 September 2017.

Islam, M.R., 2011. Vulnerability and coping strategies of women in disaster: a study on coastal areas of Bangladesh. Arts Facul. J. 4, 147–169.

Islam, M.R., Begum, S.F., Yamaguchi, Y., Ogawa, K., 1999. The Ganges and Brahmaputra Rivers in Bangladesh: basin denudation and sedimentation. Hydrol. Process. 17, 2907–2923.

Islam, M.R., Begum, S.F., Yamaguchi, Y., Ogawa, K., 2002. Distribution of suspended sediment in the coastal sea off the Ganges–Brahmaputra River mouth: observation from TM data. J. Mar. Syst. 32, 307–321.

Islam, M.R., Yamaguchi, Y., Ogawa, K., 2001. Suspended sediment in the Ganges and Brahmaputra Rivers in Bangladesh: observation from TM and AVHRR data. Hydrol. Process 15, 493–509.

Islam, M.S., Islam, A.R.M.T., Rahman, F., Ahmed, F., Haque, M.N., 2014. Geomorphology and land use mapping of northern part of Rangpur district, Bangladesh. Int. J. Geomat. Geosci. 2 (4), 145–150.

Islam, M.S., Sultana, S., Saifunnahar, M., Miah, M.A., 2014. Adaptation of char livelihood in flood and river erosion areas through indigenous practice: a study on Bhuapur riverine area in Tangail. J. Environ. Sci. Nat. Resour. 7 (1), 13–19.

Islam, S.N., 2000. Char people, living with the Padma River and fragile environment: char study report March 2000. Gono Unnayan Prochesta (GUP), Dhaka, Bangladesh.

Iwahashi, J., Pike, R.J., 2007. Automated classifications of topography from DEMs by an unsupervised nested-means algorithm and a three-part geometric signature. Geomorphology 86, 409–440.

Iwahashi, J., Yamazaki, D., 2022. Global polygons for terrain classification divided into uniform slopes and basins. Prog. Earth Planet. Sci. 9, 33.

Iwahashi, J., Yamazaki, D., Nakano, T., Endo, R., 2021. Classification of topography for ground vulnerability assessment of alluvial plains and mountains of Japan using 30 m DEM. Prog. Earth Planet. Sci. 8, 3.

Ives, J.D., Messerli, B., 1989. The Himalayan dilemma reconciling development and conservation. Routledge and UNU press, London, New York, pp. xxvii+295. https://lib.icimod.org/record/9778

Jahan, C.S., Rahaman, M.F., Arefin, R., Ali, S., Mazumder, Q.H., 2018. Morphometric analysis and hydrological inference for water resource management in Atrai-Sib River Basin, NW Bangladesh using remote sensing and GIS technique. J. Geol. Soc. India 91, 613–620.

Jain, V., Tandon, S.K., 2010. Conceptual assessment of (dis) connectivity and its application to the Ganga River dispersal system. Geomorphology 118 (3–4), 349–358.

Jain, V., Tandon, S.K., Sinha, R., 2012. Application of modern geomorphic concepts for understanding the spatio-temporal complexity of the large Ganga river dispersal system. Curr. Sci. 103 (11), 1300–1319.

James, L.A., Hodgson, M.E., Ghoshal, S., Latiolais, M.M., 2012. Geomorphic change detection using historic maps and DEM differencing: the temporal dimension of geospatial analysis. Geomorphology 137(1), 181–198.

James, M.R., Robson, S., 2012. Straightforward reconstruction of 3D surfaces and topography with a camera: accuracy and geoscience application. J. Geophys. Res. 117, 1–17.

James, M.R., Robson, S., d'Oleire-Oltmanns, S., Niethammer, U., 2017. Optimising UAV topographic surveys processed with structure-from-motion: Ground control quality, quantity and bundle adjustment. Geomorphology 280, 51–66.

JICA (Japan International Cooperation Agency), 2005. The feasibility study of Padma Bridge in the people's republic of Bangladesh. Nippon KOEI Co., Ltd. In association with Construction Project Consultants, INC. Final report volume 5: River studies.

Jenson, S.K., Domingue, J.O., 1988. Extracting topographic structure from digital elevation data for geographic information system analysis. Photogramm. Eng. Remote Sens. 54 (1), 593–600.

Jiang, W., Han, Z., Zhang, J., Jiao, Q., 2016. Stream profile analysis, tectonic geomorphology and neotectonic activity of the Damxung-Yangbajain rift in the south Tibetan Plateau. Earth Surf. Process Landf. 41 (10), 1312–1326.

Jing, Y., Zhao, Q., Lu, M., Wang, A., Yu, J., Liu, Y., Ding, S., 2022. Effects of road and river networks on sediment connectivity in mountainous watersheds. Sci. Total Environ. 826, 154189.

Joerg, P.C., Zemp, M., 2014. Evaluating volumetric glacier change methods using airborne laser scanning data. Geogr. Ann. A: Phys. Geogr. 96 (2), 135–145.

Jourgholami, M., Karami, S., Tavankar, F., Lo Monaco, A., Picchio, R., 2021. Effects of slope gradient on runoff and sediment yield on machine-induced compacted soil in temperate forests. Forests 12 (1), 49.

Kabir, M.A., Salauddin, M., Hossain, K.T., Tanim, I.A., Saddam, M.M.H., Ahmad, A.U., 2020. Assessing the shoreline dynamics of Hatiya Island of Meghna estuary in Bangladesh using multiband satellite imageries and hydro-meteorological data. Region Stud. Marine Sci. 35, 101167.

Kalantari, Z., Nickman, A., Lyon, S.W., Olofsson, B., Folkeson, L., 2014. A method for mapping flood hazard along roads. J. Environ. Manag. 133, 69–77.

Kale, V. S., 2002. Fluvial geomorphology of Indian rivers: an overview. Prog. Phys. Geogr. 26 (3), 400–433.

Kale, V.S., 2003. Geomorphic effects of monsoon floods on Indian rivers. Nat. Hazards 28, 65–84.

Kale, V.S., 2005. Fluvial hydrology and geomorphology of monsoon dominated Indian rivers. Rev. Bras. de Geomorfol. 6 (1), 63–73.

Kaliraj, S., Chandrasekar, N., Ramachandran, K.K., Srinivas, Y., Saravanan, S., 2017. Coastal landuse and land cover change and transformations of Kanyakumari coast, India using remote sensing and GIS. Egypt. J. Remote. Sens. 20 (2), 169–185.

Kamal, A.S.M.M., Midorikawa, S., 2004. GIS-based geomorphological mapping using remote sensing data and supplementary geoinformation: a case study of the Dhaka city area, Bangladesh. Int. J. Appl. Earth Obs. Geoinf. 6, 111–125.

Kanhaiya, S., Singh, B.P., Singh, S., Mittal, P., Srivastava, V.K., 2018. Morphometric analysis, bedload sediments, and weathering intensity in the Khurar River Basin, Central India. Geol. J. 54 (1), 466–481.

Karan, P.P., 2015. Climate change in Bangladesh: confronting impending disasters. Assoc. Am. Geogr. Rev. Books 3 (2), 63–65.

Karim, S., Akther, K.M., Khatun, M., Ali, R.M.E., 2019. Geomorphology and geology of the Dhaka city corporation area-an approach of remote sensing and GIS technique. Int. J. Astron. Astrophys. Space Sci. 6 (2), 7–16.

Karra, K., Kontgis, C., Statman-Weil, Z., Mazzariello, J.C., Mathis, M.M., Brumby, S.P., 2021. Global land use/land cover with Sentinel 2 and deep learning. In: 2021 IEEE International Geoscience and Remote Sensing Symposium IGARSS, Brussels, Belgium. pp. 4704–4707.

Kaushal, R.K., Sarkar, A., Mishra, K., Sinha, R., Nepal, S., Jain, V., 2020. Spatio-temporal variability in stream power distribution in the Upper Kosi River basin, central Himalaya: controls and geomorphic implications. Geomorphology 350, 106888.

Khalil, M.G., Hossain, M.M., Hoque, M.M., 1995. On siltation in the rivers of Bangladesh: causes and consequences. J. Natl. Ocean Marit. Inst. 12, 11–20.

Khan, A., 2001. Morphological changes due to construction of a barrage on the Teesta River. [online] Lib.buet.ac.bd. Available at: http://lib.buet.ac.bd:8080/xmlui/handle/123456789/188

Khan, A.S., Hossain, M. M., 2001. Assessment of morphological changes due to construction of a barrage in the Teesta River. The 45th convention of IEB, Khulna, 16–18 February.

Khan, M.S.S., Islam, A.R.M.T., 2015. Anthropogenic impact on morphology of Teesta River in Northern Bangladesh: an exploratory study. J. Geosci. Geomat. 3 (3), 50–55.

Khan, M.Y., Shafique, M., Turab, S.A., Ahmad, N., 2021. Characterization of an unstable slope using geophysical, UAV, and geological techniques: Karakoram Himalaya. North Pak Front. Earth Sci. 9, 668011.

Khan, S., Sinha, R., Whitehead, P., Sarkar, S., Jin, L., Futter, M.N., 2018. Flows and sediment dynamics in the Ganga River under present and future climate scenarios. Hydrol. Sci. J. 63 (5), 763–782.

Khan, Y.A., Lateh, H., Baten, M.A., Kamil, A.A., 2012. Critical antecedent rainfall conditions for shallow landslides in Chittagong City of Bangladesh. Environ Earth Sci. 67, 97–106.

Khosravi, K., Nohani, E., Maroufinia, E., Pourghasemi, H.R., 2016. A GIS-based flood susceptibility assessment and its mapping in Iran: a comparison between frequency ratio and weights-of-evidence bivariate statistical models with multi-criteria decision making technique. Nat. Hazards 83, 947–987.

Kibler, K., Biswas, R., Juarez Lucas, A., 2014. Hydrologic data as a human right? Equitable access to information as a resource for disaster risk reduction in transboundary river basins. Water Policy 16, 36–58.

Kiedrzyńska, E., Kiedrzyński, M., Zalewski, M., 2015. Sustainable floodplain management for flood prevention and water quality improvement. Nat. Hazards 76, 955–977.

Kirby, E., Whipple, K., 2001. Quantifiying differential rock uplift rates via stream profile analysis. Geology 29 (5), 415–418.

Klaassen, G.J., Masselink, G., 1992. Planform changes of a braided river with fine sand as bed and bank material. In: Proceedings of the 5th international symposium on river sedimentation, Karlsruhe, Germany, pp. 459–471

Knight, J., Harrison, S., 2014. Mountain glacial and paraglacial environments under global climate change: lessons from the past, future directions and policy implications. Geografiska Annaler. Ser A Phys. Geogr. 96, 245–264.

Kondolf, G, M., Bizzi, S., 2022. Stream Geomorphology. In: Mehner, T., Tockner, K., (Eds.), Encyclopedia of inland waters (Second Edition), Elsevier, pp. 249–257.

Kraaijenbrink, P., Meijer, S.W., Shea, J.M., Pellicciotti, F., De Jong, S.M., Immerzeel, W.W., 2016. Seasonal surface velocities of a Himalayan glacier derived by automated correlation of unmanned aerial vehicle imagery. Ann. Glaciol. 57 (71), 103–113.

Kristensen, P., 2004. The DPSIR framework. National Environmental Research Institute, Denmark.http://fis.freshwatertools.eu/files/MARS_resources/Info_lib/Kristensen%282004%29DPSIR%20Framework.pdf (accessed on 12 Dec 2023).

Kubo, S., 1993. Geomorphological features of Northwestern Bangladesh and some problems on flood mitigation. GeoJournal 31 (4), 313–318.

Lane, S.N., 2013. 21st century climate change: Where has all the geomorphology gone? Earth Surf. Proc. Land. 38, 106–110.

Lane, S.N., Richards, K.S., 1997. Linking river channel form and process: time, space and causality revisited. Earth Surf. Proc. Land. 22, 249–260.

Langat, P.K., Kumar, L., Koech, R., 2019. Monitoring river channel dynamics using remote sensing and GIS techniques. Geomorphology 325, 92–102.

Langhammer, J., Vacková, T., 2018. Detection and mapping of the geomorphic effects of flooding using UAV photogrammetry. Pure Appl. Geophys. 175 (9), 3223–3245.

Le Heron, D.P., Vandyk, T.M., Kuang, H., Liu, Y., Chen, X., Wang, Y., Yang, Z., Scharfenberg, L., Davies, B., Shields, G., 2019. Bird's-eye view of an Ediacaran subglacial landscape. Geology 47, 705–709.

Leb, C., Henshaw, T., Iqbal, N., Bescos, I.R., 2018. Promoting development in shared river basins: tools for enhancing transboundary basin management. Washington, DC, World Bank.

Lewin, J., Brewer, P.A., Wohl, E., 2018. Fluvial Geomorphology. In: Alderton, D., Elias, S.A., (Eds.), Encyclopedia of geology (Second edition), Academic Press, pp. 729–744.

Li, H., Zhao, J., Yan, B., Yue, L., Wang, L., 2022. Global DEMs vary from one to another: an evaluation of newly released Copernicus, NASA and AW3D30 DEM on selected terrains of China using ICESat-2 altimetry data. Int. J. Digit. Earth 15 (1), 1149–1168.

Li, J., Liu, S., Shi, X., Chen, M., Zhang, Hui., Zhu, A., Cui, J., Khokiattiwong, S., Kornkanitnan, N., 2020. Provenance of terrigenous sediments in the central Bay of Bengal and its relationship to climate changes since 25 ka. Prog. Earth Planet Sci. 7, 16.

Li, J., Zhao, Y., Bates, P., Neal, J., Tooth, S., Hawker, L., Maffei, C., 2020. Digital Elevation Models for topographic characterization and flood flow modelling along low-gradient, terminal dryland rivers-a comparison of space borne datasets for the Río ColoradoBolivia. J. Hydrol. 591, 125617.

Li, Z., Chen, J., Tan, C., Zhou, X., Li, Y., Han, M., 2021. Debris flow susceptibility assessment based on topo-hydrological factors at different unit scales: a case study of Mentougou district Beijing. Environ. Earth Sci. 80, 365.

Liu, W., Shi, C., Ma, Y., Li, H., Ma, X., 2021. Land use and land cover change-induced changes of sediment connectivity and their effects on sediment yield in a catchment on the Loess Plateau in China. Catena 207 (11), 105688.

Llena, M., Vericat, D., Cavalli, M., Crema, S., Smith, M.W., 2019. The effects of land use and topographic changes on sediment connectivity in mountain catchments. Sci. Total Environ. 660, 899–912.

Lombana, L., Martínez-Graña, A., 2021. Multiscale hydrogeomorphometric analysis for fluvial risk management application in the Carrión River, Spain. Remote Sens. 13, 2955.

López-Vicente, M., Poesen, J., Navas, A., Gaspar, L., 2013. Predicting runoff and sediment connectivity and soil erosion by water for different land use scenarios in the Spanish pre-pyrenees. Catena 102, 62–73.

López-Vicente, M., Sun, X., Onda, Y., Kato, H., Gomi, T., Hiraoka, M., 2017. Effect of tree thinning and skidding trails on hydrological connectivity in two Japanese forest catchments. Geomorphology 292, 104–114.

Lukram, I.M., Tandon, S.K., 2022. Tributary fans of the Middle Teesta basin in Sikkim-Darjeeling Himalaya, NE India: their contribution to valley-filling processes. Geological Journal 57 (2), 593–610.

Lupker, M., France-Lanord, C., Galy, V., Lavé, J., Gaillardet, J., Gajurel, A.P., Guilmette, C., Rahman, M., Singh, S.K., Sinha, R., 2012. Predominant floodplain over mountain weathering of Himalayan sediments (Ganga basin). Geochimica et Cosmochimica Acta 84, 410–432.

Lutz, A. F., Immerzeel, W.W., Shrestha, A.B., Bierkens, M.F.P., 2014. Consistent increase in High Asia's runoff due to increasing glacier melt and precipitation. Nat. Clim. Chang. 4, 587–592.

Mahala, A., 2020. The significance of morphometric analysis to understand the hydrological and morphological characteristics in two different morpho-climatic settings. Appl. Water Sci. 10, 33.

Mahanta, C., Zaman, A.M., Newaz, S.M.S., Rahman, S.M., Mazumdar, T.K., Choudhury, R., Borah, P.J., Saikia, L., 2014. Physical Assessment of the Brahmaputra River. IUCN, International Union for Conservation of Nature, Dhaka, Bangladesh. pp. xii+74. https://portals.iucn.org/library/sites/library/files/documents/2014-083.pdf (accessed on 15 March 2021).

Mahapatra, M., Ramakrishnan, R., Rajawat, A.S., 2014. Coastal vulnerability assessment using analytical hierarchical process for South Gujarat coast, India. Nat. Hazards 76, 136–159.

Mahmud, M.I., Sultana, S., Hasan, M.A., Ahmed, K.M., 2017. Variations in hydrostratigraphy and groundwater quality between major geomorphic units of the Western Ganges Delta plain, SW Bangladesh. Appl. Water Sci. 7, 2919–2932.

Malik, A., Kumar, A., Kushwaha, D.P., Kisi, O., InanSalih, Q.S., Al-Ansari, N., Yaseen, Z.M., 2019. The implementation of a hybrid model for hilly sub-watershed prioritization using morphometric variables: case study in India. Water 11 (6), 1138.

Mandal, S.P., Chakrabarty, A., 2016. Flash flood risk assessment for upper Teesta river basin: using the hydrological modeling system (HEC-HMS) software. Model. Earth Syst. Environ. 2, 59.

Martini, L., Faes, L., Picco, L., Iroumé, A., Lingua, E., Garbarino, M., Cavalli, M., 2020. Assessing the effect of fire severity on sediment connectivity in Central Chile. Sci. Total Environ. 728, 139006.

Martini, L., Picco, L., Iroumé, A., Cavalli, M., 2019. Sediment connectivity changes in an andean catchment affected by volcanic eruption. Sci. Total Environ. 692, 1209–1222.

Masmood, M., Yeh, P.J.F., Hanasaki, N., Takeuchi, K., 2015. Model study of the impacts of future climate change on the hydrology of Ganges-Brahmaputra-Meghna basin. Hydrol. Earth Syst. Sci. 19, 747–770.

Medhioub, E., Bouaziz, M., Achour, H., Bouaziz, S., 2019. Monthly assessment of TRMM 3B43 rainfall data with high-density gauge stations over Tunisia. Arab. J. Geosci. 12 (2), 1–14.

Messenzehl, K., Hoffmann, T., Dikau, R., 2014. Sediment connectivity in the high-alpine valley of Val Müschauns, Swiss National Park-linking geomorphic field mapping with geomorphometric modelling. Geomorphology 221, 215–229.

Miah, J., Hossain, K.T., Hossain, M.A., Najia, S.I., 2020. Assessing coastal vulnerability of Chittagong District, Bangladesh using geospatial techniques. J. Coast. Conserv. 24, 66.

Miah, M.M., 1988. Flood in Bangladesh: a hydro morphological study of the 1987 flood. Academic Publishers, Dhaka.

Milan, D.J., Heritage, G.L., Large, A.R., Fuller, I.C., 2011. Filtering spatial error from DEMs: Implications for morphological change estimation. Geomorphology 125 (1), 160–171.

Miller, J.C., 1953. A quantitative geomorphic study of drainage basin characteristics in the Clinch mountain area, Virginia and Tennessee. In: Technical report 3, Department of Geology, Columbia University, New York. pp. 389–402.

Mishra, V., Avtar, R., Prathiba, A. P., Mishra, P. K., Tiwari, A., Sharma, S. K., Singh, C. H., Yadav, B. C., Jain, K., 2023. Uncrewed aerial systems in water resource management and monitoring: a review of sensors, applications, software, and issues. Adv. Civ. Eng. 3544724.

Milliman, J.D., Meade, R.H., 1983. World-wide delivery of river sediment to the oceans. J. Geol. 91 (1), 1–21.

Milliman, J.D., Syvitski, J.P.M., 1992. Geomorphic/tectonic control of sediment discharge to the ocean: the importance of small mountain rivers. J. Geol. 100, 525–544.

Minar, M., Hossain, M.B., Shamsuddin, M., 2013. Climate Change and coastal zone of Bangladesh: vulnerability, resilience and adaptability. Middle-East J. Sci. Res., 13, 114–120.

Mishra, K., Sinha, R., Jain, V., Nepal, S., Uddin, K., 2019. Towards the assessment of sediment connectivity in a large Himalayan river basin. Sci. Total Environ. 661, 251–265.

Mojaddadi, H., Pradhan, B., Nampak, H., Ahmad, N., Ghazali, A.H.B., 2017. Ensemble machine-learning based geospatial approach for flood risk assessment using multi-sensor remote-sensing data and GIS. Geomat. Nat. Hazards Risk 8 (2), 1080–1102.

Mondal, M.S., 2022. Local scour at complex bridge piers in Bangladesh rivers: reflections from a large study. Water, 14, 2405.

Mondal, M.S.H., Islam, M.S., 2017. Chronological trends in maximum and minimum water flows of the Teesta River, Bangladesh, and its implications. Jamba J. Disas. Risk Stud. 9 (1), a373.

Mondal, M.S.H., Murayama, T., Nishikizawa, S., 2020. Assessing the flood risk of riverine households: a case study from the right bank of the Teesta River Bangladesh. Int. J. Disaster Risk Reduct. 51, 101758.

Montgomery, D., Dietrich, W.E., 1989. Channel initiation, drainage density and slope. Water Resour. Res. 25, 1907–1918.

Montgomery, D.R., Brandon, M.T., 2002. Topographic controls on erosion rates in tectonically active mountain ranges. Earth Planet. Sci. Lett. 201 (3), 481–489.

Moore, I.D., Burch, G.J., 1986. Physical basis of the length-slope factor in the universal soil loss equation. Soil Sci. Soc. Am. J. 50, 1294–1298.

Moore, I.D., Gesseler, P.E., Nielsen, G.A., Peterson, G.A., 1993. Soil attribute prediction using terrain analysis. Soil Sci. Soc. Am. J. 57, 443–452.

Moore, I.D., Grayson, R., Ladson, A., 1991. Digital terrain modelling: a review of hydrological, geomorphological, and biological applications. Hydrol. Process 5 (1), 3–30.

Morgan, R.P.C., 2009. Soil erosion and conservation. John Wiley and Sons, Hoboken.

Morris-Oswald, T., Sinclair, A.J., 2005. Values and floodplain management: case studies from the Red River Basin, Canada. Environ. Hazards 6 (1), 9–22.

Mukherjee, A., Fryar, A.E., Thomas, W.A., 2009. Geologic, geomorphic and hydrologic framework and evolution of the Bengal basin, India and Bangladesh. J. Asian Earth Sci. 34(3), 227–244.

Mullick, R.A., Babel, M.S., Perret, S.R., 2010. Flow characteristics and environmental flow requirements for the Teesta River, Bangladesh. In: Proceedings of International Conference on Environmental Aspects of Bangladesh (ICEAB10), Fukuoka, Japan, September 04, 2010, pp. 159–162.

Najafi, S., Dragovich, D., Heckmann, T., Sadeghi, S.H., 2021. Sediment connectivity concepts and approaches. Catena 196, 104880.

Narayan, D., Tandon, S.K., Joshi, D.D., 1983. Erosion intensity in a mountain watershed in the Himalayan region. Geol. Soc. India 24, 533–539.

NASA JPL, 2020. NASADEM Merged DEM Global 1 Arc Second V001 [Data Set]. NASA EOSDIS Land Processes DAAC. doi:10.5067/MEaSUREs/NASADEM/NASADEM_HGT.001 (accessed on 11 May 2021).

NASA, 2017. README document for the Tropical Rainfall Measurement Mission (TRMM). Goddard Earth Sciences Data and Information Services Center (GES DISC). https://disc2.gesdisc.eosdis.nasa.gov/data/TRMM_L3/TRMM_3B43/doc/README.TRMM_V7.pdf (accessed on 15 June 2021).

NEDECO (Netherlands Engineering Consultants), 1967. East Pakistan Inland Water Transport Authority, Survey of Inland Waterways and Ports, 1963-1967. NEDECO, The Hague.

Nepal, S., 2012. Evaluating upstream–downstream linkages of hydrological dynamics in the Himalayan Region. PhD thesis, Friedrich Schiller University, Jena, Germany.

Nepal, S., Flügel, W.A., Shrestha, A.B., 2014. Upstream-downstream linkages of hydrological processes in the Himalayan region. Ecol. Process. 3, 19.

Nepal, S., Shrestha, A. B., Goodrich, C. G., Mishra, A., Prakash, A., Bhuchar, S., Vasily, L. A., Khadgi, V., Pradhan, N. S., (Eds.), 2019. Multiscale integrated river basin management from a Hindu Kush Himalayan perspective. Resource book, ICIMOD, Kathmandu, Nepal. https://doi.org/10.53055/ICIMOD.757

NPDM (National Plan for Disaster Management), 2006. Ministry of Food and Disaster Management, Government of the People's Republic of Bangladesh. Draft National Plan 6.

O'Callaghan, J.F., Mark, D.M., 1984. The extraction of drainage networks from digital elevation data. Comput. Graph. Image Process. 28, 328–344.

Oguchi, T., Hayakawa, Y.S., Wasklewicz, T., 2022. 6.50-remote data in fluvial geomorphology: characteristics and applications. Shroder, J.F., (Eds.), Treatise on geomorphology, 2nd ed. Academic Press, pp. 1116–1142. https://doi.org/10.1016/B978-0-12-818234-5.00103-6

Oguchi, T., Wasklewicz, T., Hayakawa, Y.S., 2013. Remote data in fluvial geomorphology: characteristics and applications. In: Shroder, J., Wohl, E., (Eds.), Treatise on geomorphology. Academic Press, San Diego, Fluvial Geomorphology 9, pp. 711–729.

Oguchi, T., Wasklewicz, T.A., 2011. Geographic information systems in geomorphology. The Sage handbook of geomorphology. Sage, London, pp. 227–245.

Ogura, T., Mizuno, T., Katayama, D., Yamanaka, D., Sato, Y., 2023. Estimating the amount of excavated soil using RTK-UAV in excavation projects that consider the habitat of rare species. Ecol. Civil Eng. 22-00012. https://doi.org/10.3825/ece.22-00012

Olivetti, V., Cyr, A.J., Molin, P., Faccenna, C., Granger, D.E., 2012. Uplift history of the Sila Massif, southern Italy, deciphered from cosmogenic 10Be erosion rates and river longitudinal profile analysis. Tectonics 31(3).

Ortega, J.A., Razola, L., Garzón, G., 2014. Recent human impacts and change in dynamics and morphology of ephemeral rivers. Nat. Hazards Earth Syst. Sci. 14 (3), 713–730.

Otto, J.C., Prasicek, G., Blöthe, J., Schrott, L., 2018. GIS applications in geomorphology. Comprehensive geographic information systems. Elsevier, pp. 81–111.

Oya, M., 1979. An applied geomorphological study on the selected bridge site along the Brahmaputra–Jamuna River in Bangladesh (in Japanese with English abstract). Geogr. Rev. Jpn 52 (8), 407–425.

Oyedotun, T.D.T., 2016. Sediment characterisation in an Estuary-beach system. J. Coast. Zone Manag. 19 (2), 433.

Oyedotun, T.D.T., 2020. Quantitative assessment of the drainage morphometric characteristics of Chaohu Lake Basin from SRTM DEM Data: a GIS-based approach. Geol. Ecol. Landsc. 6 (3), 174–187.

Özcan, O., Özcan, O., 2021. Multi-temporal UAV based repeat monitoring of rivers sensitive to flood. J. Maps. 17 (3), 163–170.

Ozdemir, H., Bird, D., 2009. Evaluation of morphometric parameters of drainage networks derived from topographic maps and DEM in point of floods. Environ. Geol. 56 (7), 1405–1415.

Ozulu, İ., Gökgöz, T., 2018. Examining the stream threshold approaches used in hydrologic analysis. ISPRS Int. J. Geo-Inf. 7 (6), 201.

Palash, W., Bajracharya, S.R., Shrestha, A.B., Wahid, S., Hossain, M.S., Mogumder, T.K., Mazumder, L.C., 2023. Climate change impacts on the hydrology of the Brahmaputra River Basin. Climate 11, 18.

Panagos, P., Borrelli, P., Meusburger, K., 2015. A new European slope length and steepness factor (LS Factor) for modeling soil erosion by water. Geosciences 5 (2), 117–126.

Pangare, G., Nishat, B., Liao, X., Qaddumi, H.M., 2021. The restless river. World Bank, Washington, DC. https://doi.org/10.1596/36258 (accessed in March 2022).

Pant, N., Dubey, R.K., Bhatt, A., Rai, S.P., Semwal, P., Mishra, S., 2020. Soil erosion and flood hazard zonation using morphometric and morphotectonic parameters in Upper Alaknanda river basin. Nat. Hazards 103, 3263–3301.

Papaioannou, G., Vasiliades, L., Loukas, A., 2014. Multi-criteria analysis framework for potential flood prone areas mapping. Water Resour. Manag. 29, 399–418.

Pareta, K., Pareta, U., 2015. Geomorphological Interpretation through satellite imagery & DEM data. Am. J. Geophys. Geochem. Geosyst. 1 (2), 19–36.

Parizi, E., Khojeh, S., Hosseini, S.M., Moghadam, Y.J., 2022. Application of unmanned aerial vehicle DEM in flood modeling and comparison with global DEMs: case study of Atrak River Basin, Iran. J. Environ. Manage. 317, 115492.

Parveen, R., Kumar, U., Singh, V.K., 2012. Geomorphometric characterization of upper south Koel basin, Jharkhand: a remote sensing & GIS approach. J. Water Resour. Prot. 4 (12), 1042–1050.

Patton, P.C., Baker, V.R., 1976. Morphometry and floods in small drainage basins subject to diverse hydrogeomorphic controls. Water Resour. Res. 12 (5), 941–952.

Pei, T., Qin, C.Z., Zhu, A.X., Yang, L., Luo, M., Li, B., Zhou, C., 2010. Mapping soil organic matter using the topographic wetness index: a comparative study based on different flow-direction algorithms and kriging methods. Ecol. Ind. 10 (3), 610–619.

Pelletier, J.D., 2003. Drainage basin evolution in the rainfall erosion facility: dependence on initial conditions. Geomorphology 53, 183–196.

Persichillo, M.G., Bordoni, M., Cavalli, M., Crema, S., Meisina, C., 2018. The role of human activities on sediment connectivity of shallow landslides. Catena 160, 261–274.

Peters, J.J., 1993. Morphological studies and data needs. In: Proceedings of the internationals workshop on morphological behaviour of major rivers in Bangladesh (Dhaka, 1993).

Petts, G.E., 1995. Changing river channels: the geographical tradition. In: Gurnell, A.M., Petts, G.E., (Eds.), Changing river channels. Wiley, Chichester, pp. 1–23.

Picco, L., Pellegrini, G., Iroumé, A., Lenzi, M., Rainato, R., 2023. The role of in-channel vegetation in driving and controlling the geomorphic changes along a gravel-bed river. Geomorphology 437, 108803.

Piégay, H., Kondolf, G.M., Minear, J.T., Vaudor, L., 2015. Trends in publications in fluvial geomorphology over two decades: A truly new era in the discipline owing to recent technological revolution? Geomorphology 248, 489–500.

Pike, R.J., Evans, I., Hengl, T., 2009. Chapter 1 Geomorphometry: A brief guide. In: Hengl, T., Reuter, H.I., (Eds.), Developments in soil science 33, pp. 3–33.

Poeppl, R.E., Fryirs, K.A., Tunnicliffe, J., Brierley, G.J., 2020. Managing sediment (dis)connectivity in fluvial systems. Sci. Total Environ. 736, 139627.

Poeppl, R.E., Keesstra, S.D., Maroulis, J., 2017. A conceptual connectivity framework for understanding geomorphic change in human-impacted fluvial systems. Geomorphology 277, 237–250.

Pradhan, N.S., Das, P.J., Gupta, N., Shrestha, A.B., 2021. Sustainable management options for healthy rivers in South Asia: the case of Brahmaputra. Sustainability 13 (3), 1087.

Prasai, S., Surie, M.D., 2013. Political economy analysis of the Teesta River Basin. The Asia foundation, New Delhi. http://waterbeyondborders.net/wp-content/uploads/2017/06/TheAsiaFoundation.PoliticalEconomyAnalysisoftheTeestaRiverBasin.March20131.pdf

Prasanna, V., Subere, J., Das, K.D., Govindarajan, S., Yasunari, T., 2014. Development of daily gridded rainfall dataset over the Ganga, Brahmaputra and Meghna river basins. Meteorol. Appl. 21, 278–293.

R Development Core Team, 2020 [Software]. A language and environment for statistical computing. R foundation for statistical computing. https://www.R-project.org.

Rabby, Y.W., Ishtiaque, A., Rahman, M.S., 2020. Evaluating the effects of digital elevation models in landslide susceptibility mapping in Rangamati District, Bangladesh. Remote Sens. 12, 2718.

Rabby, Y.W., Li, Y., 2018. An integrated approach to map landslides in Chittagong hilly areas, Bangladesh, using Google Earth and field mapping. Landslides (Technical note); Springer-Verlag GmbH Germany part of Springer Nature.

Rabby, Y.W., Li, Y., 2019. An integrated approach to map landslides in Chittagong hilly areas, Bangladesh, using Google Earth and field mapping. Landslides 16, 633–645.

Rabby, Y.W., Li, Y., 2020. Landslide inventory (2001–2017) of Chittagong hilly areas, Bangladesh. Data 5 (1), 4.

Raff, J. L., Goodbred, S. L., Pickering, J. L., Sincavage, R. S., Ayers, J. C., Hossain, M. S., Wilson, C. A., Paola, C., Steckler, M. S., Mondal, D. R., Grimaud, J., Grall, C. J., Rogers, K. G., Ahmed, K. M., Akhter, S. H., Carlson, B. N., Chamberlain, E. L., Dejter, M., Gilligan, J. M., Hale, R. P., Khan, M. R., Muktadir, M. G., Rahman M. M., Williams, L. A., 2023. Sediment delivery to sustain the Ganges-Brahmaputra delta under climate change and anthropogenic impacts. Nat. Commun. 14, 2429.

Rafaelli, S.G., Montgomery, D.R., Greenberg, H.M., 2001. A comparison of thematic mapping of erosional intensity to GIS-driven process models in an Andean drainage basin. J. Hydrol. 244, 33–42.

Rahman, S.H., Faisal, B.M.R., Rahman M.T., Taher T. B., 2016. Analysis of VIA and EbA in a river bank erosion prone area of Bangladesh applying DPSIR framework. Climate 4 (4), 52.

Rahaman, M.F., Jahan, C.S., Arefin, R., Mazumder, Q.H., 2017. Morphometric analysis of major watersheds in Barind Tract, Bangladesh: a remote sensing and GIS-based approach for water resource management. Hydrology 8 (6), 86–95.

Rahaman, M.M., Varis, O., 2009. Integrated water management of the Brahmaputra Basin: perspectives and hope for regional development. Nat. Resour. Forum 33, 60–75.

Rahman, M., Dustegir, M., Karim, R., Haque, A., Nicholls, R.J., Darby, S.E., Nakagawa, H., Hossain, M., Dunn, F.E., Akter, M., 2018. Recent sediment flux to the Ganges–Brahmaputra-Meghna delta system. Sci.Total Environ. 643, 1054–1064.

Rahman, M.M., 2012. Time-series analysis of coastal erosion in the Sundarbans mangrove. International archives of the photogrammetry, remote sensing and spatial information sciences. In: 22nd ISPRS Congress, 25 August–01 September 2012, Melbourne, Australia, XXXIX-B8, pp. 425–429.

Rahman, M.M., Arya, D.S., Goel, N.K., Dhamy, A.P., 2011. Design flow and stage computations in the Teesta River, Bangladesh, using frequency analysis and MIKE 11 modeling. J. Hydrol. Eng. 16, 176–186.

Rahman, M.M., Rahaman, M.M., 2018. Impacts of Farakka barrage on hydrological flow of Ganges river and environment in Bangladesh. Sustain. Water Resour. Manag. 4, 767–780.

Rahman, M.S., Ahmed, B., Di, L., 2017. Landslide initiation and runout susceptibility modeling in the context of hill cutting and rapid urbanization: a combined approach of weights of evidence and spatial multi-criteria. J. Mt. Sci. 14 (10), 1919–1937.

Rahman, R., Salehin, M., 2013. Flood risks and reduction approaches in Bangladesh. In: Shaw, R., Mallick, F., Islam, A., (Eds.), Disaster risk reduction approaches in Bangladesh. Springer, Tokyo, pp. 65–90.

Rahim M.M., Quamruzzaman, C., Alim, M.S., Swapan K.B., Ahmed, M.T., Antora, S.G., Alam B.M., 2008. Proposal for dredging of a ferry route in Mawa-Kaorakandi with proper protection system due to sedimentation. Int. J. Emerg. Technol. Adv. Eng. 6 (7), 197–202.

Rahmati, O., Samadi, M., Shahabi, H., Azareh, A., Rafiei-Sardooi, E., Alilou, H., Melesse, A.M., Pradhan, B., Chapi, K., Shirzadi, A., 2019. SWPT: an automated GIS-based tool for prioritization of sub-watersheds based on morphometric and topo-hydrological factors. Geosci. Front. 10 (6), 2167–2175.

Rai, N., Neupane, S., Rana, S., Belbase, D., Khawas, V., 2019. Built on sand an examination of the practice of sand mining in south Asia with reflections from the Mahakali and the Teesta rivers. Policy Entrepreneurs Incorporated (PEI), Bakhundole, Lalitpur. www.pei.center

Rai, P.K., Mishra, V.N., Mohan, K., 2017. A study of morphometric evaluation of the Son basin, India using geospatial approach. Remote Sens. Appl.: Soc. Environment 7, 9–20.

Rajakumari, S., Mahesh, R., Sarunjith, K.J., Ramesh, R., 2022. Volumetric change analysis of the Cauvery delta topography using radar remote sensing. Egypt. J. Remote Sens. Space Sci. 25 (3), 687–695.

Rajbanshi, J., Das, S., Patel, P., 2022. Planform changes and alterations of longitudinal connectivity caused by the 2019 flood event on the braided Brahmaputra River in Assam, India. Geomorphology 403, 108174.

Ramsankaran, R., Navinkumar, P.J., Dashora, A., Kulkarni, A., 2020. UAV-based survey of Glaciers in Himalayas: opportunities and challenges. J. Indian Soc. Remote Sens. 49, 1171–1187.

Rao, M.P., Cook, E.R., Cook, B.I., D'Arrigo, R.D., Palmer, J.G., Lall, U., Woodhouse, C.A., Buckley, B.M., Uriarte, M., Bishop, D.A., Jian, J., Webster, P.J., 2020. Seven centuries of reconstructed Brahmaputra River discharge demonstrate underestimated high discharge and flood hazard frequency. Nat. Commun. 11, 6017.

Rashid, M.B., Habib, M.A., Khan, R., Islam, A.R.M.T., 2021. Land transform and its consequences due to the route change of the Brahmaputra River in Bangladesh. Int. J. River Basin Manag. https://doi.org/10.1080/15715124.2021.1938095

Rashid, T., Suzuki, S., Sato, H., Monsur, M.H., Saha, S.k., 2013. Relative Sea-level changes during the Holocene in Bangladesh. J. Asian Earth Sci. 64, 136–150.

Rasul, G., 2014. Why Eastern Himalayan countries should cooperate in transboundary water resource management. Water Policy 16 (1), 19–38.

Rasul, G., 2015. Water for growth and development in the Ganges, Brahmaputra, and Meghna basins: an economic perspective. Int. J. River Basin Manag. 13 (3), 387–400.

Ravenscroft, P., 2003. Overview of the hydrogeology of Bangladesh. In: Rahman, A.A., Ravenscroft, P., (Eds.), Groundwater resources and development in Bangladesh-background to the arsenic crisis, agricultural potential and the environment. Bangladesh Centre for advanced studies. University Press Ltd, Dhaka, Bangladesh, pp. 43–86.

Ray, P.A., Yang, Y.C.E., Wi, S., Khalil, A., Chatikavanij, V., Brown, C., 2015. Room for improvement: hydroclimatic challenges to poverty-reducing development of the Brahmaputra River basin. Environ Sci. Policy 54, 64–80.

Rhee, D.S., Kim, Y.D., Kang, B., Kim, D., 2018. Applications of unmanned aerial vehicles in fluvial remote sensing: An overview of recent achievements. KSCE J. Civ. Eng. 22, 588–602.

Rhoads, B., 2020. The vertical dimension of rivers: longitudinal profiles, profile adjustments, and step-pool morphology. In: River dynamics: geomorphology to support management. Cambridge University Press, pp. 294–318.

Richards, A., Parrish, R., Harris, N., Argles, T., Zhang, L., 2006. Correlation of lithotectonic units across the eastern Himalaya, Bhutan. Geology 34, 341–344.

Rickenmann, D., Zimmermann, M., 1993. The 1987 debris flows in Switzerland: documentation and analysis. Geomorphology 8 (2–3), 175–189.

Rinaldi, M., Belletti, B., Bussettini, M., Comiti, F., Golfieri, B., Lastoria, B., Surian, N., 2017. New tools for the hydromorphological assessment and monitoring of European streams. J. Environ. Manag. 202, 363–378.

Rinaldo, A., Marani, A., Rigon, R., 1991. Geomorphological dispersion. Water Resour. Res. 27, 513–525.

Roy, L., Das, S., 2021. GIS-based landform and LULC classifications in the Sub-Himalayan Kaljani Basin: special reference to 2016 flood. Egypt. J. Remote Sens. Space Sci. 24 (3), 755–767.

Rozo, M.G., Nogueira, A.C.R., Castro, C.S., 2014. Remote sensing-based analysis of the planform changes in the upper Amazon River over the period 1986–2006. J. South Am. Earth Sci. 51, 28–44.

Różycka, M., Migoń, P., 2021. Morphometric properties of river basins as indicators of relative tectonic activity-problems of data handling and interpretation. Geomorphology 389, 107807.

Rudra, K., 2014. Changing river courses in the western part of the Ganga–Brahmaputra delta. Geomorphology 227, 87–100.

Rudraiah, M., Govindaiah, S., Srinivas, V.S., 2008. Morphometry using remote sensing and GIS techniques in the sub basins of Kagna river basin, Gulburga district, KarnatakaIndia. J. Indian Soc. Remote Sens. 36, 351–360.

Rumsby, B., Brasington, J., Langham, J., McLelland, S., Middleton, R., Rollinson, G., 2008. Monitoring and modelling particle and reach-scale morphological change in gravel-bed rivers: Applications and challenges. Geomorphology 93, 40–54.

Rusnák, M., Sládek, J., Kidová, A., Lehotský, M., 2018. Template for high-resolution river landscape mapping using UAV technology. Measurement 115, 139–151.

Saaty, T.L., 1977. A scaling method for priorities in hierarchical structures. J. Math Psychol. 15(3), 234–281.

Saha, U.D., Bhattacharya, S., 2019. Reconstructing the channel shifting pattern of the Torsa River on the Himalayan Foreland Basin over the last 250 years. Bull. Geogr. Phys. Geogr. Ser. 16 (1), 99–114.

Saha, U.D., Bhattacharya, S., 2021. Channel avulsion in the Torsa River course and its response to topographic and hydrological controls on the Himalayan Foreland Basin. J Earth Syst. Sci. 130, 184.

Saito, H., Uchiyama, S., Hayakawa, Y.S., Obanawa, H., 2018. Landslides triggered by an earthquake and heavy rainfalls at Aso volcano, Japan, detected by UAS and SfM-MVS photogrammetry. Prog. Earth Planet Sci. 5, 15.

Saito, M., Ichikawa, K., Wakuta, Y., Amaya, K., Nasuno, A., Odashima, K., Ikeuchi, K., Ishikawa, Y., 2018. Study of river channel management methods using multi-temporal measurement data in UAV photogrammetry. Proceedings of River Technology 24, 257–262. https://doi.org/10.11532/river.24.0_257

Salandra, M.L., Roseto, R., Mele, D., Dellino, P., Capolongo, D., 2022. Probabilistic hydro-geomorphological hazard assessment based on UAV-derived high-resolution topographic data: the case of Basento River (Southern Italy). Sci. Total Environ. 156736.

Salmoral, G., Rivas Casado, M., Muthusamy, M., Butler, D., Menon, P.P., Leinster, P., 2020. Guidelines for the use of unmanned aerial systems in flood emergency response. Water, 12 (2), 521.

Sangireddy, H., Carothers, R.A., Stark, C.P., Passalacqua, P., 2016. Controls of climate, topography, vegetation, and lithology on drainage density extracted from high resolution topography data. J. Hydrol. 537, 271–282.

Sanyal, J., Lu, X.X., 2004. Application of remote sensing in flood management with special reference to Monsoon Asia: a review. Nat. Hazards 33, 283–301.

Sarkar, S.K., Ansar, S.B., Ekram, K.M.M., Khan, M.H., Talukdar, S., Naikoo, M.W., Islam, A.R.T., Rahman, A., Mosavi, A., 2022. Developing robust flood susceptibility model with small numbers of parameters in highly fertile regions of Northwest Bangladesh for sustainable flood and agriculture management. Sustainability 14, 3982.

Sarker, A.A., Rashid, A.K.M.M., 2013a. Landslide and flashflood in Bangladesh. In: Shaw, R., Mallick, F., Islam, A., (Eds.), Disaster risk reduction approaches in Bangladesh. Springer, Berlin, pp. 165–189.

Sarker, A.A., Rashid, A.K.M.M., 2013b. Landslide and flashflood in Bangladesh. In: Shaw, R., Mallick, F., Islam, A., (Eds.), Disaster risk reduction approaches in Bangladesh. Disaster risk reduction (methods, approaches and practices). Springer, Tokyo, pp.165–189.

Sarker, M.H., 2004. Impact of upstream human interventions on the morphology of the Ganges-Gorai System. Water Science and Technology Library, pp. 49–80.

Sarker, M.H., Akhand, M.R., Rahman, S.M.M., Molla, F., 2013. Mapping of coastal morphological changes of Bangladesh using RS, GIS and GNSS technology. J. Remote Sens. GIS 1 (2), 27–34.

Sarker, M.H., Akter, J., Ruknul, M., 2011. River bank protection measures in the BrahmaputraJamuna River: Bangladesh experience. International Seminar on River, Society and Sustainable Development. Dibrugarh University, India, 121, pp. 1–14.

Sarker, M.H., Thorne, C.R., Aktar, M.N., Ferdous, M.R., 2014. Morpho-dynamics of the Brahmaputra–Jamuna River, Bangladesh. Geomorphology 215, 45–59.

Sarma, J.N., 2004. An overview of the Brahmaputra river system. In: Singh, V.P., Sharma, N., Ojha, C.S.P., (Eds.), The Brahmaputra basin water resources. Water Science and Technology Library, 47. pp. 72–87.

Sarma, J.N., 2005. Fluvial process and morphology of the Brahmaputra River in Assam, India. Geomorphology 70, 226–256.

Sarwar, G.M., 2013. Sea-level rise along the coast of Bangladesh. In: Shaw, R., Mallick, F., Islam, A., (Eds.), Disaster risk reduction approaches in Bangladesh. Disaster Risk Reduction, Springer, Japan, pp. 217–231.

Sarwar, M., Woodroffe, C.D., 2013. Rates of shoreline change along the coast of Bangladesh. J. Coast. Conserv. 17 (3), 515–526.

Sattar, A., 2023. Sikkim glacial lake outburst spotlights climate vulnerability of the Himalayas. Nat. India. https://doi.org/10.1038/d44151-023-00152-7 (accessed 17 Oct. 2023).

Schumm, S.A., 1956. Evolution of drainage systems and slopes in badlands at Perth Amboy, New Jersey. Geol. Soc. Am. Bull. 67 (5), 597–646.

Schwanghart, W., Scherler, D., 2017. Bumps in river profiles: uncertainty assessment and smoothing using quantile regression techniques. Earth Surf. Dynam. 5 (4), 821–839.

Schwat, E., Istanbulluoglu, E., Horner-Devine, A., Anderson, S., Knuth, F., Shean, D., 2023. Multi-decadal erosion rates from glacierized watersheds on Mount Baker, Washington, USA, reveal topographic, climatic, and lithologic controls on sediment yields. Geomorphology 438, 108805.

Sear, D. A., Newson, M. D., Brookes, A., 1995. Sediment-related river maintenance: The role of fluvial geomorphology. Earth Surf. Process. Landf. 20 (7), 629–647.

Seeber, L., Gornitz, V., 1983. River profiles along the Himalayan arc as indicators of active tectonics. Tectonophysics 92 (4), 335–367.

Şerban, G., Rus, I., Vele, D., Breţcan, P., Alexe, M., Petrea, D., 2016. Flood-prone area delimitation using UAV technology, in the areas hard-to-reach for classic aircrafts: case study in the north-east of Apuseni Mountains, Transylvania. Nat. Hazards 82 (3), 1817–1832.

Serra-Llobet, A., Jähnig, S.C., Geist. J., Kondolf, G.M., Damm, C., Scholz, M., Lund, J., Opperman, J.J., Yarnell, S.M., Pawley, A., Shader, E., Cain, J., Zingraff-Hamed, A., Grantham, T.E., Eisenstein, W., Schmitt, R., 2022. Restoring rivers and floodplains for habitat and flood risk reduction: experiences in multi-benefit floodplain management from California and Germany. Front. Environ. Sci. 9, 778568.

Shamsuzzaman, M., Islam, M.S., Islam, M.B., 2005. Morphogeology of Pabna sadar upazila, Bangladesh. Bangladesh J. Water Resour. Res BUET 20, 65–79.

Sharma, A., 2010. Integrating terrain and vegetation indices for identifying potential soil erosion risk area. Geo-spat. Info. Sci. 13 (3), 201–209.

Sharma, J.N., 2005. Fluvial process and morphology of the Brahmaputra River in Assam, India. Geomorphology 70, 226–256.

Sharma, N., Sarkar, A., Akhter, P., Kumar, N., 2012. National Disaster Management Authority of India (NDMA) final report on study of Brahmaputra River erosion and its control. Conducted by Department of Water Resource Development and Management, India Institute of Technology, Roorkee. https://ndma.gov.in/sites/default/files/PDF/Technical%20Documents/NDMA%20Final%20Report%20Brahmaputra%20River.pdf (accessed on 25 June 2021)

Sharma, S., Sarma, J.N., 2013. Drainage analysis in a part of the Brahmaputra Valley in Sivasagar District, Assam, India, to detect the role of nontectonic activity. J. Indian Soc. Remote Sens. 41 (4), 895–904.

Sharma, T.P.P., Zhang, J., Koju, U.A., Zhang, S., Bai, Y., Suwal, M.K., 2019. Review of flood disaster studies in Nepal: A remote sensing perspective. Int. J. Disaster Risk Reduct. 34, 18–27.

Shi, X., Yang, Z., Dong, Y., Qu, H., Zhou, B., Cheng, B., 2020. Geomorphic indices and longitudinal profile of the Daba Shan, northeastern Sichuan Basin: evidence for the late Cenozoic eastward growth of the Tibetan Plateau. Geomorphology 353, 107031.

Shibly, A.M., Takewaka, S., 2012. Morphological changes along Bangladesh coast derived from satellite images. In: Proceedings of coastal engineering, JSCE, volume 3, November, pp. 41–45.

Shrestha, M.S., Artan, G.A., Bajracharya, S.R., Sharma, R.R., 2008. Using satellite-based rainfall estimates for streamflow modelling: Bagmati Basin. J. Flood Risk Manag. 1, 89–99.

Shukla, A.K., Ojha, C.S.P., Garg, R.D., 2014. Satellite based estimation and validation of monthly rainfall distribution over upper Ganga river basin. Int. Arch. Photogramm. Remote Sens. Spatial Inf. Sci. 399–404, XL–8.

Siddiqui, S., Chohan, S., Das, P.J., 2018. Reimagining Brahmaputra: policy and regulatory aspects of transboundary water governance. New Delhi, India, Oxfam.

Simon, A., Rinaldi, M., 2006. Disturbance, stream incision, and channel evolution: the roles of excess transport capacity and boundary materials in controlling channel response. Geomorphology 79 (3–4), 361–383.

Singh, M., Singh, I.B., Muller, G., 2007. Sediment characteristics and transportation dynamics of the Ganga River. Geomorphology 86, 144–175.

Singh, M., Sinha, R., Tandon, S.K., 2021. Geomorphic connectivity and its application for understanding landscape complexities: a focus on the hydro-geomorphic systems of India. Earth Surf. Proc. Land. 46, 110–130.

Singh, S.K., 2007. Erosion and weathering in the Brahmaputra river system. In: Gupta, A. (Eds.), Large rivers: geomorphology and management. John Wiley & Sons, Ltd., pp. 373–393.

Singh, S.K., France-Lanord, C., 2002. Tracing the distribution of erosion in the Brahmaputra watershed from isotopic compositions of stream sediments. Earth Planet. Sci. Lett. 202 (3–4), 645–662.

Singh, S.K., Santosh, K.R., Krishnaswami, S., 2008. Sr and Nd isotopes in river sediments from the Ganga Basin: sediment provenance and spatial variability in physical erosion. J. Geophys. Res. 113 (F03006), 18.

Singh, V.P., Sharma, B., Shekhar, C., Ojha, P., 2004. The Brahmaputra basin water resources. Kluwer Academic Publishers, Dordrecht, Boston.

Sinha, R., 2004. Geomorphology of the Ganges fluvial system in the Himalayan foreland: an update. Rev. Bras. de Geomorfol. 5 (1), 71–83.

Sinha, R., Das, S., Dikshit, O., 2002. GIS-assisted mapping of catchment-scale erosion and sediment sources, Garhal Himalayan, India. Z. Geomorpho. N.F. 46 (2), 146–165.

Sinha, R., Friend, P.F., 1994. River systems and their sediment flux, Indo-Gangetic plains, northern Bihar, India. Sedimentology 41, 825–845.

Sinha, R., Jain, V., Babu, G.P., Ghosh, S., 2005. Geomorphic characterization and diversity of the rivers of the Gangetic plains. Geomorphology 70, 207–225.

Sinha, R., Jain, V., Tandon, S.K., 2013. River systems and river science in india: major drivers and challenges. In: Sinha, R., Ravindra, R., (Eds.), Earth system processes and disaster management. Society of Earth Scientists Series. Springer, Berlin, Heidelberg, pp. 67–90.

Sinha, R., Ravindra, R., 2013. Earth system processes and disaster management. Society of Earth Scientists Series, Springer, Berlin, Heidelberg.

Slaymaker, O., Embleton-Hamann, C., 2018. Advances in global mountain geomorphology. Geomorphology 308, 230–264.

Śledź, S., Ewertowski, M., Piekarczyk, J., 2021. Applications of Unmanned Aerial Vehicle (UAV) surveys and Structure from motion photogrammetry in glacial and periglacial geomorphology. Geomorphology 378, 107620.

Smith, M.W., Carrivick, J.L., Quincey, D.J., 2015. Structure from motion photogrammetry in physical geography. Progr. Phys. Geogr. 40, 1–29.

Smith, P.N.H., 1997. Hydrologic data development system. Transp. Res. Rec. 1599 (1), 118–127.

Sørensen, R., Seibert, J., 2007. Effects of DEM resolution on the calculation of topographical indices: TWI and its components. J. Hydrol. 347 (1–2), 79–89.

Sørensen, R., Zinko, U., Seibert, J., 2006. On the calculation of the topographic wetness index: evaluation of different methods based on field observations. Hydrol. Earth Syst. Sci. 10, 101–112.

Sreedevi, P.D., Owais, S., Khan, H.H., Ahmed, S., 2009. Morphometric analysis of a Watershed of South India using SRTM data and GIS. J. Geol. Soc. India 73, 543–552.

Stanley, E.H., Boulton, A.J., 2000. River size as a factor in conservation. In: Boon, P.J., Davies, B.R., Petts, G.E., (Eds.), Global perspectives on river conservation: science, policy and practice. Wiley, New York, pp. 403–413.

Stark, C.P., Stark, G.J., 2001. A channelization model of landscape evolution. Am. J. Sci. 301 (4–5), 486– 512.

Steckler, M.S., Nooner, S.L., Akhter, S.H., Chowdhury, S.K., Bettadpur, S., Seeber, L., Kogan, M.G., 2010. Modeling Earth deformation from monsoonal flooding in

Bangladesh using hydrographic, GPS, and Gravity Recovery and Climate Experiment (GRACE) data. J. Geophys Res. 115, 1–18.

Stewart, R.J., Hallet, B., Zeitler, P.K., Malloy, M.A., Allen, C.M., Trippett, D., 2008. Brahmaputra sediment flux dominated by highly localized rapid erosion from the easternmost Himalaya. Geology 36, 711–714.

Stoffel, M., Marston, R.A., 2013. Mountain and hillslope geomorphology: an introduction. Treat Geomorphol. 7, 1–3.

Stott, T., 2013. Review of research in fluvial geomorphology 2010–2011. Prog. Phys. Geogr. 37 (2), 248–258.

Strahler, A.N., 1952. Hypsometric (area-altitude) analysis of erosional topography. Geol. Soc. Am. Bull. 63 (11), 1117–1142.

Strahler, A.N., 1964. Quantitative geomorphology of drainage basins and channel networks. In: Chow, V., (Eds.), Handbook of applied hydrology. McGrawHill, New York, pp. 439–476.

Subramanian, V., Ramanathan, A.L., 1996. Nature of sediment load in the Ganges–Brahmaputra river systems in India. In: Milliman, J.D., Haq, B.U., (Eds.), Sea-level rise and coastal subsidence. Coastal systems and continental margins. Kluwer, pp. 151–168.

Sujatha, E.R., Selvakumar, R., Rajasimman, U.A.B., 2014. Watershed prioritization of Palar sub-watershed based on the morphometric and land use analysis. J. Mt. Sci. 11 (4), 906–916.

Sulser, T.B., Ringler, C., Zhu, T., Msangi, S., Bryan, E., Rosegrant, M.W., 2010. Green and blue water accounting in the Ganges and Nile basins: implications for food and agricultural policy. J. Hydrol. 384, 276–291.

Sultana, M.R., 2022. Bank Erosion and Sediment Deposition in Teesta River: A Spatiotemporal Analysis. In: Bhunia, G.S., Chatterjee, U., Lalmalsawmzauva, K., Shit, P.K., (Eds.), Anthropogeomorphology. Geography of the physical environment. Springer, Cham.

Surian, N., Rinaldi, M., 2003. Morphological response to river engineering and management in alluvial channels in Italy. Geomorphology 50 (4), 307–326.

Swarnkar, S., Sinha, R., Tripathi, S., 2020. Morphometric diversity of supply-limited and transport-limited river systems in the Himalayan foreland. Geomorphology 348, 106882.

Szlafsztein, C., Sterr, H., 2007. A GIS-based vulnerability assessment of coastal natural hazards, state of Pará, Brazil. J. Coast. Conserv. 11 (1), 53–66.

Szlafsztein, C., Sterr, H., 2010. Coastal zone management tool: a GIS based. In: Saint-Paul, U., Schneider, H., (Eds.), Mangrove dynamics and management in North Brazil, ecological studies. Springer, Berlin, pp. 365–385.

Takagi, T., Oguchi, T., Matsumoto, J., Grossma, M.J., Sarker, M.H., Matin, M.A., 2007. Channel braiding and stability of the Brahmaputra River, Bangladesh, since 1967: GIS and remote sensing analyses. Geomorphology 85, 294–305.

Takagi, T., Oguchi, T., Zaiki, M., Matsumoto, J., 2005. Geomorphological and geological studies for Bangladesh: a review (in Japanese with English abstract). Trans. Jpn. Geomorphol. Union 26 (4), 405–422.

Takahashi, T., 1981. Estimation of potential debris flows and their hazardous zones: soft countermeasures for a disaster. J. Nat. Disaster Sci. 3, 57–89.

Takahashi, Y., 2013. A scope of asian micro-satellite consortium. IEEE workshop on geoscience and remote sensing 2013, Melaka, Malaysia.

Talukder, S., Islam, M.S., 2006. Morphogeology of Natore Town and adjacent areas, Bangladesh. Rajshahi University Studies, J. Sci. 34 (part B), 211–222.

Tang, C., Tanyas, H., Van Westen, C.J., Tang, C., Fan, X., Jetten, V.G., 2019. Analysing post-earthquake mass movement volume dynamics with multi-source DEMs. Eng. Geol. 248, 89–101.

Tarannum, T., Bhuyan, A., Badhon, F.F., 2018. Morphological changes of river Teesta during the last decade. In: Proceedings of the 1st National conference on water resources engineering (NCWRE-2018), 21-22 March, CUET, Chittagong, Bangladesh.

Tarboton, D., 1997. A new method for the determination of flow directions and upslope areas in grid digital elevation models. Water Resour. Res. 33 (1), 309–319.

Tarek, M.H., Hassan, A., Bhattacharjee, J., Choudhury, S.H., Badruzzaman, A.B.M., 2017. Assessment of TRMM data for precipitation measurement in Bangladesh. Meteorol. Appl. 24, 349–359.

Tarolli, P., 2014. High-resolution topography for understanding earth surface processes: opportunities and challenges. Geomorphology 216, 295–312.

Tarolli, P., Sofia, G., 2016. Human topographic signatures and derived geomorphic processes across landscapes. Geomorphology 255, 140–161.

Tempa, K., Peljor, K., Wangdi, S., Ghalley, R., Jamtsho, K., Ghalley, S., Pradhan, P., 2021. UAV technique to localize landslide susceptibility and mitigation proposal: a case of Rinchending Goenpa landslide in Bhutan. Nat. Hazards Res. 1 (4), 171–186.

Thapa, B., Watanabe, T., Regmi, D., 2022. Flood assessment and identification of emergency evacuation routes in Seti River basin, Nepal. Land, 11 (1), 82.

Thieler, E.R., Hammar-Klose, E.S., 1999. National assessment of coastal vulnerability to future sea-level rise: Preliminary results for the U.S. Atlantic Coast. U.S. Geological Survey Open-File Report, pp. 99–593.

Thorne, C.R., 2002. Geomorphic analysis of large alluvial rivers. Geomorphology 44, 203–219.

Thorne, C.R., Russell, A.P.G., Alam, M.K., 1993. Planform pattern and channel evolution of the Brahmaputra River, Bangladesh. Geol. Soc. Lond. Spec Publ. 75 (1), 257–276.

Tingsanchali, T., Karim, M.F., 2005. Flood hazard and risk analysis in the southwest region of Bangladesh. Hydrol. Process 19, 2055–2069.

Tran, T., Nguyen, B.Q., Vo, N.D., Le, M., Nguyen, Q., Lakshmi, V., Bolten, J.D., 2023. Quantification of global digital elevation model (DEM)–a case study of the newly released NASADEM for a river basin in Central Vietnam. J. Hydrol. Regional Studies 45, 101282.

TRMM (Tropical Rainfall Measuring Mission), 2011. TRMM (TMPA/3B43) Rainfall Estimate L3 1 Month 0.25 Degree x 0.25 Degree V7, Greenbelt, MD, Goddard Earth Sciences Data and Information Services Center (GES DISC) (accessed on 20 March 2021).

Tseng, C.M., Lin, C.W., Stark, C.P., Liu, J.K., Fei, L.Y., Hsieh, Y.C., 2013. Application of a multi-temporal, LiDAR-derived, digital terrain model in a landslide-volume estimation. Earth Surf. Process Landf. 38, 1587–1601.

Tsunetaka, H., Hotta, N., Hayakawa, Y. S., Imaizumi, F., 2020. Spatial accuracy assessment of unmanned aerial vehicle-based structures from motion multi-view stereo photogrammetry for geomorphic observations in initiation zones of debris flows, Ohya landslide, Japan. Prog. Earth Planet Sci. 7 (1), 1–14.

Tucker, G.E., Bras, R.L., 1998. Hillslope processes, drainage density and landscape morphology. Water Resour. Res. 34, 2751–2764.

Turley, M., Hassan, M.A., Slaymaker, O., 2021. Quantifying sediment connectivity: moving toward a holistic assessment through a mixed methods approach. Earth Surf. Process. Landforms. 46 (12), 2501–2519.

Turnbull, L., Wainwright, J., Brazier, R.E., 2008. A conceptual framework for understanding semi-arid land degradation: eco-hydrological interactions across multiple-space and time scales. Ecohydrology 1, 23–34.

Umitsu, M., 1985. Natural levees and landform evolutions in the Bengal lowlands. Geogr. Rev. Jpn Ser. B 58 (2), 149–164.

Umitsu, M., 1987. Late quaternary sedimentary environment and landform evolution in the Bengal Lowland. Geogr. Rev. Jpn Ser. B 60 (2), 164–178.

Umitsu, M., 1993. Late quaternary sedimentary environments and landforms in the Ganges Delta. Sed. Geol. 83, 177–186.

Uuemaa, E., Ahi, S., Montibeller, B., Muru, M., Kmoch, A., 2020. Vertical accuracy of freely available global digital elevation models (ASTER, AW3D30, MERIT, TanDEM-X, SRTM, and NASADEM). Remote Sens. 12 (21), 3482.

Vaidyanathan, N.S., Sharma, G., Sinha, R., Dikshit, O., 2002. Mapping of erosion intensity in the Garhwal Himalayan. Int. J. Remote Sens. 23 (20), 4125–4129.

Van Denderen, R.P., Kater, E., Jans, L.H., Schielen, R.M.J., 2022. Disentangling changes in the river bed profile: the morphological impact of river interventions in a managed river. Geomorphology 408, 108244.

Van Dine, D., 1996. Debris flow control structures for forest engineering. Research Branch, Ministry of Forests, Victoria. BC. Working Paper 08/1996. https://www.for.gov.bc.ca/hfd/pubs/docs/wp/wp22.pdf (accessed on 10 May 2021).

Van Iersel, W.K., Addink, E.A., Straatsma, M.W., Middelkoop, H., 2016. River floodplain vegetation classification using multi-temporal high-resolution colour infrared UAV imagery. In Proceedings of the GEOBIA 2016: Solutions and Synergies, Enschede, The Netherlands, 14–16 September 2016.

Van Rees, C.B., Waylen, K. A., Schmidt-Kloiber, A., Thackeray, S.J., Kalinkat, G., Martens, K., Domisch, S., Lillebø, A.I., Hermoso, V., Grossart, H.P., Schinegger, R., Decleer, K., Adriaens, T., Denys, L., Jarić, I., Janse, J. H., Monaghan, M. T., De Wever, A., Geijzendorffer, I., Adamescu, M. C., Jähnig, S. C., 2021. Safeguarding freshwater life beyond 2020: recommendations for the new global biodiversity framework from the European experience. Conservation Lett. 14 (1), e12771.

Van Woerkom, T., Steiner, J.F., Kraaijenbrink, P.D.A., Miles, E.S., Immerzeel, W.W., 2019. Sediment supply from lateral moraines to a debris-covered glacier in the Himalaya. Earth Surf. Dyn. 7, 411–427.

Vázquez-Tarrío, D., Ruiz-Villanueva, V., Garrote, J., Benito, G., Calle, M., Lucía, A., Díez-Herrero, A., 2024. Effects of sediment transport on flood hazards: lessons learned and remaining challenges. Geomorphology, 446, 108976.

Vijith, H., Dodge-Wan, D., 2019. Modelling terrain erosion susceptibility of logged and regenerated forested region in northern Borneo through the Analytical Hierarchy Process (AHP) and GIS techniques. Geoenvironmental Disasters 6, 8.

Wainwright, J., Turnbull, L., Ibrahim, T.G., Lexartza-Artza, I., Thornton, S.F., Brazier, R.E., 2011. Linking environmental regimes, space and time: interpretations of structural and functional connectivity. Geomorphology 126, 387–404.

Wallick, J.R., Grant, G.E., Lancaster, S.T., Bolte, J.P., Denlinger, R.P., 2007. Patterns and controls on historical channel change in the Willamette River, Oregon, USA. In: Gupta, A., (Eds.), Large rivers: geomorphology and management. Wiley, pp. 491–516.

Wang, S., Ren, Z., Wu, C., Lei, Q., Gong, W., Ou, Q., Zhang, H., Ren, G., Li, C., 2019. DEM generation from Worldview-2 stereo imagery and vertical accuracy assessment for its application in active tectonics. Geomorphology 336, 107–118.

Wang, T., Watanabe, T., 2022. Monitoring campsite soil erosion by structure-from-motion photogrammetry: a case study of Kuro-dake Campsites in Daisetsuzan National Park, Japan. J. Environ. Manage. 314, 115106.

Warner, J.F., Van Staveren, M.F., Van Tatenhove, J., 2018. Cutting dikes, cutting ties? Reintroducing flood dynamics in coastal polders in Bangladesh and the Netherlands. Int. J. Disast. Risk Reduct. 32, 106–112.

Wasson, R.A., 2003. A sediment budget for the Ganga–Brahmaputra catchment. Curr. Sci. 84, 1041–1047.

Watson, C.S., Kargel, J.S., Tiruwa, B., 2019. UAV-Derived Himalayan topography: hazard assessments and comparison with global DEM products. Drones 3 (1), 18.

Weiss, A.D., 2001. Topographic position and landform analysis. In: Poster presentation, ESRI users conferences, San Diego, CA.

Wellmeyer, J.L., Slattery, M.C., Phillips, J.D., 2005. Quantifying downstream impacts of impoundment on flow regime and channel planform lower Trinity River. Texas Geomorphol. 69 (1–4), 1–13.

Wheaton, J.M., Brasington, J., Darby, S.E., Sear, D.A., 2010. Accounting for uncertainty in DEMs from repeat topographic surveys: improved sediment budgets. Earth Surf. Process Landf. 35, 136–156.

Whipple, K.X., Tucker, G.E., 1999. Dynamics of the stream-power river incision model: implications for height limits of mountain ranges, landscape response timescales, and research needs. J. Geophys. Res. 104, 17661–17674.

White, S.M., Apitz, S.E., 2008. Conceptual and strategic frameworks for sediment management at the river basin scale. In: Owens, P.N., (Eds.), Sediment management of sediment resources: sediment management at the river basin scale. Elsevier BV, pp. 31–53.

Williams, R.D., 2012. DEMs of difference. Geomorphological techniques (Eds.), British Society for Geomorphology, pp. 17.

Winchell, M.F., Jackson, S.H., Wadley, A.M., Srinivasan, R., 2008. Extension and validation of a geographic information system-based method for calculating the revised universal

soil loss equation length-slop factor for erosion risk assessments in large watersheds. J. Soil Water Conserv. 63 (3), 105–111.

Wischmeier, W.H., Smith, D.D., 1978. Predicting rainfall erosion losses: a guide to conservation planning. In: US Department of agriculture handbook, No. 537, Washington DC. https://naldc.nal.usda.gov/download/CAT79706928/PDF (accessed on 20 May 2021).

Wobus, C., Whipple, K.X., Kirby, E., Synder, N., Johnson, J., Spyropolon, K., Crosby, B., Sheehan, D., 2006. Tectonics from topography: Procedures, promise, and pitfalls. In: Willett, S.D., Hovius, N., Brandon, M.T., Fisher, D.M., (Eds.), Tectonics, climate, and landscape evolution. Geol. Soc. Am. Special paper 398, pp. 55–73.

Wohl, E., 2014. Time and the rivers flowing: fluvial geomorphology since 1960. Geomorphology 216 (1), 263–282.

Wohl, E., Brierley, G., Cadol, D., Coulthard, T.J., Covino, T., Fryirs, K.A., Grant, G., Hilton, R.G., Lane, S.N., Magilligan, F.J., Meitzen, K.M., Passalacqua, P., Poeppl, R.E., Rathburn, S.L., Sklar, L.S., 2019. Connectivity as an emergent property of geomorphic systems. Earth Surf. Process Landf. 44 (1), 4–26.

Wohl, E., Merritt, D.M., 2008. Reach-scale channel geometry of mountain streams. Geomorphology 93 (3–4), 168–185.

Wolman, M.G., Miller, J.P., 1960. Magnitude and frequency of forces in geomorphic processes. J. Geol. 68, 54–74.

Woodget, A.S., Carbonneau, P.E., Visser, F., Maddock, I.P., 2014. Quantifying submerged fluvial topography using hyperspatial resolution UAS imagery and structure from motion photogrammetry. Earth Surf. Process Landf. 40, 47– 64.

World Bank Group, 2015. Toward efficient and sustainable river basin operational services in Indonesia.World Bank, Washington, DC https://openknowledge.worldbank.org/handle/10986/23241 (accessed on May 2021).

Xiao, H., Liu, G., Liu, P., Zheng, F., Zhang, J., Hu, F., 2017. Sediment transport capacity of concentrated flows on steep loessial slope with erodible beds. Sci. Rep. 7, 2350.

Xie, C., Cui, B., Xie, T., Yu, S., Liu, Z., Chen, C., Shao, X., 2020. Hydrological connectivity dynamics of tidal flat systems impacted by severe reclamation in the Yellow River Delta. Sci. Total Environ. 739, 139860.

Yamagata, K., Haruyama, S., Murooka, M., Wang, D., 2015. Changes in wetland and floodplain sedimentation processes in the middle reach of the Amur River basin. In: Haruyama, S., Shiraiwa, T., (Eds.), Environmental change and the social response in the Amur River basin. Springer, Tokyo, International Perspectives in Geography 5, PP. 91–103.

Yang, C., Jen, C., Cheng, Y., Lin, J., 2021. Quantification of mudcracks-driven erosion using terrestrial laser scanning in laboratory runoff experiment. Geomorphology 375, 107527.

Yao, Z., Ta, W., Jia, X., Xiao, J., 2011. Bank erosion and accretion along the Ningxia-Inner Mongolia reaches of the Yellow river from 1958 and 2008. Geomorphology 127, 99–106.

Yasuda, Y., Aich, D., Hill, D., Huntjens, P., Swain, A., 2017. Transboundary water cooperation over the Brahmaputra River: legal political economy analysis of current and future potential cooperation. The Hague Institute for Global Justice. https://siwi.org/wp-content/uploads/2018/01/brahmaputra-basin-report-final_design.pdf. (accessed on 10 March 2022).

Yong, B., Chen, B., Gourley, J.J., Ren, L., Hong, Y., Chen, X., Wang, W., Chen, S., Gong, L., 2014. Inter comparison of the version-6 and version-7 TMPA precipitation products over high and low latitudes basins with independent gauge networks: is the newer version better in both real-time and post-real-time analysis for water resources and hydrologic extremes? J. Hydrol. 508, 77–87.

Zarfl, C., Lumsdon, A.E., Berlekamp, J., Tydecks, L., Tockner, k., 2015. A global boom in hydropower dam construction. Aquat. Sci. 77, 161–170.

Zanandrea, F., Michel, G.P., Kobiyama, M., Cardozo, G.L., 2019. Evaluation of different DTMs in sediment connectivity determination in the Mascarada River Watershed, southern Brazil. Geomorphology 332, 80–87.

Zanandrea, F., Michel, G.P., Kobiyama, M., Censi, G., Abatti, B.H., 2021. Spatial-temporal assessment of water and sediment connectivity through a modified connectivity index in a subtropical mountainous catchment. Catena 204, 105380.

List of abbreviations

ADTree: Alternating Decision Tree

AHP: Artificial Hierarchy Process

AIC: Akaike Information Criterion

ALOS: Advanced Land Observing Satellite

ARIMA: Autoregressive Integrated Moving Average

ASCII: American Standard Code for Information Interchange

ASTER: Advanced Spaceborne Thermal Emission and Reflection Radiometer

AVHRR: Advanced Very-High-Resolution Radiometer

AW3D: ALOS Global Digital Surface Model

BoB: Bay of Bengal

BIWTA: Bangladesh Inland Water Transport Authority

BWDB: Bangladesh Water Development Board

CDMP: Comprehensive Disaster Management Program

CHT: Chittagong Hill Tracts

CVI: Coastal Vulnerability Index

DEM: Digital Elevation Model

DPSIR: Driver-Pressure-State-Impact-Response

DoD: DEM of Difference

DTM: Digital Terrain Model

EGM96: Earth Gravitational Model 1996

ESA: European Space Agency

ESRI: Environmental System Research Institute Inc.

FDP: Fluvial Deltaic Plain

FTDP: Fluvio-Tidal Deltaic Plain

GB: Ganges–Brahmaputra

GBM: Ganges–Brahmaputra–Meghna

GCD: Geomorphic Change Detection

GCPs: Ground Control Points

GDEM: Global Digital Elevation Models

GJC: Ganges–Jamuna Confluence

GLAS: Geoscience Laser Altimeter System

GLMMs: Generalized Linear Mixed Models

GLOFs: Glacial Lake Outburst Flood

GLONASS: Global Navigation Satellite System

GNSS: Global Navigation Satellite System

GRDC: Global Runoff Data center

GSI: Geospatial Information Authority of Japan

HAE: Height Above Ellipsoid

HAND: Height Above The Nearest Drainage

HHC: High Himalayan Crystalline Sequence

IC: Connectivity Index

ICESat-GLAS: Ice, Cloud, and Land Elevation Satellite-Geoscience Laser Altimeter System

IMD: India Meteorological Department

ITS: Indus–Tsangpo Suture

IUCN: International Union for Conservation of Nature and Natural Resources

IWRM: Integrated Water Resources Management

JAXA: Japan Aerospace Exploration Agency

JRC: Joint River Commission

LH: Lesser Himalayas

LiDAR: Light Detection and Ranging

LPDAAC: Land Processes Distributed Active Archive Center

LPET: Longitudinal Profile Extraction Tool

LS: Slope-Length

LULC: Land-Use/Land-Cover

MEaSUREs: Making Earth System Data Records for Use in Research Environments

MERIT DEM: Multi-Error-Removed Improved-Terrain DEM

NASA: National Aeronautics and Space Administration

NASADEM: National Aeronautics and Space Administration DEM

NetCDF: Network Common Data Form

NPDM: National Plan for Disaster Management

NGOs: Non-Government Organizations

PALSAR: Phased Array-Type L-Band Synthetic Aperture Radar

PMC: Padma–Meghna Confluence

PRISM: Panchromatic Remote-Sensing Instrument for Stereo Mapping

QPSO: Quantum Particle Swamp Optimization

REEs: Rare Earth Elements

RTK: Real-Time Kinematic

SAR: Synthetic Aperture Radar

SfM-MVS: Structure from Motion Multiview Stereo Workflow

SAWI: South Asia Water Initiative

SoB: Survey of Bangladesh

SMAT: Semi-automated Morphometric Assessment Tools

SPI: Stream Power Index

SRTM: Shuttle Radar Topographic Mission

SSC: Suspended Sediment Concentration

STI: Sediment Transport Index

STPM: Sediment Transport Potential Maps

TanDEM-X: Terrasar-X Add-On for Digital Elevation Measurement

TauDEM: Terrain Analysis Using Digital Elevation Models

THB: Trans-Himalayan Batholiths

TLS: Terrestrial Laser Scanning

TPI: Topographic Position Index

TRET: TRMM Data Extraction Tool

TRM: Tidal River Management

TRMM: Tropical Rainfall Measuring Mission

TSS: Tethyan Sedimentary Series

TWI: Topographic Wetness Index

UAS: Unmanned Aerial System

UAVs: Unmanned Aerial Vehicles

WLC: Weighted Linear Combination